

การศึกษาการผลิตเอทิลแอลกอฮอล์จากแป้งข้าวเหนียวที่ได้ออกจากการหมัก  
โดยกระบวนการกลั่นแบบมีปฏิริยา

นางสาวบุญประดับ แดงประดับ



วิทยานิพนธ์นี้เป็นส่วนหนึ่งของการศึกษาตามหลักสูตรปริญญาวิศวกรรมศาสตรมหาบัณฑิต  
สาขาวิชาวิศวกรรมเคมี  
มหาวิทยาลัยเทคโนโลยีสุรนารี  
ปีการศึกษา 2557

**STUDY OF ETHYL LACTATE PRODUCTION FROM  
FERMENTATION-DERIVED MAGNESIUM LACTATE  
BY REACTIVE DISTILLATION**

**Boonpradab Daengpradab**



**A Thesis Submitted in Partial Fulfillment of the Requirements for the  
Degree of Master of Engineering in Chemical Engineering**

**Suranaree University of Technology**

**Academic Year 2014**

**STUDY OF ETHYL LACTATE PRODUCTION FROM  
FERMENTATION-DERIVED MAGNESIUM LACTATE  
BY REACTIVE DISTILLATION**

Suranaree University of Technology has approved this thesis submitted in partial fulfillment of the requirements for a Master's Degree.

Thesis Examining Committee

---

(Dr. Terasut Sookkumnerd)

Chairperson

---

(Asst. Prof. Dr. Panarat Rattanaphanee)

Member (Thesis Advisor)

---

(Asst. Prof. Dr. Boris Golman)

Member

---

(Asst. Prof. Dr. Atichat Wongkoblaph)

Member

---

(Prof. Dr. Sukit Limpijumnong)

Vice Rector for Academic Affairs  
and Innovation

(Assoc. Prof. Flt. Lt. Dr. Kontorn Chamniprasart)

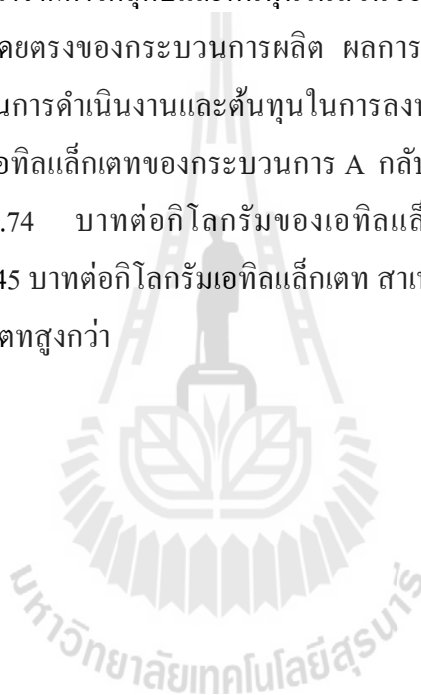
Dean of Institute of Engineering

บุญประดับ แดงประดับ : การศึกษาการผลิตเอทิลแล็กเตทจากแมกนีเซียมแล็กเตทที่ได้จากการหมักโดยกระบวนการกลั่นแบบมีปฏิกิริยา (STUDY OF ETHYL LACTATE PRODUCTION FROM FERMENTATION-DERIVED MAGNESIUM LACTATE BY REACTIVE DISTILLATION) อาจารย์ที่ปรึกษา : ผู้ช่วยศาสตราจารย์ ดร.พนารัตน์ รัตนพานี, 262 หน้า.

ในวิทยานิพนธ์ฉบับนี้ ได้ศึกษาความเป็นไปได้ในการผลิตเอทิลแล็กเตท โดยกระบวนการกลั่นแบบมีปฏิกิริยาที่ใช้แมกนีเซียมแล็กเตทจากการหมักเป็นสารตั้งต้นโดยตรง การดำเนินการศึกษาวิจัยแบ่งออกได้เป็น 3 ส่วนหลัก ส่วนแรกคือการศึกษาจลนพลศาสตร์ของปฏิกิริยาเอสเทอร์พีเคชันระหว่างเอทานอลกับกรดแล็กติกในสารละลายแมกนีเซียมแล็กเตทโดยใช้กรดซัลฟูริกเป็นตัวเร่งปฏิกิริยาเอกพันธ์ ตัวแปรในการศึกษาได้แก่ อุณหภูมิของปฏิกิริยา อัตราส่วนโดยโมลเริ่มต้นระหว่างเอทานอลต่อกรดแล็กติก และความเข้มข้นของตัวเร่งปฏิกิริยาในระบบ ขั้นตอนนี้ใช้แบบจำลองสัมประสิทธิ์แอกติวิตี UNIQUAC และ UNIFAC ในการแสดงความไม่เป็นอุดมคติของสารละลายในปฏิกิริยาและเปรียบเทียบผลการศึกษาที่ได้กับจลนพลศาสตร์ของปฏิกิริยาเอสเทอร์พีเคชันระหว่างเอทานอลกับกรดแล็กติกความบริสุทธิ์สูง ผลการศึกษาพบว่าปฏิกิริยาเอสเทอร์พีเคชันที่ใช้แมกนีเซียมแล็กเตทเป็นสารตั้งต้นนั้น มีค่าคงที่ของปฏิกิริยาและค่าคงที่สมดุลของปฏิกิริยาต่ำกว่า และมีความคลาดเคลื่อนระหว่างค่าคงที่ทั้งสองที่ได้จากการทดลองและจากการคำนวณสูงกว่าปฏิกิริยาที่ใช้กรดแล็กติกความบริสุทธิ์สูงเป็นสารตั้งต้น ซึ่งน่าจะมีสาเหตุจากการมีแมกนีเซียมซัลเฟตที่เกิดจากปฏิกิริยาระหว่างแมกนีเซียมแล็กเตทกับกรดซัลฟูริกอยู่ในระบบ

การศึกษาวิจัยส่วนที่สองคือการออกแบบเบื้องต้น การจำลอง และการหาสภาวะที่เหมาะสมของกระบวนการกลั่นแบบมีปฏิกิริยาเพื่อผลิตเอทิลแล็กเตทด้วยโปรแกรม Aspen Plus โดยศึกษาและเปรียบเทียบประสิทธิภาพของกระบวนการผลิต 2 แบบที่มีความสามารถในการผลิตเริ่มต้นที่ 50 ลิตรของน้ำหมักในหนึ่งวัน ในกระบวนการแบบแรก (กระบวนการ A) เอทิลแล็กเตทที่ผลิตได้ถูกเก็บเป็นผลิตภัณฑ์ที่ด้านบนของหอกลั่นแบบมีปฏิกิริยา ขณะที่ในกระบวนการแบบที่สอง (กระบวนการ B) เอทิลแล็กเตทเป็นผลิตภัณฑ์ที่ด้านล่างของหอดังกล่าว ผลการศึกษาพบว่ากระบวนการ A มีอัตราการผลิตและผลได้ของเอทิลแล็กเตทสูงกว่ากระบวนการ B แต่กระบวนการ B ให้ผลิตภัณฑ์สุดท้ายเป็นสารละลายเอทิลแล็กเตทที่มีความเข้มข้นสูงกว่า และใช้จำนวนหอกลั่นลำดับส่วนและปริมาณความร้อนในกระบวนการผลิตน้อยกว่ากระบวนการ A

การศึกษาวิจัยส่วนสุดท้ายคือการประเมินต้นทุนการผลิตเอทิลแอลกอฮอล์ของกระบวนการผลิตที่ออกแบบไว้ในการศึกษาส่วนที่สองที่มีความสามารถในการผลิตที่ 50 ลิตรของน้ำหมักในหนึ่งวันเท่านั้น ต้นทุนทั้งหมดในการลงทุนสามารถคำนวณด้วยวิธี Percentage delivered-equipment cost ซึ่งพิจารณาค่าใช้จ่ายในการลงทุนต่างๆเป็นสัดส่วนกับค่าใช้จ่ายในการจัดซื้อหน่วยปฏิบัติการของกระบวนการผลิตที่ซึ่งสามารถคำนวณได้จากสหสัมพันธ์ของ Guthrie สำหรับต้นทุนการดำเนินงานของกระบวนการผลิตพิจารณาจากค่าวัตถุดิบและต้นทุนในส่วนของพลังที่ใช้ในกระบวนการผลิตเป็นหลัก ค่าใช้จ่ายในการผลิตรายปีคำนวณได้จากต้นทุนการดำเนินงานของกระบวนการผลิตที่พิจารณาจากค่าวัตถุดิบและต้นทุนในส่วนของพลังงานที่ใช้ในกระบวนการผลิตและค่าต้นทุนการลงทุนโดยตรงของกระบวนการผลิต ผลการศึกษาในส่วนนี้แสดงให้เห็นว่าแม้กระบวนการ A จะมีต้นทุนการดำเนินงานและต้นทุนในการลงทุนสูงกว่ากระบวนการ B แต่กลับมีต้นทุนการผลิตต่อหน่วยเอทิลแอลกอฮอล์ของกระบวนการ A กลับต่ำกว่า กล่าวคือกระบวนการ A มีต้นทุนการผลิตอยู่ที่ 767.74 บาทต่อกิโลกรัมของเอทิลแอลกอฮอล์ ขณะที่ต้นทุนการผลิตของกระบวนการ B อยู่ที่ 833.45 บาทต่อกิโลกรัมเอทิลแอลกอฮอล์ สาเหตุหลักเนื่องมาจากกระบวนการ A มีอัตราการผลิตเอทิลแอลกอฮอล์สูงกว่า



สาขาวิชา วิศวกรรมเคมี

ปีการศึกษา 2557

ลายมือชื่อนักศึกษา \_\_\_\_\_

ลายมือชื่ออาจารย์ที่ปรึกษา \_\_\_\_\_

BOONPRADAB DAENGPRADAB : STUDY OF ETHYL LACTATE  
PRODUCTION FROM FERMENTATION-DERIVED MAGNESIUM  
LACTATE BY REACTIVE DISTILLATION. THESIS ADVISOR : ASST.  
PROF. PANARAT RATTANAPHANEE, Ph.D., 262 PP.

ETHYL LACTATE/MAGNESIUM LACTATE/ESTERIFICATION/REACTIVE  
DISTILLATION/COST ANALYSIS

In this study, feasibility study of ethyl lactate synthesis via reactive distillation process using fermentation-derived magnesium lactate directly as a starting material was investigated. The study was divided into 3 parts. The first part was a kinetic study of esterification between ethanol and lactic acid in magnesium lactate solution using sulfuric acid as a homogeneous catalyst. Variables of interest were reaction temperature, molar ratio of ethanol to lactic acid, and concentration of the catalyst in the system. Non-idealities of the components in the reaction solution were represented by UNIQUAC and UNIFAC activity coefficient model. The results obtained were compared with kinetics of esterification between ethanol and high purity lactic acid. It was found that reaction rate constant and equilibrium constant of the reaction using magnesium lactate as a reactant were lower than those obtained from the reaction on high purity lactic acid. Larger deviation between the experimental and calculated kinetic parameters was observed in the reaction with magnesium lactate, which could likely be due to a presence of magnesium sulfate, a product from the reaction between magnesium lactate and sulfuric acid in the system.

The second part of this thesis was a preliminary design, simulation and optimization of the reactive distillation process for production of ethyl lactate using Aspen Plus. Efficiencies of two process schemes with capacity of 50 L fermentation broth per day were evaluated and compared. In the first scheme (Process A), the produced ethyl lactate was harvested at the top of the reactive distillation column. In the second process (Process B), on the other hand, it was collected at the bottom of the reactive distillation column. It was found that Process A gave higher production rate and yield of ethyl lactate, but the final ethyl lactate solution obtained from Process B was of higher concentration. In addition, the number of fractional distillation columns required to purify ethyl lactate, hence amount of energy required, in Process B was less than that required in Process A.

The last part of this thesis dealt with estimation of ethyl lactate production cost using both processes designed in the second part with the same capacity of 50 L/day of broth. Total capital cost was calculated by percentage delivered-equipment cost method which considers other expenses as the percentage of purchased equipment cost calculated by Guthire's correlation. Annual production cost was estimated by the operating costs, which were mainly consisted of the raw material and utility costs, and the fixed-capital cost. The production cost of ethyl lactate from Process A was 767.74 THB/kg<sub>ethyl lactate</sub>, while that from Process B was 833.45 THB/kg<sub>ethyl lactate</sub>. It should be noted that Process A had higher annual production cost and capital cost than Process B. The lower ethyl lactate production cost obtained from Process A was, therefore, likely due to its higher production rate compared to the one given by Process B.

School of Chemical Engineering

Academic Year 2014

Student's Signature \_\_\_\_\_

Advisor's Signature \_\_\_\_\_

## ACKNOWLEDGEMENT

I am grateful to all the people who have helped in the completion of this thesis. Firstly and foremost, I would like to express my sincere thanks and gratitude to my thesis advisor, Asst. Prof. Dr. Panarat Rattanaphanee for her invaluable help and continuous encouragement throughout the course of this research. She gave many suggestions and many helps in my study in both Bachelor's degree and Master's degree level, especially in conducting the research and writing this thesis. Her guiding motivation and patience was the most important source of my accomplishment.

I would like to thank Dr. Terasut Sookkumnerd, Asst. Prof. Dr. Boris Golman and Asst. Prof. Dr. Atichat Wongkoblap for their suggestions on this work and their valuable time to serve as my committee member. I also would like to thank all the lecturers in School of Chemical Engineering, Suranaree University of Technology, who teach me in all subjects and give a lot of motivations to be a good Chemical Engineer.

I am thankful to Chemical Engineering laboratory technician, Mr. Saran Dokmajkun, for his great help with the laboratory facilities and for the valuable recommendations.

Lastly, I would like to express my deep sense of gratitude to my family, especially my father, for all the support and encouragement they give me throughout the course of this study.

Boonpradab Daengpradab

# TABLE OF CONTENTS

	<b>Page</b>
ABSTRACT (THAI).....	I
ABSTRACT (ENGLISH).....	III
ACKNOWLEDGEMENTS.....	V
TABLE OF CONTENTS.....	VI
LIST OF TABLES.....	XIII
LIST OF FIGURES.....	XVIII
SYMBOLS AND ABBREVIATIONS.....	XXVI
<b>CHAPTER</b>	
<b>I INTRODUCTION.....</b>	<b>1</b>
1.1 Background and Significance of the Problem.....	1
1.2 Objectives of the Research.....	4
1.3 Scope and Limitation of the Research.....	4
1.4 Output of the Research.....	5
1.5 References.....	5
<b>II KINETIC STUDY OF LACTIC ACID ESTERIFICATION.....</b>	<b>7</b>
2.1 Abstract.....	7
2.2 Introduction.....	8
2.3 Literature Review.....	9

## TABLE OF CONTENTS (Continued)

	<b>Page</b>
2.4 Theory.....	13
2.4.1 Esterification Reaction.....	13
2.4.2 Equilibrium .....	15
2.4.2.1 Vapor-Liquid Equilibrium.....	15
2.4.3 Thermodynamic Models .....	18
2.4.3.1 The Universal Quasi-Chemical (UNIQUAC) Model.....	18
2.4.3.2 The Universal Functional Activity Coefficient (UNIFAC) Model.....	21
2.5 Procedures.....	24
2.5.1 Chemicals.....	24
2.5.2 Experimental Procedure.....	24
2.5.2.1 Preparation of Magnesium Lactate Solution Study.....	24
2.5.2.2 Preparation of Magnesium Lactate Solution .....	24
2.5.2.3 Kinetic Study of Esterification.....	25
2.5.3 Analysis of the Compositions.....	25
2.5.3.1 Gas Chromatography (GC) Analysis of Ethyl Lactate .....	25



## TABLE OF CONTENTS (Continued)

	<b>Page</b>
3.4.3 DSTWU model.....	81
3.4.4 RADFRAC model.....	83
3.5 Methodology.....	84
3.5.1 Phase Equilibrium and Kinetic Modeling.....	85
3.5.2 Simulation and Optimization.....	86
3.6 Results and Discussion.....	87
3.6.1 Process A Configuration.....	88
3.6.1.1 Reactive Distillation Column, RD.....	89
3.6.1.2 First Fractional Distillation Column, DIS1.....	99
3.6.1.3 Reactive Distillation Column and First Fraction Distillation with Recycle Stream.....	101
3.6.1.4 Second Fractional Distillation Column, DIS2.....	106
3.6.1.5 Last Fractional Distillation Column, DIS3.....	108
3.6.2 Process B Configuration.....	114
3.6.2.1 Reactive Distillation Column, RD.....	115
3.6.2.2 First Fractional Distillation Column, DIS1.....	124
3.6.2.3 Second Fractional Distillation Column, DIS2.....	127
3.6.2.4 Process B with Recycle Stream.....	129

## TABLE OF CONTENTS (Continued)

	<b>Page</b>
3.7	Conclusions.....141
3.8	References.....142
<b>IV</b>	<b>PRELIMINARY PRODUCTION COST</b>
	<b>ESTIMATATION.....145</b>
4.1	Abstract.....145
4.2	Introduction.....146
4.3	Literature Reviews.....147
4.4	Theory.....155
4.4.1	Capital Cost.....155
	4.4.1.1 Fixed Capital Investment.....155
	4.4.1.2 Working Capital Investment.....156
	4.4.1.3 Estimation of Capital Investment.....157
	4.4.1.4 Purchased Equipment Cost.....159
4.4.2	Operating Cost.....159
	4.4.2.1 Raw Material Cost.....160
	4.4.2.2 Utilities Cost.....160
4.4.3	Production Cost.....161
4.5	Methodology.....162
4.6	Results and Discussions.....163
4.6.1	Capital Cost.....163

## TABLE OF CONTENTS (Continued)

	<b>Page</b>
4.6.1.1 Equipment Purchased Cost.....	163
4.6.1.1.1 Column Purchased Cost.....	164
4.6.1.1.2 Heat Exchanger Cost .....	166
4.6.1.2 Total Capital Cost.....	168
4.6.2 Operating Cost.....	170
4.6.2.1 Raw Material Cost.....	170
4.6.2.1.1 Magnesium Lactate Fermentation Cost .....	170
4.6.2.1.2 Other Raw Material Cost.....	173
4.6.2.2 Utilities Cost.....	174
4.6.3 Production Cost.....	179
4.7 Conclusions.....	181
4.8 References.....	182
<b>V CONCLUSIONS AND RECOMMENDATIONS.....</b>	<b>185</b>
5.1 Conclusions.....	185
5.2 Recommendations.....	187
 <b>APPENDICES</b>	
APPENDIX A      PROPERTIES OF ETHYL LACTATE AND MAGNESIUM LACTATE.....	188

## TABLE OF CONTENTS (Continued)

		<b>Page</b>
APPENDIX B	EXAMPLE OF CALCULATION FOR PREPARATION OF MAGNESIUM LACTATE SOLUTION .....	192
APPENDIX C	EXAMPLE OF COMPONENT ANALYSIS OF LACTIC ACID AND ETHYL LACTATE .....	194
APPENDIX D	LIQUID EQUILIBRIUM BY UNIQUAC AND UNIFAC MODELS IN MATLAB® .....	198
APPENDIX E	EXAMPLE OF CALCULATION OF CONSTANT IN ESTERIFICATION REACTION .....	220
APPENDIX F	EXAMPLE OF APSEN PLUS SIMULATOR .....	223
APPENDIX G	PRICE OF CHEMICAL AND CORRECTION FACTOR USED IN COST ESTIMATION .....	246
APPENDIX H	LIST OF PUBLICATIONS .....	253
BIOGRAPHY .....		261

## LIST OF TABLES

<b>Table</b>		<b>Page</b>
1.1	Example of solvent applications.....	1
2.1	Composition of lactic acid and its oligomers in feed solution.....	10
2.2	Effect of molar quantity, concentration, and volume of sulfuric acid in acidification of magnesium lactate.....	26
2.3	UNIQUAC binary interaction parameters for the quaternary system of ethanol+water+ethyl lactate+lactic acid at 101.33 kPa, $\tau_{ij} = \exp\left(-\left(a_{ij} + b_{ij}T\right)/T\right)$ .....	30
2.4	UNIFAC group specifications.....	31
2.5	The Arrhenius parameters of magnesium lactate and commercial lactic acid esterification.....	37
2.6	Kinetic parameters of magnesium lactate esterification with ethanol.....	44
2.7	Kinetic parameters of commercial lactic acid esterification with ethanol.....	45
2.8	Experimental and calculated reaction rate constant of magnesium lactate esterification.....	54
2.9	Experimental and calculated reaction rate constant of commercial lactic acid esterification.....	54
2.10	Effect of magnesium sulfate on the reaction kinetics parameters of commercial lactic acid esterification with ethanol.....	60

## LIST OF TABLES (Continued)

<b>Table</b>		<b>Page</b>
3.1	Composition and molar flow rate of feed streams.....	87
3.2	Initial specification of reactive distillation column in Process A.....	90
3.3	Stream composition of reactive distillation column in Process A.....	99
3.4	Specification of DIS1 column in Process A from DSTWU model.....	100
3.5	Stream composition in Process A with reactive distillation column and first fractional distillation column with ethanol recycle.....	106
3.6	Specification of DIS2 column in Process A from DSTWU model.....	107
3.7	Stream composition obtained from optimization of column DIS2.....	108
3.8	Specification of DIS3 column in Process A from DSTWU model.....	109
3.9	Composition of each stream in Process A.....	112
3.10	Unit operation specification in Process A.....	113
3.11	Heat duty of each unit in Process A.....	113
3.12	Initial specification of reactive distillation column in Process B.....	116
3.13	Stream composition of reactive distillation column in Process B.....	124
3.14	Specification of DIS1 column in Process B from DSTWU model.....	125
3.15	Stream compositions of DIS1 column of Process B.....	126
3.16	Specification of DIS2 column in Process B from DSTWU model.....	128
3.17	Stream compositions of DIS2 column of Process B.....	129
3.18	Stream compositions of the process with ethanol recycle operating under the optimal conditions of each column.....	130

## LIST OF TABLES (Continued)

<b>Table</b>	<b>Page</b>
3.19 Highest recovery of ethanol in stream ET at each total number of stages.....	133
3.20 Composition of each stream in Process B.....	139
3.21 Unit operation specification of Process B.....	141
3.22 Heat duty of operating unit in Process B.....	141
4.1 Expenses related to the fixed capital investment.....	156
4.2 Ratio factors for estimating capital investment items based on purchased equipment cost.....	158
4.3 Examples of operating cost.....	160
4.4 Summary of the production cost.....	162
4.5 Column costs of Process A.....	165
4.6 Column costs of Process B.....	165
4.7 Heat exchanger cost of Process A.....	168
4.8 Heat exchanger cost of Process B.....	168
4.9 Total equipment purchased cost of Process A and Process B.....	168
4.10 Total capital cost of Process A and Process B.....	169
4.11 Original composition of culture media broth.....	171
4.12 Price of MRS culture broth with different carbon sources.....	172
4.13 Costs of magnesium lactate fermentation based on 50 L of fermentation broth per day.....	173

## LIST OF TABLES (Continued)

Table	Page
4.14 Raw material costs of ethyl lactate production from fermentation-derived magnesium lactate process .....	174
4.15 Energy content of different fuels .....	175
4.16 Price of different energy sources .....	175
4.17 Quantities and cost of energy required in Process A .....	177
4.18 Quantities and cost of energy required in Process B .....	178
4.19 Annual production cost of Process A and Process B .....	180
4.20 Ethyl lactate production cost of Process A and B .....	181
A.1 Physical and chemical properties of ethyl lactate .....	190
A.2 Physical and chemical properties of magnesium lactate .....	191
F.1 Composition and molar flow rate of each component in fermentation-derived magnesium lactate solution .....	225
F.2 Molar flow rate and mole fraction of feed stream F1 .....	225
F.3 Arrhenius's parameter of reaction obtained from UNIQUAC model .....	226
G.1 Price of chemicals in culture media .....	247
G.2 Price of culture media with original Sigma Aldrich formula .....	248
G.3 Price of culture media with original Neogen formula .....	248
G.4 Price of culture media with Sigma Aldrich formula which was applied with cassava starch .....	249

## LIST OF TABLES (Continued)

<b>Table</b>		<b>Page</b>
G.5	Price of culture media with Neogen formula which was applied with cassava starch.....	249
G.6	Price of other raw material.....	250
G.7	Pressure correction factors of column.....	250
G.8	Material correction factor of column.....	250
G.9	Correction factors for column trays.....	251
G.10	Material factors of heat exchanger.....	251
G.11	Correction factors for pressure of heat exchanger.....	251
G.12	Correction factors for type of heat exchanger.....	251

## LIST OF FIGURES

Figure	Page
1.1	Molecular structure of ethyl lactate .....2
2.1	Effect of sulfuric acid molar quantity to mole of lactic acid dissolved in acidification of magnesium lactate .....27
2.2	Effect of sulfuric acid concentration to mole of lactic acid dissolved in acidification of magnesium lactate .....28
2.3	Magnesium lactate solution which acidify by various sulfuric acid concentrations; (a) Magnesium lactate solution before evaporation; (b) Magnesium lactate solution after partially water removed .....29
2.4	Effect of reaction temperature on conversion of lactic acid in esterification of (a) magnesium lactate, (b) commercial lactic acid with the UNIQUAC model .....34
2.5	Effect of reaction temperature on conversion of lactic acid in esterification of (a) magnesium lactate, (b) commercial lactic acid with the UNIFAC model .....35
2.6	Arrhenius plots of (a) UNIQUAC Model and (b) UNIFAC Model .....36
2.7	Effect of initial ethanol-to-lactic acid molar ratio on conversion of lactic acid in esterification of (a) magnesium lactate, (b) commercial lactic acid with the UNIQUAC model .....39

## LIST OF FIGURE (Continued)

Figure	Page
2.8	Effect of initial ethanol-to-lactic acid molar ratio on conversion of lactic acid in esterification of (a) magnesium lactate, (b) commercial lactic acid with the UNIFAC model..... 40
2.9	Effect of catalyst loading on conversion of lactic acid in esterification of (a) magnesium lactate, (b) commercial lactic acid with the UNIQUAC model..... 42
2.10	Effect of catalyst loading on conversion of lactic acid in esterification of (a) magnesium lactate, (b) commercial lactic acid with the UNIFAC model..... 43
2.11	Plots between reaction rate constant and catalyst loading of (—●—) magnesium lactate and (--○--) commercial lactic acid esterification from UNIQUAC model..... 47
2.12	Plots between reaction rate constant combined effects of catalyst loading and initial molar ratio of ethanol-to-lactic acid of (—●—) magnesium lactate and (--○--) commercial lactic acid esterification..... 49
2.13	Plots between log k and reciprocal of the absolute temperature of (—●—) magnesium lactate and (--○--) commercial lactic acid esterification from UNIQUAC model..... 50

## LIST OF FIGURE (Continued)

Figure	Page
2.14 Plots between experimental and calculated reaction rate constant of magnesium lactate esterification for (a) UNIQUAC model and (b) UNIFAC model.....	56
2.15 Plots between experimental and calculated reaction rate constant of commercial lactic acid esterification for (a) UNIQUAC model and (b) UNIFAC model.....	57
2.16 Effect of magnesium sulfate concentration on reaction conversion for esterification of commercial lactic acid with ethanol.....	59
3.1 Flow sheet of ethyl acetate production process.....	70
3.2 Process flow diagram for the recovery of lactic.....	71
3.3 The process scheme for a reaction sequence $A + B \rightleftharpoons D + C$ .....	75
3.4 Schematic for counter-current vapor-liquid contacting in tray column.....	76
3.5 Schematic for counter-current vapor-liquid contacting in packed column.....	76
3.6 The shape of packing of catalyst pellets.....	77
3.7 Multi-stage reactive distillation column configurations.....	78
3.8 Process flow sheet of Process A.....	88
3.9 Effect of total number of stages of reactive distillation column in Process A on (●) conversion of lactic acid; (○) recovery of ethyl lactate; (▼) yield of ethyl lactate.....	91

## LIST OF FIGURE (Continued)

Figure	Page
3.10 Effect of molar distillate rate of reactive distillation column in Process A on (●) conversion of lactic acid; (○) recovery of ethyl lactate; (▼) yield of ethyl lactate .....	92
3.11 Effect of reflux ratio of reactive distillation column in Process A on (●) conversion of lactic acid; (○) recovery of ethyl lactate; (▼) yield of ethyl lactate .....	93
3.12 Influence of the distillate rate and reflux ratio of reactive distillation column in Process A on yield of ethyl lactate .....	94
3.13 Sensitivity analysis of (a) effect of tray diameter and (b) effect of tray spacing on (●) conversion of lactic acid; (○) recovery of ethyl lactate; (▼) yield of ethyl lactate in reactive distillation column of Process A .....	96
3.14 Influence of feed stage on yield of ethyl lactate in reactive distillation column of Process A .....	97
3.15 Influence of feed temperature on yield of ethyl lactate in reactive distillation column of Process A .....	98
3.16 Process schematic for operation of reactive distillation column and fractional distillation column DIS1 with recycle stream .....	101
3.17 Liquid phase molar composition in reactive distillation of Process A .....	103
3.18 Temperature profile of reactive distillation column of Process A; (●) liquid phase temperature and (○) vapor phase temperature .....	104

## LIST OF FIGURE (Continued)

Figure	Page
3.19 Molar ratio of ethanol-to-lactic acid profile in the reactive distillation column in Process A.....	105
3.20 Process flow sheet of Process A with optimal conditions.....	111
3.21 Process flow sheet of Process B.....	114
3.22 Influence of total number of stages of the reactive distillation column on (●) conversion of lactic acid; (○) recovery of ethyl lactate; (▼) yield of ethyl lactate.....	117
3.23 Influence of total number of stages of reactive distillation column in Process B on molar flow rate of ethanol in its bottom product stream.....	117
3.24 Influence of bottom rate of reactive distillation column on in Process B on (●) conversion of lactic acid; (○) recovery of ethyl lactate; (▼) yield of ethyl lactate.....	118
3.25 Influence of reflux ratio of reactive distillation column in Process B on (●) conversion of lactic acid; (○) recovery of ethyl lactate; (▼) yield of ethyl lactate.....	119
3.26 Influence of bottom rate and reflux ratio of reactive distillation column in Process B on yield of ethyl lactate.....	120
3.27 Influence of feed location of reactive distillation column in Process B on yield of ethyl lactate.....	121

## LIST OF FIGURE (Continued)

Figure	Page
3.28	Influence of feed temperature of reactive distillation column in Process B on yield of ethyl lactate.....122
3.29	Influence of the tray diameter and tray spacing of reactive distillation column on yield of ethyl lactate.....123
3.30	Liquid phase composition of reactive distillation column in Process B.....135
3.31	Temperature profile of reactive distillation column of Process B; (●) liquid phase temperature and (○) vapor phase temperature.....136
3.32	Molar ratio of ethanol-to-lactic acid profile in the reactive distillation column in Process B.....136
3.33	Process flow sheet of Process B with optimal conditions.....138
4.1	Process scheme of lactic acid production.....148
4.2	Process flow diagram of biodiesel production process.....150
4.3	Schematic diagrams of n-butyl acetate production system.....151
4.4	Process schematic for 95% pure lactic acid production.....153
4.5	Flowchart of supercritical methanol process.....154
A.1	Structural formula of ethyl lactate.....189
A.2	Structural formula of magnesium lactate.....190
C.1	Calibration standard curve of lactic acid.....195
C.2	Calibration standard curve of ethyl lactate.....195
C.3	Chromatogram of lactic acid from HPLC.....196

## LIST OF FIGURE (Continued)

<b>Figure</b>	<b>Page</b>
C.4 Chromatogram of ethyl lactate from GC.....	197
D.1 Flowchart of non-linear least square combined with ode45.....	200
F.1 Aspen Plus startup window.....	227
F.2 Properties window.....	228
F.3 Find components.....	229
F.4 All component specification.....	229
F.5 Next Input button in the toolbar.....	230
F.6 Thermodynamic method specification.....	230
F.7 Binary interaction parameter of UNIQUAC model input.....	231
F.8 Details of process flow sheet window.....	232
F.9 Selection of unit operation.....	233
F.10 Adding streams to the column.....	234
F.11 Feed stream details input.....	235
F.12 Reactive distillation column setup.....	236
F.13 Section of reaction in reactive distillation column.....	236
F.14 Tray specification.....	237
F.15 Reaction specification.....	237
F.16 Control Panel.....	238
F.17 Streams result of simulation.....	239
F.18 Selecting manipulated variable in sensitivity analysis.....	239

## LIST OF FIGURE (Continued)

<b>Figure</b>	<b>Page</b>
F.19 Define variable to be studied in the sensitivity analysis.....	240
F.20 Input variable to table result.....	240
F.21 FORTRAN statements input.....	241
F.22 Sensitivity result.....	241
F.23 Identify flowsheet variables in optimization.....	242
F.24 Identify objective function in optimization.....	242
F.25 Selecting manipulated variable in optimization.....	243
F.26 Results of flowsheet variables in optimization.....	244
F.27 Objective function value in optimization.....	244
F.28 Optimal manipulated variables in optimization.....	245

## SYMBOLS AND ABBREVIATIONS

$a_i$	=	Activity of component i
A	=	Area of heat exchanger, ft <sup>2</sup>
$A_0$	=	Pre-exponential factor or frequency factor, s <sup>-1</sup>
B	=	Bottom rate, kmol hr <sup>-1</sup>
BP	=	Bottom product stream
C	=	Catalyst loading
$C_2H_5^-$	=	Ethyl ion
$C_3H_5O_3^-$	=	Lactate ion
$C_i$	=	Concentration of component i, mol L <sup>-1</sup>
D	=	Column diameter, ft
DIS1	=	The first fractional distillation column
DIS2	=	The second fractional distillation column
DIS3	=	The third fractional distillation column
DR	=	Distillate rate, kmol hr <sup>-1</sup>
E/L	=	Initial molar ratio of ethanol to lactic acid
EtLA	=	Ethyl lactate
EtOH	=	Ethanol
$E_A$	=	Activation energy, J mol <sup>-1</sup>
f	=	Fugacity
F	=	Feed molar flow rate, mol h <sup>-1</sup>

## SYMBOLS AND ABBREVIATIONS (Continued)

$F_c$	=	Correction factor
$F_d$	=	Design type of heat exchanger correction factor
$F_m$	=	Material correction factor
$F_p$	=	Pressure correction factor
$F_s$	=	Tray spacing correction factor
$F_t$	=	Tray type correction factor
F1	=	Fresh feed stream 1
F2	=	Fresh feed stream 2
FM1	=	Feed stream 1
FM2	=	Feed stream 2
$g$	=	Partial Gibbs free energy
$H$	=	Enthalpy, $\text{J mol}^{-1}$
$\text{H}^+$	=	Hydrogen ion
$\text{H}_2\text{SO}_4$	=	Sulfuric acid
HEAT1	=	First heat exchanger
HEAT2	=	Second heat exchanger
HI	=	Column height, ft
$k$	=	Reaction rate constant, $\text{s}^{-1}$
$k_1$	=	Forward reaction rate constant, $\text{s}^{-1}$
$k_{-1}$	=	Backward reaction rate constant, $\text{s}^{-1}$
$K$	=	K-value

## SYMBOLS AND ABBREVIATIONS (Continued)

Ke	=	Equilibrium constant
L	=	Liquid molar flow rate, mol h <sup>-1</sup>
LA	=	Lactic acid
LD	=	Liquid molar flow rate from condenser, mol h <sup>-1</sup>
m	=	Initial molar ratio of ethanol to lactic acid
M	=	Molar concentration, mol L <sup>-1</sup>
M1	=	Mixing stream 1
Mg <sup>2+</sup>	=	Magnesium (II) ion
MgLA <sub>2</sub>	=	Magnesium lactate
MgSO <sub>4</sub>	=	Magnesium sulfate
MgCO <sub>3</sub>	=	Magnesium carbonate
MIX1	=	Mixer
M&S	=	Marshall and Swift index
n	=	Initial molar ratio of water to lactic acid
N	=	Number of stage
P	=	Total pressure
q	=	Surface area parameter
q <sub>F</sub>	=	Mole of saturated liquid on the feed tray per mole feed
Q	=	heat duty, J h <sup>-1</sup>
Q <sub>k</sub>	=	Area parameter of functional group k
r	=	Volume parameter
r <sub>ji</sub>	=	Reaction rate of component i in stage j

## SYMBOLS AND ABBREVIATIONS (Continued)

$-r_{LA}$	=	Reaction rate of lactic acid, $s^{-1}$
R	=	Universal gas constant
$R_k$	=	Volume parameter of functional group k
$R^2$	=	Coefficient of determination
RD	=	Reactive distillation column
RE	=	Recovery of ethyl lactate
RES1	=	Residual stream 1
RES2	=	Residual stream 2
RR	=	Reflux ratio
S1	=	Stream 1
S2	=	Stream 2
$SS_{err}$	=	Sum of squared error
$SS_{tot}$	=	Total sum of squared error
t	=	Time, s
T	=	Absolute temperature
THB	=	Thai Baht
TP	=	Top product stream
U	=	Overall heat transfer coefficient, $Btu\ hr^{-1}\ ^\circ F^{-1}\ ft^{-2}$
$U_j$	=	Liquid holdup on stage j, mol
USD	=	United State Dollar
V	=	Vapor molar flow rate, $kmol\ hr^{-1}$

## SYMBOLS AND ABBREVIATIONS (Continued)

$w$	=	Weight
$W$	=	Water
$x$	=	Mole fraction in liquid phase
$X$	=	Conversion
$\bar{X}$	=	Average value of conversion
$y$	=	Mole fraction in vapor phase
$Y$	=	Yield of ethyl lactate
$z$	=	Coordination number
$z_i$	=	Mole fraction of component $i$ in feed

### Greek Symbols

$X$	=	Mole fraction of group $m$ in mixture
$\Delta$	=	Differential
$\Phi^*$	=	Segment fraction
$\Gamma$	=	Group residual activity coefficient
$\Theta_m$	=	Area fraction of group $m$
$\Psi_{mn}$	=	Group interaction parameter
$\alpha$	=	Relative volatility
$\gamma$	=	Activity coefficient
$\varphi$	=	Fugacity coefficient
$\nu_k$	=	Number of functional group of type $k$ in molecule $i$

## SYMBOLS AND ABBREVIATIONS (Continued)

$\theta^*$	=	Poynting correction factor
$\theta$	=	Area fraction
$\tau_{ij}$	=	Interaction parameter of component i and j

### Subscripts

0	=	Initial condition
A	=	Process A
B	=	Process B
BP	=	Bottom product
C	=	Condenser
Cal	=	Calculated
D	=	Distillate
D1	=	DIS1 column
D2	=	DIS2 column
e	=	Equilibrium state
EtLA	=	Ethyl lactate
EtOH	=	Ethanol
Exp	=	Experimental
HK	=	Heavy key component
i	=	Component i
j	=	Component j or number of stage j

## SYMBOLS AND ABBREVIATIONS (Continued)

k	=	Functional group k
LA	=	Lactic acid
LK	=	Light key component
min	=	Minimum
M	=	Number of component
N	=	Number of stage
r	=	Reaction
RD	=	Reactive distillation column
W	=	Water
<b>Superscripts</b>		
*	=	Reference stage, Saturated
C	=	Combinatorial part
E	=	Excess property
F	=	Feed
i	=	Component i
l	=	Liquid phase
R	=	Residual part
v	=	Vapor phase

# CHAPTER I

## INTRODUCTION

### 1.1 Background and Significance of the Problem

Generally definition of solvent is any substance that dissolves another substance so that the resulting mixture is a homogeneous solution. This is the most widespread class of chemicals in household and chemical industries. It has been used for thousand years in separation and extraction procedures as well as cleaning solvents (Anastas, 2002). Some applications of solvents are shown in Table 1.1.

**Table 1.1** Example of solvent applications (Kerton, 2009).

Application	Description
Solvent extraction	In wastewater treatment or a degreaser and cleaning agent To recover natural products from plants or from fermentation liquors
Organic chemistry	As a reaction medium and diluents in separations and purification As a dehydrator (also in materials chemistry)
Polymer and materials chemistry	As a binder to achieve cohesiveness in composite materials Production of powders, coatings, films, etc.
Household and others	Fuels, lubricants, paints, varnishes, adhesives, dyes, etc. Antifreeze, Cleaning fluids Emulsions within cosmetics and pharmaceuticals

Common industrial solvents that widely used in products and processes include chloroform, carbon tetrachloride, benzene, xylene, toluene, acetone, methyl ethyl ketone etc. Most solvents inherit some hazard such as flammability, explosive, toxicity, stratospheric ozone depletion and atmospheric ozone depletion as well as global warming potential (Anastas, 2002). Green solvents, therefore, have gained more attention in the search for alternative safer chemicals.

Green solvent is one application of green chemistry. The idea of “green” solvents expresses the goal to minimize the environmental impact resulting from the use of solvents in chemical production. It can reduce or eliminate the intrinsic hazard of traditional solvent. Green solvent is biodegradable and renewable. There are many alternative green solvents such as aqueous solvents, supercritical carbon dioxide (ScCO<sub>2</sub>), glycerol carbonate, 2-Methyltetrahydrofuran (2-MeTHF), cyclopentyl methyl ether (CPME), as well as fatty acid ester. (Anastas et al., 2000, Anastas, 2002 and Kerton, 2009).

Ethyl lactate is one of important esters in lactate ester family. It is also known as lactic acid ethyl ester or IUPAC name: Ethyl (S)-2-hydroxypropanoate. The molecular formula of ethyl lactate is C<sub>5</sub>H<sub>10</sub>O<sub>3</sub> and its molecular structure is shown in Figure 1.1.

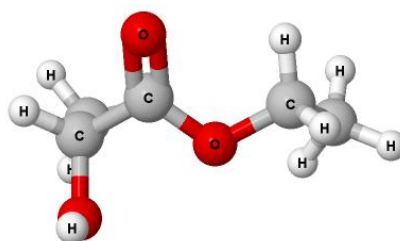


**Figure 1.1** Molecular structure of ethyl lactate.

Ethyl lactate can be considered as green solvent due to its nontoxic, biodegradable, renewable as well as excellent solvent properties. It is clear to slightly yellow liquid with fruit-like odor. It can be used in many industries such as pharmaceutical, fragrances and also as coating (Asthana et al., 2005 and Pereira et al., 2011). In addition, ethyl lactate has been approved by USA Food and Drug Administration (FDA) to be used as additives in food products (Aparicio and Alcalde, 2009). The major advantages of ethyl lactate are listed as follows:

- 100% Biodegradable
- Renewable-made from corn and other carbohydrates
- Non carcinogenic
- Non corrosive
- Stable in solvent formulations until exposed to water
- High solvency power for resins, polymers and dyes
- Rinses easily with water
- High boiling point
- Low vapor pressure and low VOC
- Not an ozone depleting chemical
- Easy and inexpensive to recycle

The demand of ethyl lactate is about 150 billion pound per year and tends to increase in the future. It is normally sold for 60 to 150 baht per kilogram depending on its quality (Jones et al., 2003). In order to obtain lower price of ethyl lactate, therefore the alternative productions of the ethyl lactate are interesting. Ethyl lactate can be produced either by esterification of lactic acid with ethanol or combination of acetaldehyde with hydrogen cyanide to form acetaldehyde cyanohydrin, which is

converted into ethyl lactate by treatment with ethanol and an inorganic acid (Lewix, 2007). The second method is quite complicated thus ethyl lactate is normally produced by esterification of high-purity of lactic acid with ethanol. However, this method is expensive due to high cost of lactic acid separation and purification processes, which have been estimated to be about 50% of total production cost of ethyl lactate (Pereira et al., 2011). Therefore, synthesis of ethyl lactate directly from a fermentation-derived lactate salt might help decreasing the production cost since several pre-treatment, separation and purification steps can be omitted resulting in the process with fewer operating units and shorter processing time (Filachione and Costello, 1952 and Kasinathan et al., 2010).

## **1.2 Objectives of the Research**

The objectives of this research are to study the kinetics of fermentation-derived magnesium lactate esterification with ethanol catalyzed by sulfuric acid and to investigate feasibility of ethyl lactate production from the fermentation-derived magnesium lactate via reactive distillation process as well as to perform cost analysis of such production.

## **1.3 Scope and Limitation of the Research**

1.3.1 Study kinetics of sulfuric acid-catalyzed esterification between ethanol and acidified fermentation-derived magnesium lactate.

1.3.2 Perform conceptual design and cost analysis of reactive distillation for ethyl lactate production from fermentation-derived magnesium lactate.

## 1.4 Output of the Research

1.4.1 Kinetics data for esterification between ethanol and lactic acid obtained from fermentation-derived magnesium lactate.

1.4.2 Preliminary cost analysis for ethyl lactate production from fermentation-derived magnesium lactate.

## 1.5 References

Anastas, P.T. (2002). Green chemistry as applied to solvents. **American Chemical Society**. Washington, DC.

Anastas, P.T., Heine, L.G., and Williamson, T.C. (2000). Green chemical syntheses and processes: Introduction. **American Chemical Society**. Washington, DC.

Aparicio, S. and Alcalde, R. (2009). The green solvent ethyl lactate: an experimental and theoretical characterization. **Green Chemistry**. 11: 65-78.

Asthana, N., Kolah, A., Vu, D.T., Lira, C.T., and Miller, D.J. (2005). A continuous reactive separation process for ethyl lactate formation. **Organic Process Research and Development**. 9: 599-607.

Filachione, E.M. and Costello, E.J. (1952). Lactic esters by reaction of ammonium lactate with alcohols. **Industrial and Engineering Chemistry**. 44: 2189-2191.

Jones, J., Pham, T., Smart, K., Splinter, D., and Steele, M. (2003). Ethyl lactate production. <http://www.ou.edu/>.

Kasinathan, P., Kwak, H., Lee, U., Kwang, D.W., Hwang, Y.K., Chang, J. (2010). Synthesis of ethyl lactate from ammonium lactate solution by coupling solvent extraction with esterification. **Separation and Purification Technology**. 76: 1-7.

Kerton, F.M. (2009). **Alternative Solvents for Green Chemistry**. Cambridge, UK.

Lewis, R.J. (2007). **Hawley's Condensed Chemical Dictionary** (15th ed.). John Wiley & Sons.

Pereira, C.S.M., Silva, V.M.T.M, and Rodrigues, A.E. (2011). Ethyl lactate as a solvent: Properties, applications and production processes – a review. **Green Chemistry**. 13: 2658-2671.



## CHAPTER II

### KINETIC STUDY OF LACTIC ACID ESTERIFICATION

#### 2.1 Abstract

In this chapter, procedure for preparation of lactic acid solution by acidification of magnesium lactate powder with sulfuric acid and optimal concentration and quantity of sulfuric acid on acidification were established. Kinetics of magnesium lactate solution esterification with ethanol was investigated by using sulfuric acid as homogeneous catalyst. Effects of reaction temperature, initial molar ratio of ethanol-to-lactic acid, and catalyst loading on the conversion of lactic acid were investigated. Reaction rate constant and equilibrium constant were determined with activity coefficients of all the components predicted by UNIQUAC and UNIFAC model. As the same process conditions, kinetic parameters from two esterification systems were compared. The parameters obtained from magnesium lactate esterification were lower than those obtained from esterification of lactic acid. This result may be due to a present of magnesium sulfate in magnesium lactate solution. Correlation between reaction rate constant and all process variables were established. Good agreement between experimental and calculated reaction rate constant was obtained especially in experiments with high initial molar ratio of ethanol-to-lactic acid. Moreover, effect of magnesium sulfate, a major impurity of this process, on kinetics of the reaction was studied with system of commercial high-purity lactic acid esterification and found that increasing of salt quantity decreased kinetic parameters.

## 2.2 Introduction

In recent years, environment benign chemicals synthesis has been gained more interest because the fossil based chemicals have many hazards and pollutions. One of attractive environmental benign solvent is ethyl lactate, also known as lactic acid ethyl ester. It is nontoxic, biodegradable, and excellent solvent properties (Asthana et al., 2005). The conventional ethyl lactate production is esterification of lactic acid with ethanol which catalyzed by acid catalyst. Nevertheless, this production is expensive due to the cost of separation and purifying of lactic acid. Using direct lactate salts as a reactant is one of alternative ways to reduce the ethyl lactate production cost since lactic acid purifying step can be excluded (Filachione and Costello, 1952). The interesting method is esterification of fermentation-derived magnesium lactate with ethanol which magnesium lactate directly obtained from lactic acid production.

There are several studies concerned mechanism and kinetics of esterification between commercially high-purity lactic acid and ethanol. Many kinetic information and kinetic variables of this system are reported. Important parameters that influence the reaction kinetics are temperature, initial molar ratio of reactants and amount of catalyst loading.

However, the kinetics of lactic acid esterification in a presence of salts has not been studied before. Therefore, it is important to study the kinetic of magnesium lactate esterification for understanding the impact of key variables to this reaction.

## 2.3 Literature Review

There are several kinetics studies of esterification of lactic acid with alcohol. Troupe and DiMilla (1957) investigated the esterification reaction between lactic acid and ethanol using sulfuric acid as homogeneous catalyst. Lactic acid with different purity, i.e. 85 and 44 w/w%, was used as the feed of the reaction carried out in a sealed tube. In addition, they developed rate equation of this system to use in a flow reactor. Effect of reaction temperature, amount of catalyst loading, and initial reactant molar ratio were examined. It was found that temperature and catalyst loading did not have great effect on equilibrium constant of the reaction but the initial reactant molar ratio did. A relationship between reaction rate constant and involved parameters was also established.

Zhang et al. (2004) studied the kinetics of lactic acid esterification with ethanol catalyzed by cation-exchange resins. Five different types of cation-exchange resin were used. Effects of catalyst type, catalyst loading, and temperature on the reaction kinetics were investigated. It was found that the equilibrium constant of this reaction nearly did not change with increase of catalyst loading. However, the time required to reach reaction equilibrium was reduced as the catalyst loading increased. They found that 002 and NKC type catalysts have the highest activity. Moreover, Langmuir-Hinshelwood model was applied in this study and it is indicated that ethanol and water adsorbed much stronger than lactic acid and ethyl lactate.

Asthana et al. (2006) studied kinetics of esterification of lactic acid and its oligomers with ethanol over Amberlyst 15 cation-exchange resin in batch reactor. They suggested that, at concentrations of more than 20 w/w% lactic acid in water, the acid could undergo oligomerization to form a linear oligomer acid, which was

believed to adversely affect ethyl lactate yield in the reaction. Different starting concentration of lactic acid solutions, 20 w/w%, 50 w/w%, and 88 w/w%, reaction temperature and catalyst loading were used to investigate the reaction kinetic. In addition, compositions of different lactic acid concentrations are tabulated in Table 2.1. They found that lactic acid conversion and reaction rate were directly dependent on reaction temperature, initial feed molar ratio and the catalyst loading. Reversible  $n^{\text{th}}$ -order rate expression for esterification and oligomerization reaction was fitted with experimental data, and the results were in good agreement over a wide range of reaction conditions. It appeared that predicting the reaction with starting lactic acid concentration of 88 w/w% required a more-complex model than that with 20 w/w% and 50 w/w% lactic acid solutions, which might be due to the presence of acid oligomers.

**Table 2.1** Composition of lactic acid and its oligomers in feed solution.

Parameter	Feed Designation (Nominal)		
	20 w/w% lactic acid	50 w/w% lactic acid	88 w/w% lactic acid
Feed component			
LA1	23 w/w% (5.6 mol%)	46 w/w% (15.2 mol%)	58 w/w% (43.5 mol%)
LA2		3 w/w% (0.5 mol%)	22 w/w% (9.2 mol%)
LA3			6 w/w% (1.8 mol%)
LA4			2 w/w% (0.4 mol%)
H <sub>2</sub> O	77 w/w% (94.4 mol%)	51 w/w% (84.3 mol%)	12 w/w% (45.1 mol%)

\*Where LA1 is monomer lactic acid, LA2-LA4 are linear oligomer acids

Delgado et al. (2007) studied the kinetics of lactic acid esterification with ethanol and ethyl lactate hydrolysis catalyzed by Amberlyst 15 cation-exchange resin in a stirred batch reactor using dilute solution of lactic acid (20 w/w% lactic acid) to avoid the presence of lactic acid oligomers. Effect of reaction temperature, catalyst loading, and initial reactant molar ratio were studied. The reaction rate was found to increase with temperature and catalyst loading while the equilibrium conversion was found to increase with the initial reactant molar ratio. Pseudo-homogeneous model and Langmuir-Hinshelwood model were correlated with the kinetic experimental data. It was observed that water was the most strongly adsorbed molecule, followed by ethanol, lactic acid and ethyl lactate. Both models gave a good agreement with the experimental data.

In addition, Pereira et al. (2008) investigated thermodynamic equilibrium and reaction kinetics for esterification of lactic acid (88 w/w%) with ethanol catalyzed by the Amberlyst 15-wet in batch reactor. Concentrated lactic acid solution was used in order to increase yield of the reaction. Presence of the acid oligomers was neglected because of percentages of lactic acid and ethyl lactate oligomers were less than 5% at equilibrium. Langmuir-Hinshelwood model was used to describe the mechanism of the reaction. Good agreement between experiment and numerical simulation was achieved, and it was concluded that the most polar molecule, water and alcohol, have the strongest adsorption strength on the surface of Amberlyst 15.

Chooklin et al. (2009) studied the effect of ethanol concentration (90 w/w%, 95 w/w%, and 99.7 w/w%) on lactic acid conversion and ethyl lactate selectivity based on other products. Lactic acid solution with 88 w/w% concentration was used as the starting feed, and Amberlyst 15 was the catalyst. The reaction was carried out

in a semi-batch catalytic distillation. They found that increasing ethanol concentration led to increase conversion and selectivity of the ethyl lactate as well as the weight percentage of unknown component from the oligomerization of the concentrated lactic acid. Because of decreasing water content in ethanol solution, adsorption of water on the catalyst surface was reduced.

In addition, the esterification of lactate salt that directly obtained from lactic acid production, such as ammonium lactate, has been investigated. In 1952, Filachione and Costello studied the production of lactic esters by reaction of ammonium lactate with various alcohols. They observed that primary alcohols have higher conversion to ester than secondary alcohols did. Moreover, they found that high boiling point of primary alcohol gave the highest conversion to lactic ester, 73% to 75%, and conversion to ammonia was usually 80% or higher. They found that the reaction proceeded through dissociation of the ammonium lactate to ammonia and lactic acid and that the latter undergoes esterification with n-butanol. They investigated that increasing n-butanol to ammonium lactate ratio increased the formation of butyl lactate. Catalyst, such as boric acid, trihexylamine, basic aluminum acetate, as well as silica gel, helped reducing the reaction time by approximately one half but did not greatly affect the conversion. Furthermore the yield of lactic ester increased if the by-products of the reaction were recycled.

Kasinathan et al. (2010) synthesized ethyl lactate from aqueous ammonium lactate solution by coupling solvent extraction with esterification. They found that when ammonium lactate reacted directly with ethanol without solvent, the ethyl lactate yield was quite low because of the formation of oligomer and lactamide in the process. They approved ethyl lactate yield by using lactic acid solution, which was

extracted from ammonium lactate with solvents. They found that tributyl phosphate, used as the solvent in salt slitting technique of lactic acid, gave the highest ethyl lactate yield.

## 2.4 Theory

### 2.4.1 Esterification Reaction

Esterification is a reaction between carboxylic acid (R-COOH) and alcohol (R-OH) to form an ester and water as the reaction products. This reaction is reversible, and the reaction conversion is generally limited by chemical equilibrium. To enhance the equilibrium conversion of the reaction, Le Chatelier's principle was used. This is normally done by using an excess amount of one of the reactants or continuously removing one of the products from the reaction mixture (Kumar and Mahajani, 2007). In addition, catalysts are always used to enhance the reaction rate.

The esterification of lactic acid (LA) with ethanol (EtOH) to produce ethyl lactate (EtLA) and water (W) can be written as:



Reaction rate of lactic acid esterification with ethanol can be expressed in equation (2.2).

$$-r_{LA} = \frac{dX_{LA}}{dt} = k \left( C_{LA} C_{EtOH} - \frac{C_{EtLA} C_W}{Ke} \right) \quad (2.2)$$

where  $-r_{LA}$  is reaction rate of lactic acid,  $s^{-1}$ .

$C_i$  is concentration of component  $i$ ,  $molL^{-1}$ .

$k$  is reaction rate constant,  $s^{-1}$ .

$t$  is reaction time, s.

$Ke$  is equilibrium constant.

$X_{LA}$  is conversion of lactic acid which can be written as:

$$X_{LA} = \frac{C_{LA,0} - C_{LA}}{C_{LA,0}} \quad (2.3)$$

where  $C_{LA,0}$  is initial concentration of lactic acid,  $molL^{-1}$ .

$C_{LA}$  is concentration of lactic acid at time  $t$ ,  $molL^{-1}$ .

In order to account for the non-ideality of the solution, the reaction rate can be expressed in term of activity instead of concentration as in equation (2.4) and (2.5).

$$-r_{LA} = \frac{dX_{LA}}{dt} = k \left( a_{LA} a_{EtOH} - \frac{a_{EtLA} a_W}{Ke} \right) \quad (2.4)$$

$$Ke = \frac{a_{EtLA,e} a_{W,e}}{a_{EtOH,e} a_{LA,e}} = \left( \frac{x_{EtLA,e} x_{W,e}}{x_{EtOH,e} x_{LA,e}} \right) \left( \frac{\gamma_{EtLA,e} \gamma_{W,e}}{\gamma_{EtOH,e} \gamma_{LA,e}} \right) \quad (2.5)$$

where  $a_i$  is activity of component  $i$ .

$x_{i,e}$  is mole fraction of component  $i$  at equilibrium.

$\gamma_i$  and  $\gamma_{i,e}$  are activity coefficient and equilibrium activity coefficient of component  $i$ , respectively.

## 2.4.2 Equilibrium

The equilibrium is a word that mean to a static condition in which absence of change. In thermodynamics it means not only the absence of change but the absence of any tendency toward change on a macroscopic scale. Therefore, a system at equilibrium exists under conditions such that no change in state can occur. Because any tendency toward change is caused by a driving force of one kind or another, the absence of such a tendency indicates also the absence of any driving force. Hence for a system at equilibrium all forces are in exact balance. Whether a change actually occurs in a system not at equilibrium depends on resistance as well as one driving force. In many systems subject to appreciable driving forces change occurs at a negligible rate, because the resistance to change is very large (Smith et al., 2005).

### 2.4.2.1 Vapor-Liquid Equilibrium

Vapor-Liquid equilibrium (VLE) is the state of coexistence of liquid and vapor phased. Basic relationship for each component in vapor and liquid phase of the multicomponent system is the equality of fugacity in all phase.

$$f_i^v = f_i^l \quad (2.6)$$

where  $f_i^v$  and  $f_i^l$  are the fugacity of component  $i$  in the vapor phase and liquid phase, respectively.

The fugacities in vapor phase and liquid phase can be represented by measurable state variables by two methods: the equation-of-stage method and the activity-coefficient method.

The fugacity in vapor phase can be written as:

$$f_i^v = \phi_i^v y_i P \quad (2.7)$$

where  $\phi_i^v$  is vapor phase fugacity coefficient of component  $i$ .

$y_i$  is mole fraction of component  $i$  in the vapor phase.

$P$  is total system pressure.

For vapor phase at low to moderate pressure,  $\phi_i^v$  is close to unity. Thus, equation (2.7) can be reduced into:

$$f_i^v = y_i P \quad (2.8)$$

As for the liquid phase, in an ideal liquid solution system, the liquid fugacity of each component in the mixture is directly proportional to the mole fraction of the component as:

$$f_i^l = x_i f_i^{*,l} \quad (2.9)$$

where  $x_i$  is mole fraction of component  $i$  in the liquid phase.

$f_i^{*,l}$  is liquid phase reference fugacity of component  $i$ .

However, in the systems of non-ideal in liquid mixtures, liquid activity coefficient ( $\gamma_i$ ) can be used to represent the deviation of the mixture from ideality. Thus, equation (2.9) is modified as:

$$f_i^l = x_i \gamma_i f_i^{*,l} \quad (2.10)$$

The liquid phase reference fugacity  $f_i^{*,l}$  from the above equation is computed as:

$$f_i^{*,l} = \phi_i^{*,v}(T, P_i^*) P_i^* \theta_i^* \quad (2.11)$$

where  $\phi_i^{*,v}$  is fugacity coefficient of pure component  $i$  at the system temperature and vapor pressures, as calculated from the vapor phase equation of state.

$P_i^*$  is liquid vapor pressure of component  $i$  at the system temperature.

$\theta_i^*$  is Poynting correction for pressure =  $\exp\left(\frac{1}{RT} \int_{P_i^*}^P V_i^{*,l} dP\right)$ .

At low system pressures, the Poynting correction is near unity and can be ignored. Thus the overall vapor-liquid equilibrium (VLE) relationship for the mixture systems can be described as the following equation:

$$y_i P = x_i \gamma_i P_i^* \quad (2.12)$$

Equation (2.12) also can be called modified Raoult's Law, and the liquid activity coefficient can be estimated from activity coefficient models that related to the system (Luyben and Chien, 2010).

### 2.4.3 Thermodynamic Models

#### 2.4.3.1 The Universal Quasi-Chemical (UNIQUAC) Model

The UNIQUAC model is used for determine the liquid-phase activity coefficients in fluid-phase equilibria. This model was developed by Abrams and Prausnitz (1975). The UNIQUAC model comprised of two additive parts, a combinatorial part to describe the dominant entropic distribution and molecular size as well as shape differences and the residual part to account for intermolecular forces that are responsible for the enthalpy of mixing.

$$\frac{g^E}{RT} = \left( \frac{g^E}{RT} \right)^C + \left( \frac{g^E}{RT} \right)^R \quad (2.13)$$

From the fundamental excess-property relation:

$$\ln \gamma_i = \frac{g^E}{RT} \quad (2.14)$$

Therefore, equation (2.13) became to

$$\ln \gamma_i = \ln \gamma_i^C + \ln \gamma_i^R \quad (2.15)$$

where  $g^E$  is partial excess Gibbs energy.

$\gamma_i$  is activity coefficient for component  $i$ .

$R$  is the universal gas constant.

$T$  is the absolute temperature.

Superscript  $C$  and  $R$  referred to combinatorial and residual, respectively.

For multicomponent system, the combinatorial and residual parts can be written as equation (2.16) and (2.17).

$$\ln \gamma_i^C = \sum_{i=1}^m x_i \ln \frac{\Phi_i^*}{x_i} + \frac{z}{2} \sum_{i=1}^m q_i x_i \ln \frac{\theta_i}{\Phi_i^*} \quad (2.16)$$

$$\ln \gamma_i^R = - \sum_{i=1}^m q_i' x_i \ln \left( \sum_{j=1}^m \theta_j' \tau_{ji} \right) \quad (2.17)$$

where  $z$  is the coordination number which is set equal to 10.

$x_i$  is mole fraction of component  $i$  in the system.

$m$  is total number of component in the system.

Subscript  $i$  identifies component in the system.

Subscript  $j$  is a dummy index.

The segment fraction  $\Phi^*$  and area fractions  $\theta$  and  $\theta'$  are given by

$$\Phi_i^* = \frac{r_i x_i}{\sum_{j=1}^m r_j x_j} \quad (2.18)$$

$$\theta_i = \frac{q_i x_i}{\sum_{j=1}^m q_j x_j} \quad (2.19)$$

$$\theta_i' = \frac{q_i' x_i}{\sum_{j=1}^m q_j' x_j} \quad (2.20)$$

where  $r_i$  is pure-component volume parameter for component  $i$ .

$q_i$  and  $q_i'$  are pure-component surface areas parameter of component  $i$ .

In original formulation,  $q_i=q_i'$ . To obtain better agreement for system containing of water or lower alcohols,  $q_i'$  values for water and lower alcohol were adjusted empirically because of the effect of hydrogen bonding in the molecules, then the surface of interaction  $q_i'$  is smaller than the geometric external surface  $q_i$ . For other fluid,  $q_i=q_i'$ .

For each system, the interaction parameter with the effect of temperature are given by

$$\tau_{ij} = \exp\left(-\frac{a_{ij}}{T}\right) \quad (2.21)$$

$$\tau_{ji} = \exp\left(-\frac{a_{ji}}{T}\right) \quad (2.22)$$

where  $a_{ij}$  is binary parameter for component  $i$  and component  $j$ .

$a_{ji}$  is binary parameter for component  $j$  and component  $i$ .

Note that  $\tau_{ij} \neq \tau_{ji}$ ; however, when  $i = j$ , then  $\tau_{ij} = \tau_{ji} = 1$ .

Thus, for any component  $i$ , the activity coefficient is given by

$$\ln \gamma_i = \ln \frac{\Phi_i^*}{x_i} + \frac{z}{2} q_i \ln \frac{\theta_i}{\Phi_i^*} + l_i - \frac{\Phi_i^*}{x_i} \sum_{j=1}^m x_j l_j - q_i' \ln \left( \sum_{j=1}^m \theta_j' \tau_{ji} \right) + q_i' - q_i' \sum_{j=1}^m \frac{\theta_j' \tau_{ij}}{\sum_{k=1}^m \theta_k' \tau_{kj}} \quad (2.23)$$

where 
$$l_j = \frac{z}{2}(r_j - q_j) - (r_j - 1) \quad (2.24)$$

The main advantages of UNIQUAC model are first, from its relative simplicity, using only two adjustable parameters, and second, from its wide range of applicability due to the UNIQUAC model can be used in wide variety of non-electrolyte of liquid mixtures containing nonpolar or polar fluids such as hydrocarbons, alcohols, nitriles, ketones, organic acids, etc. and water, including partially miscible mixtures (Praunitz et al., 1999).

#### 2.4.3.2 The Universal Functional Activity Coefficient (UNIFAC)

##### Model

Based on the UNIQUAC equation, the UNIFAC model was developed by Fredenslund, Jones and Prausnitz (1975). They provided the method for estimation activity coefficients depends on the concept that a liquid mixture may be considered a solution of the structural units from which the molecules are formed rather than a solution of the molecules themselves. A molecule is divided into functional groups and molecule-molecule interactions are considered.

According to UNIFAC model is based on the UNIQUAC model then the model comprised of two additive parts, a combinatorial part and residual part.

$$\ln \gamma_i = \ln \gamma_i^C + \ln \gamma_i^R \quad (2.25)$$

For multicomponent system, the combinatorial and residual parts can be written as:

$$\ln \gamma_i^C = \ln \frac{\Phi_i^*}{x_i} + \frac{z}{2} q_i \ln \frac{\theta_i}{\Phi_i^*} + l_i - \frac{\Phi_i^*}{x_i} \sum_{j=1}^m x_j l_j \quad (2.26)$$

$$\ln \gamma_i^R = \sum_k v_k^{(i)} [\ln \Gamma_k - \ln \Gamma_k^{(i)}] \quad (2.27)$$

where  $Z$  is the coordination number which is set to 10.

$x_i$  is mole fraction of component  $i$  in the system.

$m$  is total number of component in the system.

$v_k^{(i)}$  is number of functional group of type  $k$  in molecule  $i$ .

$\Gamma_k$  is activity coefficient of group  $k$ .

$\Gamma_k^{(i)}$  is activity coefficient of group  $k$  in pure component  $i$ .

Subscript  $i$  is identifies component in the system.

Subscript  $j$  is a dummy index.

Subscript  $k$  is functional group in the molecule  $i$ .

The segment fraction  $\Phi_i^*$ , area fractions  $\theta$  and  $l_i$  are similarly with in UNIQUAC model. The parameter  $r_i$  and  $q_i$  are calculated as the sum of group volume and area parameters,  $R_k$  and  $Q_k$ , given as:

$$r_i = \sum_k v_k^{(i)} R_k \quad (2.28)$$

$$q_i = \sum_k v_k^{(i)} Q_k \quad (2.29)$$

The group residual activity coefficient,  $\Gamma_k$ , can be expressed in term of following equation:

$$\ln \Gamma_k = Q_k \left[ 1 - \ln \left( \sum_m \Theta_m \Psi_{mk} \right) - \sum_m \left( \frac{\Theta_m \Psi_{km}}{\sum_n \Theta_n \Psi_{nm}} \right) \right] \quad (2.30)$$

where  $\Theta_m$  is the area fraction of group  $m$  which is calculated by

$$\Theta_m = \frac{Q_m X_m}{\sum_n Q_n X_n} \quad (2.31)$$

where  $X_m$  is the mole fraction of group  $m$  in the mixture.

The group interaction parameter  $\Psi_{mn}$  is given by

$$\Psi_{mn} = \exp \left( -\frac{a_{mn}}{T} \right) \quad (2.32)$$

where  $a_{mn}$  is energy interaction parameters of functional group  $m$  and  $n$ .

$T$  is absolute temperature.

Note that  $a_{mn}$  has units of degree Kelvin and  $a_{nm} \neq a_{mn}$ .

In additional, equation (2.30) also holds for  $\ln \Gamma_k^{(i)}$ . The UNIFAC model has been successfully used for the design of distillation columns (including azeotropic and extractive distillation) where the required multicomponent activity coefficients were estimated because of a lack of experimental information (Praunitz et al., 1999).

## **2.5 Procedures**

### **2.5.1 Chemicals**

Lactic acid (88 w/w%), absolute ethanol (99+ w/w%), and sulfuric acid (96 w/w%) were obtained from CARLO ERBA. Magnesium lactate powder is produced from lactic acid fermentation using magnesium oxide as neutralizing agent. Deionized water was obtained from Aquinity P LifeScience TI.

### **2.5.2 Experimental Procedure**

#### **2.5.2.1 Preparation of Magnesium Lactate Solution Study**

Effect of molar quantity and concentration of sulfuric acid on concentration of lactic acid obtained from acidified magnesium lactate was investigated by acidifying the salt with different volume of 1 M sulfuric acid solution and different concentration of sulfuric acid at equal volume. In all experiments, 20 g of fermentation-derived magnesium lactate powder was dissolved with sulfuric acid solution. Total molar quantity of 1 M sulfuric acid was varied from 0.050, 0.099 and 0.150 mole to investigate optimal molar amount of sulfuric acid. For optimal concentration, concentration of sulfuric acid was varied from 1 M to 4 M with the total number of mole of sulfuric acid was kept at 0.099 mole, which is the stoichiometric amount of the acid in acidification reaction. Solubility of magnesium lactate in the solution was observed, and lactic acid concentration in the solution was analyzed by HPLC.

#### **2.5.2.2 Preparation of Magnesium Lactate Solution**

Magnesium lactate powder was dissolved in 1 M sulfuric acid solution. The solution was stirred for 10 minutes before it was left for precipitation for 90 minutes. Solid residue was separated by vacuum filtration. In order to reduce

interference of water in the esterification reaction, about 60% of its volume was removed from the solution by rotary evaporator. Lactic acid concentration in remained magnesium lactate solution was analyzed by HPLC.

### **2.5.2.3 Kinetic Study of Esterification**

Kinetic study was performed for the homogeneous catalytic esterification of lactic acid from fermentation-derived magnesium lactate with ethanol at atmospheric pressure in glass reactor. Reaction was carried out at varied initial feed molar ratio of ethanol to lactic acid from 3:1, 10:1 and 30:1, reaction temperature from 85, 80, 75, and 65°C and catalyst loading from 1, 2, and 3 v/v% and using sulfuric acid as a catalyst. The solution was stirred by magnetic stirrer and control temperature by heating oil bath. Samples were analyzed for ethyl lactate produced by GC at regular interval time for 6 hour. Another set of experiments with the same conditions were performed using high purity lactic acid as the starting material in order to elucidate the effect of lactic acid source and purity on the kinetics of the reaction.

## **2.5.3 Analysis of the Compositions**

### **2.5.3.1 Gas Chromatography (GC) Analysis of Ethyl Lactate**

Quantities of ethyl lactate produced from esterification reaction were analyzed by a Shimadzu GC-14B equipped with flame ionization detector (FID) using helium (99.999% purity) as a carrier gas. A TR-FFAP with 30m × 0.53mm × 0.5µm capillary column was used to separate the sample. The samples were diluted with deionized water before analysis. The oven was operated at variable-programmed temperature. Initially, the temperature of the oven was held at 50°C for 3 minutes,

before it was increased to 60°C at a rate of 10°C per minute and held for 1 minute. Temperature of injector and detector were at 250°C.

### 2.5.3.2 High Pressure Liquid Chromatography (HPLC) Analysis of Lactic Acid

HPLC from Agilent Technologies equipped with a Hypersil BDS-C18 column and a UV detector with a wavelength of 210 nm was used to analyze lactic acid. Sulfuric acid of 0.005 M concentration was used as a mobile phase at a flow rate of 0.7 ml/min. The column oven temperature was maintained at 60 °C. The samples were diluted with water and injected in amount of 0.1 µL.

## 2.6 Results and Discussion

### 2.6.1 Preparation of Magnesium Lactate Solution Study

In this part, optimum condition for preparing the magnesium lactate solution by acidification of fermentation-derived magnesium lactate with sulfuric acid was investigated. Effect of molar quantity, concentration and volume of sulfuric acid on dissolution of magnesium lactate during acidification were studied and tabulated in Table 2.2.

**Table 2.2** Effect of molar quantity, concentration, and volume of sulfuric acid in acidification of magnesium lactate.

Amount of MgLA <sub>2</sub> (g)	Mole of MgLA <sub>2</sub>	H <sub>2</sub> SO <sub>4</sub> concentration (M)	Volume of H <sub>2</sub> SO <sub>4</sub> (ml)	Mole of H <sub>2</sub> SO <sub>4</sub>	Mole of LA dissolved	% LA dissolved
20.0602	0.099	1	50.00	0.050	0.12	60.5
20.0896	0.099	1	99.00	0.099	0.18	90.8
20.0497	0.099	1	150.00	0.150	0.179	90.4
20.0262	0.099	2	49.50	0.099	0.151	76.5
20.0170	0.099	3	33.00	0.099	0.116	58.8
20.0220	0.099	4	24.75	0.099	0.118	59.5

The effect of sulfuric molar quantity was studied by varying molar quantity of 1 M sulfuric acid from 0.050 to 0.150 mol. Amount of magnesium lactate was kept constant at 20 g. As the Figure 2.1, it was found that amount of lactic acid dissolved into the solution depended on molar quantity of sulfuric acid used. If the sulfuric acid molar quantity less than that required by the stoichiometric were used, magnesium lactate did not completely dissolve then amount of lactic acid in the solution decreased. The stoichiometric quantity of sulfuric acid gave the highest concentration of lactic acid in magnesium lactate solution. Therefore, suitable molar quantity of sulfuric acid is stoichiometric required.

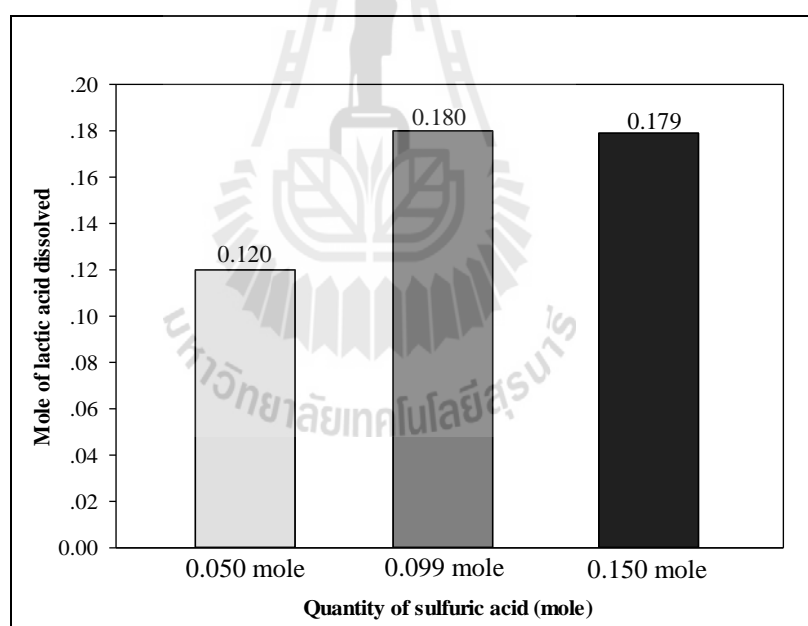


**Figure 2.1** Effect of sulfuric acid molar quantity on mole of lactic acid dissolved in acidification of magnesium lactate. Molar quantity of sulfuric acid 1 M:  
□ 0.05 mol; ■ 0.099 mol; ■ 0.15 mole.

In order to study effect of sulfuric acid concentration on acidification of fermentation-derived magnesium lactate, the molar quantity of various sulfuric acid concentration was kept constant at stoichiometric required. Concentration of sulfuric acid was varied from 1 to 4 M of sulfuric acid. Figure 2.2 showed the result of effect of sulfuric acid concentration to amount of dissolved lactic acid in the magnesium lactate solution. It was found that increasing of sulfuric acid concentration, amount of lactic acid in the solution trend to be decreased. Higher concentration of sulfuric acid, which constant molar quantity, had lower volume of sulfuric acid thus magnesium lactate powder incompletely dissolved and yield to lower amount of lactic acid released into the solution.

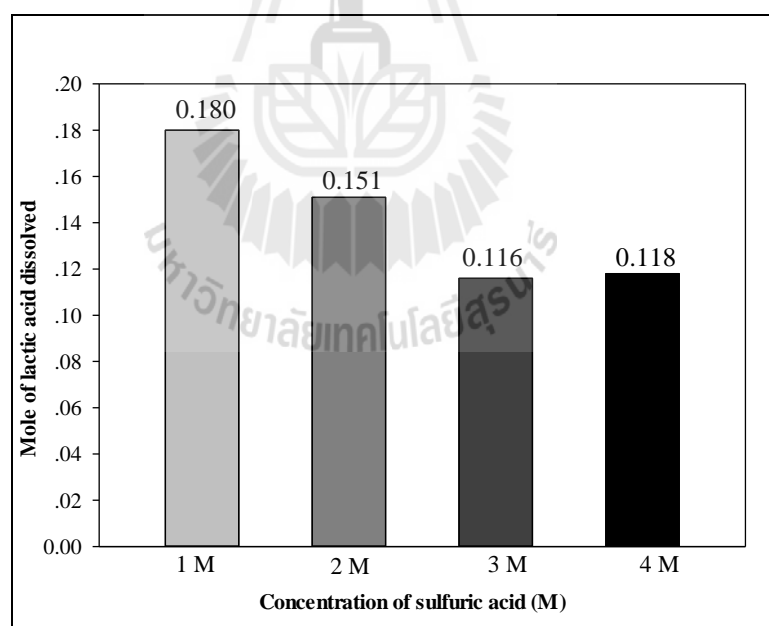


**Figure 2.2** Effect of sulfuric acid concentration on mole of lactic acid dissolved in acidification of magnesium lactate. Concentration of sulfuric acid:

□ 1M; ■ 2M; ■ 3 M; ■ 4 M.

Moreover, higher sulfuric acid showed the magnesium lactate solution after partially removal of water in black color this might be due to high acidity of concentrated sulfuric acid, see in Figure 2.3.

Therefore, the optimal quantity and concentration of sulfuric acid in preparing magnesium lactate solution by acidification is stoichiometric amount with magnesium lactate powder at concentration of sulfuric acid of 1 M.

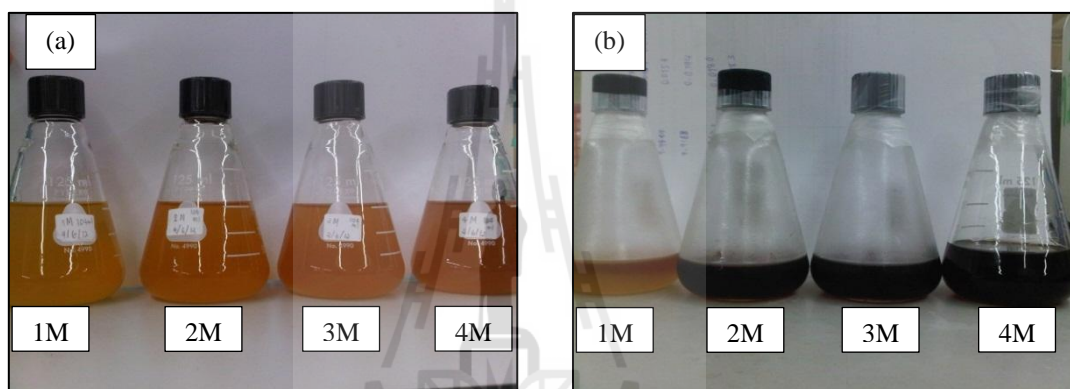


**Figure 2.3** Magnesium lactate solution which acidify by various sulfuric acid concentrations; (a) Magnesium lactate solution before evaporation; (b) Magnesium lactate solution after partially water removed.

### 2.6.2 Kinetic Study

The reaction rate equations of lactic acid esterification with ethanol used in calculation were shown in equation (2.4) and (2.5). According to reaction occur in liquid phase, the activity coefficients of each component in liquid phase were calculated from UNIQUAC and UNIFAC models, due to non-ideal solution behavior. The binary interaction parameters of each pair component for UNIQUAC model were obtained from Delgado et al. (2007) which study vapor-liquid equilibrium of the

quaternary reactive system of ethanol-water-ethyl lactate-lactic acid without salts. For UNIFAC model, group interaction parameters were calculated from functional-group of each component in the solution which obtained from Chan et al. (2001). The UNIQUAC and UNIFAC interaction parameters were shown in Table 2.3 and 2.4, respectively. The calculation of mole fractions was described in Appendix E.

**Table 2.3** UNIQUAC binary interaction parameters for the quaternary system of ethanol+water+ethyl lactate+lactic acid at 101.33 kPa,

$$\tau_{ij} = \exp\left(-\frac{(a_{ij} + b_{ij}T)}{T}\right) \text{ (Delgado et al., 2007).}$$

Component		i j		Binary interaction parameter	
1	2	i	j	$a_{ij}$ (K)	$b_{ij}$
Ethanol (EtOH)	Lactic acid (LA)	EtOH	LA	191.28	
		LA	EtOH	-43.32	
Ethanol (EtOH)	Ethyl lactate (EtLA)	EtOH	EtLA	-148.67	
		EtLA	EtOH	341.77	
Ethanol (EtOH)	Water (W)	EtOH	W	728.97	-2.0046
		W	EtOH	-756.95	2.4936
Water (W)	Lactic acid (LA)	W	LA	-39.61	
		LA	W	155.18	
Water (W)	Ethyl lactate (EtLA)	W	EtLA	64.53	
		EtLA	W	99.8	
Ethyl lactate (EtLA)	Lactic acid (LA)	EtLA	LA	52.64	
		LA	EtLA	125.29	

**Table 2.4** UNIFAC group specifications (Chan et al., 2001).

Molecule	Group name	Group number		Volume ( $R_k$ )	Surface area ( $Q_k$ )
		Main	Secondary		
Ethanol	CH <sub>3</sub>	1	1	0.9011	0.848
	CH <sub>2</sub>	1	2	0.6744	0.540
	OH	5	14	1.0000	1.200
Lactic acid	CH <sub>3</sub>	1	1	0.9011	0.848
	CH	1	3	0.4469	0.228
	OH	5	14	1.0000	1.200
	COOH	20	42	1.3013	1.224
Ethyl lactate	CH <sub>3</sub>	1	1	0.9011	0.848
	CH <sub>2</sub>	1	2	0.6744	0.540
	CH	1	3	0.4469	0.228
	OH	5	14	1.0000	1.200
	COO	41	77	0.1380	1.200
Water	H <sub>2</sub> O	7	16	0.9200	1.400

The flow chart of simulation and the computer program were shown in Appendix D. Equilibrium constant ( $K_e$ ) was calculated from the experiments while reaction rate constant ( $k$ ) was determined by minimizing the sum of squared errors ( $SS_{err}$ ) between the experimental ( $X_{exp}$ ) and the calculated conversion ( $X_{cal}$ ) as shown in equation (2.32).

$$SS_{err} = \sum_1^n (X_{exp} - X_{cal})^2 \quad (2.32)$$

The calculated conversion was evaluated by 4<sup>th</sup>-order Runge-Kutta method. Agreement between the experimental and calculated conversion was judged by coefficient of determination or  $R^2$ , computed by

$$R^2 = 1 - \frac{SS_{err}}{SS_{tot}} \quad (2.33)$$

where  $SS_{tot}$  is the total sum of squared error which can be calculated from by

$$SS_{tot} = \sum_1^n (X_{exp} - \bar{X}_{exp})^2 \quad (2.34)$$

where  $\bar{X}_{exp}$  is average value of experimental conversion.

The relationship between the reaction rate constant and reaction temperature is expressed by Arrhenius equation:

$$k = A_0 \exp\left(-\frac{E_A}{RT}\right) \quad (2.35)$$

where  $A_0$  is pre-exponential factor,  $s^{-1}$ .

$E_A$  is activation energy,  $Jmol^{-1}$ .

$R$  is the universal gas constant,  $8.314 Jmol^{-1}K^{-1}$ .

$T$  is absolute temperature, K.

In kinetics study, the experiments were performed with reaction temperature, initial ethanol-to-lactic molar ratio, and catalyst loading ranges of 338.15 to 358.15 K, 3:1 to 30:1 and 1 to 3 v/v%, respectively.

### 2.6.2.1 Effect of Reaction Temperature

The influence of reaction temperature on the kinetic of both esterification of magnesium lactate solution and commercial lactic acid were carried out under the reaction temperature of 358.15, 353.15, 348.15, and 338.15 K with

constant initial ethanol-to-lactic acid at 3:1 and catalyst loading at 2 v/v%. The results were shown in Figure 2.4 and Figure 2.5 for UNIQUAC and UNIFAC model, respectively. As expected, conversion of lactic acid in both processes was increased with reaction temperature. However, the conversion of magnesium lactate esterification was lower than that obtained from the system of commercial lactic acid. This could be due to a presence of impurities in magnesium lactate solution, one of which is magnesium sulfate formed during acidification of magnesium lactate with sulfuric acid. Same effect is noticed on the equilibrium conversion of both systems.

The reaction rate were determined and found that the reaction rate increases with the reaction temperature. Higher temperature will increase the number of molecule that able to react. Consequently, reaction rate increase with temperature (Masel, 2001). The effects of temperature on the reaction rate are shown by Arrhenius plots in Figure 2.6.

The linearity of the Arrhenius plots in Figure 2.6 was shown by the coefficients of determination ( $R^2$ ). For Figure 2.6 (a), values of  $R^2$  of the UNIQUAC model were found to be 0.8651 and 0.8687 for magnesium lactate and commercial lactic acid esterification. As well as in Figure 2.6 (b),  $R^2$  of UNIFAC model for both esterification systems were found to be 0.8055 and 0.8442, respectively. Table 2.5 shows the calculated Arrhenius parameters from both processes.

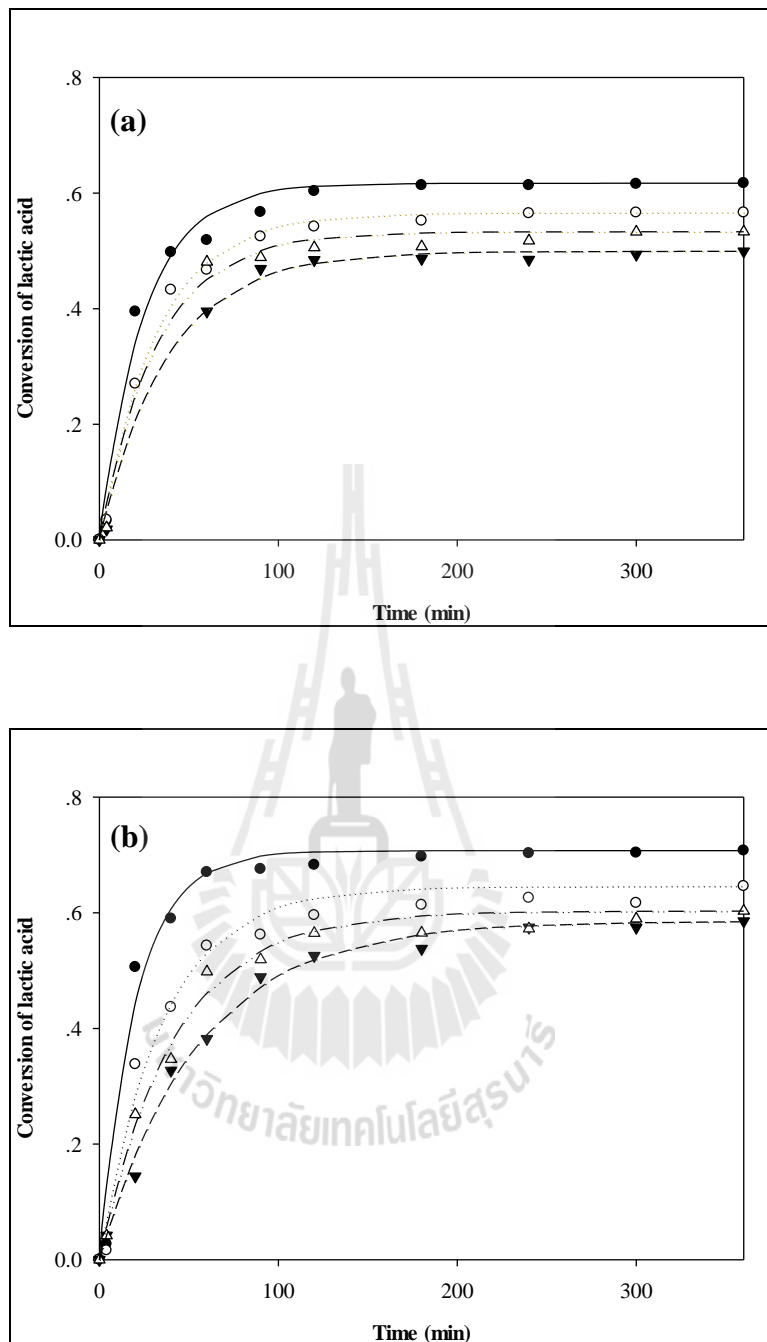


**Figure 2.4** Effect of reaction temperature on conversion of lactic acid in esterification of (a) magnesium lactate, (b) commercial lactic acid with the UNIQUAC model. Reaction conditions: (●) 358.15 K, (○) 353.15 K, (Δ) 348.15 K, (▼) 338.15 K. Line indicated the calculated conversion.

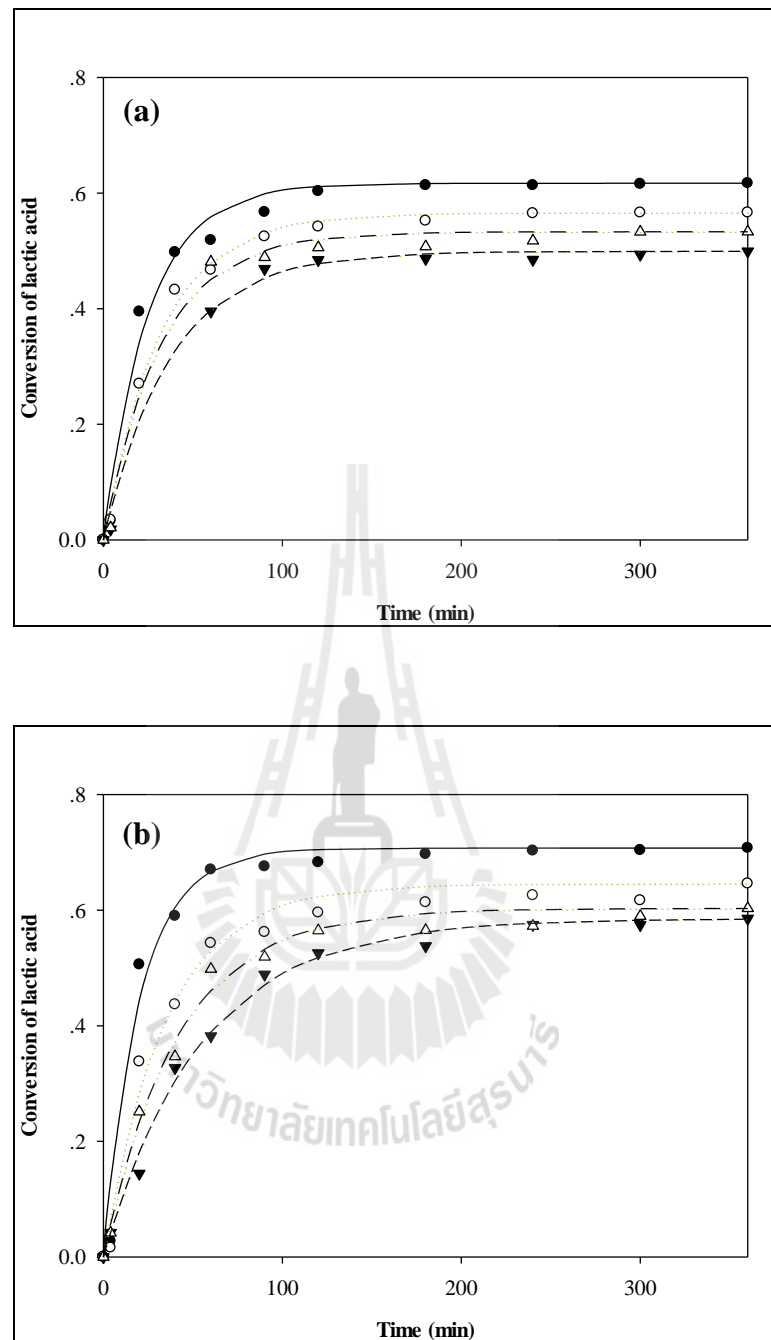


**Figure 2.5** Effect of reaction temperature on conversion of lactic acid in esterification of (a) magnesium lactate, (b) commercial lactic acid with the UNIFAC model. Reaction conditions: (●) 358.15 K, (○) 353.15 K, (△) 348.15 K, (▼) 338.15 K. Line indicated the calculated conversion.

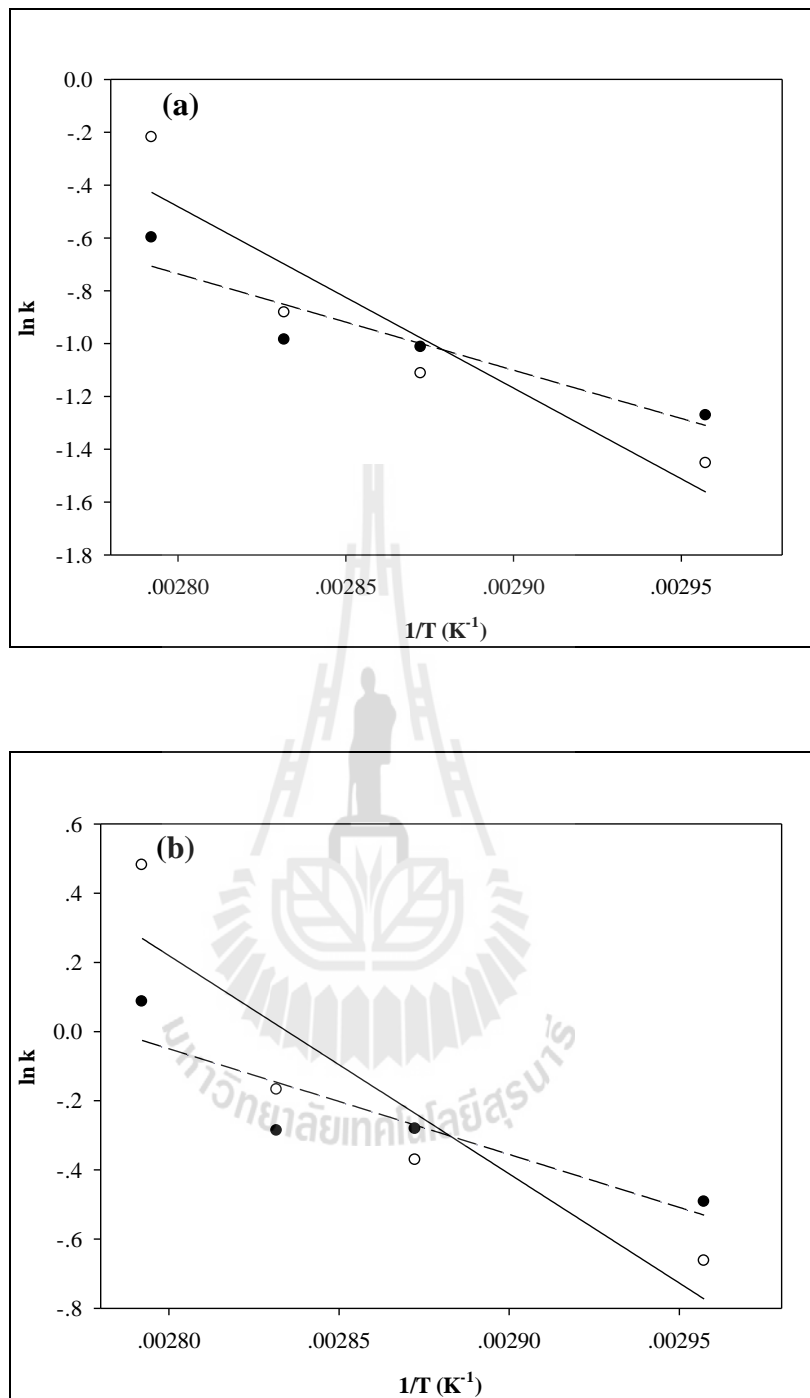


**Figure 2.6** Arrhenius plots of (a) UNIQUAC Model and (b) UNIFAC Model. The systems are (—●—) magnesium lactate esterification and (—○—) commercial lactic acid esterification.

**Table 2.5** The Arrhenius parameters of magnesium lactate and commercial lactic acid esterification.

System	$E_A$ (kJ/mol)	$A_0$ (s <sup>-1</sup> )
<i>Magnesium Lactate</i>		
UNIQAUC model	30.4	$1.33 \times 10^4$
UNIFAC model	25.4	$5.01 \times 10^3$
<i>Commercial Lactic Acid</i>		
UNIQAUC model	57.1	$1.41 \times 10^8$
UNIFAC model	52.5	$5.92 \times 10^7$

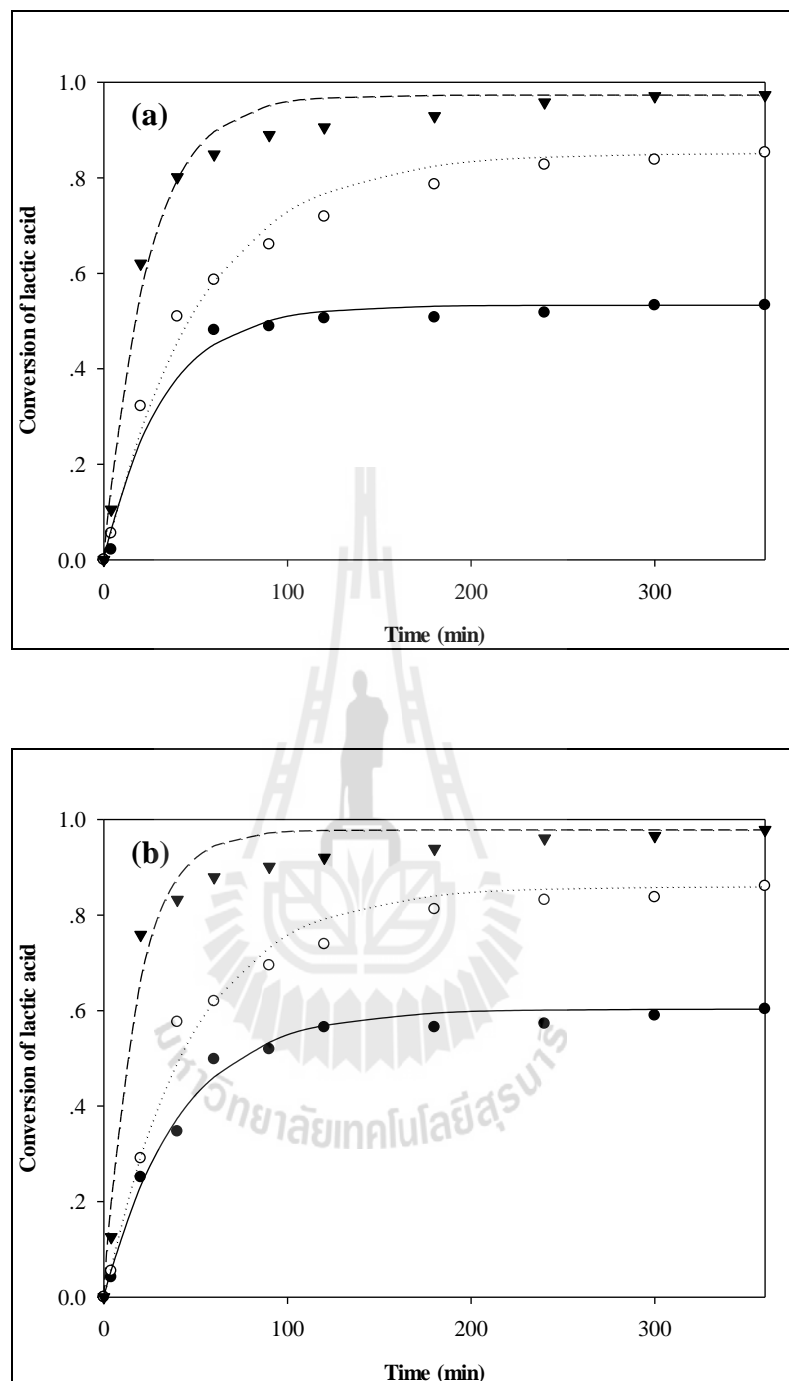
The activation energy is referred to the lowest energy required to overcome the reaction or the height of the energy barrier at the transition state (Levenspiel, 1999 and Masel, 2001). Then, magnesium lactate esterification with less activation energies should have higher reaction rate than the esterification of commercial lactic acid. In contrast, the values of pre-exponential factor from commercial lactic acid esterification were very higher than the magnesium lactate system. This pre-exponential factor is concerned about the frequency of collision between reactant molecules at the transition state to produce the products and this factor is directly effect to the reaction rate. As mentioned before, magnesium lactate solution has some impurity and this impurity may be the cause of interruption of collision between reactant molecules and lead to reduce the reaction rate. Furthermore, for reactions which taking places in solutions, solvent or ionic in the solution also have effect to these Arrhenius parameters (Masel, 2001). Therefore, the

reaction rates of commercial lactic acid esterification were higher than the magnesium lactate esterification.

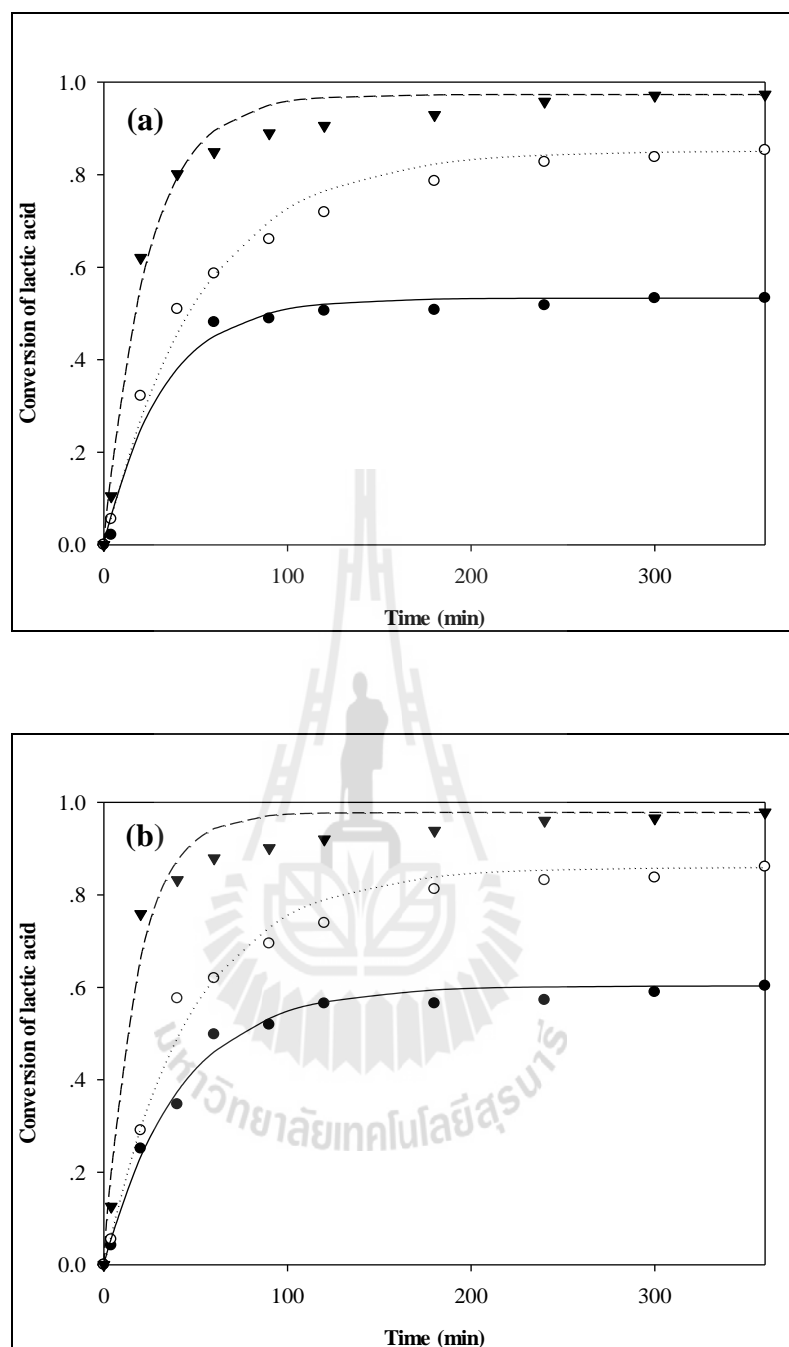
Moreover, the reaction rate constant of commercial lactic acid are in proximity of the values reported by Troupe and Dimilla (1957) who obtained the activation energies of 62.4 and 50.6 kJ/mol for esterification of H<sub>2</sub>SO<sub>4</sub>-catalyzed esterification of 85 and 44 w/w% commercial lactic acid, respectively.

#### **2.6.2.2 Effect of Initial Feed Molar Ratio**

The effect of initial feed molar ratio was investigated by varying the initial ethanol-to-lactic acid molar ratio from 3:1 to 30:1. All the reactions in this study were carried out at 348.15 K with the catalyst loading of 2 v/v%. The results were shown in Figure 2.7 and 2.8 for UNIQUAC and UNIFAC model, respectively. It was found that the conversion of lactic acid in both processes was increased with the initial feed molar ratio. According to Le Chatelier's principle, increasing of initial feed molar ratio will increase forward reaction rate. In this situation, ethyl lactate is produced more, and the conversion of lactic acid is increased.



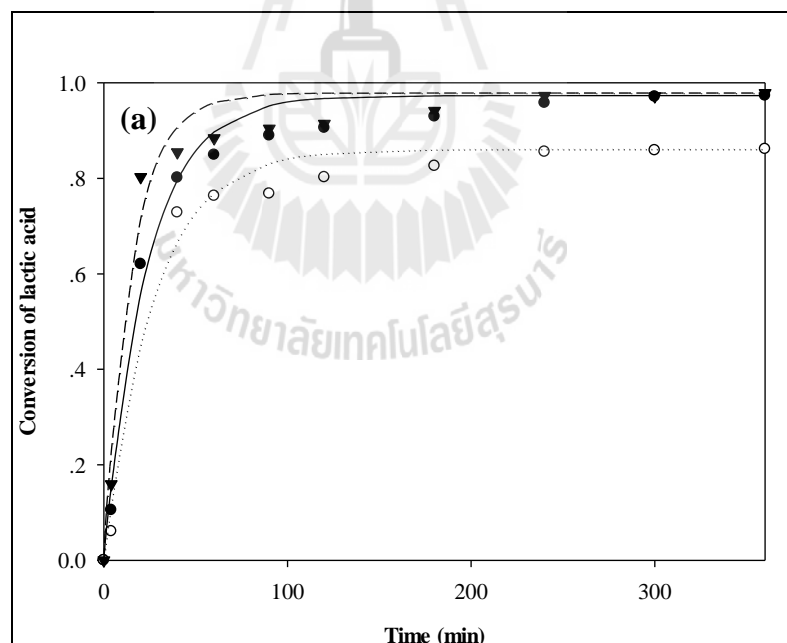
**Figure 2.7** Effect of initial ethanol-to-lactic acid molar ratio on conversion of lactic acid in esterification of (a) magnesium lactate, (b) commercial lactic acid with the UNIQUAC model. Reaction conditions: (▼) 30:1, (○) 10:1, (●) 3:1. Line indicated the calculated conversion.

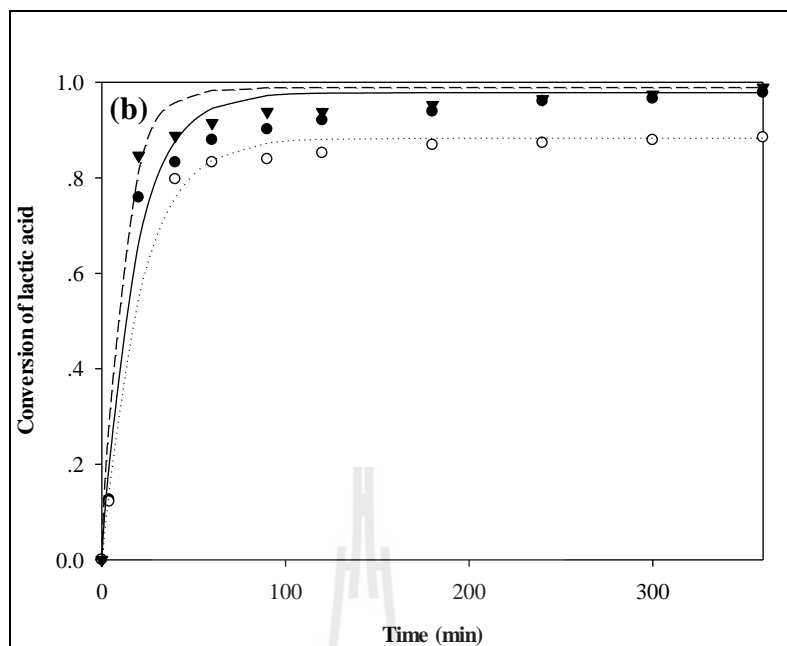


**Figure 2.8** Effect of initial ethanol-to-lactic acid molar ratio on conversion of lactic acid in esterification of (a) magnesium lactate, (b) commercial lactic acid with the UNIFAC model. Reaction conditions: (▼) 30:1, (○) 10:1, (●) 3:1. Line indicated the calculated conversion.

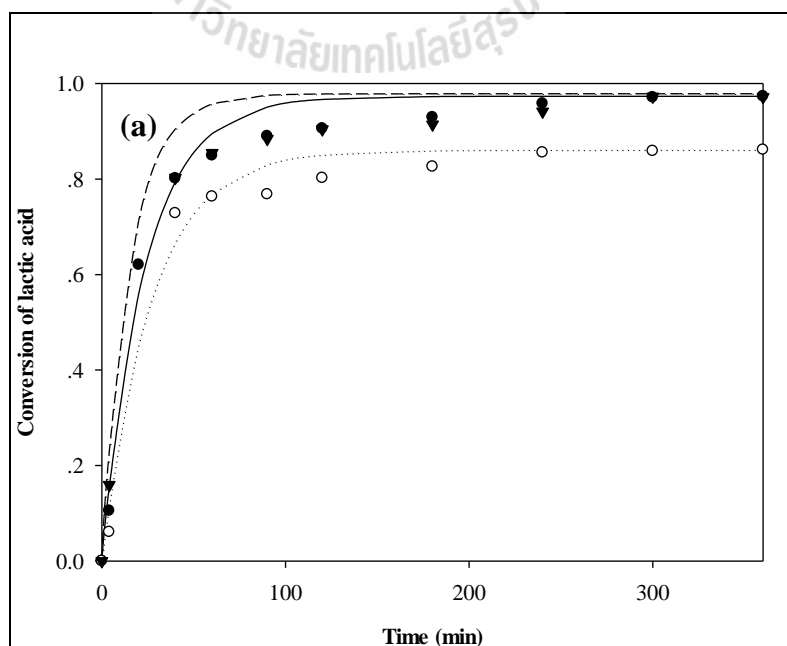
### 2.6.2.3 Effect of Catalyst Loading

Effect of catalyst loading was investigated by varying concentration of sulfuric acid in the reaction solution from 1 to 3 v/v% (or 0.02 to 0.06 w/w%) with constant reaction temperature at 348.15 K and initial ethanol-to-lactic acid molar ratio at 30:1. The results were shown in Figure 2.9 and 2.10 for UNIQUAC and UNIFAC model, respectively. Since an autocatalytic reaction that favors the acidic environment (Pereira et al, 2011) and the catalyst will decrease the activation energy of the reaction (Masel, 2001), thus rate of reaction increases with catalyst amount. Therefore, the conversion of lactic acid in both processes was increased with concentration of sulfuric acid in the process.





**Figure 2.9** Effect of catalyst loading on conversion of lactic acid in esterification of (a) magnesium lactate, (b) commercial lactic acid with the UNIQUAC model. Reaction conditions: (▼) 3 v/v%, (●) 2 v/v%, (○) 1 v/v%. Line indicated the calculated conversion.



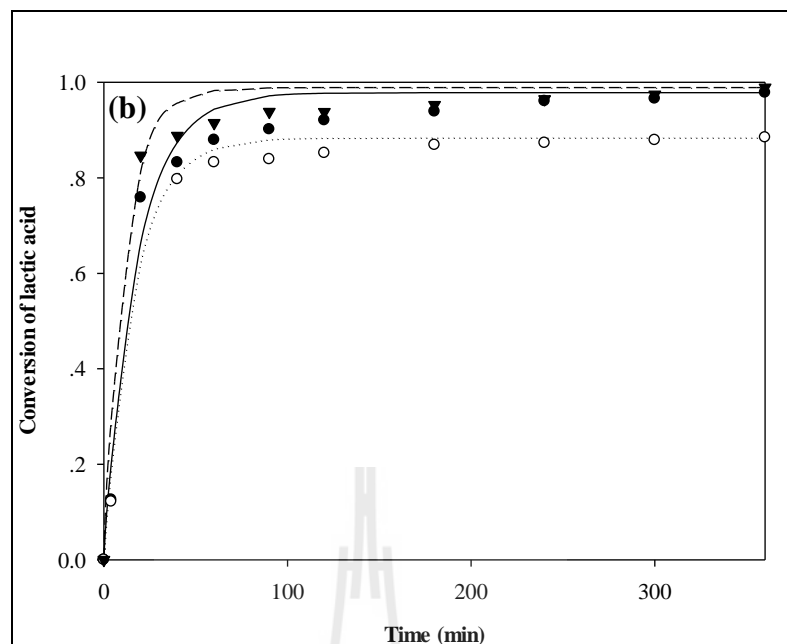


**Figure 2.10** Effect of catalyst loading on conversion of lactic acid in esterification of (a) magnesium lactate, (b) commercial lactic acid with the UNIFAC model. Reaction conditions: ( $\blacktriangledown$ ) 3 v/v%, ( $\bullet$ ) 2 v/v%, ( $\circ$ ) 1 v/v%. Line indicated the calculated conversion.

#### 2.6.2.4 Kinetic Parameters

The kinetic parameters: reaction rate constant and equilibrium constant, of esterification of magnesium lactate and commercial lactic acid were determined and shown in Table 2.6 and Table 2.7, respectively. The coefficient of determination ( $R^2$ ) in every experiment was in the range of 0.970-0.990, which indicated quite good agreement between the experimental conversion and the calculated conversion. The activity coefficients were calculated from UNIQUAC and UNIFAC models in order to considering the non-ideality of the solution, thus the kinetic parameters obtained of both systems and models were compared.

It was found that the kinetic parameters were increased with reaction temperature, initial molar ratio of ethanol-to-lactic acid, as well as catalyst loading. The reaction rate constant and equilibrium constant of magnesium lactate esterification were mostly lower than those obtained from commercial lactic acid esterification excepted at reaction temperature of 338.15 and 348.15 K. This could be due to lower solubility of magnesium sulfate at lower temperature. At low temperature, magnesium sulfate not dissolved and magnesium ions not released to affect the kinetic of the reactions. Moreover, the activation energy of magnesium lactate esterification was lower than the commercial lactic acid system. Therefore, at lower temperature with less impurity magnesium ions to interrupt the collision of reactant molecules, the reaction rates of magnesium lactate esterification were lower than that of commercial lactic acid.

**Table 2.6** Kinetic parameters of magnesium lactate esterification with ethanol.

Temperature (K)	Initial feed molar ratio	Catalyst loading (v/v%)	UNIQUEAC			UNIFAC		
			k	Ke	R <sup>2</sup>	k	Ke	R <sup>2</sup>
358.15	3:1	2	0.5497	7.0842	0.982	1.0909	9.1412	0.982
353.15	3:1	2	0.3736	5.3238	0.995	0.7509	6.7743	0.995
338.15	3:1	2	0.2803	4.2532	0.995	0.6115	5.4650	0.995
348.15	3:1	2	0.3630	4.9338	0.905	0.7547	6.3017	0.990
348.15	10:1	2	0.4647	10.5452	0.988	0.9997	13.6201	0.989
348.15	30:1	2	1.2867	21.498	0.985	2.9473	30.1436	0.985
348.15	30:1	1	0.8622	2.9723	0.908	1.9962	4.2683	0.985
348.15	30:1	3	1.7903	23.6763	0.973	4.1278	33.8002	0.973

**Table 2.7** Kinetic parameters of commercial lactic acid esterification with ethanol.

Temperature (K)	Initial feed molar ratio	Catalyst loading (v/v%)	UNIQUAC			UNIFAC		
			k	Ke	R <sup>2</sup>	k	Ke	R <sup>2</sup>
358.15	3:1	2	0.8036	11.1585	0.978	1.6183	14.9392	0.978
353.15	3:1	2	0.4140	7.9631	0.982	0.8457	10.4832	0.983
338.15	3:1	2	0.2339	6.3426	0.994	0.5154	8.3990	0.994
348.15	3:1	2	0.3287	6.8799	0.990	0.6901	9.0273	0.990
348.15	10:1	2	0.5122	11.1272	0.986	1.1004	14.3840	0.987
348.15	30:1	2	1.6516	25.3862	0.974	3.7904	35.8537	0.974
348.15	30:1	1	1.1042	3.3787	0.995	2.5718	4.9060	0.995
348.15	30:1	3	2.2731	43.6529	0.978	5.2951	62.9260	0.978

Normally, equilibrium constant depends on the reaction temperature only. However, from Table 2.6 and 2.7, it can be seen that equilibrium constant was increased with reaction temperature, initial molar ratio of ethanol-to-lactic acid and catalyst loading. Increasing of initial feed molar ratio and catalyst loading with constant total volume of reaction solution at 250 mL have influence on the initial composition in the solution and yield to effect on amount of product produced in the solution. Higher equilibrium concentration of products, which were ethyl lactate and water, in the reaction solution was obtained when higher reaction temperature, initial feed molar ratio as well as catalyst loading were used. Therefore, the equilibrium constant in this thesis depended on all process variables.

Moreover, it should be noted that the difference between the kinetic parameters obtained from UNIQUAC and UNIFAC model are quite substantial. This may be because of the different value of interaction parameter that used to calculate the activity coefficient of each model as mention in Table 2.3 and 2.4. In addition, using of binary interaction parameters from the system without salt

might affect to the accuracy of kinetic parameters because the reaction solution were highly non-ideality solution which consisted of ions, such as  $H^+$ ,  $Mg^{2+}$  and  $SO_4^{2-}$ , and lactic acid oligomers while the binary interaction parameters were considered only pure component. Therefore, it might have some error in the kinetic parameters obtained from both models. In order to enhance accuracy of kinetic parameters, the binary interaction parameters from the system with salts and oligomers should be investigated.

The relationship between reaction rate constant and reaction temperature, initial feed molar ratio, and catalyst loading for esterification of commercial lactic acid with concentration of 85 w/w% and 44 w/w% were correlated by Troupe and Dimilla (1957), but they did not consider the non-ideality of the solution. In this research, the relationships between reaction rate constant and corresponding parameters of magnesium lactate and commercial lactic acid esterification that incorporated with considering of non-ideal solution system were correlated to replicate the correlation from Troupe and Dimilla (1957).

For UNIQUAC model, the reaction rate constants of magnesium lactate and lactic acid esterification were plotted against catalyst loading in w/w% at constant initial feed molar ratio and temperature as shown in Figure 2.11.

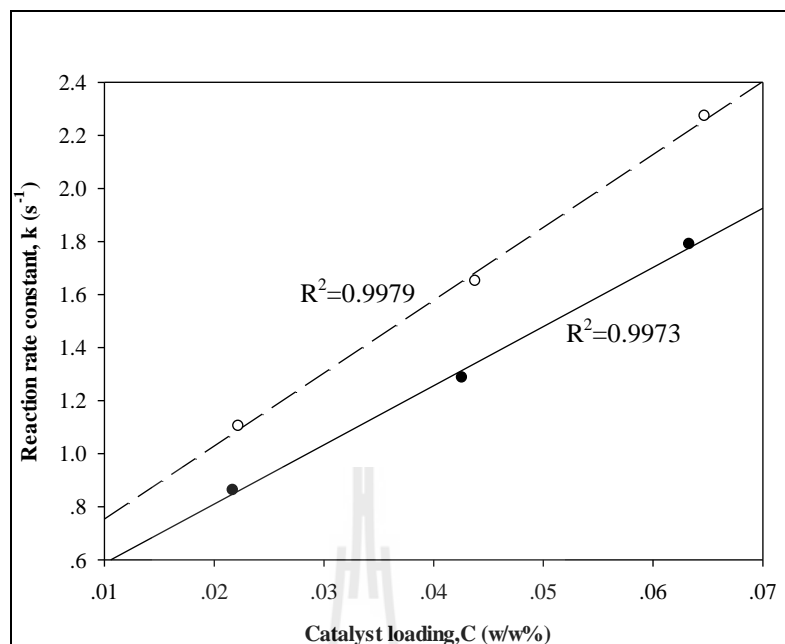


**Figure 2.11** Plots between reaction rate constant and catalyst loading of (—●—) magnesium lactate and (--○--) commercial lactic acid esterification from UNIQUAC model.

The relationship between reaction rate constant and catalyst loading of magnesium lactate and lactic acid esterification obtained from plots were shown in equation (2.36) and (2.37).

For esterification of magnesium lactate:

$$k = 22.307C + 0.3642 \quad (2.36)$$

For esterification of commercial lactic acid:

$$k = 22.494C + 0.4785 \quad (2.37)$$

It can be seen from equation (2.36) and (2.37) that the intercepts of these equations are not at origin, which indicates the autocatalytic nature of the reaction. The difference in coefficients of the correlation for esterification of magnesium lactate and commercial lactic acid shown in this study is likely due to the process impurities and the value of interaction parameters as previously explained.

The effect of initial molar ratio of ethanol-to-lactic acid (E/L) on the reaction rate constant of magnesium lactate and commercial lactic acid esterification were established by plotting the reaction rate constant that combined effect of catalyst loading against the initial ethanol-to-lactic acid molar ratio as shown in Figure 2.12. The reaction rate constant which combined effect of catalyst loading in Figure 2.12 was estimated by rearranged equation (2.36) and (2.37) with substitution of catalyst loading in unit of w/w% which equivalent to 2 v/v% because the influence of initial molar ratio was studied at constant catalyst loading of 2 v/v%. The correlation involved effect of initial feed molar ration and catalyst loading obtained from Figure 2.12 can be written as equation (2.38)-(2.39).

For esterification of magnesium lactate:

$$k = 0.8387(E/L)(C) - 4.0247(C) + 0.3642 \quad (2.38)$$

For esterification of commercial lactic acid:

$$k = 1.1589(E/L)(C) - 8.5676(C) + 0.4785 \quad (2.39)$$

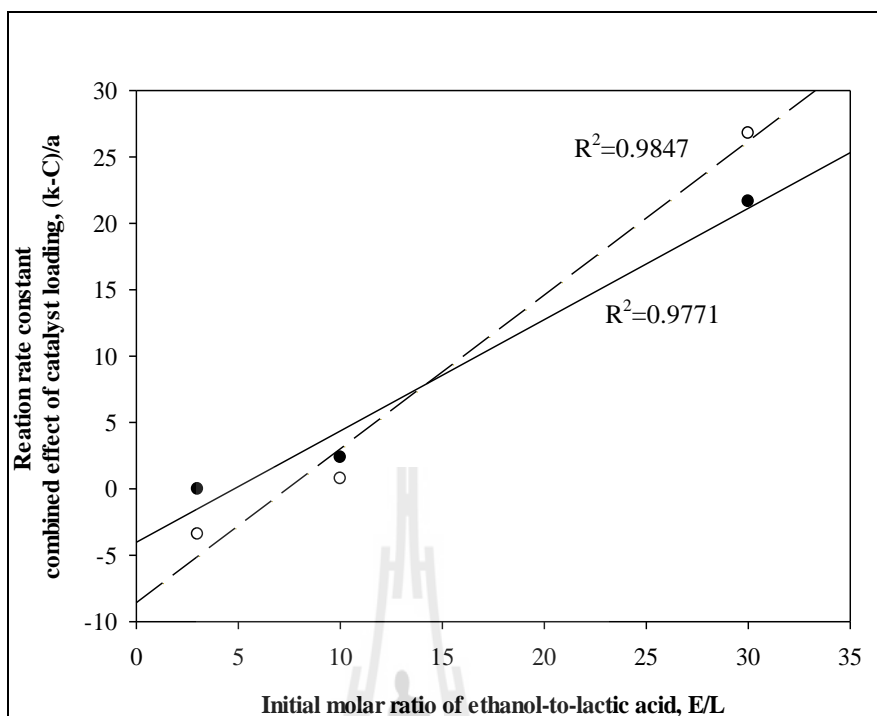


**Figure 2.12** Plots between reaction rate constant combined effects of catalyst loading and initial molar ratio of ethanol-to-lactic acid of (—●—) magnesium lactate and (--○--) commercial lactic acid esterification.

Effect of the reaction temperature to reaction rate constant were acquired by plotting  $\log k$  against the reciprocal of the absolute temperature at constant initial ethanol-to-lactic acid molar ratio and catalyst loading as shown in Figure 2.13.

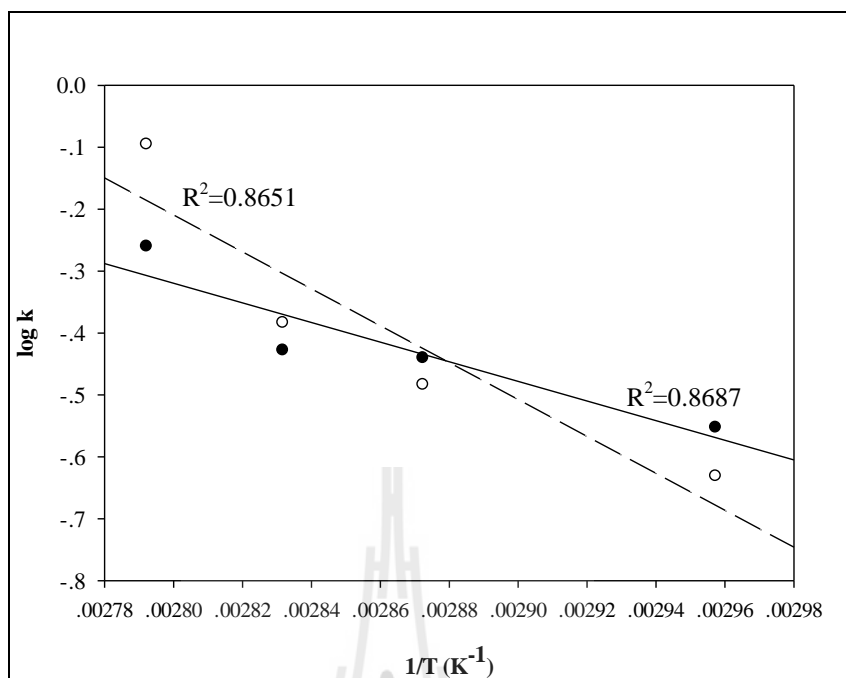


**Figure 2.13** Plots between log k and reciprocal of the absolute temperature of (—●—) magnesium lactate and (--○--) commercial lactic acid esterification from UNIQUAC model.

According to this research were studied effect of initial ethanol-to-lactic acid molar ratio and catalyst loading at constant reaction temperature at 75°C or 348.15 K. Therefore, the equation can be able to express in form of the ratio between the reaction rate constant at any temperature and at 348.15 K. The expression can be written as in equation (2.40) and (2.41).

For esterification of magnesium lactate:

$$\frac{k_{T(K)}}{k_{348.15K}} = \frac{10^{\left(4.1244 - \frac{15871}{T}\right)}}{0.3679} \quad (2.40)$$

For esterification of commercial lactic acid:

$$\frac{k_{T(K)}}{k_{34815K}} = \frac{10^{\left(\frac{8.1485 - 29848}{T}\right)}}{0.3760} \quad (2.41)$$

Equation (2.38) and (2.39) were combined with equation (2.40) and (2.41) to obtain the correlations between the reaction rate constant with involved parameter, yield:

Correlation for magnesium lactate esterification:

$$k = (0.8387(E/L)(C) - 4.0257(C) + 0.3642) \left( \frac{10^{\left(\frac{4.1244 - 15871}{T}\right)}}{0.3679} \right) \quad (2.42)$$

Correlation for commercial lactic acid esterification:

$$k = (1.1589(E/L)(C) - 8.5671C) + 0.4785 \left( \frac{10^{\left(\frac{8.1485 - 29848}{T}\right)}}{0.3760} \right) \quad (2.43)$$

The relationships between the reaction rate constant and process variables determined from UNIFAC model can be established in the similarly procedures. The correlations were expressed in equation (2.44) and (2.45):

Correlation for magnesium lactate esterification:

$$k = (1.9900(E/L)(C) - 11.5630(C) + 0.8447) \left( \frac{10^{\left( \frac{3.6998 - \frac{13290}{T}}{0.7893} \right)}}{0.7893} \right) \quad (2.44)$$

Correlation for commercial lactic acid esterification:

$$k = (2.7208(E/L)(C) - 21.5460(C) + 1.0959) \left( \frac{10^{\left( \frac{7.7726 - \frac{27418}{T}}{0.7893} \right)}}{0.7893} \right) \quad (2.45)$$

In addition, in this thesis, correlation between reaction rate constant and process parameters of both systems were established in the common form as follows (Fogler, 2006):

$$k = k_0 \exp \left( \frac{E_A}{R} \left( \frac{1}{T_0} - \frac{1}{T} \right) \right) \quad (2.46)$$

where  $k$  is reaction rate constant,  $s^{-1}$ .

$k_0$  is specific reaction rate constant at specific temperature  $T_0$ .

$T$  is absolute reaction temperature, K.

$T_0$  is specific temperature which equal to 348.15 K.

$E_A$  is activation energy,  $\text{kJmol}^{-1}$ .

$R$  is universal gas constant,  $\text{Jmol}^{-1}\text{K}^{-1}$ .

The relationship between reaction rate constant and process variables, in form of equation (2.46), of magnesium lactate and lactic acid

esterification calculated by UNIQUAC and UNIFAC model can be written as in equation (2.47) to (2.50).

Correlation for magnesium lactate esterification from UNIQUAC model:

$$k = (0.8387(E/L)(C) - 4.0257(C) + 0.3642) \exp\left(3654.4K\left(\frac{1}{348.15K} - \frac{1}{T}\right)\right) \quad (2.47)$$

Correlation for commercial lactic acid esterification from UNIQUAC model:

$$k = (1.1589(E/L)(C) - 8.5671(C) + 0.4785) \exp\left(6872.8K\left(\frac{1}{348.15K} - \frac{1}{T}\right)\right) \quad (2.48)$$

Correlation for magnesium lactate esterification from UNIFAC model:

$$k = (1.9900(E/L)(C) - 11.5630(C) + 0.8447) \exp\left(3060.1K\left(\frac{1}{348.15K} - \frac{1}{T}\right)\right) \quad (2.49)$$

Correlation for commercial lactic acid esterification from UNIFAC model:

$$k = (2.7208(E/L)(C) - 21.5460(C) + 1.0959) \exp\left(6313.3K\left(\frac{1}{348.15K} - \frac{1}{T}\right)\right) \quad (2.50)$$

Recalculate the reaction rate constant of both esterification systems and both models by these correlations. Table 2.8 and 2.9 showed the comparison between recalculated reaction rate constant and the experimental reaction rate constant.

**Table 2.8** Experimental and calculated reaction rate constant of magnesium lactate esterification.

Temperature (K)	Initial feed molar ratio	Catalyst loading (w/w%)	UNIQUAC Model			UNIFAC Model		
			$k_{exp}$	$k_{cal}$	Deviation (%)	$k_{exp}$	$k_{cal}$	Deviation (%)
358.15	3:1	0.04	0.5497	0.4020	26.863	1.0909	0.7751	28.934
353.15	3:1	0.04	0.3736	0.3479	6.866	0.7509	0.6868	8.538
338.15	3:1	0.04	0.2803	0.2199	21.568	0.6115	0.4676	23.531
348.15	3:1	0.04	0.3630	0.2999	17.396	0.7547	0.6064	19.648
348.15	10:1	0.04	0.4647	0.5500	18.348	0.9997	1.1999	20.024
348.15	30:1	0.04	1.2867	1.2646	1.717	2.9473	2.8953	1.763
348.15	30:1	0.02	0.8622	0.8228	4.562	1.9962	1.8893	5.356
348.15	30:1	0.06	1.7903	1.7084	4.574	4.1278	3.9062	5.367

**Table 2.9** Experimental and calculated reaction rate constant of commercial lactic acid esterification.

Temperature (K)	Initial feed molar ratio	Catalyst loading (w/w%)	UNIQUAC Model			UNIFAC Model		
			$k_{exp}$	$k_{cal}$	Deviation (%)	$k_{exp}$	$k_{cal}$	Deviation (%)
358.15	3:1	0.04	0.8036	0.4434	44.815	1.6183	0.8457	47.743
353.15	3:1	0.04	0.4140	0.3379	18.378	0.8457	0.6589	22.085
338.15	3:1	0.04	0.2339	0.1425	39.056	0.5154	0.2981	42.149
348.15	3:1	0.04	0.3287	0.2555	22.247	0.6901	0.5097	26.138
348.15	10:1	0.04	0.5122	0.6109	19.273	1.1004	1.3439	22.126
348.15	30:1	0.04	1.6516	1.6261	1.549	3.7904	3.7273	1.665
348.15	30:1	0.02	1.1042	1.0601	3.986	2.5718	2.4296	5.527
348.15	30:1	0.06	2.2731	2.1736	4.378	5.2951	4.9829	5.896

From Table 2.8 and 2.9, it was found that good agreement between the calculated and experimental reaction rate constant was achieved with high initial feed molar ratio of ethanol to lactic acid. High deviation between calculated and experimental reaction rate constant of magnesium lactate esterification might be due to effect of impurities in the magnesium lactate solution. For commercial lactic acid esterification which not has process impurities, large deviation might be effected by the lactic acid oligomers in the solution. According to lactic acid have two functional groups in its molecule; the hydroxyl group could be interacted to another carboxylic group of other lactic acid molecule and appear in form of the oligomers of lactic acid. The presence of oligomeric ester depended on concentration of lactic acid and could be observed at high concentration of lactic acid, above 20 w/w% of lactic acid, as well as high reaction temperature (Vu et al., 2005 and Asthana et al., 2005-2006). In this research, concentrations of lactic acid used were about 30 w/w%. Therefore, the oligomers of lactic acid could be occurred and affected to the kinetics of the reaction especially in lower initial ethanol-to-lactic acid molar ratio which have high amount of lactic acid, and higher reaction temperature.

The average deviations between the calculated and experimental reaction rate for magnesium lactate esterification are 12.74% and 14.15% for UNIQUAC model and UNIFAC model, and for commercial lactic acid esterification are 19.21% and 21.67% for UNIQUAC model and UNIFAC model, respectively.

In addition, Figure 2.14 and 2.15 showed the plots between experimental and calculated reaction rate constant of each system to observe the agreement between both parameters. It was found that agreement between both

reaction rate constant from UNIQUAC model were better than that obtained from UNIFAC model. Therefore, the kinetic parameters from UNIQUAC model was selected to be used in preliminary process design to synthesis ethyl lactate from magnesium lactate solution by reactive distillation system in the next chapter.

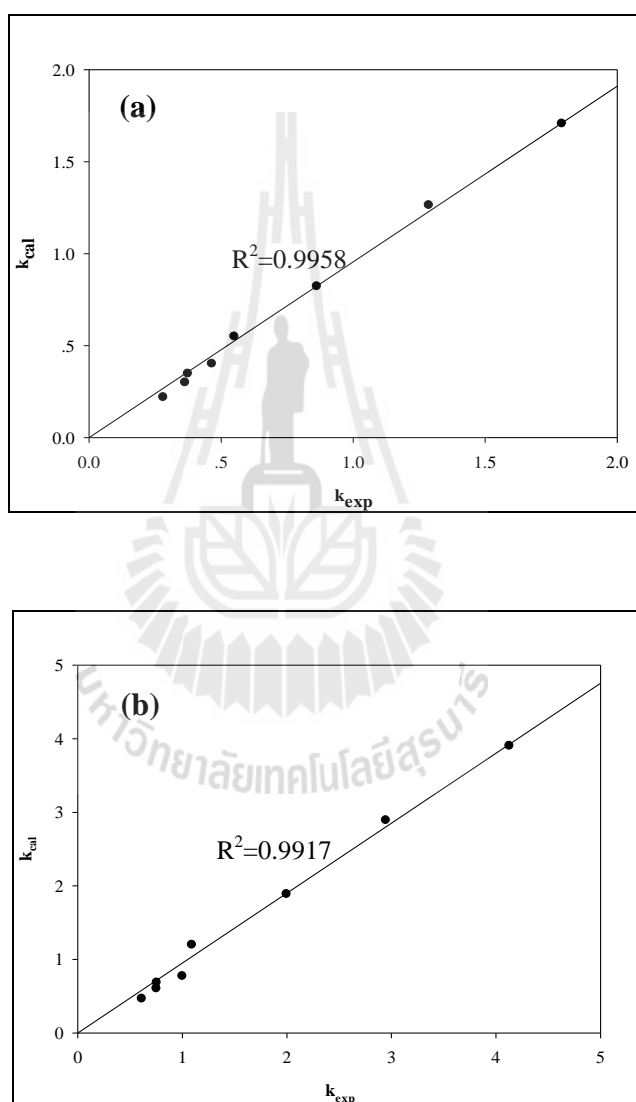


**Figure 2.14** Plots between experimental and calculated reaction rate constant of magnesium lactate esterification for (a) UNIQUAC model and (b) UNIFAC model.

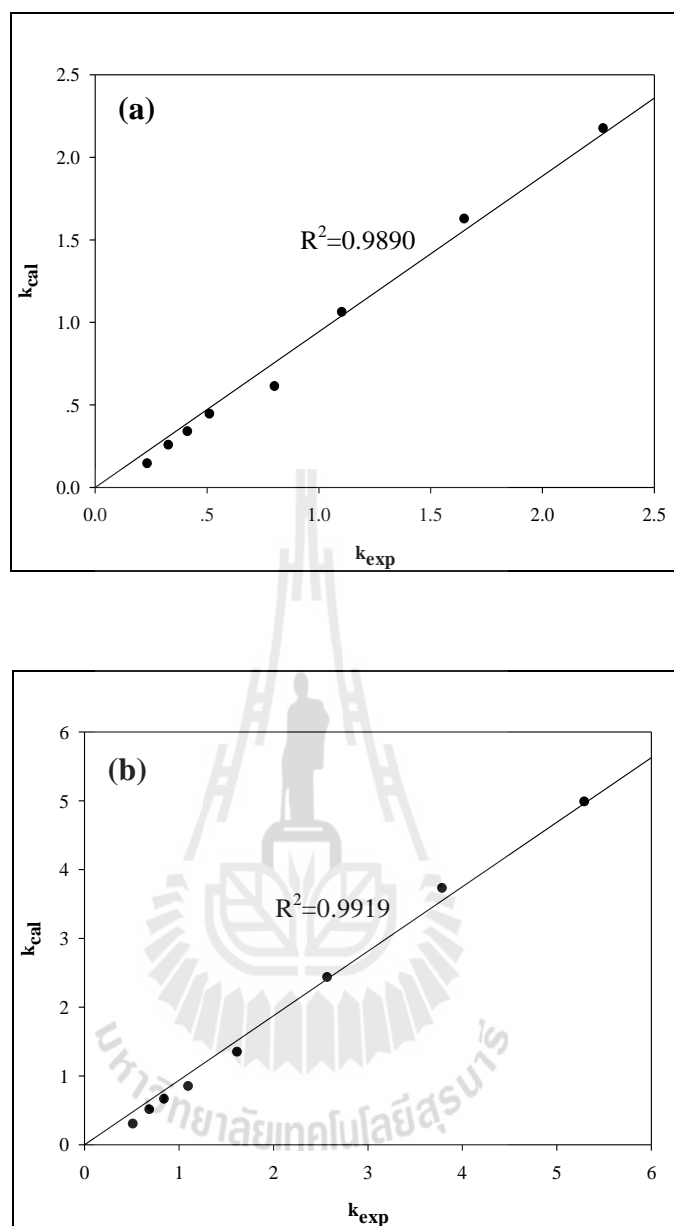


**Figure 2.15** Plots between experimental and calculated reaction rate constant of commercial lactic acid esterification for (a) UNIQUAC model and (b) UNIFAC model.

### 2.6.2.5 Effect of Magnesium Sulfate Concentration on the Reaction

#### Kinetics

According to difference in conversions and kinetic parameters that obtained from magnesium lactate and commercial lactic acid esterification, the effect of magnesium sulfate which is the major impurity of this process on the kinetics of lactic acid esterification was studied. The concentration of magnesium sulfate in the reaction solution was varied from 0 to 0.08 mg/L. The reactions were carried out at constant reaction temperature, initial ethanol-to-lactic acid molar ratio, and catalyst loading of 348.15 K, 3:1, and 2 v/v%, respectively.

The results of this part were shown in Figure 2.16. It was found that lactic acid conversion decreased with increasing concentration of magnesium sulfate. It can be considered as two ranges of magnesium sulfate concentration, 0-0.04 g/mL and 0.06-0.08 g/mL. The solubility of magnesium sulfate in water is 62.9 g/100 mL, at 80°C, and it slightly soluble in alcohol (Green and Perry, 2007). Therefore, when small concentrations of magnesium sulfate were used, total magnesium sulfate was dissolved in the reaction solution. Magnesium ion ( $Mg^{2+}$ ), which decomposed from magnesium sulfate, may interact with lactate ion ( $CH_3CHOHCOO^-$ ) in the solution and amount of lactate ion to produced ethyl lactate was decreased as well as the conversion. Since magnesium sulfate is slightly soluble in alcohol and the most composition in the reaction is alcohol. Therefore, at higher concentration of magnesium sulfate, magnesium sulfate may not dissolve and interrupt the contraction between ethyl ion ( $C_2H_5^+$ ) and lactate ion ( $CH_3CHOHCOO^-$ ) in the solution and conversion of the reaction was greatly decreased. Moreover, addition of magnesium sulfate salt into the solution may introduce ionic forces that affect to the equilibrium

of the system (Aznar et al., 2000). The salt in the solution have an ionic strength that exhibited by the concentration of salt. Salting in and Salting out effect can be occurred. Salting in effect reduces the volatility of one component, while, salting out effect promote that another causing an increase in the relative volatility. Therefore, the activity coefficient and equilibrium constant of the reaction may change with ionic strength of solution (Banat et al., 2002 and Banat et al., 2003).

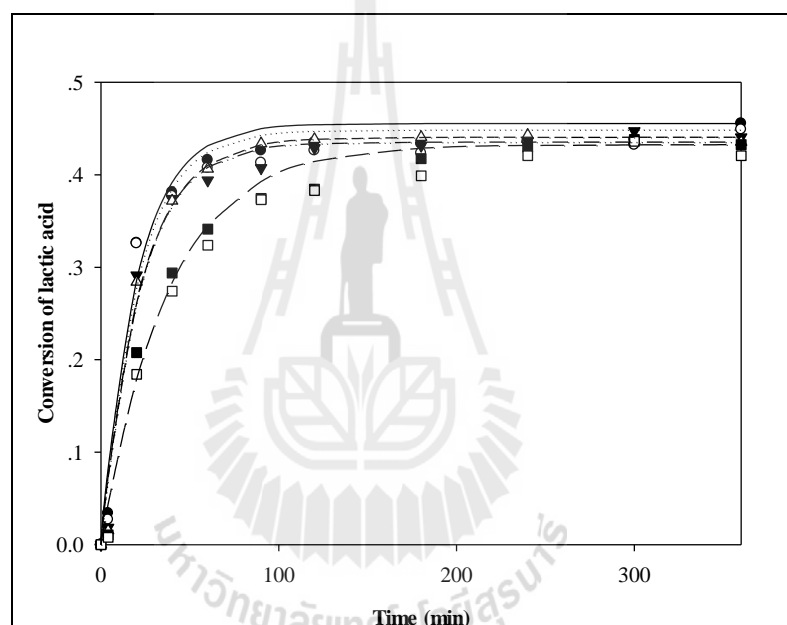


**Figure 2.16** Effect of magnesium sulfate concentration on reaction conversion for esterification of commercial lactic acid with ethanol. Reaction conditions: (●) 0 g/mL, (○) 0.008 g/mL, (▼) 0.020 g/mL, (△) 0.040 g/mL, (■) 0.060 g/mL, (□) 0.080 g/mL of magnesium sulfate concentration. Lines indicate the calculated conversion from UNIQUAC model.

The effect of concentration of magnesium sulfate on kinetics of commercial lactic acid esterification was studied. The UNIQUAC model was used in calculation and the kinetic parameters were shown in Table 2.10. It found that both reaction rate constant and equilibrium constant were decreased with increasing concentration of magnesium sulfate in the reaction solution as expected. Therefore, one of cause of difference kinetic parameters from magnesium lactate and commercial lactic esterification is due to amount of magnesium sulfate in magnesium lactate solution. Thus magnesium sulfate should be removed before the esterification. Since deviation of reaction rate constant that obtained from the relationship, equation (2.43) and (2.44), are still quite high, in order to develop these relationships more accurately, the effect of oligomers and effect of impurity in the reaction solution such as magnesium sulfate should be taken into consider. Moreover, activity coefficient model concerning effect of magnesium sulfate on the reaction kinetics must be specifically developed in order to gain extensive perception of this process and to get the better agreement between experimental and calculated data.

**Table 2.10** Effect of magnesium sulfate on the reaction kinetics parameters of commercial lactic acid esterification with ethanol.

Concentration of MgSO <sub>4</sub> (g/mL)	Conversion at equilibrium	UNIQUAC Model			UNIFAC Model		
		k	Ke	R <sup>2</sup>	k	Ke	R <sup>2</sup>
0.000	0.4555	0.5133	3.6825	0.977	1.0707	4.597	0.977
0.008	0.449	0.5057	3.5874	0.971	1.0546	4.4689	0.971
0.020	0.4406	0.4501	3.4603	0.982	0.9383	4.2987	0.982
0.040	0.4354	0.4608	3.3877	0.986	0.9602	4.2015	0.986
0.060	0.4326	0.2626	3.349	0.987	0.5471	4.1499	0.987
0.080	0.4206	0.2407	3.1787	0.991	0.5012	3.9234	0.991

## 2.7 Conclusions

The optimal molar quantity and concentration of sulfuric acid in acidifying magnesium lactate is stoichiometric amount with magnesium lactate powder at concentration of sulfuric acid of 1 M. The kinetics of magnesium lactate esterification with ethanol was investigated and compared with commercial lactic acid esterification. The activities of each component were calculated from UNIQUAC and UNIFAC model. The activation energies of magnesium lactate esterification obtained from UNIQUAC and UNIFAC were found to be 30.3 and 25.4 kJ/mol, respectively. The kinetics parameters, reaction rate constant and equilibrium constant, were determined from both models and found that both of parameters were influenced by the reaction temperature, initial feed molar ratio of ethanol to lactic acid, catalyst loading, as well as the amount of magnesium sulfate in the reaction solution. The relationship between the reaction rate constant and involved process variables was established. Good agreement between the experimental and calculated reaction rate constant were achieved in high initial feed molar ratio of ethanol to lactic acid. The deviation between experimental and calculated reaction rate constant may be from formation of the oligomers and high concentration of magnesium sulfate in the reaction where small initial ethanol-to-lactic acid molar ratio and high reaction temperature were used. To obtain more accurate relationship of reaction rate constant with corresponding parameters, the influence of oligomers and impurity, amount of magnesium sulfate, in the reaction should be taken to consider.

## 2.8 References

- Abrams, D.S. and Prausnitz, J.M. (1975). Statistical thermodynamics of liquid mixtures: A new expression for the excess Gibbs energy of partly or completely miscible systems. **AIChE**. 21: 116-128.
- Asthana, N., Kolah, A., Vu, D.T., Lira, C.T., and Miller, D.J. (2005). A continuous reactive separation process for ethyl lactate formation. **Organic Process Research and Development**. 9: 599-607.
- Asthana, N.S., Kolah, A.K., Vu, D.T., Lira, C.T., and Miller, D.L. (2006). A kinetic model for the esterification of lactic acid and its oligomers. **Industrial and Engineering Chemistry Research**. 45: 5251-5257.
- Aznar, M., Araujo, R. N., Romanato, J. F., Santos, G. R., and d'Avila, S. G. (2000). Salt Effects on Liquid-Liquid Equilibrium in Water+Ethanol+Alcohol+Salt Systems. **Journal of Chemical and Engineering Data**. 45: 1055-1059.
- Banat, F., Al-Asheh, S., Simandi, J. (2002). Effect of dissolved inorganic salts on the isothermal vapor-liquid equilibrium of the propionic acid-water mixer. **Chemical Engineering and Processing**. 41: 793-798.
- Banat, F., Al-Asheh, S., Simandi, J. (2003). Vapor-liquid equilibria of propionic acid-water system in the presence of different types of inorganic salts: effect of temperature and salt concentration. **Chemical Engineering and Processing**. 42: 917-923.
- Chan, C.K., Peng, C., Chan, M.N. (2001). UNIFAC Structural Groups and Parameters. [www.aim.env.uea.ac.uk/aim/info/UNIFACgroups.html](http://www.aim.env.uea.ac.uk/aim/info/UNIFACgroups.html)
- Chooklin, S., Kaewsichan, L., Kaewsichan, J., and Sura-apinan, P. (2009). [http://infor.eng.psu.ac.th/kpi\\_fac/file\\_link/P1253FPaper.pdf](http://infor.eng.psu.ac.th/kpi_fac/file_link/P1253FPaper.pdf)

- Dassy, S., Wiame, H., and Thyron, F.C. (1994). Kinetics of the liquid phase synthesis and hydrolysis of butyl lactate catalysed by cation exchange resin. **Journal of Chemical Technology and Biotechnology**. 59: 149-156.
- Delgado, P., Sanz, M.T., and Beltran, S. (2007). Isobaric vapor-liquid equilibrium for the quaternary reactive system: Ethanol + water + ethyl lactate + lactic acid at 101.33kPa. **Fluid Phase Equilibria**. 255: 17-23.
- Delgado, P., Sanz, M.T., and Beltran, S. (2007). Kinetic study for esterification of lactic acid with ethanol and hydrolysis of ethyl lactate using an ion-exchange resin catalyst. **Chemical Engineering Journal**. 126: 111-118.
- Filachione, E.M. and Costello, E.J. (1952). Lactic esters by reaction of ammonium lactate with alcohols. **Industrial and Engineering Chemistry**. 44: 2189-2191.
- Fredenslund, A., Jones, R.L., and Prausnitz, J.M. (1975). Group-contribution estimation of activity coefficients in nonideal liquid mixtures. **AIChE**. 21: 1086-1099.
- Fogler, H. S. (2006). **Elements of Chemical Reaction Engineering**. (4th ed.). New Jersey: Prentice-Hall.
- Kasinathan, P., Kwak, H., Lee, U., Kwang, D.W. (2010). Synthesis of ethyl lactate from ammonium lactate solution by coupling solvent extraction with esterification. **Separation and Purification Technology**. 76: 1-7.
- Kumar, R. and Mahajani, S.M. (2007). Esterification of lactic acid with n-butanol by reactive distillation. **Industrial and Engineering Chemistry Research**. 46: 6873-6882.

- Luyben, W. L. and Chien, I-L. (2001) **Design and Control of Distillation Systems for Separating Azeotropes**. John Wiley and Sons.
- Masel, R. I. (2001). **Chemical Kinetics and Catalysis**. New York.
- Pereira, C.S.M., Pinho, S.P., Silva, V.M.T.M, and Rodrigues, A.E. (2008). Thermodynamic equilibrium and reaction kinetics for the esterification of lactic acid with ethanol catalysed by acid ion-exchange resin. **Industrial and Engineering Chemistry Research**. 47: 1453-1463.
- Pereira, C. S., Silva, V. M., Rodrigues, A. E. (2011). Ethyl lactate as a solvent: properties, applications and production process - a review. **Green Chem.** 13: 2658-2671.
- Green, D. W. and Perry, R. H. (2007). **Perry's chemical Engineers' handbook**. (8th ed.). New York: McGraw-Hill.
- Prausnitz, J.M., Lichtenthaler, R.N., and de Azevedo, E.G. (1999). **Molecular Thermodynamics of Fluid-Phase Equilibrium**. (3rd ed.). New Jersey: Prentice-Hall.
- Smith, J.M., Van Ness, H.C., and Abbott, M.M. (2005). **Introduction to Chemical Engineering Thermodynamics**. (7th ed.). New York: McGraw-Hill Education (Asia).
- Troupe, R.A. and DiMilla, E. (1957). Kinetics of the ethyl alcohol-lactic acid reaction. **Chemical Processes**. 49: 847-855.
- Vu, D. T., Kolah, A. K., Asthana, N. S., Peereboom, L., Lira, C. T., and Miller, D. J. (2005). Oligomer Distribution in Concentrated Lactic Acid Solutions. **Fluid Phase Equilibria**. 236: 125-135.

Zhang, Y., Ma, L., and Yang, J. (2004). Kinetics of esterification of lactic acid with ethanol catalysed by cation-exchange resins. **Reactive and Functional Polymer**. 61: 101-104.



## CHAPTER III

### PRELIMINARY PROCESS DESIGN

#### 3.1 Abstract

Preliminary process for synthesis of ethyl lactate directly by magnesium lactate esterification with ethanol using sulfuric acid as a homogeneous catalyst was designed and simulated by Aspen Plus simulator. RADFRAC model was used for reactive distillation column and fractional distillation column configuration. All of the columns were designed as tray column in order to avoid clogging of magnesium sulfate which could happen if a packed column were used. Non-idealities of the reaction mixture were represented by UNIQUAC property model. The process scheme was designed for the target of initial fifty liters of magnesium lactate fermentation broth per day. Moreover, the process was designed as two schematics which called Process A and B. In Process A, ethyl lactate produced in the reactive distillation was emitted from column via the top product stream. On the other hand, ethyl lactate was emitted via the bottom product stream by Process B. The optimal conditions and configurations of all units in each process were investigated. From the results, it was found that number of fractional distillation column used in purification of ethyl lactate in Process A was higher than in Process B for one unit. The number of unit operation has an affected on the energy consumption. Therefore, the energy required for Process A was higher than that required from Process B. Moreover, overall yields of ethyl lactate obtained from both processes were compared. The

overall yield of ethyl lactate in these preliminary process designs was defined as conversion of lactic acid in reactive distillation column divided by total recovery of ethyl lactate in the process. It was found that the overall yield of ethyl lactate obtained from Process A was found to be 93.30% while from Process B was 73.33%. The production rates of ethyl lactate were found to be 0.047 kmol/day or 5.599 kg/day and 0.037 kmol/day or 4.400 kg/day for Process A and B, respectively. Ethyl lactate produced in both process schemes was in form of an aqueous solution. However, concentration of ethyl lactate obtained from Process A was significantly lower than the obtained from Process B. The concentration of ethyl lactate produced in Process A was 37.18 w/w% or 8.27 mole% while Process B was 76.79 w/w% or 33.52 mole%, respectively.

### **3.2 Introduction**

Ethyl lactate is well known as one of green chemicals. It can be used in many industries (Pereira et al., 2011). Ethyl lactate is produced industrially via esterification of commercial lactic acid with ethanol using either homogeneous or heterogeneous acid catalyst. This process is, however, expensive due to the costly separation and purification processes, which has been estimated to be about a half of the total cost for production of highly purified lactic acid. Synthesis of ethyl lactate directly from lactate salts, such as ammonium lactate, obtained from lactic acid fermentation might help to reduce the production cost of the process. (Filachione and Costello, 1952 and Kasinathan et al., 2010).

In the present, the integration of several functions in the single apparatus is gained more attentions. The combinations of applications into one single unit have

several advantages such as cost reduction, environmental protection and significant increase of computational power (They et al., 2005). Reactive distillation is a unit operation that combines chemical reaction and separation in the same vessel. Due to its multifunctional nature, the unit has its merit in reducing both capital and operational cost of the process. It is also considered as a high potential process for carrying out reversible reactions such as esterification, hydrolysis, transesterification, etherification, and alkylation as it can promote the reaction conversion in these equilibrium-limited reactions. Moreover, other advantages of reactive distillation are high selectivity, the heat of reaction can be used in situ for distillation, and increase the separation of product in the process (Sundmacher and Kienle, 2003).

Feasibility of synthesis of ethyl lactate by esterification of fermentation-derived lactate salt in reactive distillation has never been studied. Therefore, in this chapter, preliminary process for producing ethyl lactate from esterification of fermentation-derived magnesium lactate was designed and simulated using Aspen Plus simulator.

### **3.3 Literature Reviews**

In the past several decades, reactive distillation process has been found to become prominent and important alternative to the usual reaction separation process which is equilibrium limited. First patent about the reactive distillation were exhibited by Backhaus in 1920s. There are many applications of reactive distillation in industries. The most famous industrial application of reactive distillation process is the esterification to produce methyl acetate by the Eastman Chemical Co. (Agreda et al., 1984). Eastman Chemical Co. was the first company which used the reactive

distillation with the commercial production. Nowadays, there are many researches about the applications and principles as well as designing of the reactive distillation.

Smejkal et al. (2001) studied the production of 2-methylpropylacetate from 2-methylpropanal and acetic acid by reactive distillation. They simulated the reactive distillation using ASPEN Plus simulator. The results of the feed stages position showed that separate feed to the lower and upper part of the reaction zone gave the best result on the organic phase distillate composition. The concentrations of raw materials, acetic acid and 2-methylpropanol, which contaminated to the organic phase were lowest at the optimal feed stages. Moreover, they found that adding an equilibrium reactor prior to the reactive distillation column improved the product quality. In addition, they compared the simulation results with the pilot plant experimental data. They obtained very good agreement between experimental data and the simulation result.

Luo and Xiao (2001) presented the feasibility of reactive distillation process to produce diethyl carbonate by transesterification of ethanol and dimethyl carbonate. Potassium carbonate,  $K_2CO_3$ , was used as the homogeneous catalyst in this system. They presented the equilibrium model in the reactive distillation column. The influence of holdup of the tray, feed locations of the raw materials, reflux ratio, and Murphree tray efficiency on dimethyl carbonate conversion and diethyl carbonate selectivity were investigated. They found that more than 99.5% of selectivity of diethyl carbonate and completed conversion of dimethyl carbonate were achieved in this process.

Tang and coworkers (2003) designed and developed complete ethyl acetate production by reactive distillation column system. The homogeneous catalytic



lactic acid and performance of batch reactive distillation were strongly dependent on efficiency of water removal. Moreover, they studied the recovery of lactic acid from the formation of n-butyl lactate by continuous reactive distillation column. The results from continuous process were compared with the simulation results by ASPEN Plus simulator. They used UNIQUAC model to estimate the vapor-liquid equilibrium with concerning about non-ideality of the liquids phase. The effect of operating parameters, for example, catalyst loading, boilup heat, feed mole ratio, feed concentration, as well as the number of total stages on lactic acid conversion and n-butyl lactate in the product stream were investigated. The comparison of concentration and temperature profile from experimental were resulted in good agreement. Moreover, they proposed the process configuration for recovery of lactic acid as shown in Figure 3.2.

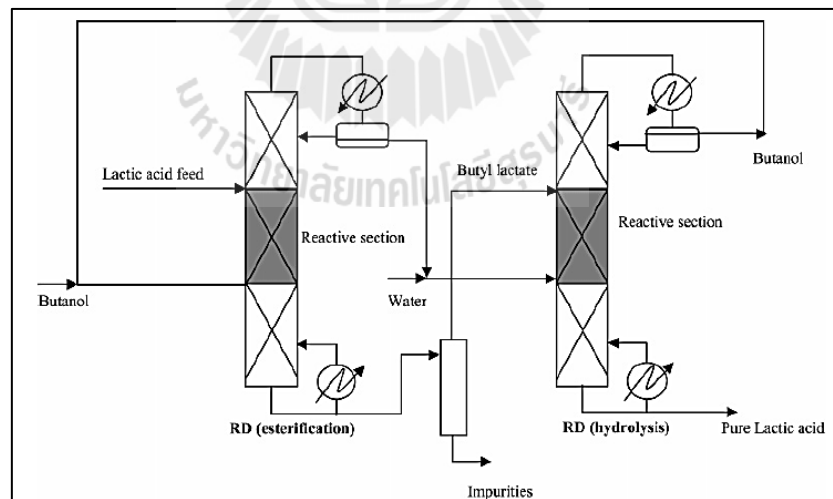


**Figure 3.2** Process flow diagram for recovery of lactic acid by Kumar and Mahajani (2007).

Gao et al. (2007) presented the ethyl lactate synthesis from solid super acid catalyzed reactive distillation process. They did the experiment with packed bed reactive distillation column and simulated the process using ASPEN Plus simulator. The influence of reflux ratio, mole ratio of reactant feed, feed flow rate, and the feed positions on yield of ethyl lactate were investigated in the experiment. They found that ethyl lactate quality strongly depended on the reaction performance section as well as feed location. Moreover, they obtained maximum yield of ethyl lactate was 51.64% and increased to 82.00% compared with the simple esterification reactor. Optimal conditions for the reactive distillation column were reflux ratio was 1:1, feed mole ratio of ethanol to lactic acid was 4:1 with feed rate of lactic acid was  $0.6284 \text{ molh}^{-1}$ , and feed location were upper stage and lower stage of the reactive zone for lactic acid and ethanol, respectively. Furthermore, they compared top and bottom product composition from the experiment with the simulation results. They found that the simulation results fitted with the experimental results well.

In addition to applications of reactive distillation, there are many review articles and study about modeling development and designing of the reactive distillation. One of the good review articles on reactive distillation modeling was performed by Taylor and Krishna (2000). The background information and modeling development on the reactive distillation were presented. They also discussed about column configurations in the system of both homogenous and heterogeneous catalytic reactive distillation. Moreover, the conceptual designs of the reactive distillation were proposed.

Melles and coworker (2000) presented the conceptual design of reactive distillation column including optimization of the total number of trays and the total

liquid holdup in the column. They showed the feasibility of designing the reactive distillation column with different liquid holdup in the column sections. Furthermore, they presented that sensitivity curve or sensitivity analysis was the useful method to study influence of operating parameters in the process.

They et al. (2005) established the preliminary design of reactive distillation column. They proposed a three-step procedure to design the reactive distillation unit, which combined with the feasibility analysis, synthesis, and design of reactive distillation. Moreover, they presented examples of proposed methodology with the production of methyl-tert-butyl-ether (MTBE) and methyl acetate process.

## **3.4 Theory**

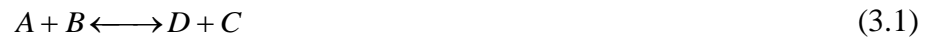
### **3.4.1 Reactive Distillation**

Reactive distillation (RD) is a unit operation where chemical reaction and separation occur in the same single vessel. As it is an integration of reaction and distillation, the continuous separation of the products can drive the reversible reaction to be completed by Le Chatelier's principle. It is normally called "catalytic distillation" when the catalysts were applied in the reactive distillation (Coker, 2010).

Due to the advantages of this integration, the reactive distillation is a high potential process for carrying out the reaction which chemical equilibrium limited such as esterification, hydrolysis, transesterification, and alkylation as well as etherification. Moreover, both capital and operation cost of the process can be reduced by the reactive distillation when compared with ordinary or conventional process. Therefore, the reactive distillation has shown great economical and environmental benefits in many existing applications. The examples of applying the reactive

distillation were production of methyl tertiary butyl ether (MTBE), ethyl tertiary butyl ether (ETBE) and methyl acetate (Sundamacher and Kienle, 2003).

Let consider a reversible reaction which expressed in as follow:



The boiling point of the components follows the sequence A, C, D, and B. Where A and B are the reactants, D and C are both desired products of the reaction.

The conventional process flow sheet of this reaction is a reactor followed by a series of distillation columns as shown in Figure 3.3 (a). The mixture of A and B is fed to the reactor, where the reaction takes place in the presence of catalyst and reaches reaction equilibrium. Three distillation columns are required to purify the products C and D. The unreacted components, A and B, are recycled back to the reactor. In practice the series of distillation columns could be much more complex than the one displayed in Figure 3.3 (a) if one or more azeotropes are formed in the mixture. The alternative reactive distillation process is shown in Figure 3.3 (b). The reactive distillation column consists of a reactive section in the middle with non-reactive rectifying and stripping sections at the top and bottom. The task of the rectifying section is to recover reactant B from the product stream C. In the stripping section, the reactant A is stripped from the product stream D. In the reactive section the products are separated in situ, driving the equilibrium toward formation of C and D and preventing any undesired side reactions between the reactants A (or B) with the product C (or D). For a properly designed reactive distillation column, virtually 100% conversion can be achieved (Taylor and Krishna, 2000).

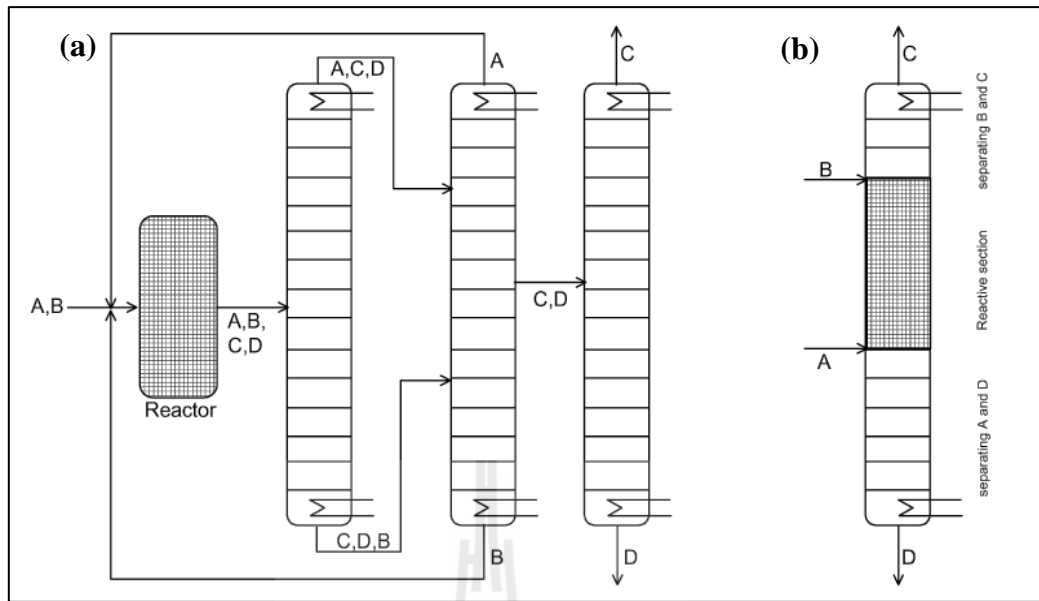


**Figure 3.3** The process scheme for a reaction sequence  $A + B \rightleftharpoons D + C$ ; (a) The traditional convention process; (b) The reactive distillation configuration (Taylor and Krishna, 2000).

The reaction in reactive distillation unit usually takes place in the liquid phase or at the surface of a solid catalyst in contact with liquid reactant. For homogeneous catalytic reactive distillation process, counter-current vapor-liquid contacting can be achieved in a multi-tray column, as showed in Figure 3.4, or a column with random or structured packing, as showed in Figure 3.5.

For heterogeneous catalytic process, the sizes of catalyst particles used in such operation are usually in the range of 1-3 mm of particle diameter (Taylor and Krishna, 2000). The catalyst pellets have to be enveloped within wire gauze enveloped column packing to overcome the limitations of flooding. Most commonly, the catalyst envelopes are packed inside the column. There are several shapes of column packing used in the industrials as showed in Figure 3.6.

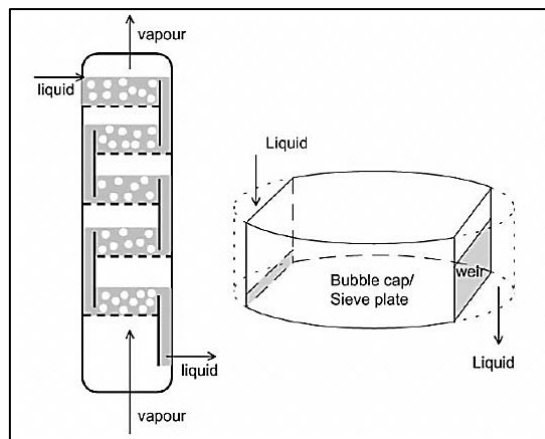


**Figure 3.4** Schematic for counter-current vapor-liquid contacting in tray column  
(Taylor and Krishna, 2000).

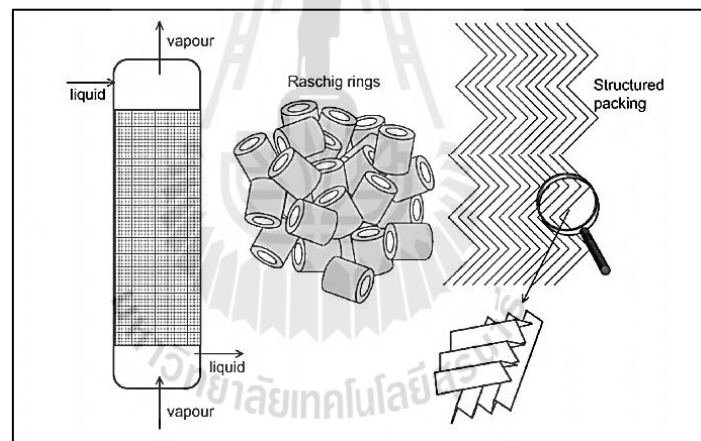


**Figure 3.5** Schematic for counter-current vapor-liquid contacting in packed column  
(Taylor and Krishna, 2000).

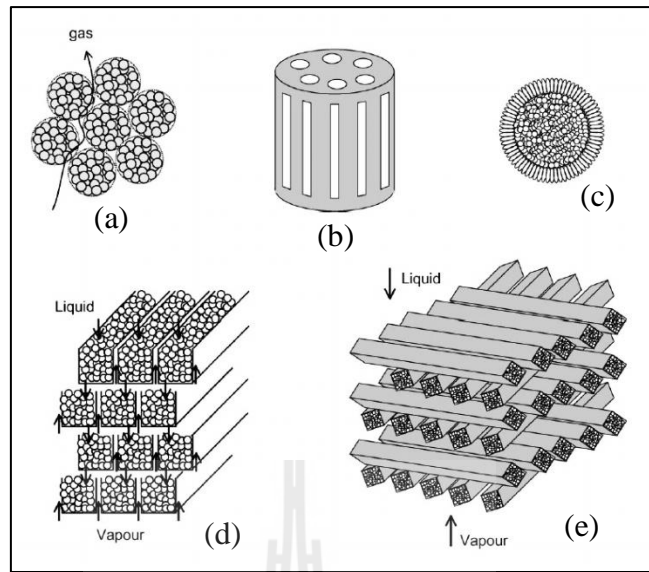


**Figure 3.6** The shape of packing of catalyst pellets; (a) porous spheres filled with catalyst inside them; (b) cylindrical shaped envelopes with catalyst inside them; (c) wire gauze envelopes with the sphere shapes; (d) wire gutters with the catalyst particles inside them; (e) tube or gutters with the catalyst pellets inside them.

### 3.4.2 Mathematical Modeling in Reactive Distillation

Due to the integration of reaction and separation in one single vessel, the numerical modeling involved in reactive distillation is very complex. There are two types of models that have been proposed for the conventional distillation columns, equilibrium stage model (EQ) and non-equilibrium state model (NEQ). Both of models are suitable to apply for the reactive distillation columns (Luo and Xiao, 2001). Generally, the equilibrium model and the non-equilibrium model consist of the so-called MERQ equations (material balance, energy balance, rate equations for mass transfer, and phase equilibrium at vapor-liquid interface). Since the non-equilibrium

model is much more complex, the equilibrium model is more convenient to be used (Luo and Xiao, 2001).

The equations that the equilibrium stage model are generally called MESH model (Material balance, vapor-liquid equilibrium equations, mole fraction summations, and heat balance). Vapor from the stage below and liquid from the stage above are brought into contact on the stage together. The vapor and liquid leaving the stage are assumed to be in equilibrium with each other (Taylor and Krishna, 2000).

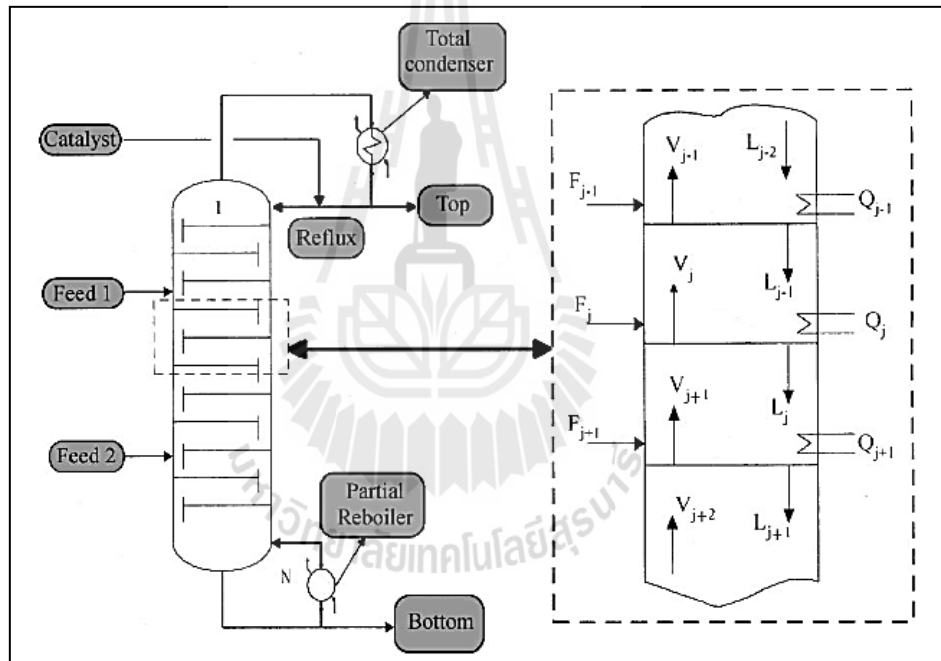


**Figure 3.7** Multi-stage reactive distillation column configurations.

Equilibrium stages in reactive distillation unit are schematically shown in Figure 3.7. The stages are numbered from top of the column (condenser) to the column bottom (re-boiler). In addition, modeling of the equilibrium model comes with assumptions: (i) steady state operation, (ii) the reactions take place entirely in the

bulk liquid phase, (iii) the fugacity coefficients of the vapor phase are unity because of the low pressure, and (iv) the pressure drop along the column is neglected to simplify the calculation. Equations used in this model are as follows:

The component material balance equations:

$$L_{j-1}x_{j-1,i} + V_{j+1}y_{j+1,i} + F_j z_{j,i} - V_j y_{j,i} - L_j x_{j,i} - r_{j,i} = U_j \frac{dx_{j,i}}{dt} \quad (3.2)$$

$$(j=1,2,\dots,N-1; i=1,2,\dots,M)$$

$$L_{N-1}x_{N-1,i} - (V_N y_{N,i} + L_N x_{N,i}) = 0 \quad (3.3)$$

$$(N=\text{stage re-boiler}; i=1,2,\dots,M)$$

$$V_1 y_{1,i} - (L_0 + LD)x_{0,i} = 0 \quad (3.4)$$

$$(0 \text{ stage condenser}; i=1,2,\dots,M)$$

where  $LD$  is liquid flow from the condenser,  $\text{mol h}^{-1}$ .

$F_j$  is feed flow rate,  $\text{mol h}^{-1}$ .

$L_j$  is liquid flow rate,  $\text{mol h}^{-1}$ .

$V_j$  is vapor flow rate,  $\text{mol h}^{-1}$ .

$M, N$  are number of components and stages, respectively.

$r_{j,i}$  is reaction rate of  $i$  component on stage  $j$ ,  $\text{mol h}^{-1}$ .

$U_j$  is liquid hold-up on stage  $j$ ,  $\text{mol}$ .

$x_{i,j}, y_{i,j}$  are mole fraction of component  $i$  in liquid and vapor phase, respectively, at stage  $j$ .

$z_{i,j}$  is molar composition of component  $i$  at the feed stage  $j$

The phase equilibrium equations:

$$y_{j,i}P = x_{j,i}\gamma_i P_i^* \quad (j=1,2,\dots,N; i=1,2,\dots,M) \quad (3.5)$$

where  $P$  is pressure, Pa.

$P_i^*$  is saturated vapor pressure of component  $i$ , Pa.

$\gamma_i$  is activity coefficients of component  $i$ .

The summation equations:

$$\sum_{i=1}^M x_{j,i} - 1 = 0 \quad (j=1,2,\dots,N) \quad (3.6)$$

$$\sum_{i=1}^M y_{j,i} - 1 = 0 \quad (j=1,2,\dots,N) \quad (3.7)$$

And the energy balance equations:

$$L_{j-1}H_{j-1}^L + V_{j+1}H_{j+1}^V + F_jH_j^F - L_jH_j^L - V_jH_j^V + Q_r = 0 \quad (3.8)$$

$$(j=1,2,\dots,N-1)$$

$$L_{N-1}H_{N-1}^L - (V_NH_N^V + L_NH_N^L) + Q_b = 0 \quad (N^{\text{th}} \text{ stage re-boiler}) \quad (3.9)$$

$$V_1H_1^V - (L_0 + LD)H_N^L + Q_c = 0 \quad (0^{\text{th}} \text{ stage condenser}) \quad (3.10)$$

where  $H_j^F$  is feed enthalpy of component  $j$ ,  $\text{J mol}^{-1}$ .

$H_j^L$  is liquid enthalpy of component j, J mol<sup>-1</sup>.

$H_j^V$  is vapor enthalpy of component j, J mol<sup>-1</sup>.

$Q_b$ , is heat duty of reboiler, J h<sup>-1</sup>.

$Q_c$  is heat duty of condenser, J h<sup>-1</sup>.

$Q_r$  is heat of reaction, J h<sup>-1</sup>.

### 3.4.3 DSTWU model

The DSTWU model stands for DiSTillation-Winn-Underwood. This model is suitable for both binary and multicomponent systems. The DSTWU model is developed for the systems presented constant relative volatility by performing a Winn-Underwood-Gilliland shortcut design calculation for a single feed, two products distillation column, with a partial or total condenser (Bruce, 2006 and Ralph, 2010).

The DSTWU model is based on the Gilliland correlation which relates minimum and operating reflux ratios,  $RR_{min}$  and  $RR$ , to minimum and actual number of theoretical stages,  $N_{min}$  and  $N$ . The Gilliland correlation, which developed by Molokanov et al. in 1972, is shown in equation (3.11) (Ralph, 2010).

$$\frac{N - N_{min}}{N + 1} = 1 - \exp\left(\frac{1 + 54.4X}{11 + 117.2X} \left(\frac{X - 1}{X^{0.5}}\right)\right) \quad (3.11)$$

where 
$$X = \frac{RR - RR_{min}}{RR + 1} \quad (3.12)$$

The minimum reflux ratio ( $RR_{min}$ ) is obtained from Underwood's correlation (1946) which is shown in equation (3.13).

$$RR_{min} + 1 = \sum_i \frac{\alpha_i x_{i,D}}{\alpha_i - \theta} \quad (3.13)$$

where  $x_{i,D}$  is the mole fraction of component  $i$  in the distillate.

$\alpha_i$  is the relative volatility of component  $i$ .

$\theta$  is the root of equation calculated from equation (3.14).

$$1 - q_F = \sum_i \frac{\alpha_i z_i}{\alpha_i - \theta} \quad (3.14)$$

where  $z_i$  is the mole fraction of component  $i$  in feed.

$q_F$  is the mole of saturated liquid on the feed tray per mole of feed.

The Winn's method (1958), which is a modification of the Fenske's equation, is used to calculate the minimum number of total stages ( $N_{min}$ ) as shown in equation (3.15).

$$N_{min} = \frac{\ln \left[ \frac{x_{LK,D}}{x_{LK,BP}} \left( \frac{x_{HK,BP}}{x_{HK,D}} \right)^{\theta_{LK}} \right]}{\ln \beta_{LK/HK}} \quad (3.15)$$

where  $BP$  is the bottom product of the column.

$D$  is the distillate of the column.

$HK$  is the heavy key component.

$LK$  is the light key component.

$x$  is mole fraction of liquid phase.

$\beta_{LK/HK}$  and  $\theta_{LK/HK}$  are constants at a fixed pressure and can be estimated from the K-values for the light key and heavy key at the top and bottom temperature.  $\beta_{LK/HK}$  and  $\theta_{LK/HK}$  are related to each other by

$$\beta_{LK/HK} = \frac{K_{LK}}{(K_{HK})^{\theta_{LK}}} \quad (3.16)$$

The DSTWU model is normally used to estimate one of the following variables:

- Reflux ratio at a given number of theoretical stages
- Number of theoretical stages at a given reflux ratio

#### 3.4.4 RADFRAC model

The RADFRAC model is the rigorous distillation modeling workhorse of Aspen Plus simulator. It is based on the inside-out formulation of Boston and Sullivan (1974), which employs a reorganization of the basic equations and the sequence of calculation. The inside-loop convergence methods used in inside-out algorithms for RADFRAC model are Broyden, Wegstein, Newton, and Schubert methods. Detailed description of the method may be found in Seader and Henley (1998) (Ralph, 2010 and Aspen plus reference, Aspen plus simulator V7.3.2).

RACFRAC model is suitable for all types of multistage vapor-liquid fractionation operations such as ordinary distillation, absorption, stripping, extractive and azeotropic distillation. Moreover, it can be used to model columns in which chemical reactions occur. Reactions can have fixed conversion or they can be the equilibrium or rate-controlled as well as electrolytic reaction. They can also occur in either liquid and/or vapor phase (Aspen plus reference, Aspen plus simulator V7.3.2).

### 3.5 Methodology

The preliminary processes to produce ethyl lactate from fermentation-derived magnesium lactate esterification with ethanol in homogeneous phase catalytic by sulfuric acid were designed and modeled using Aspen Plus simulator (Aspen, Version 7.3.2). Since this thesis was a part of project that had objective to study the feasibility of ethyl lactate production from fermentation-derived magnesium lactate. Magnesium lactate was produced in small capacity of batch fermentation process. Thus, the process capacity of the process design was aimed to handle 50 liters of fermentation broth daily. The operation was at atmospheric pressure.

The reaction was carried out in the reactive distillation column which represented by RADFRAC module. Ethyl lactate, which is the desired product of this process, was purified by a series of fractional distillation columns. Efficiency of two process schemes was investigated and compared. In the first scheme, Process A, ethyl lactate was emitted from the top of the reactive distillation column along with other light compounds in the process, i.e. ethanol and water. In Process B, on the other hand, ethyl lactate was discharged from the bottom of reactive distillation column. The bottom product stream in Process B mainly consisted of unreacted lactic acid, sulfuric acid, and magnesium sulfate, which were regarded as heavy components.

All columns in the processes were designed as tray-type in order to avoid clogging of magnesium sulfate in the packing materials. The stages are numbered from top to bottom of the column. Therefore, a condenser is the 1<sup>st</sup>-stage and a reboiler is the n<sup>th</sup>-stage. In both processes, excess ethanol was fed back as the recycle stream. Optimal conditions and configurations of the process in all schemes were

investigated by sensitivity analysis and optimization method. Overall yield of ethyl lactate produced from Process A and Process B were compared.

### 3.5.1 Phase Equilibrium and Kinetic Modeling

In order to design the reactive distillation process, phase equilibrium and reaction kinetic data are needed. It is assumed in this study that the vapor phase is ideal gas. The activities of components in non-ideal liquid phase were related to their activity coefficient ( $\gamma$ ), which were calculated using UNIQUAC model. The binary interaction parameters were obtained from Delgado et al. (2007).

In this study, the kinetic parameters of esterification of lactic acid in fermentation-derived magnesium lactate solution with ethanol using sulfuric acid as homogeneous catalyst was obtained from previous chapter. Due to the non-idealities of the reaction mixture the reaction rate is expressed in term of activity ( $a$ ) instead of concentration as shown in equation (3.17).

$$-r_{LA} = k_1(a_{EtOH}a_{LA}) - k_{-1}(a_{EtLA}a_W) \quad (3.17)$$

where  $a_i$  is the activity of component  $i$ .

$k_1$  is the forward reaction rate constant,  $s^{-1}$ .

$k_{-1}$  is the backward reaction rate constant,  $s^{-1}$ .

The reaction rate constant for forward ( $k_1$ ) and backward ( $k_{-1}$ ) reaction are function of reaction temperature as expressed in equation (3.18) and (3.19), respectively.

$$k_1 = 13300s^{-1} \exp\left(-\frac{30400J/mol}{RT}\right) \quad (3.18)$$

$$k_{-1} = 0.799s^{-1} \exp\left(-\frac{7022.67J/mol}{RT}\right) \quad (3.19)$$

where  $R$  is the universal gas constant,  $J\ mol^{-1}\ K^{-1}$ .

$T$  is absolute temperature, K.

In order to enhance forward reaction and increase yield of ethyl lactate in the process with limitation of kinetic information of reaction and concerning of process economical, the initial molar ratio of ethanol-to-lactic acid of 3:1 and catalyst loading of 2 v/v% were selected to be used in the process design.

### 3.5.2 Simulation and Optimization

The process simulation was carried out using Aspen Plus simulator equipped with RADFRAC module, which is normally used for rigorous modeling of distillation process. Since the reaction solution has highly non-ideal behavior, the strongly non-ideal liquid convergence method was selected. Maximum number of iteration for convergence of the simulation was fixed at fifty. The manipulated variables in optimization of the RD column in Process A and B were the distillate rate or bottom rate and the reflux ratio. The target variables, which were also used to evaluate the process efficiency, were conversion of lactic acid ( $X_{LA}$ ) in esterification reaction and overall yield of ethyl lactate ( $Y_{EiLA}$ ) achieved in the final products. Both terms are defined in equation (3.20) and (3.21).

$$X_{LA} = \frac{\text{Mole of ethyl lactate produced in RD column}}{\text{Mole of lactic acid in process feed}} \quad (3.20)$$

$$Y_{EiLA} = \frac{\text{Mole of ethyl lactate in final product}}{\text{Mole of lactic acid in process feed}} \quad (3.21)$$

### 3.6 Results and Discussion

The synthesis of ethyl lactate by esterification of fermentation-derived magnesium lactate was designed to handle 50 liters of magnesium lactate fermentation broth per day. Technical assessments of two processes are performed as previously mentions. Two feed streams were introduced into the reactive distillation unit of each process. The first feed stream was lactic acid solution prepared by acidification of magnesium lactate powder obtained from lactic acid fermentation. The second feed stream was absolute ethanol. Sulfuric acid, the homogeneous catalyst for esterification reaction, was mixed with the lactic acid feed stream before being charged into the column. The composition of each feed stream and the molar flow rate of each composition in the feeds based on 3:1 of initial molar ratio of ethanol-to-lactic acid and 2 v/v% of catalyst loading were showed in Table 3.1.

**Table 3.1** Composition and molar flow rate of feed streams.

Feed stream	Composition	Normal boiling point (°C)	Molar flow rate (mol/hr)	Mole fraction
F1	Lactic acid	216.63	2.120	0.0773
	Water	100.02	23.530	0.8590
	Magnesium sulfate	9726.85	1.370	0.0500
	Sulfuric acid	274.80	0.380	0.0137
F2	Ethanol	78.31	6.350	1

From Table 3.1, F1 and F2 represented lactic acid and ethanol feed stream, respectively. The normal boiling point of each composition was obtained from ASPEN Plus simulator data base.

### 3.6.1 Process A Configuration

In Process A, ethyl lactate was removed from reactive distillation column after it was produced via top product stream of the column. The ester was purified with a series of fractional distillation column. The process flow sheet of this scheme is displayed in Figure 3.8. This process consists of one reactive distillation column (RD), three fractional distillation columns (DIS1, DIS2 and DIS3), one mixer (M1) and two heaters (HEAT1 and HEAT2).

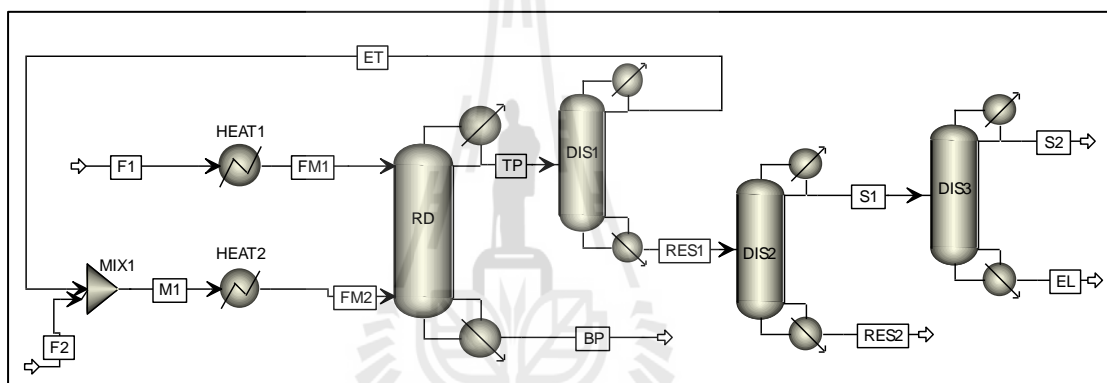


**Figure 3.8** Process flow sheet of Process A.

Lactic acid was charged to the reactive distillation column as acidified magnesium lactate solution in feed stream F1, while absolute ethanol was charged in feed stream F2. Ethyl lactate was produced in the reactive distillation column and removed with the top product stream TP. Since the normal boiling points of ethanol and water were lower than the normal boiling point of ethyl lactate, therefore, the stream TP contains excess ethanol, by-product water in addition to the desired product ethyl lactate. Heavy product of the reactive distillation column was a mixture of unreacted lactic acid, sulfuric acid, and a major process impurity magnesium sulfate,

which is discharged from reactive distillation column in a bottom product stream BP. Stream TP was fed to the first distillation column, DIS1, to partially remove excess ethanol and recycle it back to the reactive distillation column via stream ET. The bottom product of DIS1 column was fed to the second distillation column, DIS2, via the stream RES1. The main purpose of this column was to remove the rest of unreacted lactic acid and the remained sulfuric from the product stream. These components were discharged from the process via stream RES2. The top product stream of DIS2 column was, then, sent to the last distillation column, DIS3, where all the remained ethanol and some of water were separated out of the process via stream S2. The final product from this process is received as an aqueous solution of ethyl lactate in stream EL.

### 3.6.1.1 Reactive Distillation Column, RD

Initial specification and operating parameters of the reactive distillation column are shown in Table 3.2. The feed stages are fixed at stage 2<sup>nd</sup> for feed stream F1 and stage N-1<sup>th</sup> for feed stream F2 where N is the total number of the stages in the column.

The appropriate total number of the stages of the RD column was investigated by sensitivity analysis. Effect of total number of stages on yield of ethyl lactate produced in the reactive distillation column was studied. The expression of ethyl lactate yield in the reactive distillation column was showed in equation (3.22).

$$\%Y_{RD,A} = \frac{\text{Mole of ethyl lactate in stream TP}}{\text{Mole of lactic acid in feed stream F1}} \times 100\% \quad (3.22)$$

**Table 3.2** Initial specification of reactive distillation column in Process A.

Operating parameter	Value	Unit
Distillate rate (DR)	0.032	kmol/hr
Reflux ratio (RR)	0.001	-
Tray diameter	0.15	m
Tray spacing	0.10	m
Weir height	1	inch
Temperature of feed		
F1	110	°C
F2	75	°C

It was found that ethyl lactate yield ( $\%Y_{RD,A}$ ) was increased with increasing total number of stages. However, the simulation cannot be converged when the total number of stage was higher than 14. This could be due to the limitation of simulation convergence when the maximum number of iterations was set at 50 in order to avoid the multiple optimum of the process. The maximum ethyl lactate yield obtained was 93.60% at the total number of stages was 14. The total number of stages was also found to affect the lactic acid conversion ( $\%X_{RD,A}$ ) and ethyl lactate recovery ( $\%RE_{RD,A}$ ) in the reactive distillation column. These two parameters were determined by equation (3.23) and (3.24).

$$\%X_{RD,A} = \frac{\text{Total mole of ethyl lactate produced in RD column}}{\text{Mole of lactic acid in feed stream F1}} \times 100\% \quad (3.23)$$

$$\%RE_{RD,A} = \frac{\text{Mole of ethyl lactate in stream TP}}{\text{Mole of ethyl lactate produced in RD column}} \times 100\% \quad (3.24)$$

Where total mole of ethyl lactate produced in the reactive distillation column was the summation between mole of ethyl lactate in the stream TP and the stream BP. Influences of total number of stages on each parameter were showed in Figure 3.9.

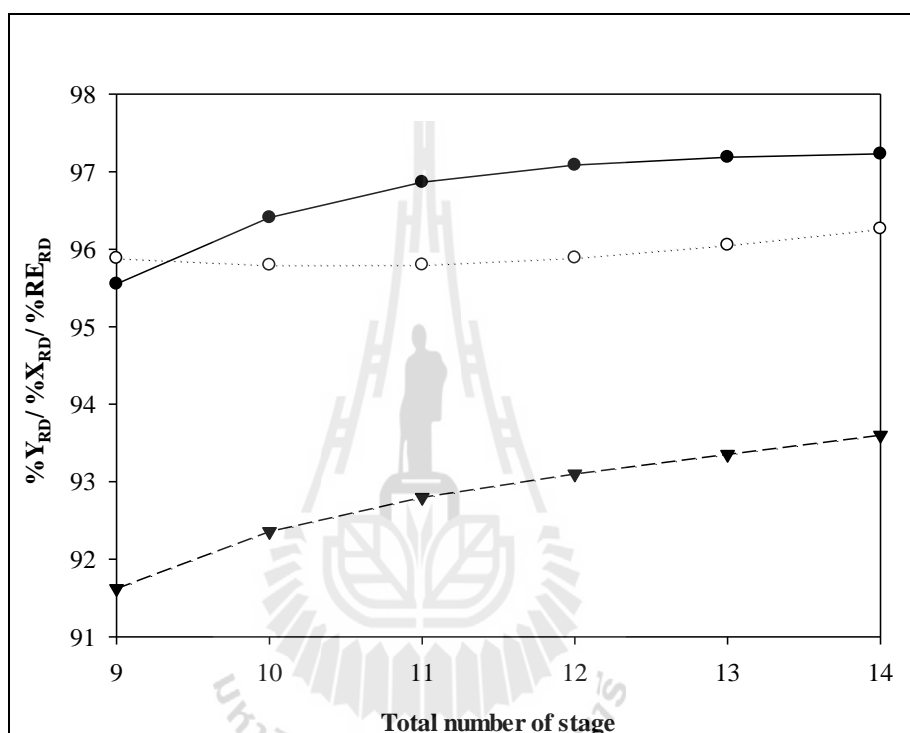


**Figure 3.9** Effect of total number of stages of reactive distillation column in Process A on (●) conversion of lactic acid; (○) recovery of ethyl lactate; (▼) yield of ethyl lactate.

The total number of stages of the reactive distillation column was, therefore, selected to be 14 stages in this process scheme. Other operating parameters of the reactive distillation column, such as distillate rate, reflux ratio, tray space and diameter, feed position, as well as feed temperature were also investigated

by sensitivity analysis and optimization. When one parameter was studied, other parameters were fixed at their initial values.

The molar distillate rate of the reactive distillation column (kmol/hr) was studied by sensitivity analysis method. The results were showed in Figure 3.10. It was found that the yield of ethyl lactate produced in this column was increased with the distillate rate. The rate of distillate has an effected on ethyl lactate flow rate in the stream TP and the yield of ethyl lactate. The highest yield of ethyl lactate was obtained when the distillate rate equaled to 0.032 kmol/hr.

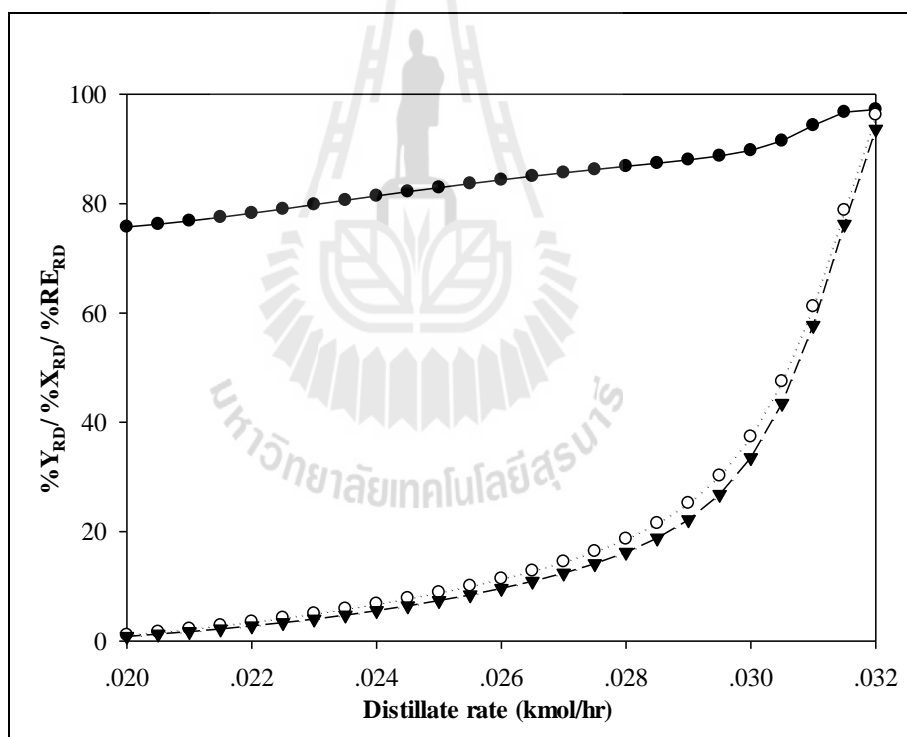


**Figure 3.10** Effect of molar distillate rate of reactive distillation column in Process A on (●) conversion of lactic acid; (○) recovery of ethyl lactate; (▼) yield of ethyl lactate.

Influence of molar reflux ratio of the reactive distillation column on the yield of ethyl lactate was analyzed using the same method and the results were showed in Figure 3.11. It can be seen that increasing reflux ratio seemed to reduce the yield of ethyl lactate. Since reflux ratio is the ratio of reflux flow rate to the distillate flow rate. Increasing of the reflux ratio increased amount of product fed to the column via reflux stream. As the nature of esterification reaction is reversible process therefore ethyl lactate has a chance to react with water via backward reaction due to high quantity of water in the column. Conversion of lactic acid was significantly decreased due to higher amount of product.

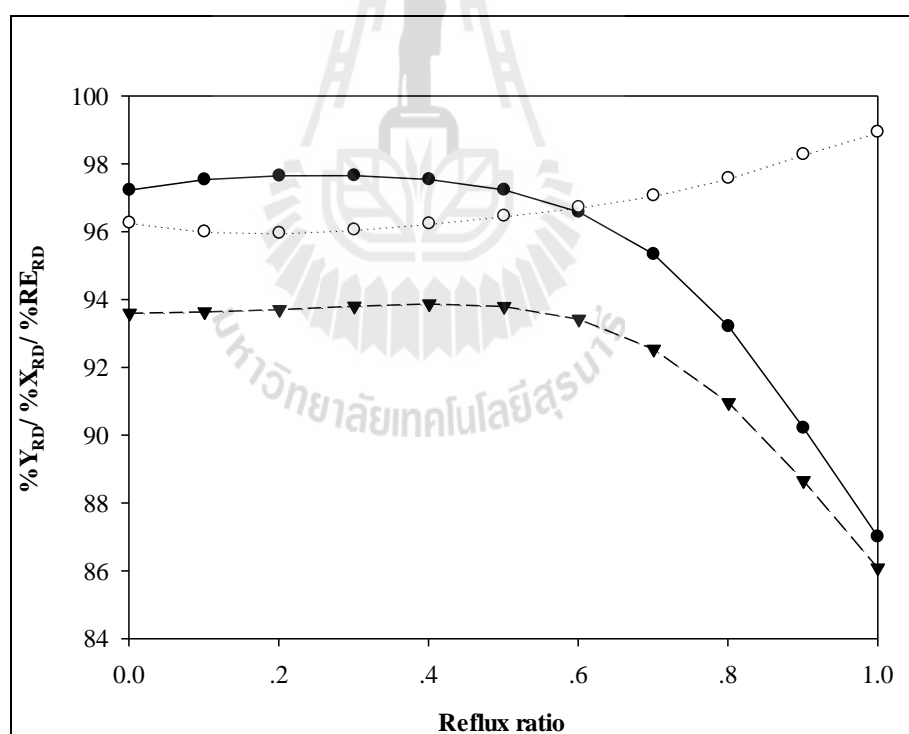


**Figure 3.11** Effect of reflux ratio of reactive distillation in Process A on

(●) conversion of lactic acid; (○) recovery of ethyl lactate;

(▼) yield of ethyl lactate.

Sensitivity analysis to explore effect of distillate rate combined with reflux ratio on yield of ethyl lactate in reactive distillation column was also investigated. When consider influence of distillate rate and reflux ratio at the same time, if the distillate rate lower than 0.029 kmol/hr and the reflux ratio higher than 0.1 the simulation can not be converged due to the complexity of the model. Therefore, the range of distillate rate and reflux ratio used in simultaneously sensitivity were 0.029-0.032 kmol/hr and 0.001-0.1, respectively. The results were showed in Figure 3.12 and it was found that the highest yield of ethyl lactate obtained when distillate rate was 0.032 kmol/hr and reflux ratio was 0.001.

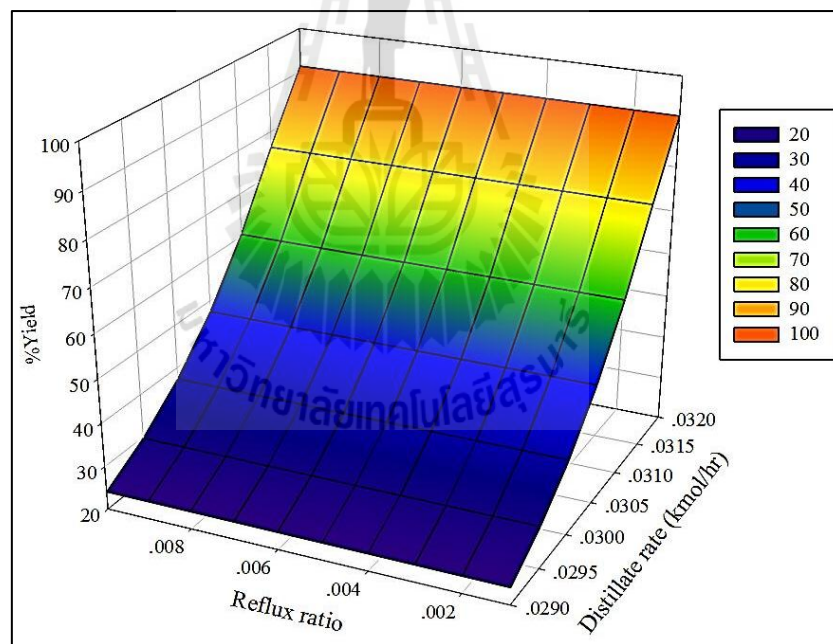


**Figure 3.12** Influence of the distillate rate and reflux ratio of reactive distillation column in Process A on yield of ethyl lactate.

The lactic acid feed flow rate that corresponds to the process capacity for handling 50 liters of fermentation broth per day was approximately to

2.120 mol/hr or 0.191 kg/hr, therefore, the column to use in this process should not have too large configurations. The effect of tray specifications such as tray diameter and tray spacing on yield of ethyl lactate, conversion of lactic acid as well as recovery of ethyl lactate was investigated by sensitivity analysis. The range of both parameters in the study was 0.1 to 0.5 m. The results shown in Figure 3.13 and indicated that increasing of both tray diameter and tray spacing decreased the yield of ethyl lactate. Since the reaction in this process was assumed to occur only in liquid phase, contact between ethanol vapor and lactic acid in the liquid phase might be decreased if the column were too large in diameter or in tray spacing. This led to the decrease in conversion of lactic acid and yield of ethyl lactate. The suitable tray diameter and tray spacing were found to be 0.1 m with weir height of 1 inch.

In addition, the influences of feed stage and feed temperature were studied. Since the first stage and the last stage of the column are condenser and reboiler units therefore the feed stage was varied from 2<sup>nd</sup>-13<sup>th</sup> stage. In the counter-current flow column, the heavier reactant liquid phase flow down and reacted with the lighter reactant, which is in the flow up gas phase. Then, lactic acid feed stream F1 was varied from 2<sup>nd</sup> stage to 7<sup>th</sup> stage, and ethanol stream F2 was varied from 8<sup>th</sup> stage to 13<sup>th</sup> stage.

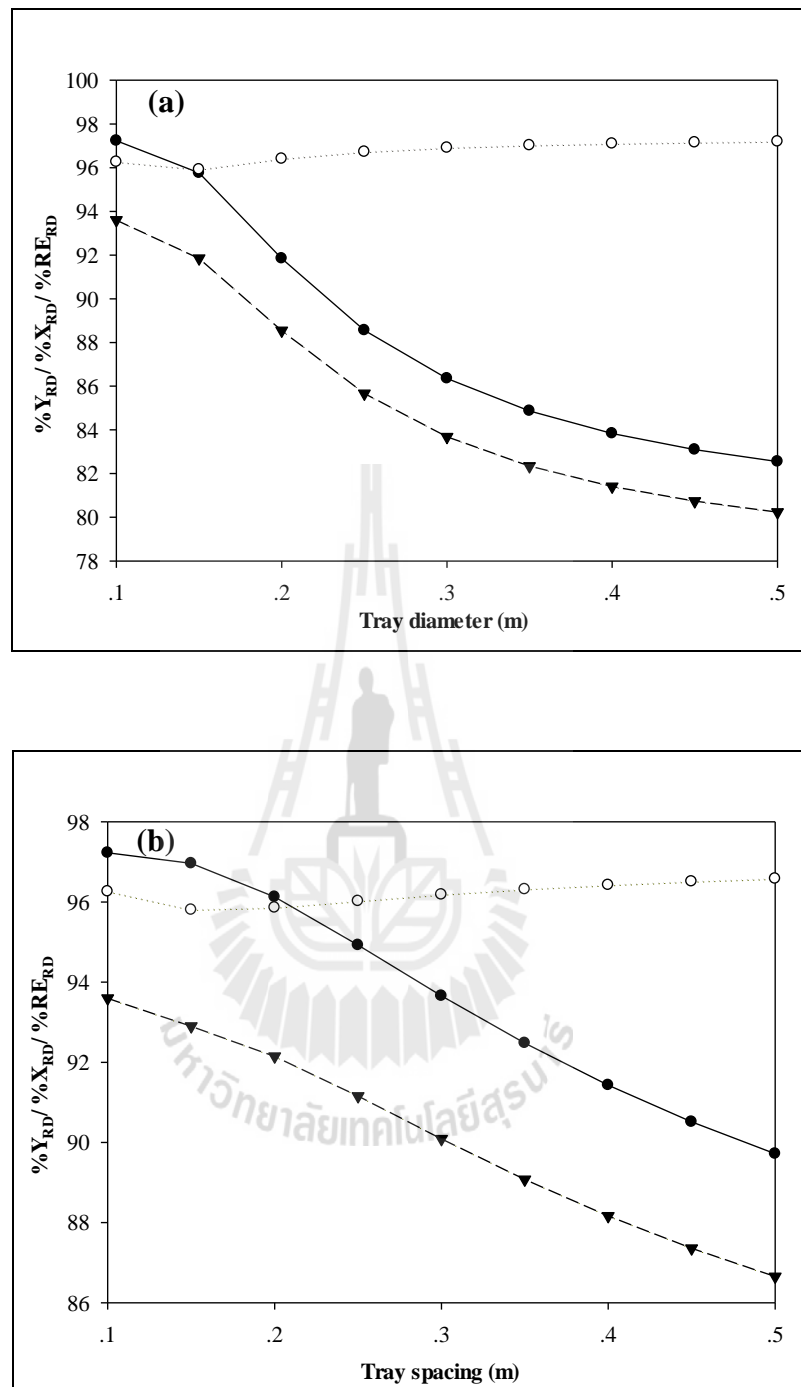


**Figure 3.13** Sensitivity analysis of (a) effect of tray diameter and (b) effect of tray spacing on (●) conversion of lactic acid; (○) recovery of ethyl lactate; (▼) yield of ethyl lactate in reactive distillation column of Process A.

Influence of feed stage on yield of ethyl lactate is shown in Figure 3.14. As expected, the yield of ethyl lactate depended on the feed position of both feed streams. The higher the lactic acid stream and the lower the ethanol stream were fed, the reaction section in the reactive distillation column was extended. The reactants had more time to contact and react with each other, so the acid conversion was increased. The maximum yield of ethyl lactate was obtained when the feed stage of F1 and F2 stream were at the 2<sup>nd</sup> and 13<sup>th</sup> stage, respectively.

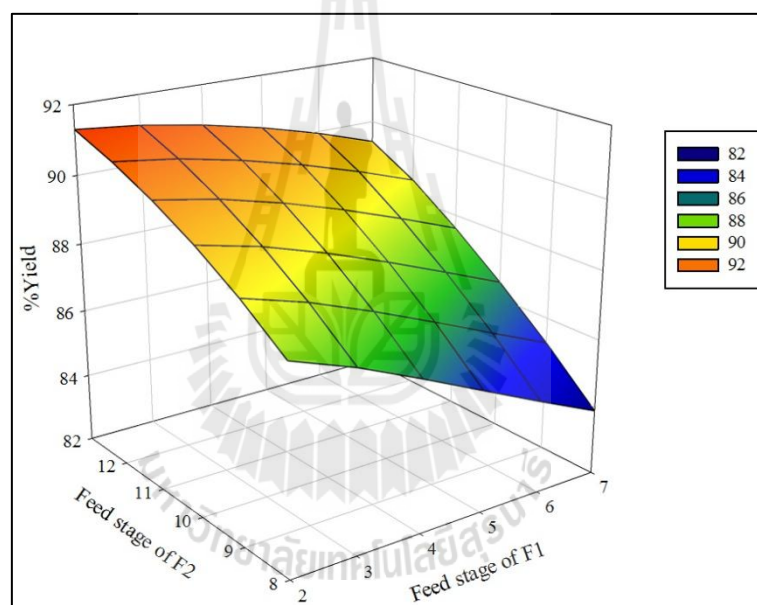


**Figure 3.14** Influence of feed stage on yield of ethyl lactate in reactive distillation column of Process A.

Influence of feed temperature on yield of ethyl lactate was also studied, and the result was showed in Figure 3.15. It was found that yield of ethyl lactate was lower than 70% when the temperature of stream F1 was lower than 105°C and temperature of stream F2 was higher than 75°C.

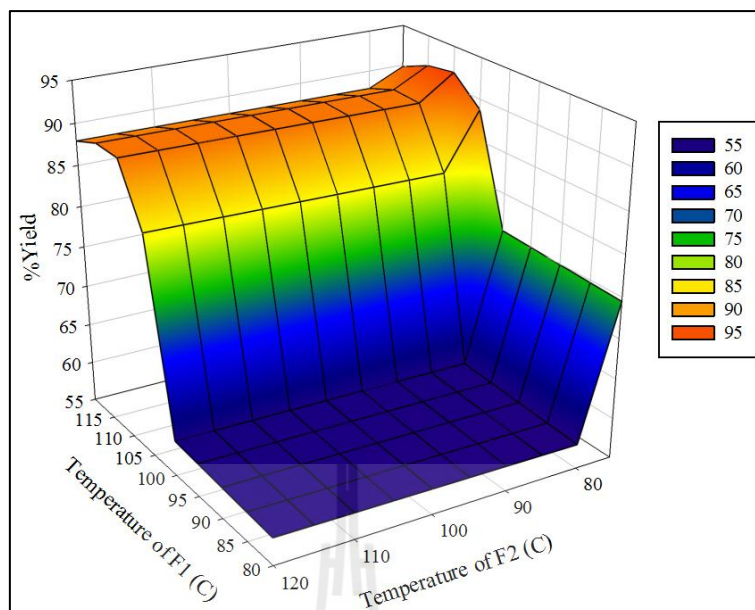


**Figure 3.15** Influence of feed temperature on yield of ethyl lactate in reactive distillation column of Process A.

When temperature of stream F1 was lower than 105°C, water which was the main component of stream F1 may not be evaporated and still remained in the liquid phase. Since water was one of the reaction products, it can be reacted with ethyl lactate which produced in the column and lead to reduce yield of ethyl lactate. If the temperature of stream F1 was higher than 105°C, water would easily evaporate and leave the column with stream TP and it would not interfere with the reaction. For ethanol stream F2, if its temperature was higher than 75°C, the yield of ethyl lactate was quite lower than that obtained from temperature of 75°C. Since the reaction was assumed to be occurred in liquid phase, increasing ethanol temperature higher than 75°C not affected to the reaction. The optimal feed temperatures were 110°C and 75°C for stream F1 and F2, respectively.

Temperature, molar flow rate and composition of each stream involving in the reactive distillation column of Process A were showed in Table 3.3. Conversion of lactic acid obtained from this column was 97.21%, yield of ethyl lactate produced was 93.58% with the recovery of ethyl lactate in the top product stream of 96.27%.

**Table 3.3** Stream composition of reactive distillation in Process A.

Description	Stream			
	F1	F2	TP	BP
Temperature (°C)	110.00	75.00	88.10	258.15
Molar flow rate (mol/hr)	27.390	6.350	32.000	1.740
Component mole fraction				
Ethanol	0	1	0.13378	0.00635
Lactic acid	0.07730	0	0.00184	0.00008
Ethyl lactate	0	0	0.06191	0.04424
Water	0.85900	0	0.79950	0.00004
Sulfuric acid	0.01370	0	0.00297	0.16117
Magnesium sulfates	0.05000	0	0	0.78813

### 3.6.1.2 First Fractional Distillation Column, DIS1

The top product stream TP from the reactive distillation column was fed to the first distillation column, DIS1, to remove some of the excess ethanol and recycle it back to the reaction. The bottom product of DIS1 column was fed to the next column to increase the purity of ethyl lactate.

The column specification of DIS1 was preliminary designed using DSTWU model of distillation column to find minimum number of stages and

minimum reflux ratio. The DSTWU model is based on Gilliland correlation. In simulation, water was specified to be the heavy key component and ethanol was the light key component. The minimum number of stages was designed for recovery 100% of ethanol in the stream ET. The results of DSTWU model for DIS1 column are shown in Table 3.4. The minimum number stages of DIS1 column was found to be 9.6 stages, therefore, the number of stages for DIS1 column was specified as 10 stages. The stream TP from the reactive distillation column was fed into the first distillation column, DIS1 at the 5<sup>th</sup> stage and the reflux ratio of this column was 0.5.

**Table 3.4** Specification of DIS1 column in Process A from DSTWU model.

Parameter	Value	Unit
Minimum reflux ratio:	0.368	
Actual reflux ratio:	0.500	
Minimum number of stages:	9.613	
Number of actual stages:	21.156	
Feed stage:	4.225	
Number of actual stages above feed:	3.225	
Reboiler heating required:	163.333	W
Condenser cooling required:	151.667	W
Distillate temperature:	80.150	°C
Bottom temperature:	99.580	°C
Distillate to feed fraction:	0.294	

The configuration of DIS1 column obtained from DSTWU model was applied to the RADFRAC model to find the optimal distillate rate and reflux ratio. Column specification, such as, tray diameter and spacing was fixed to be the same as in RD column. Optimization of DIS1 column was performed in order to

determine the optimal molar distillate rate and reflux ratio to recover ethanol in the stream ET. The optimization result indicated that the optimal molar distillate rate and reflux ratio of DIS1 column to obtain maximum recovery of ethanol in the stream ET were 0.069 kmol/hr and 3.728, respectively.

### 3.6.1.3 Reactive Distillation Column and First Fraction Distillation with Recycle Stream

The recycle stream ET from DIS1 column was recycled and mixed with fresh ethanol in a mixture M1 before being injected to the reactive distillation column. The manipulated variables, i.e. distillate rate and reflux ratio, of the reactive distillation column were needed to re-optimize. The process schematic for operation of the reactive distillation column and the fractional distillation column DIS1 with recycle stream is shown in Figure 3.16. Two heat exchangers, HEAT1 and HEAT2, were used to heat up the lactic acid feed stream F1 to 110°C and ethanol feed stream F2 to 75°C, respectively.

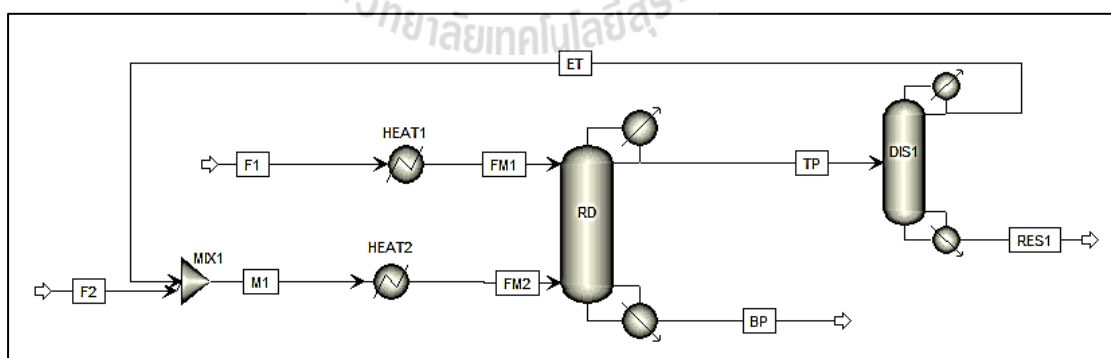


**Figure 3.16** Process schematic for operation of reactive distillation column and fractional distillation column DIS1 with recycle stream.

In optimization with recycle stream, the sequence of simulation and tear stream have to be defined. The sequence of simulation was started with RD column, DIS1 column, MIX1, and HEAT2, respectively. Tear stream was selected to be the stream FM2.

The optimization was operated to find the maximum yield of ethyl lactate produced in reactive distillation column plus column DIS1 with recycle stream. The yield of ethyl lactate in this step was defined in equation (3.25).

$$\%Y_{D1,A} = \frac{\text{Mole of ethyl lactate in stream } RES1}{\text{Mole of lactic acid in feed stream } F1} \times 100\% \quad (3.25)$$

It was found from process optimization that the optimal molar distillate rate and reflux ratio of reactive distillation column were 0.03913 kmol/hr and 0.001, respectively.

The liquid phase molar composition in the reactive distillation column after optimization was shown in Figure 3.17. It can be seen that composition of top product stream, which was the composition in the condenser or the 1<sup>st</sup> stage, were mainly consisted of water, ethanol and ethyl lactate. Since ethanol was impurity of ethyl lactate solution and high amount of ethanol still remained in the product stream therefore it needed to be removed by another distillation column.

The temperature profile of reactive distillation column after optimization was displayed in Figure 3.18. It was found that vapor phase and liquid phase temperature trended to be decreased with the stage number from the lower stage to the upper stage, from the 13<sup>th</sup> stage to the 2<sup>st</sup> stage, except the liquid phase at the 13<sup>th</sup> stage. Liquid phase temperature was found to be the lowest at this stage because

this stage was the feed location of stream F2 which was fed to the reactive distillation column with temperature of 75°C. Moreover, condenser reboiler temperatures were found to be about 84°C and 254°C, respectively.

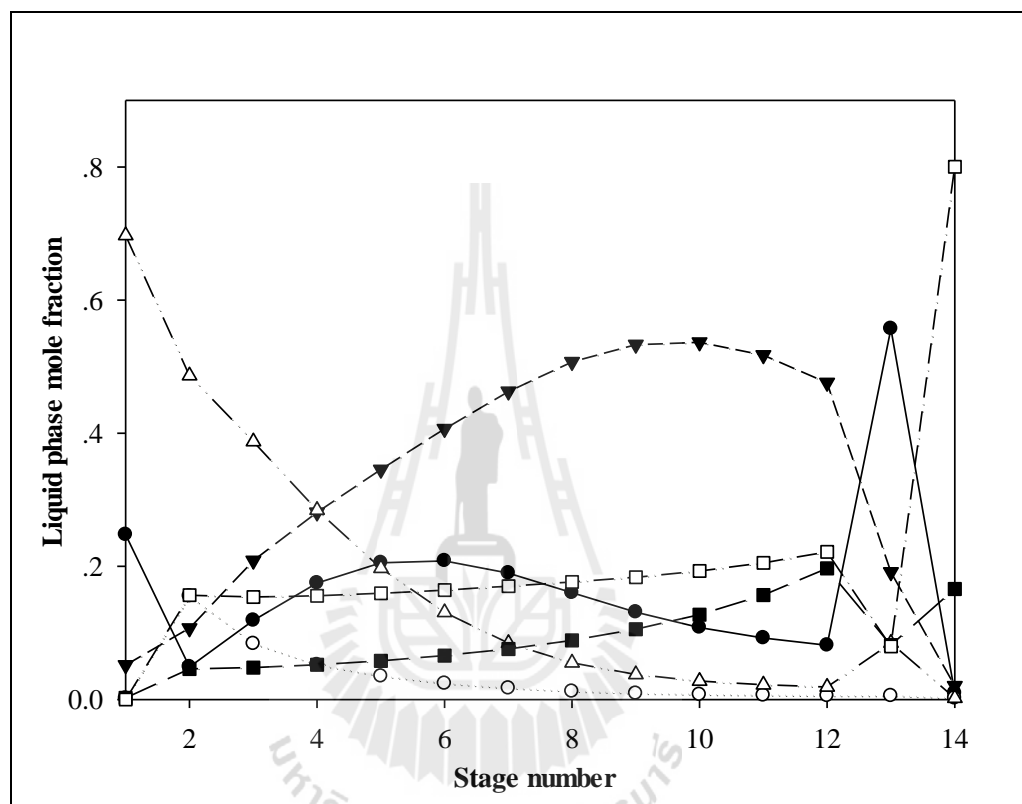


**Figure 3.17** Liquid phase molar composition in reactive distillation of Process A:

- (●) Ethanol; (○) Lactic acid; (▼) Ethyl lactate; (△) Water;
- (■) Sulfuric acid; (□) Magnesium sulfate.

In addition, molar ratio of ethanol-to-lactic acid (E/L) in each stage of reactive distillation column was shown in Figure 3.19. It can be seen that even the initial fresh feed molar ratio of ethanol-to-lactic acid used in the process was 3-to-1 but molar ratio of ethanol-to-lactic acid in each stage was not at the initial condition. That could be due to changing of liquid composition in each stage from

both of reaction and separation influences simultaneously. In the reactive distillation column, reaction was occurred from the 2<sup>nd</sup> stage to 13<sup>th</sup> stage, thus molar ratio of ethanol-to-lactic acid in each stage was not constant. In the 13<sup>th</sup> stage, ethanol was fed to the column and small of lactic acid, which fed at the 2<sup>nd</sup> stage, flow down to this stage therefore the highest molar ratio of ethanol-to-lactic acid in the column was observed in this stage. In addition, kinetic information with the effect of this parameter should be used in the process design in order to consider effect of molar ratio of ethanol-to-lactic acid in the reactive distillation column.

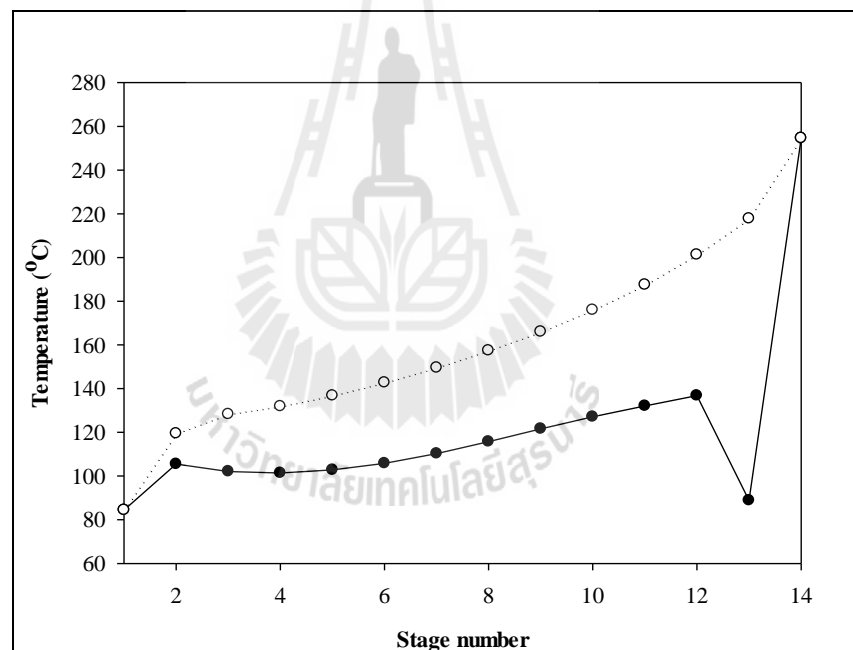


**Figure 3.18** Temperature profile of reactive distillation column of Process A;

(●) liquid phase temperature and (○) vapor phase temperature.

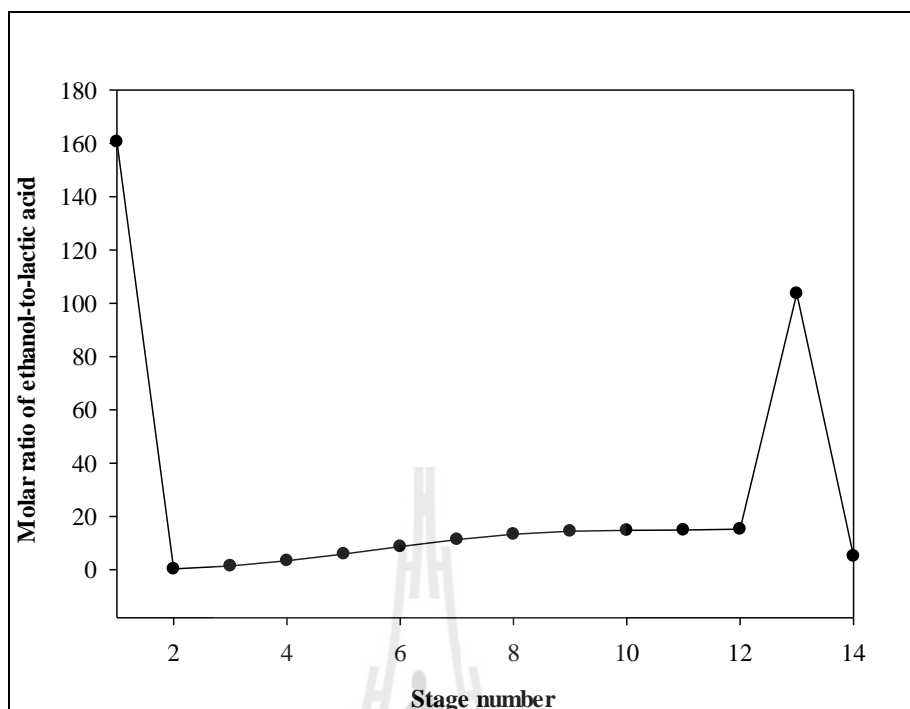


**Figure 3.19** Molar ratio of ethanol-to-lactic acid profile in the reactive distillation column in Process A.

Moreover, composition of each stream in this process was displayed in Table 3.5. It can be seen from Table 3.5 that the unreacted lactic acid and some of sulfuric acid still remained in product stream RES1. These two components could be evaporated and amalgamated in the stream TP due to high temperature of reboiler stage, as can be seen at the 14<sup>th</sup> stage in Figure 3.18. Therefore, they must be removed from the desired product using another fractional distillation column.

**Table 3.5** Stream composition in Process A with reactive distillation column and first fractional distillation column with ethanol recycle.

Description	Stream						
	FM1	M1	FM2	BP	TP	ET	RES1
Temperature (°C)	110.00	53.36	75.00	254.58	84.42	78.40	88.14
Molar flow rate (mol/hr)	27.390	13.450	13.450	1.710	39.130	7.100	32.030
Component mole fraction							
Ethanol	0	0.87361	0.87361	0.00962	0.24746	0.76063	0.13364
Lactic acid	0.07730	0	0	0.00189	0.00154	0	0.00188
Ethyl lactate	0	0	0	0.02042	0.05159	0.00001	0.06303
Water	0.85900	0.12639	0.12639	0.00179	0.69708	0.23936	0.79860
Sulfuric acid	0.01370	0	0	0.16599	0.00233	0	0.00285
Magnesium sulfate	0.05000	0	0	0.80029	0	0	0

### 3.6.1.4 Second Fractional Distillation Column, DIS2

The second distillation column was needed in order to remove unreacted lactic acid and sulfuric acid from the desired product. The column specification of DIS2 column was firstly investigated by DSTWU model using the same procedure as DIS1 column. In this unit, ethyl lactate and lactic acid were defined as light key and heavy key component, respectively. The minimum number of stages was designed for 100% recovery of ethyl lactate in stream S1 and 100% recovery of lactic acid in stream RES2.

The results of DSTWU model for DIS2 column are shown in Table 3.6. The minimum number of stage of DIS2 column was found to be 9.7 stages, therefore, the number of stage was specified as 10 stages. The feed stage was the 8<sup>th</sup> stage and the reflux ratio was 0.5.

**Table 3.6** Specification of DIS2 column in Process A from DSTWU model.

Parameter	Value	Unit
Minimum reflux ratio:	0.016	
Actual reflux ratio:	0.500	
Minimum number of stages:	9.711	
Number of actual stages:	14.974	
Feed stage:	7.259	
Number of actual stages above feed:	6.259	
Reboiler heating required:	560.000	W
Condenser cooling required:	560.000	W
Distillate temperature:	87.95	°C
Bottom temperature:	241.35	°C
Distillate to feed fraction:	0.995	

The second distillation column, DIS2, was connected with reactive distillation column RD and first fractional distillation column DIS1 with recycle stream. The configuration of column DIS2 from DSTWU model was applied with RADFRAC model. Column specification, such as, tray diameter and spacing was fixed to be the same as in reactive distillation column which were 0.1 m both.

Optimization of column DIS2 was done to find the maximum yield of ethyl lactate produced. Recovery of lactic acid in stream RES2 higher than 99.9999% was set to be constraint of optimization. Ethyl lactate yield in this step was calculated as shown in equation (3.26). The optimal molar distillate rate and reflux ratio for column DIS2 were found to be 0.03187 kmol/hr and 0.33339, respectively. The recovery of ethyl lactate in this column was found to be 99.97% and the recovery of lactic acid in stream RES2 was found to be 99.99%. Moreover, maximum yield of

ethyl lactate obtained was 95.33%. The composition of each stream was shown in Table 3.7.

$$\%Y_{D2,A} = \frac{\text{Mole of ethyl lactate in stream S1}}{\text{Mole of lactic acid in stream F1}} \times 100\% \quad (3.26)$$

**Table 3.7** Stream composition obtained from optimization of column DIS2.

Description	Stream								
	FM1	M1	FM2	BP	TP	ET	RES1	S1	RES2
Temperature (°C)	110.00	53.36	75.00	254.58	84.42	78.40	88.14	87.95	239.77
Molar flow rate (mol/hr)	27.390	13.450	13.450	1.710	39.130	7.100	32.030	31.870	0.150
Component mole fraction									
Ethanol	0	0.87361	0.87361	0.00962	0.24746	0.76063	0.13364	0.13428	0.00001
Lactic acid	0.07730	0	0	0.00189	0.00154	0	0.00188	0	0.39668
Ethyl lactate	0	0	0	0.02042	0.05159	0.00001	0.06303	0.06331	0.00335
Water	0.85900	0.12639	0.12639	0.00179	0.69708	0.23936	0.79860	0.80241	0.00014
Sulfuric acid	0.01370	0	0	0.16599	0.00233	0	0.00285	0	0.59982
Magnesium sulfate	0.05000	0	0	0.80029	0	0	0	0	0

As can be seen in Table 3.7, all the remained lactic acid and sulfuric acid were removed from the process via stream RES2. The product stream S1 contained with ethanol, water and ethyl lactate. Ethanol in this stream was the fraction remained from ethanol recovery in DIS1 column; therefore, it is necessary to be removed from the product stream.

#### 3.6.1.4 Last Fractional Distillation Column, DIS3

The last distillation column was used to remove all the remained ethanol from the product in order to obtain aqueous solution of ethyl lactate. As the same as before, DSTWU model was used to find the minimum number of stages of this column. In this unit, ethanol and ethyl lactate were defined as light key

and heavy key component, respectively. The minimum number of stage was designed for 100% recovery of ethanol in stream S2.

The results of DSTWU model for the minimum number of stages was shown in Table 3.8. It was found that the minimum number stages of column was 9.79. Therefore, the total number of stages of 10 was applied for DIS3 column. The feed position of this column was the 9<sup>th</sup> stage.

**Table 3.8** Specification of DIS3 column in Process A from DSTWU model.

Parameter	Value	Unit
Minimum reflux ratio:	0.296	
Actual reflux ratio:	0.500	
Minimum number of stages:	9.797	
Number of actual stages:	19.067	
Feed stage:	8.134	
Number of actual stages above feed:	7.134	
Reboiler heating required:	151.667	W
Condenser cooling required:	140.000	W
Distillate temperature:	79.86	°C
Bottom temperature:	99.42	°C
Distillate to feed fraction:	0.272	

Column DIS3 was applied with RADFRAC model in order to investigate optimal distillate rate and reflux ratio of the column. The tray diameter and tray spacing of this column were also fixed at 0.1 m. The distillate rate and reflux ratio were optimized to obtain maximize yield of ethyl lactate with the constraint of completely removal of ethanol remained in ethyl lactate solution. It was found that when feed location was the 9<sup>th</sup> stage, only 99.89% ethanol can be recovered and the yield of ethyl lactate was 94.33%. In order to obtain the aqueous solution of ethyl

lactate, all ethanol must be removed. Thus, the feed stage was varied to find the optimal location, and it was found that the optimal feed location was at the 6<sup>th</sup> stage. The recovery of ethanol was 99.999% and recovery of ethyl lactate obtained was 97.867%. The optimal molar distillate rate and reflux ratio were 0.008 kmol/hr and 24.565, respectively.

$$\%Y_A = \frac{\text{Mole of ethyl lactate in stream EL}}{\text{Mole of lactic acid in stream FI}} \times 100\% \quad (3.27)$$

The column DIS3 with optimal conditions was connected with the rest of column in the process. It was found that overall yield of ethyl lactate obtained from Process A, where ethyl lactate was collected at the top of the reactive distillation column, was 93.30%. Percentage of ethyl lactate lost in this process was found to be about 3.92%. The overall process flow sheet and stream compositions were shown in Figure 3.20 and Table 3.9, respectively. Specification and heat duty of each operating unit in this process were shown in Table 3.10 and 3.11.

As the results, the product of this process was in form of aqueous solution of ethyl lactate. Quite low concentration of ethyl lactate was obtained. Since the scope of this research was to produce the ethyl lactate by esterification of fermentation-derived magnesium lactate in reactive distillation therefore it was satisfied to produce aqueous solution of ethyl lactate. Hence, the concentration of ethyl lactate aqueous solution produced by Process A was 8.273 mole% or 37.18w/w%.

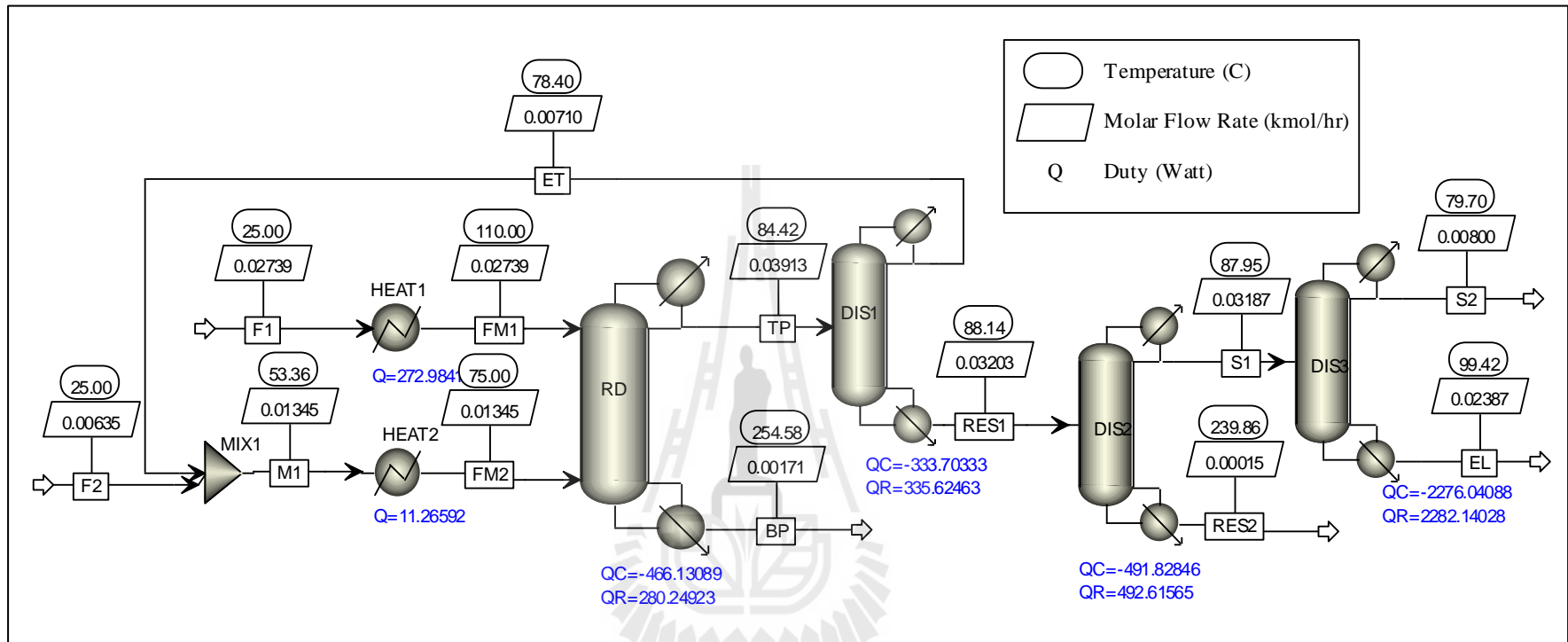


Figure 3.20 Process flow sheet of Process A with optimal condition.

**Table 3.9** Composition of each stream in Process A.

Description	Stream										
	FM1	M1	FM2	BP	TP	ET	RES1	S1	RES2	S2	EL
Temperature (°C)	110.00	53.36	75.00	254.58	84.42	78.40	88.14	87.95	239.77	79.70	99.42
Molar flow rate (mol/hr)	27.390	13.450	13.450	1.710	39.130	7.100	32.030	31.870	0.150	8.000	23.870
Component mole fraction											
Ethanol	0	0.87361	0.87361	0.00962	0.24746	0.76063	0.13364	0.13428	0.00001	0.53500	0
Lactic acid	0.07730	0	0	0.00189	0.00154	0	0.00188	0	0.39668	0	0
Ethyl lactate	0	0	0	0.02042	0.05159	0.00001	0.06303	0.06331	0.00335	0.00538	0.08273
Water	0.85900	0.12639	0.12639	0.00179	0.69708	0.23936	0.79860	0.80241	0.00014	0.45962	0.91727
Sulfuric acid	0.01370	0	0	0.16599	0.00233	0	0.00285	0	0.59982	0	0
Magnesium sulfate	0.05000	0	0	0.80029	0	0	0	0	0	0	0

**Table 3.10** Unit operation specification in Process A.

Specification	Unit					
	HEAT1	HEAT2	RD	DIS1	DIS2	DIS3
Temperature (°C)	110	75	-	-	-	-
Total number of stages	-	-	14	10	10	10
Feed stage	-	-	2 and 13	5	8	6
Column diameter (m)	-	-	0.1	0.1	0.1	0.1
Column spacing (m)	-	-	0.1	0.1	0.1	0.1
Distillate rate (mol/hr)	-	-	39.130	7.100	31.870	8.000
Reflux ratio	-	-	0.001	3.306	0.333	24.565

**Table 3.11** Heat duty of each unit in Process A.

Unit Operation		Heat Duty (W or Js <sup>-1</sup> )
Unit Name	Operation Type	
MIX1	Mixture	-
HEAT1	Heater	272.984
HEAT2	Heater	11.266
RD	Reactive distillation	
Condenser		466.131
Reboiler		280.249
DIS1	Distillation column	
Condenser		333.703
Reboiler		335.625
DIS2	Distillation column	
Condenser		491.828
Reboiler		492.616
DIS3	Distillation column	
Condenser		2276.041
Reboiler		2282.140
Total		7242.583
Total heat required per day (MJ)		625.759

### 3.6.2 Process B Configuration

In contrast to Process A, ethyl lactate produced in Process B was discharged with the bottom product of the reactive distillation column. The process flow sheet as displayed in Figure 3.21 consists of one reactive distillation column (RD), two fractional distillation columns (DIS1 and DIS2), one mixer (M1) and two heaters (HEAT1 and HEAT2). It can be seen that only two fraction distillation columns were required in this process, one column less than Process A.

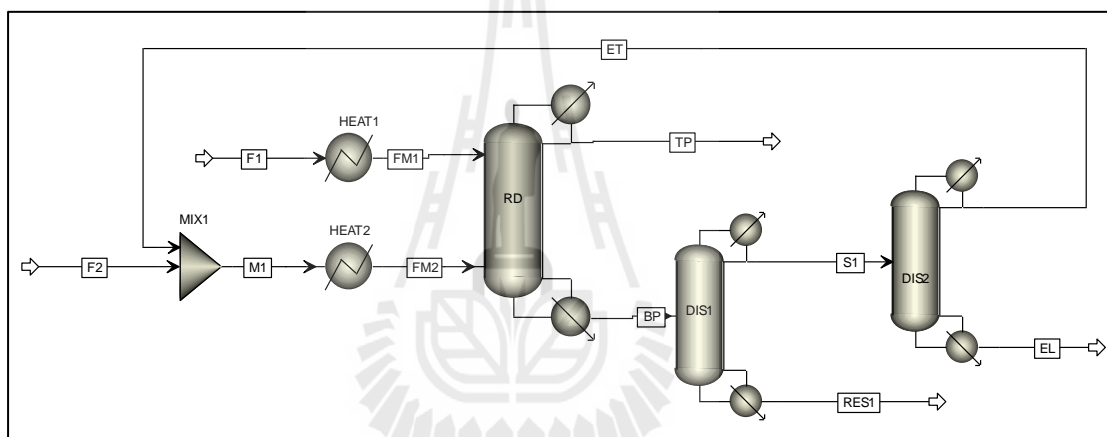


**Figure 3.21** Process flow sheet of Process B.

As the same as in Process A, lactic acid was charged into the reactive distillation column as acidified magnesium lactate solution in feed stream F1. Absolute ethanol was charged into the column as feed stream F2. After its production, ethyl lactate left the reactive distillation column with the bottom product stream BP, while most of the high volatility components like ethanol and water left the column via top product stream TP. The stream BP, which consisted of unreacted lactic acid, ethanol, water, magnesium sulfate, sulfuric acid, and most of ethyl lactate produced,

was fed to the first fractional distillation column, DIS1, to remove all of unreacted lactic acid and sulfuric acid from the process via stream RES1. The stream S1 from DIS1 which consisted of ethyl lactate, ethanol and water, was then sent to the second fractional distillation column DIS2 to remove all the excess ethanol and recycle it back to the reactive distillation column with the recycle stream ET. The desired product, ethyl lactate, from this process was received as an aqueous solution of ethyl lactate in stream EL.

All of the column specifications and the optimal operating conditions were investigated by the sequence of simulation and optimization from reactive distillation column to the last distillation column.

### 3.6.2.1 Reactive Distillation Column, RD

Simulation of the reactive distillation column was started by determination of its total number of stages using initial specifications of the column and temperature of feed stream. Feed positions of both feed stream were fixed at the 2<sup>nd</sup> and the N-1<sup>st</sup> stage. The tray diameter and spacing of all columns were specified as the same as Process A which were 0.1 m of both parameters. Feed temperature and reactive distillation column specification in Process B are shown in Table 3.12.

The number of total stages was varied from 9 to 20, as the same as in Process A, and the effect of the total number of stages on yield of ethyl lactate produced was investigated. For this process, the expression of ethyl lactate yield and recovery of ethyl lactate in the reactive distillation column were shown in equation (3.27) and (3.28).

$$\%Y_{RD,B} = \frac{\text{Mole of ethyl lactate in stream BP}}{\text{Mole of lactic acid in feed stream F1}} \times 100\% \quad (3.27)$$

$$\%R_{RD,B} = \frac{\text{Mole of ethyl lactate in stream BP}}{\text{Mole of ethyl lactate produced in RD column}} \times 100\% \quad (3.28)$$

**Table 3.12** Initial specification of reactive distillation column in Process B.

Operating parameter	Value	Unit
Temperature of feed		
F1	110	°C
F2	75	°C
Bottom rate (B)	0.0295	kmol/hr
Boilup ratio (BR)	0.2	-
Tray diameter	0.1	m
Tray spacing	0.1	m
Weir height	1	inch

Effect of total number of stages on yield of ethyl lactate is shown in Figure 3.22. It was found that, under the operating conditions shown in Table 3.12, the total of number of stages did not have significant effect on yield of ethyl lactate as the yield increased from 60.76% to just only 61.26% when the total number of stages increased from 9 to 20. Instead, ethanol molar flow rate in bottom product stream seemed to be significantly increased when number of stage was increased as shown in Figure 3.23, which indicates to increasing of ethanol mole fraction in bottom product stream. Therefore, the total number of stages for the reactive distillation column in Process B was selected to be 9 due to a concern in purity of ethyl lactate produced in this process.

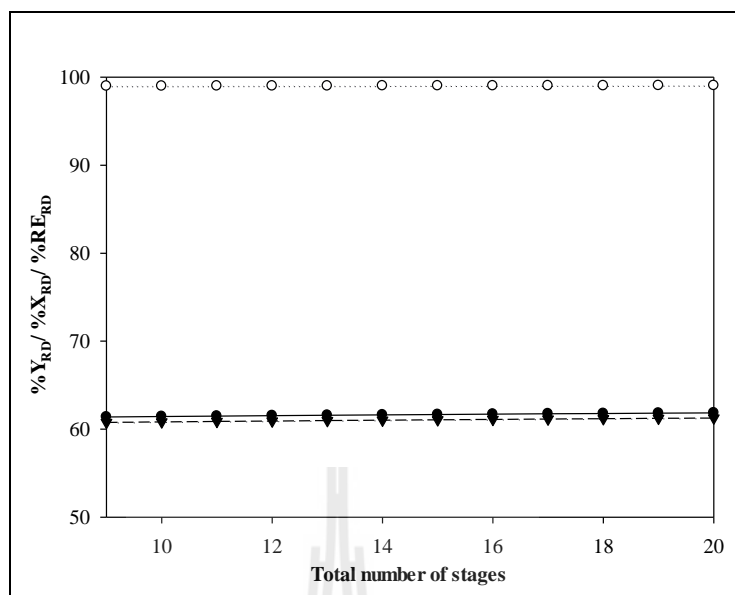


**Figure 3.22** Influence of total number of stages of the reactive distillation column in Process B on (●) conversion of lactic acid; (○) recovery of ethyl lactate; (▼) yield of ethyl lactate.

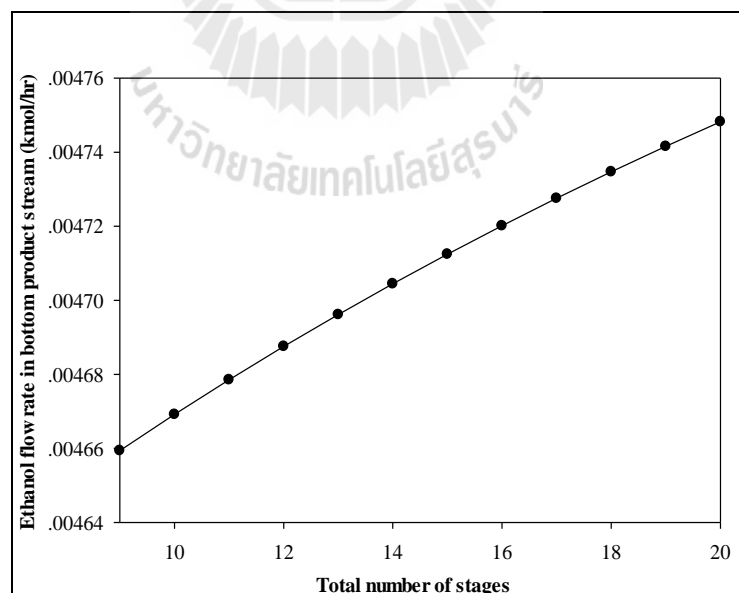


**Figure 3.23** Influence of total number of stages of reactive distillation column in Process B on molar flow rate of ethanol in its bottom product stream.

Reflux ratio and bottom rate of reactive distillation column were used as manipulated variables in optimization of Process B. Initial values of the bottom rate and reflux ratio were set at 0.0147 kmol/hr and 0.001, respectively.

Effect of bottom rate on the yield of ethyl lactate produced in reactive distillation column was studied at constant reflux ratio. The results were shown in Figure 3.24.

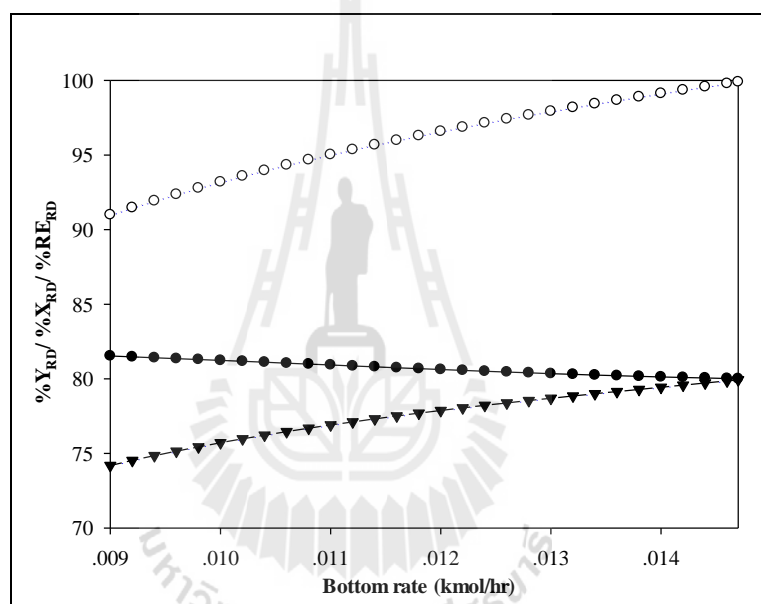


**Figure 3.24** Influence of bottom rate of reactive distillation column in Process B on (●) conversion of lactic acid; (○) recovery of ethyl lactate; (▼) yield of ethyl lactate.

Results from sensitivity analysis revealed that, at constant reflux ratio, the simulation was not converged when the bottom rate higher than 0.0147 kmol/hr. From Figure 3.24, it was found that yield of ethyl lactate in the reactive distillation column and the recovery of ethyl lactate in bottom product stream were significantly

increased with the bottom rate. Even though the conversion of lactic acid was found to decrease with the bottom rate but the recovery of ethyl lactate in the bottom product stream was found to be significantly increased. The yield of ethyl lactate was increased with the bottom rate due to the interaction of both parameters. Therefore, amount of ethyl lactate in the bottom product stream was depended on the bottom rate of the reactive distillation column. Hence, the optimal bottom rate was 0.0147 kmol/hr.

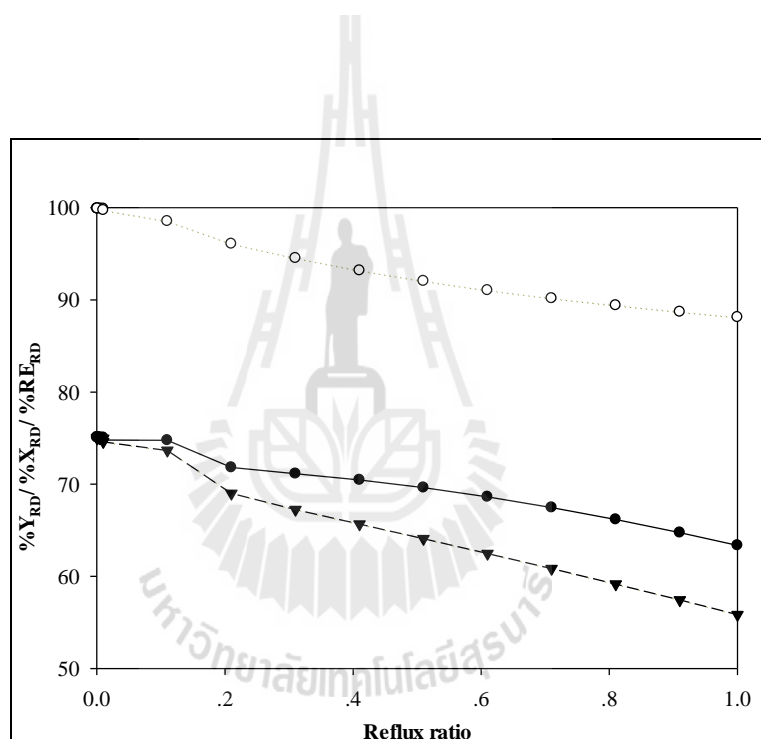


**Figure 3.25** Influence of reflux ratio of reactive distillation column in Process B on (●) conversion of lactic acid; (○) recovery of ethyl lactate; (▼) yield of ethyl lactate

Sensitivity analysis to explore effect of reflux ratio on performance of the reactive distillation column was studied. The results were displayed in Figure 3.25. It was clearly seen that yield and recovery of ethyl lactate as well as the

conversion of lactic acid were decreased with increasing the reflux ratio of the reactive distillation column. This phenomena was expectable. Since increasing the reflux ratio physically meant more water and ethyl lactate were fed back into the column, the esterification reaction was likely to be hampered by the presence of these two reaction products. The conversion of lactic acid and amount of ethyl lactate produced were, therefore, decreased with the increase of reflux ratio.

Effect of bottom rate and reflux ratio on performance of the reactive distillation column was studied simultaneously and the results were shown in Figure 3.26. The highest yield of ethyl lactate produced was obtained at 0.0147 kmol/hr of the bottom rate and 0.0005 of the reflux ratio. The yield of ethyl lactate at this operating condition was 75.05%

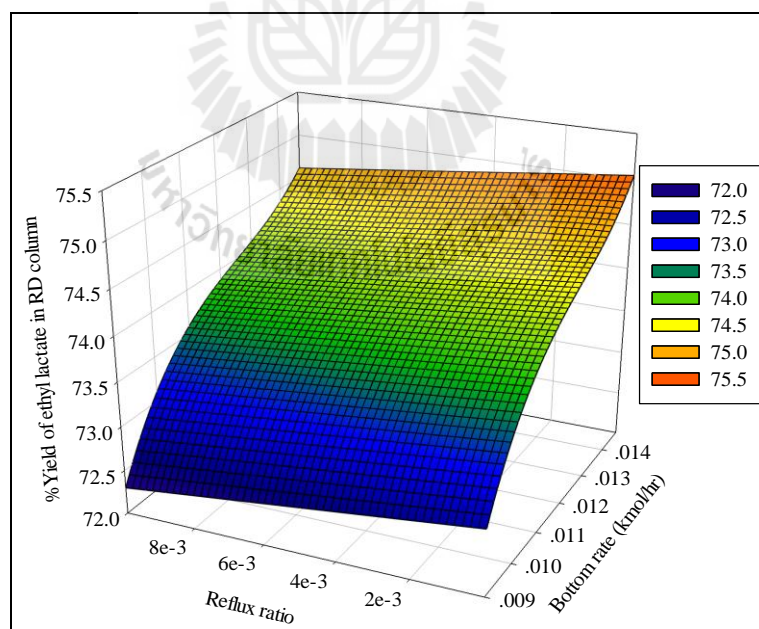


**Figure 3.26** Influence of bottom rate and reflux ratio of reactive distillation column in Process B on yield of ethyl lactate.

Next, effect of feed position and feed temperature of both feed streams were investigated. The result was shown in Figure 3.27. Since the first and the last stage of the reactive distillation column was the condenser and reboiler, the feed position of stream F1 and F2 in sensitivity analysis of the feed location were varied from 2<sup>nd</sup> stage to 4<sup>th</sup> stage and 5<sup>th</sup> stage to 8<sup>th</sup> stage, respectively. It was found that the highest yield of ethyl lactate was obtained when stream F1 and F2 were fed at the 2<sup>nd</sup> stage and the 6<sup>th</sup> stage, respectively.

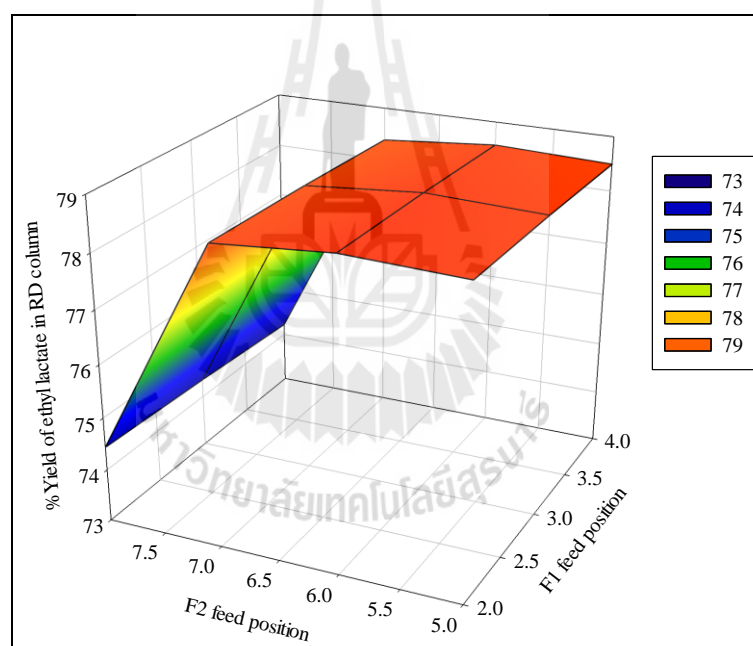


**Figure 3.27** Influence of feed location of reactive distillation column in Process B on yield of ethyl lactate.

Sensitivity analysis of feed temperature effect on performance of the reactive distillation column was shown in Figure 3.28. The result which was similar to that obtained in Process A, showed that the temperature of stream F1 significantly

affected the conversion of lactic acid as well as the ethyl lactate yield and recovery, while the temperature of stream F2 had minor effect on these process parameters. When temperature of stream F1 was lower than approximately 105°C, water which was the main component of stream F1 could not evaporate and still remained in the liquid phase. Large amount of water interrupted the forward reaction and reduced the ethyl lactate production yield. The highest yield of ethyl lactate was obtained when feed temperature of stream F1 and F2 were 110°C and 60°C, respectively.

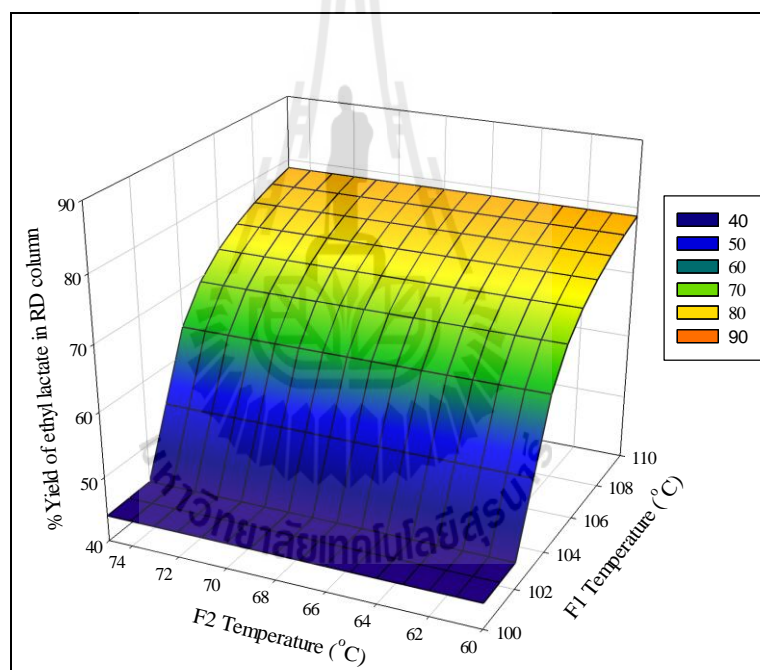


**Figure 3.28** Influence of feed temperature of reactive distillation column in Process B on yield of ethyl lactate.

Effect of tray specifications of the reactive distillation column was also studied through sensitivity analysis of tray diameter and tray spacing. The ranges of the parameters investigated were 0.1 to 0.5 for tray diameter and 0.1 to 0.2 for tray

spacing. It should be noted that the weir height of the tray was fixed at 1 inch. The results obtained were showed in Figure 3.29. The highest yield of ethyl lactate was obtained at tray diameter and tray spacing were 0.1 and 0.1 m, respectively. Therefore, the optimal tray configuration obtained from sensitivity analysis of Process B was the same as in Process A.

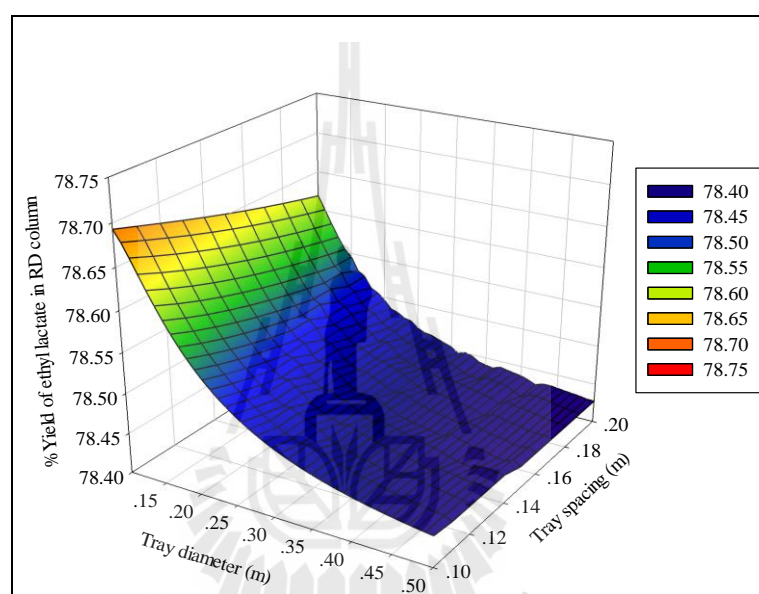


**Figure 3.29** Influence of the tray diameter and tray spacing of reactive distillation column in Process B on yield of ethyl lactate.

Operation of the reactive distillation column under all the optimal conditions resulted in yield of ethyl lactate of 80.02%, the conversion of lactic acid of 80.08% and the recovery of ethyl lactate in bottom product stream of 99.92%. The composition of each stream leaving from single reactive distillation column at the optimal conditions was shown in Table 3.13. It can be seen that the bottom product stream contained the component in the process, thus, this stream needed to be further.

**Table 3.13** Stream composition of reactive distillation column in Process B.

Description	Stream			
	F1	F2	BP	TP
Temperature (°C)	110.00	60.00	88.63	99.50
Molar flow rate (mol/hr)	27.390	6.350	14.700	19.040
Component mole fraction				
Ethanol	0	1	0.31419	0.00190
Lactic acid	0.07730	0	0.02543	0.00252
Ethyl lactate	0	0	0.11524	0.00007
Water	0.85900	0	0.42648	0.99551
Sulfuric acid	0.01370	0	0.02551	0.00001
Magnesium sulfate	0.05000	0	0.09315	0

### 3.6.2.2 First Fractional Distillation Column, DIS1

The first fractional distillation column, DIS1, was designed to remove all the remained lactic acid, sulfuric acid and magnesium sulfate in the bottom product stream discharged from the reactive distillation column, stream TP. All the impurities removed in column DIS1 left the process via stream RES1, which was the bottom product of this distillation column. The overhead product stream S1 containing the remained ethanol, water and ethyl lactate was fed to the second fractional distillation column to purify ethyl lactate.

As the same as in Process A, column configuration of column DIS1 was preliminary designed using the DSTWU model to find the minimum number of stages of the column. In order to remove the components that have higher boiling point than ethyl lactate, lactic acid was specified to be heavy key component and ethyl lactate was specified to be light key component. The minimum number of

stages in the model was designed for 100% recovery of ethyl lactate in the overhead product stream S1 while all the residuals were separated from the column via RES1 stream. The result from DSTWU model was shown in Table 3.14. It can be seen that the minimum number of stages of column DIS1 was found to be 13 while the feed stage was on the 9<sup>th</sup> stage.

**Table 3.14** Specification of DIS1 column in Process B from DSTWU model.

Parameter	Value	Unit
Minimum reflux ratio:	0.022	
Actual reflux ratio:	0.500	
Minimum number of stages:	12.377	
Number of actual stages:	19.048	
Feed stage:	8.786	
Number of actual stages above feed:	7.786	
Reboiler heating required:	244.183	Watt
Condenser cooling required:	220.928	Watt
Distillate temperature:	84.14	C
Bottom temperature:	272.94	C
Distillate to feed fraction:	0.856	

As the same procedure as in Process A, the configurations of DIS1 column obtained from DSTWU model was applied to the RADFRAC model. Other column specifications such as tray diameter and spacing were fixed at 0.1 m as before. The optimization was performed to find the optimal distillate rate and reflux ratio of DIS1 column with the RADFRAC model. The optimal conditions were evaluated to obtain the maximum removal of ethyl lactate in the top product stream and the maximum recovery of the residuals in the bottom product stream. The recovery of ethyl lactate in this optimization was defined as equation (3.29).

$$\%RE_{DI,B} = \frac{\text{Mole of ethyl lactate in stream S1}}{\text{Mole of ethyl lactate in stream BP}} \times 100\% \quad (3.29)$$

The optimization results indicated that the optimal distillate rate and reflux ratio of column DIS1 were found to be 0.01258 kmol/hr and 0.5, respectively. Stream compositions obtained from the optimization of column DIS1 were shown in Table 3.15. It can be seen that, all of ethyl lactate in the stream BP, which was produced in the reactive distillation column, was discharged from DIS1 column via stream S1. Moreover, all of lactic acid, sulfuric acid and magnesium sulfate were removed from the process via RES1 stream.

**Table 3.15** Stream compositions of DIS1 column of Process B.

Description	Stream		
	BP	RES1	S1
Temperature (°C)	88.63	272.94	84.14
Molar flow rate (mol/hr)	14.700	2.120	12.580
Component mole fraction			
Ethanol	0.31419	0	0.36708
Lactic acid	0.02543	0.17644	0
Ethyl lactate	0.11524	0	0.13464
Water	0.42648	0	0.49828
Sulfuric acid	0.02551	0.17706	0
Magnesium sulfate	0.09315	0.64650	0

After that, DIS1 column was connected with the reactive distillation column and process simulation under the optimal conditions was

performed. The yield of ethyl lactate obtained from these columns was found to be 80.02%. The yield of ethyl lactate of two columns was defined as the equation (3.30).

$$\%Y_{D1,B} = \frac{\text{Mole of ethyl lactate in stream } S1}{\text{Mole of lactic acid in feed stream } F1} \times 100\% \quad (3.30)$$

However, as shown in Table 3.15, the excess ethanol still remained in the product stream, and it must be removed by another distillation column.

### 3.6.2.3 Second Fractional Distillation Column, DIS2

The main function of the second distillation column was to remove all of remained ethanol from the final product stream and recycled it back to the reactive distillation column.

Specifications of DIS2 column were firstly investigated by DSTWU model to determine the total number of stages. In this unit, ethanol and ethyl lactate were defined as the light key and the heavy key component, respectively. The column was designed to remove total excess ethanol via the overhead product stream ET. Ethyl lactate was discharged as the final product in the bottom product stream of the column, stream EL.

The results of DSTWU model for DIS2 column were tabulated in Table 3.16. It was found that the minimum number of stages to remove all the excess ethanol was 11. The feed stage of this the column was at the 10<sup>th</sup> stage.

**Table 3.16** Specification of DIS2 column in Process B from DSTWU model.

Parameter	Value	Unit
Minimum reflux ratio:	0.142	
Actual reflux ratio:	0.500	
Minimum number of stages:	10.490	
Number of actual stages:	18.167	
Feed stage:	10.864	
Number of actual stages above feed:	9.864	
Reboiler heating required:	186.044	Watt
Condenser cooling required:	186.044	Watt
Distillate temperature:	80.40	°C
Bottom temperature:	150.94	°C
Distillate to feed fraction:	0.864	

The configuration of column DIS2 estimated by DSTWU model was applied in the RADFRAC model. Tray diameter and spacing of the column were also fixed at 0.1 m as the same as in previous column. The optimization of DIS2 column was evaluated to find the optimal distillate rate and reflux ratio to obtain maximum recovery of ethyl lactate in this column, which was defined as following equation:

$$\%RE_{D2,B} = \frac{\text{Mole of ethyl lactate in stream } EL}{\text{Mole of ethyl lactate in stream } S1} \times 100\% \quad (3.31)$$

The optimal distillate rate and reflux ratio were found to be 0.07951 kmol/hr and 13.03943, respectively. The stream compositions of DIS2 column obtained from the optimization were shown in Table 3.17. Ethyl lactate recovered in the bottom product stream was found to be 98.56% while 99.80% of ethanol was recovered in the overhead product stream.

**Table 3.17** Stream compositions of DIS2 column of Process B.

Description	Stream		
	S1	ET	EL
Temperature (°C)	84.14	79.35	100.66
Molar flow rate (mol/hr)	12.580	7.950	4.630
Component mole fraction			
Ethanol	0.36708	0.57972	0.00199
Lactic acid	0	0	0.00001
Ethyl lactate	0.13464	0.00307	0.36053
Water	0.49828	0.41721	0.63747
Sulfuric acid	0	0	0
Magnesium sulfate	0	0	0

#### 3.6.2.4 Process B with Recycle Stream

The excess ethanol recovered from process was separated in DIS2 column via stream ET and was mixed with fresh ethanol feed of ethanol before being fed to the reactive distillation column. The process flow sheet including the recycle stream was displayed in Figure 3.21. The mixed ethanol feed was injected to a heat exchanger to heat it up to the optimized temperature of 60°C. The lactic acid was heated up to 110°C. When the process was operated with the optimal conditions of each column, the stream compositions in the process with ethanol recycle were tabulated in Table 3.18.

**Table 3.18** Stream compositions of the process with ethanol recycle operating under the optimal conditions of each column.

Description	Stream								
	FM1	M1	FM2	TP	BP	S1	RES1	ET	EL
Temperature (°C)	110.00	55.11	60.00	84.38	86.28	82.09	244.09	78.21	98.55
Molar flow rate (mol/hr)	27.390	14.300	14.300	26.990	14.700	12.580	2.120	7.950	4.630
Component mole fraction									
Ethanol	0	0.91075	0.91075	0.16230	0.46159	0.53929	0	0.83947	0.02391
Lactic acid	0.07730	0	0	0.00180	0.01425	0	0.09887	0	0
Ethyl lactate	0	0	0	0.00538	0.11659	0.12316	0.07756	0	0.33462
Water	0.85900	0.08925	0.08925	0.83052	0.28891	0.33755	0	0.16053	0.64147
Sulfuric acid	0.01370	0	0	0.00001	0.02551	0	0.17706	0	0
Magnesium sulfate	0.05000	0	0	0	0.09315	0	0.64651	0	0

Conversion of lactic acid in reactive distillation in Process B was calculated by equation (3.32).

$$\%X_B = \frac{\text{Mole of ethyl lactate produced in RD column}}{\text{Mole of lactic acid in feed stream F1}} \times 100\% \quad (3.32)$$

It was found that when the process was operated, the conversion of lactic was increased from 80.08% to be 87.81%. Higher amount of ethanol kept the reaction moving forward to produce the products, conversion of lactic acid was increased. However, overall ethyl lactate yield of Process B, which was defined in equation (3.33), was decreased from 78.86% to be 73.20% due to the decreasing of overall recovery of ethyl lactate. The overall recovery of ethyl lactate was explained in equation (3.34).

$$\%Y_B = \frac{\text{Mole of ethyl lactate in stream EL}}{\text{Mole of lactic acid in feed stream F1}} \times 100\% \quad (3.33)$$

$$\%RE_B = \frac{\text{Mole of ethyl lactate in stream EL}}{\text{Mole of ethyl lactate produced in RD column}} \times 100\% \quad (3.34)$$

The decrease in overall recovery of ethyl lactate was occurred because bottom rate of reactive distillation column was fixed at the previous optimal bottom rate. Ethyl lactate produced in the reactive distillation column was more discharged from the reactive distillation column via the top product. The recovery of ethyl lactate in the reactive distillation column was significantly decreased from 99.92% to 92.19%. The lower amount of ethyl lactate recovered in the reactive distillation column has affected on the overall recovery of ethyl lactate, therefore, the overall yield of ethyl lactate was decreased. Thus the bottom rate and the reflux ratio of the reactive distillation column were re-optimized in order to obtain the highest overall yield of ethyl lactate of the process.

In order to perform the process optimization with ethanol recycle stream, the sequence of simulation and tear stream have to be defined. The sequence of simulation was started with the RD column, DIS1 column, DIS2 column, MIX1, and HEAT2, respectively. The tear stream was set as stream FM2 as the same as in Process A.

It was found from process simulation that the optimal molar bottom rate and reflux ratio of the reactive distillation column were 0.0147 kmol/hr and 0.00005, respectively. It should be note that the new optimal parameters were the same as the initial previous values before optimization. The composition of each stream was therefore the same as tabulated in Table 3.18. The overall yield of ethyl lactate was 73.20%. However, it can be seen from Table 3.18 that the stream EL was still with ethanol. Therefore, this excess ethanol in stream EL needed to be eliminated.

Since column DIS2 was used to remove all of remained ethanol from the product stream EL, total number of stages and feed location of column DIS2 were re-optimized in order to remove all ethanol from stream EL. Other specification and conditions of other columns were kept as the optimal values because optimization of whole process with higher variables was very difficult to be converged.

From the results of DSTWU model of DIS2 column in above section explored that the actual number of total stages was 19 stages, however, the number of total stages used in DIS2 column was 11 stages. Therefore, the effects of the total number of stages and the feed location of this column on the recovery of excess ethanol were investigated. The total number of stages was varied from 11 stages to 19 stages and the feed stage location was varied from the 2<sup>nd</sup> to the N-1<sup>th</sup> stage.

The optimization of each number of stages was investigated to obtain the highest overall yield of ethyl lactate with the constraint of maximum recovery of ethanol in ET stream. At any total number of stages, the feed stage location that gave the highest the recovery of ethanol was optimized. The manipulated variables were the bottom rate and the reflux ratio of the RD column. Over 99.99% of ethanol recovered in DIS2 column and the mole fraction of ethanol in the final product solution lower than 0.0001 were desired. The results of total number of stage and feed location on these two target variables were shown in Table 3.19.

**Table 3.19** Highest recovery of ethanol in stream ET at each total number of stages.

Total number of stage	Feed stage	Highest recovery of ethanol (%)	Overall yield of ethyl lactate obtained (%)	Mole fraction of ethanol in EL stream
11	9	99.700	73.104	0.00426
12	9	99.800	73.300	0.00289
13	9	99.800	73.331	0.00257
14	2	99.940	73.176	0.00084
15	2	99.950	73.182	0.00070
16	4	99.980	73.280	0.00025
17	5	99.992	73.306	0.00013
18	6	99.994	73.326	0.00010
19	6	99.998	73.326	0.00002

From the results in Table 3.19, it was found that mole fraction of ethanol in the product stream was decreased, while the recovery of ethanol in stream EL was increased with the increasing of total number of stages of DIS2 column. The desired mole fraction of ethanol in stream EL, lower than 0.0001, was obtained when the total number of stages was 18 with the feed location at the 6<sup>th</sup> stage. Mole fraction of ethanol in this stream was less than 0.0001 when the total number of stages was 19. However, the maximum yield of ethyl lactate was not different from that obtained from DIS2 column with 18 stages. Therefore, 18 stages of DIS2 column were satisfied to recover the excess ethanol. Highest overall yield of ethyl lactate obtained was 73.33% while the overall recovery of ethyl lactate and the conversion of lactic acid were 83.49% and 87.83%, respectively.

The liquid phase mole fraction of each component in reactive distillation column after process optimization was shown in Figure 3.30. It was found that ethanol was the main component in the lower part of the column because of the ethanol feed location was at the 6<sup>th</sup> stage. The temperature of ethanol was 60°C therefore the ethanol was mainly in the liquid phase. In contrast, water was the main component in the upper stages. The temperature of lactic acid feed solution was 110°C therefore some of the water was evaporated. However, some of water still remained in the lower stage and interrupted the forward reaction to produce ethyl lactate. Therefore, the conversion of lactic acid obtained from Process B was less than Process A.

The temperature profile of the reactive distillation column in Process B was displayed in Figure 3.31. Liquid phase temperature in each stage was found to be decreased with the lower stage of the column especially at the 6<sup>th</sup> stage which was the feed location of feed stream F2. For vapor phase temperature, it was observed that the highest vapor phase temperature was at the 2<sup>nd</sup> stage because this stage was the feed location of feed stream F1 with temperature of 110°C. Thus, some of water in feed stream F1 was evaporated and affected to vapor phase temperature of the column. Moreover, lower liquid phase and vapor phase temperature in Process B might be effected to conversion of lactic acid in the reactive distillation column. Therefore, the conversion of lactic acid in this process was found to be lower than that obtained from Process A.

In addition, molar ratio of ethanol-to-lactic acid in each stage of reactive distillation column was shown in Figure 3.32. It explored that the molar ratio of ethanol-to-lactic acid was not constant at 3:1. For stage upper the feed point of

ethanol stream, lower than 1:1 of ethanol-to-lactic acid molar ratio was observed. Low temperature of ethanol feed stream might be effected to quantity of ethanol that evaporated into vapor phase and flow up to upper stage of the reactive distillation column. When small of ethanol was evaporated to the upper stage, the molar ratio of ethanol-to-lactic acid was lower than 1:1. In contrast, high molar ratio of ethanol-to-lactic acid was observed at state below feed point of ethanol stream.

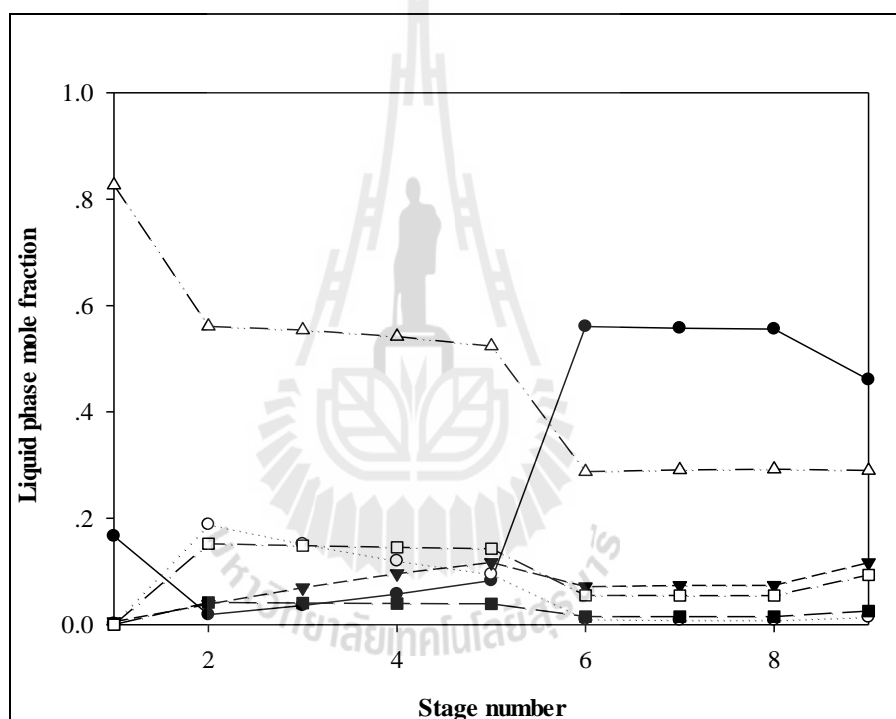


**Figure 3.30** Liquid phase composition of reactive distillation column in Process B:

(●) Ethanol; (○) Lactic acid; (▼) Ethyl lactate; (△) Water;

(■) Sulfuric acid; (□) Magnesium sulfate.

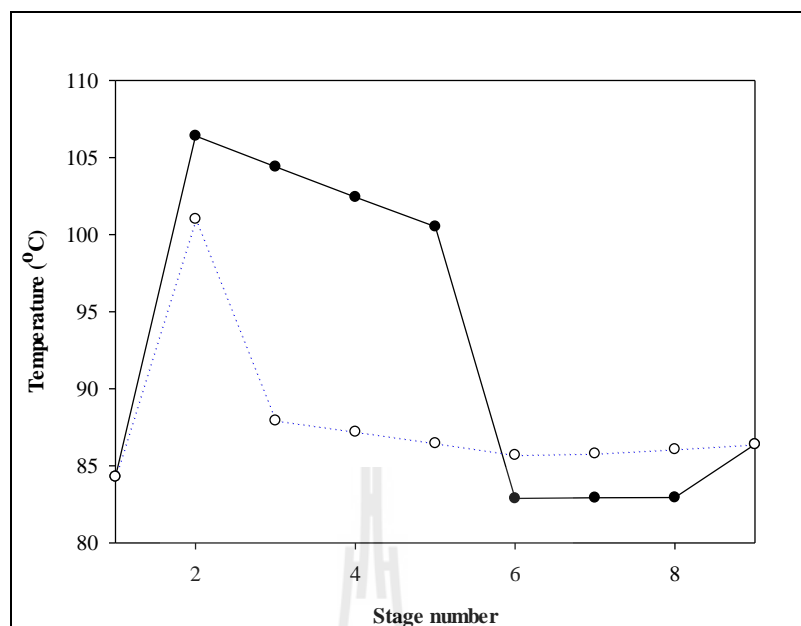


**Figure 3.31** Temperature profile of reactive distillation column of Process B

(●) liquid phase temperature and (○) vapor phase temperature.

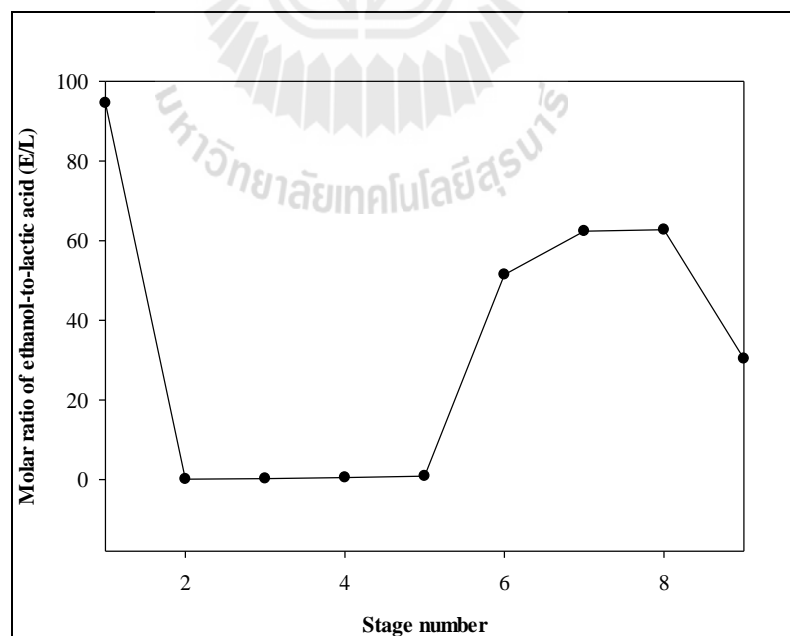


**Figure 3.32** Molar ratio of ethanol-to-lactic acid in each stage of reactive distillation

column in Process B.

The process flow sheet and the composition of each stream in Process B were shown in Figure 3.33 and Table 3.20, respectively. It can be seen that the final product stream EL was aqueous solution of ethyl lactate. The ethyl lactate solution obtained from Process B was found to be 33.52 mole%, which was higher than that obtained from Process A. The percentage loss of ethyl lactate in Process B was found to be about 7.99%. Azeotrope between ethyl lactate and water was not observed in this process. The unit operation specification and the heat duty of each unit involved in this process were shown in Table 3.21 and 3.22, respectively.

Total heat duty of all the operating units in Process B was 3612.07 watts, which was higher than the total heat duty of 7242.58 watts evaluated in Process A. The lower heat duty of Process B could likely be due to the less number of operating units in Process B since only two fractional distillation columns were required in this process instead of three columns used in Process A.

In view of production rate, it was found in this study that Process B could produce 0.037 kmol/day or 4.400 kg/day of ethyl lactate, which was lower than the rate of 0.047 kmol/day or 5.599 kg/day of ethyl lactate achieved in Process A. The overall yield of ethyl lactate in Process A was also higher than that in Process B. However, as previously mentions, 33.52% by mole ethyl lactate solution obtained from Process B was of higher concentration than the 8.27% by mole solution obtained from Process A.

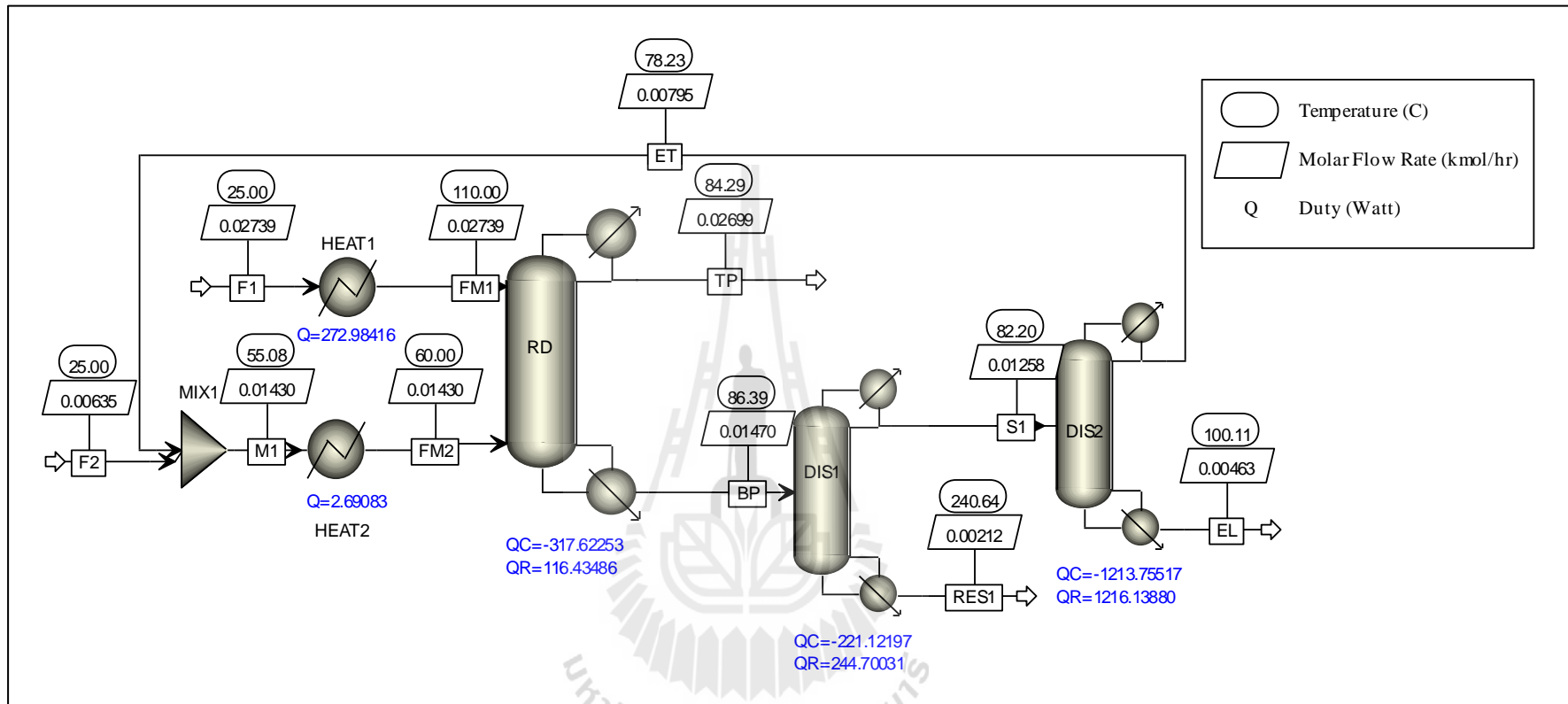


Figure 3.33 Process flow sheet of Process B with optimal condition.

**Table 3.20** Composition of each stream in Process B.

Description	Stream								
	FM1	M1	FM2	BP	TP	S1	RES1	ET	EL
Temperature (°C)	110.00	55.15	60.00	86.29	84.27	82.10	239.48	78.19	100.48
Molar flow rate (mol/hr)	27.390	14.300	14.300	14.700	26.990	12.580	2.120	7.950	4.630
Component mole fraction									
Ethanol	0	0.91755	0.91754	0.46086	0.16628	0.53826	0.00114	0.85169	0.00010
Lactic acid	0.07730	0	0	0.01429	0.00176	0	0.09915	0	0
Ethyl lactate	0	0	0	0.11638	0.00551	0.12338	0.07478	0	0.33522
Water	0.85900	0.08245	0.08246	0.28981	0.82644	0.33836	0.00138	0.14831	0.66468
Sulfuric acid	0.01370	0	0	0.02551	0.00001	0	0.17706	0	0
Magnesium sulfate	0.05000	0	0	0.09315	0	0	0.64650	0	0

**Table 3.21** Unit operation specification of Process B.

Specification	Operating Unit				
	HEAT1	HEAT2	RD	DIS1	DIS2
Temperature (°C)	110	60	-	-	-
Total number of stage	-	-	9	13	18
Feed stage	-	-	2 and 6	12	6
Column diameter (m)	-	-	0.1	0.1	0.1
Column spacing (m)	-	-	0.1	0.1	0.1
Distillate rate (mol/hr)	-	-	14.700	12.580	7.950
Reflux ratio	-	-	0.011	0.500	13.039

**Table 3.22** Heat duty of operating unit in Process B.

Unit Operation		Heat Duty (W or Js <sup>-1</sup> )
Name	Operation type	
MIX1	Mixture	
HEAT1	Heater	272.984
HEAT2	Heater	2.690
RD	Reactive distillation	
Condenser		317.622
Reboiler		116.435
DIS1	Distillation column	
Condenser		221.122
Reboiler		244.700
DIS2	Distillation column	
Condenser		1213.756
Reboiler		1216.138
	Total	3605.449
Total heat required per day (MJ)		311.511

It can be concluded here that advantage of Process A, where ethyl lactate was collected at the top of reactive distillation column, was higher production rate and yield of ethyl lactate. Process B, on the other hand, offered the less number of fractional distillation columns required to purify ethyl lactate, which led to the lower heat requirement in the process. In order to compare efficiency of processes with different process schemes more thoroughly, economic analysis was performed and discussed in Chapter IV of this thesis.

### **3.7 Conclusions**

The process for ethyl lactate production by esterification of fermentation-derived magnesium lactate with ethanol was preliminary designed. Sulfuric acid was used as a homogeneous catalyst and the kinetics information of the reaction was obtained from the study in the previous chapter. Two process schematics were designed and simulated by Aspen Plus simulator. Process A was designed where ethyl lactate was collected at the top of the reactive distillation column. In Process B, on the other hand, ethyl lactate was discharged with the bottom product stream of the reactive distillation column. The reactive and fractional distillation columns in both process schematics were designed as tray column. DSTWU model was used to determine the specification of all the distillation and process optimization was performed using RADFRAC model. UNIQUAC model was used to represent non-ideality of the reaction mixture. The process capacity was set to handle 50 liters of magnesium lactate fermentation broth per day. The optimal configurations and operating conditions of both processes were investigated. In order to compare the process efficiency, overall yield of ethyl lactate and production rate as well as

concentration of ethyl lactate obtained from both processes were compared. It was found that the overall ethyl lactate yield obtained from Process A was 93.30% with the production rate of 0.047 kmol/day or 5.599 kg/day while it was only 73.20% with 0.037 kmol/day or 4.400 kg/day of the production rate achieved from Process B. However, the concentration of ethyl lactate which was in form of aqueous solution obtained from Process A was 37.18 w/w% which was very low when compared with 76.79 w/w% from Process B. Moreover, three fractional distillation columns were required in Process A which higher than required from Process B for one. Difference in number of fractional distillation column affected to amount of heat duty required from both processes.

### 3.8 References

- Agreda, V.H. and Partin, L.R. (1984). Reactive distillation process for the production of methyl acetate. **U.S. Patent 4435595.**
- Aspen Plus library in Aspen Plus simulator (Version 7.3.2), Aspen Tech
- Backhaus, A.A. (1921). Continuous processes for the manufacture of ester, **U.S. Patent 1400849.**
- Coker, A.K. (2010). **Ludwig's Applied Process Design for Chemical & Petrochemical Plants.** 4 editions.
- Delgado, P., Sanz, M.T., and Beltran, S. (2007). Kinetic study for esterification of lactic acid with ethanol and hydrolysis of ethyl lactate using an ion-exchange resin catalyst. **Chemical Engineering Journal.** 126: 111-118.

- Filachione, E.M. and Costello, E.J. (1952). Lactic esters by reaction of ammonium lactate with alcohols. **Industrial and Engineering Chemistry**. 44: 2189-2191.
- Gao, J., Zhao, X.M., Zhou, L.Y. and Huang, Z.H. (2007). Investigation of ethyl lactate reactive distillation process. **Chemical Engineering Research and Design**. 85: 525-529.
- Kasinathan, P., Kwak, H., Lee, Uhwang., Hwang, D.W., Hwang, Y.K. and Chang, J.S. (2010). Synthesis of ethyl lactate from ammonium lactate solution by coupling solvent extraction with esterification. **Separation and Purification Technology**. 76: 1-7.
- Kumar, R. and Mahajani, S.M. (2007). Esterification of lactic acid with n-butanol by reactive distillation. **Industrial and Engineering Chemistry Research**. 46: 6873-6882.
- Luo, H.P. and Xiao, W.D. (2001). A reactive distillation process for a cascade and azeotropic reaction system: Carbonylation of ethanol with dimethyl carbonate. **Chemical Engineering Science**. 56: 403-410.
- Melles, S., Grievink, J., and Schrans, S.M. (2000). Optimization of the conceptual design of reactive distillation columns. **Chemical Engineering Science**. 55: 2089-2097.
- Pereira, C. S., Silva, V. M., Rodriuges, A. E. (2011). Ethyl Lactate as a Solvent: Properties, Applications and Production Process - a Review. **Green Chem**. 13: 2658-2671.
- Ralph, S. (2010). **Teach Yourself the Basics of Aspen Plus<sup>TM</sup>**. John Wiley and Sons.

- Smejkal, Q., Hanika, J. and Kolena, J. (2001). 2-Methylpropylacetate synthesis in a system of equilibrium reactor and reactive distillation column. **Chemical Engineering Science**. 56: 365-370.
- Sundmacher, K. and Kienle, A. (eds.). (2003). **Reactive distillation: status and future directions**. Magdeburg Germany: Wiley-VCH Verlag GmbH&Co.
- Tang, Y.T., Huang, H.P. and Chien, I.L. (2003). Design of a complete ethyl acetate reactive distillation column system. **Computer Aided Chemical Engineering**. 15: 1044-1049.
- Taylor, R. and Krishna, R. (2000). Review-Modeling reactive distillation. **Chemical Engineering Science**. 55: 5183-5229.
- They, R., Meyer, X. M., Joulia, X., Meyer, M. (2005). Preliminary design of reactive distillation columns. **Chemical Engineering Research and Design**. 84: 379-400.

## CHAPTER IV

### PRELIMINARY PRODUCTION COST ESTIMATION

#### 4.1 Abstract

In this chapter, production cost of the preliminary process for ethyl lactate synthesis was evaluated to compare efficiency of the two process schemes detailed in Chapter III processes. Total capital investment of each process was calculated using the percentage delivered-equipment cost method which considers each expense of capital cost as the percentage of purchased equipment cost. The equipment purchasing cost of Process A and Process B was considered only cost of reactive and fractional distillation columns and their heat exchangers which can be estimated from Guthrie's correlation. Column purchasing costs were dependent on height and diameter of the column. Material of column and tray was designed to be stainless steel due to its high corrosive resistance. Similarly, purchased costs of reboiler and condenser were dependent on area of heat transfer. It was found that the total capital cost of Process B was to be 1.855 million Baht which lower than 2.566 million Baht that obtained from Process A due to lower number of columns, condenser and reboiler required of Process B. Since both processes were designed to handle 50 L/day of fermentation broth which can be considered as a small production process, some expenses of operating cost, such as operating labor cost and laboratory cost, were not considered. The major expenses of the operating cost were considered to be cost of raw material and utility. Cost of raw material of both processes was equal because they were

designed to handle the same capacity of fermentation broth per day. Utility costs when different energy sources, i.e. electricity, diesel oil, LPG, and fuel oil, were evaluated and compared. Fuel oil was selected to be an energy source of the process due to its lowest cost compared with other energy sources. It was found that utilities cost of Process A was higher Process B due to the higher total heat duty required in Process A. The production cost of ethyl lactate can be evaluated from annual production cost divided by annual production rate of ethyl lactate obtained from each process. The annual production cost of each process was evaluated from the operating cost combined with the fixed capital cost. It was found that the annual production cost of Process A was found to be 1.569 million Baht per year which was higher than 1.339 million Baht per year from Process B due to higher number of operating unit and heat duty required. Although Process B has lower annual production cost but its production cost was found to be higher than Process A due to its lower production rate. The ethyl lactate production cost of Process A and B were found to be 767.74 and 833.45 THB/kg, respectively.

## 4.2 Introduction

Ethyl lactate is a benign chemical and important lactic acid ester due to its advantages such as it can be used as solvent in several industries and used as food additive in food production (Pereira et al., 2011). Normally, ethyl lactate is produced from high-purity lactic acid esterification with ethanol catalyzed by acid catalyst. This process is, therefore, quite expensive due to the high production cost of lactic acid. Lactic acid can be produced from both fermentation of carbohydrates and chemical synthesis, but fermentation process is currently dominating the industrial production

of lactic acid (Chen et al., 2014). However, the purification and recovery of the lactic acid from fermentation broth is a difficult and expensive task (Kumar and Mahajani, 2007 and Maki-Arvela et al., 2014).

In order to reduce the production cost of ethyl lactate, developing on alternative low-cost production process could be helpful. Using lactate salts obtained directly from fermentation as a reactant is one of the approaches to reduce the ethyl lactate production cost since lactic acid purifying step can be excluded (Filachione and Costello, 1952). Alternative process to produce ethyl lactate is developed in Chapter III of this thesis, where ethyl lactate produced from fermentation-derived magnesium lactate esterification with ethanol using reactive distillation column processes were explicated.

After completing the development of new production, process economic evaluation must be done since this step can provide a good indication for viability of the production (Anderson. 2009). Therefore, in this chapter, preliminary ethyl lactate production cost from fermentation-derived magnesium lactate esterification processes were performed and compared. The viability of the production is investigated.

### **4.3 Literature Reviews**

In recent years, there are many publications about the process economic evaluation because the economics feasibility is of great importance to access process viability.

Akerberg and Zacchi (2000) proposed the process for lactic acid production form fermentation of whole-wheat flour. An economical evaluation of lactic acid production cost was performed. The process scheme was showed in Figure 4.1. The

processes were simulated using BioProcSim computer program. The capacity of lactic acid production of 30,000 tons per year was assumed to be a target of this production.

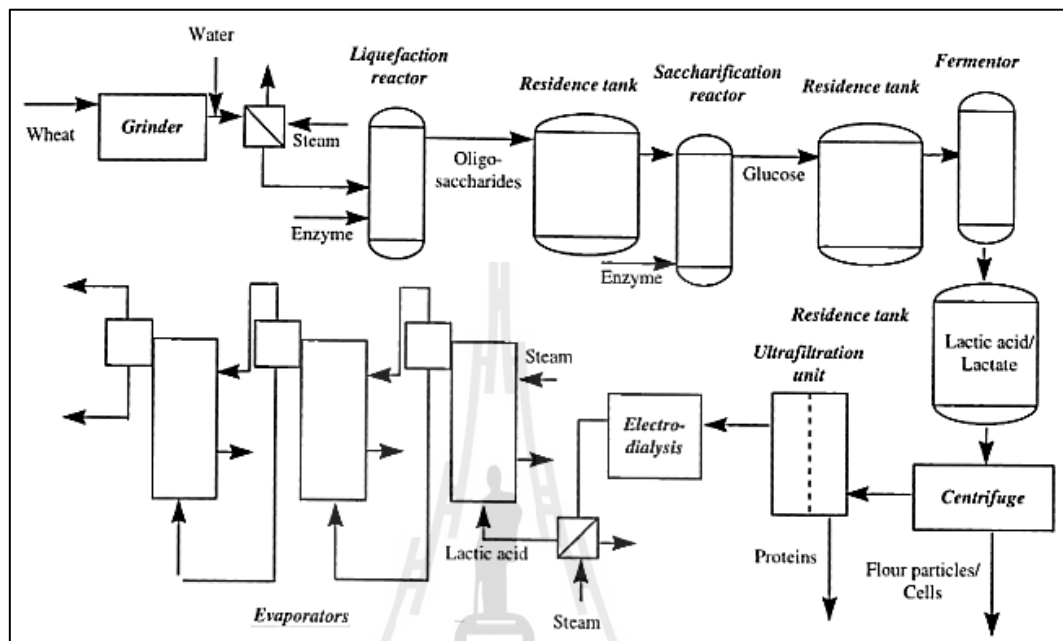


**Figure 4.1** Process scheme of lactic acid production (Akerberg and Zacchi, 2000).

It was found that the process with batch fermentation was more economical than the continuous fermentation. The operation cost of the process was about 80% of the total cost. The major production costs were the cost of raw material, saccharification, fermentation, and electro-dialysis. In order to reduce the production cost, different process alternatives were evaluated. The alternative processes studied were such as recovery of wheat flour as fodder, integrating the saccharification and fermentation steps, recovery of sodium hydroxide from the electro-dialysis step, and fermentation at a lower pH. It was found that lactic acid production cost can be reduced by lowering the pH and/or by recycling sodium hydroxide, which produced by electro-dialysis, to the fermenter. The production cost with wheat flour

concentration was optimized and it was found that 116 grams of glucose per liter of wheat flour concentration gave the lactic acid production cost of 0.88 USD/kg.

Marchetti et al. (2008) presented conceptual design and economic analysis of biodiesel production from spent oil. Three different reaction catalysts: homogeneous alkaline catalyst with acid pre-esterification, homogeneous acid catalyst and heterogeneous solid catalyst, were compared. The flow diagrams of each process were shown in Figure 4.2. SuperPro Designer simulator was used to simulate the process to produce biodiesel with purity higher than 98 w/w%. They found that all the process achieved high purity of biodiesel. For each metric ton of spent oil, 0.9884 metric ton of biodiesel was produced from the homogeneous alkaline catalyst with acid pre-esterification process while minimum production of 0.9881 metric ton of biodiesel was obtained from the process with homogeneous acid catalyst. In all processes, 76-89% of the operating cost was from raw material cost. Biodiesel production costs of each process were in range of 0.51 to 0.53 USD/kg. However, the heterogeneous solid catalyst process appeared to be more profitable and gave the highest net present value with an interest of 7% compared with other process.

In 2009, Arpornwichanop and coworkers presented economic analysis of n-butyl acetate production from dilute acetic acid with n-butanol using different reactive distillation systems. Three different reactive distillation systems used in this study were single-column reactive distillation, distillation-reactive distillation hybrid systems and pervaporation-reactive distillation hybrid system. All systems were simulated using Aspen Plus simulator. Schematic diagrams of all systems were shown in Figure 4.3.

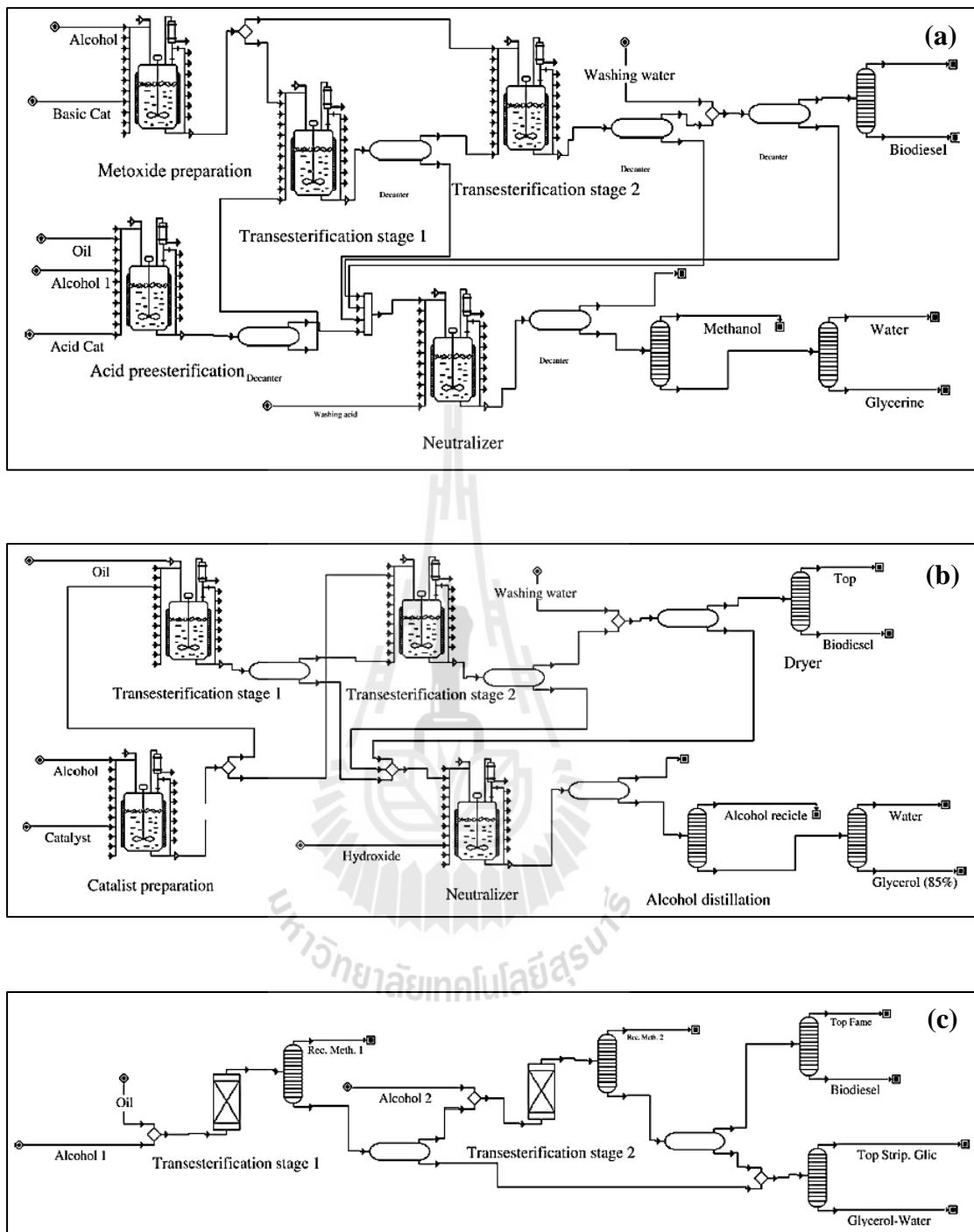


**Figure 4.2** Process flow diagram of biodiesel production process using

- (a) homogeneous alkaline catalytic with acid pre-esterification,
- (b) homogeneous acid catalyst and (c) heterogeneous solid catalyst.

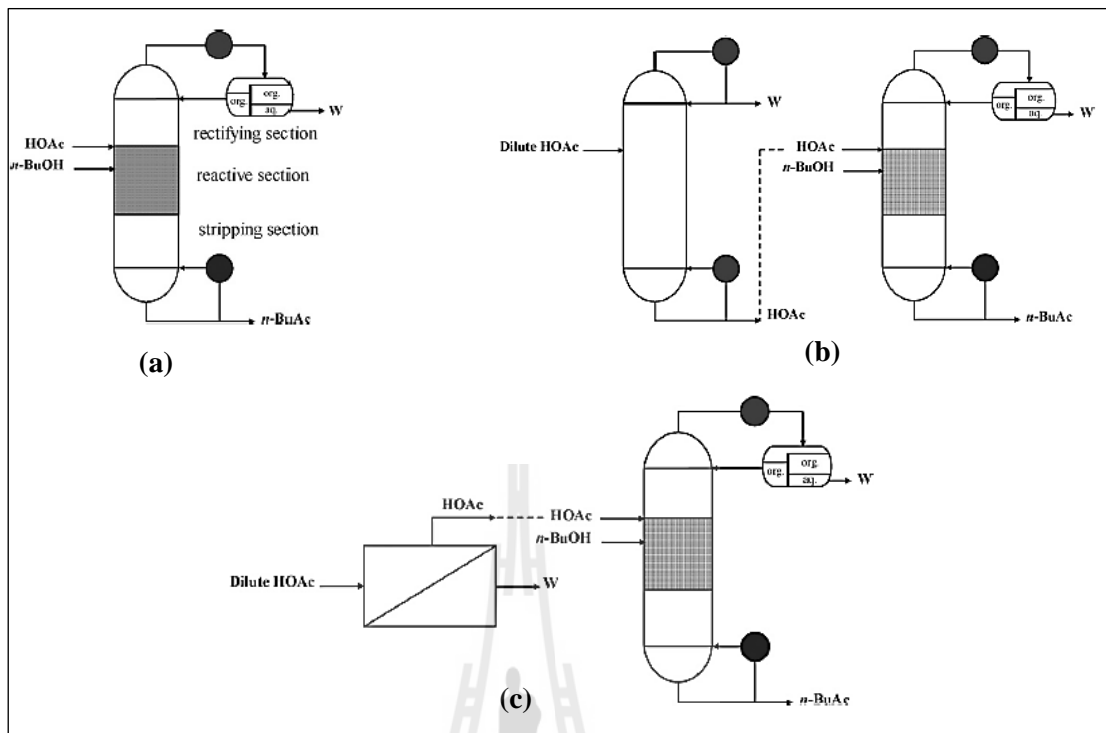


**Figure 4.3** Schematic diagrams of n-butyl acetate production system: (a) conventional reactive distillation column, (b) distillation-reactive distillation hybrid system and (c) pervaporation-reactive distillation hybrid system (Arpornwichanop et al., 2009).

Total annual cost of each process was estimated and used as criteria for choosing the optimum system to produce higher than 98 mole% of n-butyl acetate in the product stream. The total annual cost can be expressed in equation (4.1).

$$\text{Total annual cost} = \text{Operating cost} + \frac{\text{Capital cost}}{\text{Payback period}} \quad (4.1)$$

It was found that the energy requirement or overall heat duty were about 6450, 7570 and 5380 kW and total annual cost was about 1350, 1660 and 1560 \$1000/year for single-column reactive distillation, distillation-reactive distillation hybrid systems

and pervaporation-reactive distillation hybrid system, respectively. Therefore, although the pervaporation-reactive distillation hybrid system was attractive operation due to the minimum energy requirement, the single-column reactive distillation seemed to be the best system as offered the minimum total annual cost.

Sikder and coworkers (2011) proposed techno-economic analysis of lactic acid production from sugarcane juice using a membrane-integrated bioreactor system. The overall process of this production is shown in Figure 4.4. They found that about 36% of the total capital cost was in the fermentation step, where the main cost was at fermentation unit and sugarcane juice holding tank because of high cost of construction material. This cost can be reduced by using cheaper materials or removing the holding tank and sending the sugarcane juice directly to the mixing tank after sterilization step. Moreover, it was found that about 94% of the total cost was contributed by the operating cost where raw material and fermentation cost were its two major components. The operating cost can be reduced by many ways such as using a cheaper nitrogen source like silk worm larvae or yeast autolysate, installing the lactic acid plants in the sugarcane-growing areas as well as recycling the unconverted sugar from purification step to the fermenter. Based on the production rate of 16900 metric tons of 80 w/w% lactic acid, the final production cost of this process amounted to 3.15 US \$/kg.

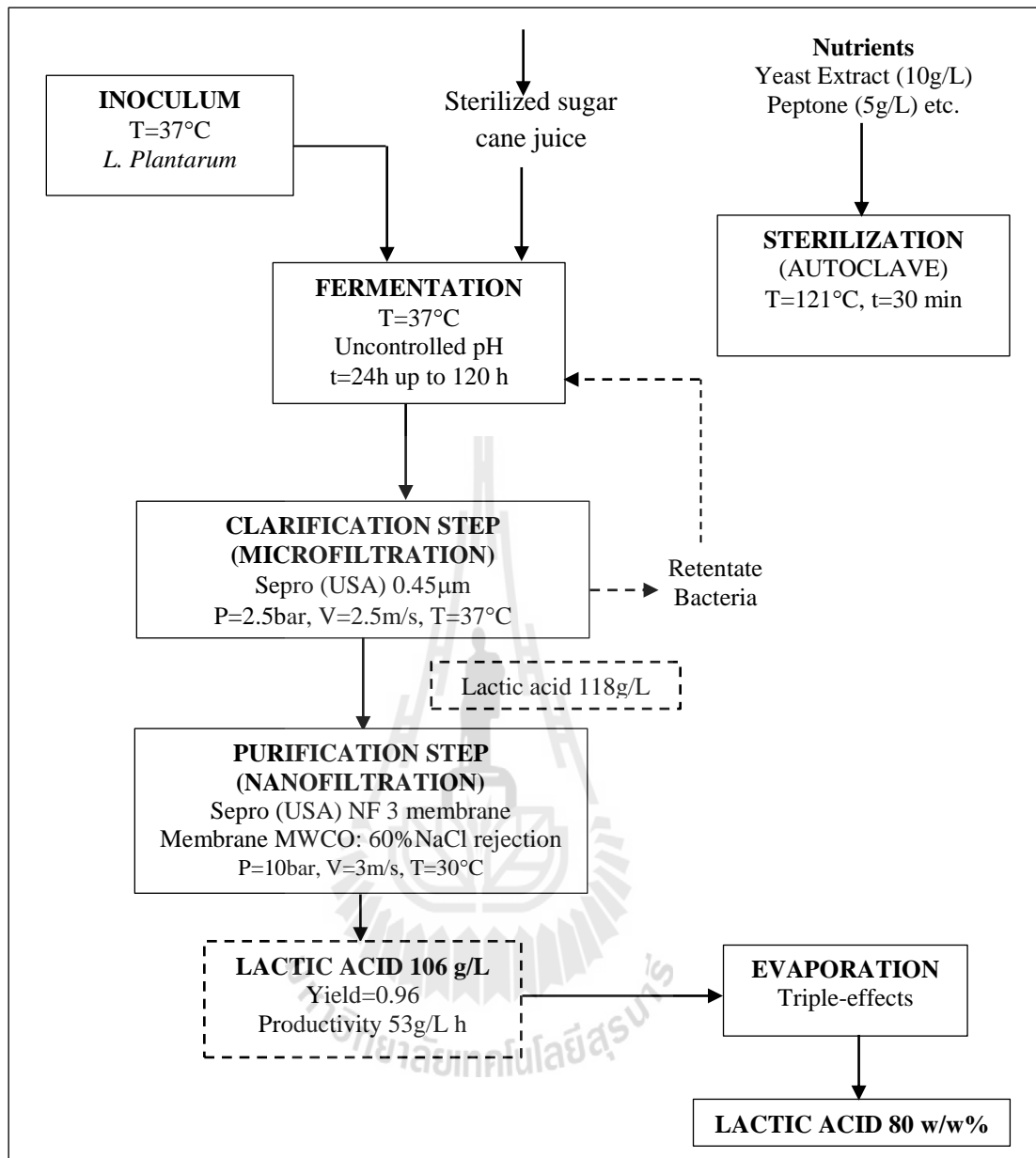


**Figure 4.4** Process schematic for 95% pure lactic acid production proposed by Sikder et al. (2011).

In 2013, Yusuf and Kamarudin proposed conceptual design and economic evaluation of biodiesel production from *Jatropha curcas* oil (JCO) by supercritical methanol process. The proposed process was shown in Figure 4.5. The reaction was

carried out in a plug flow reactor (PFR). Flash tank (FT) and the first distillation column (DC1) were used to recover methanol. Glycerol, the reaction by-product, was separated by decanter (DEC) and biodiesel was purified by the second distillation column (DC2). Material balance and energy balance of the proposed process were performed based on the capacity of 40000 tons per year of biodiesel production. Different feed stocks such as *Jatropha curcas* oil, wasted cooking oil and wasted canola oil were compared. *Jatropha curcas* oil gave the highest biodiesel purity, followed by waste cooking oil and waste canola oil. For economic evaluation, they found that raw material cost and capital cost were the major contribution of the biodiesel cost. Total production cost and operating cost from *Jatropha curcas* oil were the lowest when compared with process using waste cooking oil and waste canola oil. The production cost of biodiesel was found to be 0.78 USD/kg.

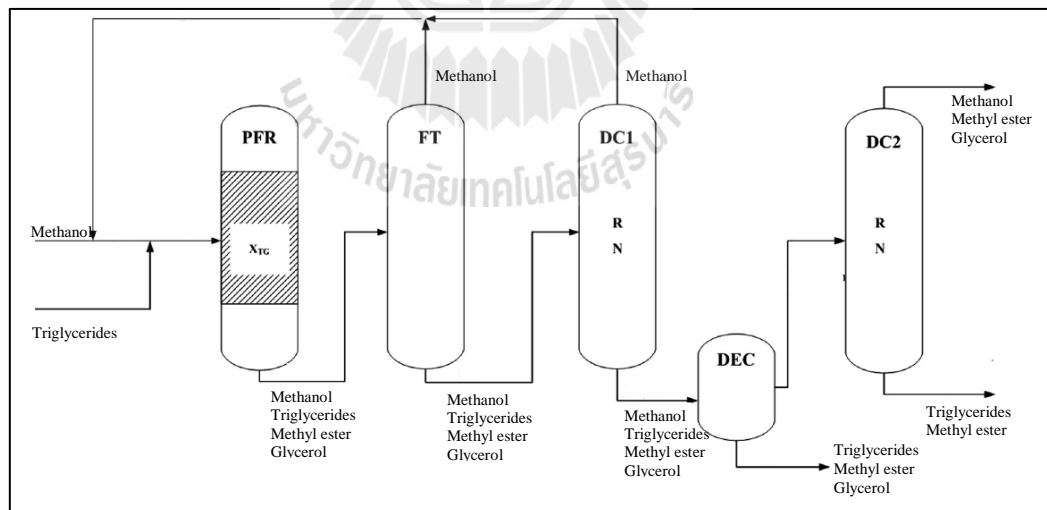


**Figure 4.5** Flowchart of supercritical methanol process

(Yusuf and Kamarudin, 2013).

## **4.4 Theory**

### **4.4.1 Capital Cost**

Capital cost or capital investment is an expense that relates to construction of a new plant or modification of an existing plant (Couper, 2003). Total capital investment (TCI) is the summation of fixed-capital investment (FCI) and working capital (WC). The fixed-capital investment is the expense that needed to supply the required manufacturing and plant facilities while the working capital is that necessary for the operation of the plant (Peter et al., 2003).

#### **4.4.1.1 Fixed Capital**

The fixed capital investment can be divided into manufacturing fixed-capital investment, also known as direct cost, and nonmanufacturing fixed-capital investment, also known as indirect cost. The manufacturing fixed capital cost represents the expense necessary for the installed process equipment with all components that are needed for complete process operation. The capital cost required for construction overhead and for all plant components that are not directly related to the process operation is designated the nonmanufacturing fixed capital investment (Peter et al., 2003). The expenses related to the fixed capital investment are tabulated in Table 4.1.

**Table 4.1** Expenses related to the fixed capital investment.

Direct costs	Indirect costs
Purchased equipment	Engineering and supervision
Purchased-equipment installation	Legal expense
Instrumentation and controls	Construction expenses
Piping	Contractor's fee
Electrical systems	Contingency
Buildings (including services)	Etc.
Yard improvements	
Service facilities	
Land	

#### 4.4.1.2 Working Capital Investment

The working capital investment is the additional investment needed, over and above the fixed capital, to start up and operate the plant to the point when income is earned. Most of the working capital cost is recovered at the end of the project (Sinnott, 1999). The working capital cost includes the expenses of:

- Start-up.
- Initial catalyst charges.
- Raw material and intermediates in the process.
- Finished product inventories.
- Funds to cover outstanding accounts from customers.

The ratio of working capital to total capital investment varies with different companies, but most chemical plants use an initial working capital amounting to 10 to 20% of the total capital investment cost. This percentage may increase to as much as 50% or more for companies producing products of seasonal demand, because of the large inventories which must be maintained for appreciable periods (Peter et al., 2003).

#### 4.4.1.3 Estimation of Capital Investment

Most of capital investment estimations are based on purchased cost of the major equipment item required for the process. The other costs, such as installed cost and land cost etc., being estimated as factors of the equipment cost (Sinnott, 1999). Accuracy of the capital cost estimation depends on the cost data and amount of design details available as well as the time spent on preparing of the estimation. In the early stages of a project only an approximate estimate will be justified based on the amount of information available (Tower and Sinnott, 2013).

There are many methods to estimate capital investment such as detailed-item estimate, unit cost estimate, Lang factor method, and percentage of delivered-equipment cost. The common method used for preliminary estimation of the capital investment is the percentage of delivered-equipment cost method. This method used the delivered equipment cost or purchased equipment cost in estimation of the fixed capital investment and total capital investment. The other items included in the total direct and indirect plant cost are estimated as the percentages of the purchase equipment cost. This is summarized in the following cost equation:

$$C_n = \sum (E + f_1E + f_2E + f_3E + \dots + f_nE) \quad (4.2)$$

where  $C_n$  is the capital cost.

$E$  is the purchased equipment cost.

$f_1, f_2, f_3, \dots, f_n$  are multiplying factors for piping, electrical, indirect costs, etc.

Additional component of the capital investment, which is the working capital, is based on average percentages of the total capital investment.

Average values of the various percentages have been determined for typical chemical plants, and these values are presented in Table 4.2. Default factors for three general process types which are solid, solid-fluid, and fluid processing are included in the table. The expected accuracy of this method is in the  $\pm 20$  to 30% range (Peter et al., 2003).

**Table 4.2** Ratio factors for estimating capital investment items based on purchased equipment cost (Peter et al., 2003).

Details	Percent of delivered-equipment cost for		
	Solid process	Solid-fluid process	Fluid process
<b>Direct costs</b>			
Purchased equipment delivered	100	100	100
purchased-equipment installation	45	39	47
Instrumentation and controls (installed)	18	26	36
Piping (installed)	16	31	68
Electrical systems (installed)	10	10	11
Buildings (including services)	25	29	18
Yard improvements	15	12	10
Service facilities (installed)	40	55	70
<b>Total direct plant cost</b>	<b>269</b>	<b>302</b>	<b>360</b>
<b>Indirect costs</b>			
Engineering and supervision	33	32	33
Construction expenses	39	34	41
Legal expenses	4	4	4
Contractor's fee	17	19	22
Contingency	35	37	44
<b>Total indirect plant cost</b>	<b>128</b>	<b>126</b>	<b>144</b>
<b>Fixed-capital investment</b>	<b>397</b>	<b>428</b>	<b>504</b>
<b>Working capital (15% of total capital investment)</b>	<b>70</b>	<b>76</b>	<b>89</b>
<b>Total capital investment</b>	<b>467</b>	<b>504</b>	<b>593</b>

#### **4.4.1.4 Purchased Equipment Cost**

There are many ways to estimate the purchasing cost of equipment. The most accurate method for determining process equipment costs is provided by a current price from sellers. Other alternative is to use the cost data on previously purchased equipment of the same type. However, for conceptual design, faster and simpler approach to estimate equipment capital cost is necessary. Faster way to estimate equipment cost is to use correlations. In the 1970s, many purchased equipment cost correlations were developed and published by Peters and Timmerhaus, Guthrie, Chilton and Happel (Douglas, 1988 and Green and Perry, 2008).

Guthrie's correlations provide more information than most other cost correlations. The purchased cost correlation proposed by Guthrie is developed for carbon-steel based equipment. Series of correction factors are needed such as material, type of equipment and pressure factor. Douglas (1988) updated Guthrie's correlations from mid-1968 values by using a ratio of the Marshall and Swift indices. Equipment costs which updated by Douglas are very useful and easy to calculate due to less number of variable required.

#### **4.4.2 Operating Cost**

Operating cost or manufacturing cost is the cost related to day-to-day operation of a chemical plant. Normally, operating cost is easy to estimate. In order to evaluate the operating cost, process information such as stream flow rate and number of operating units provided on process flow sheet diagram is required. Costs involved with operating cost can be tabulated as in Table 4.3. Variable operating cost is the

cost that varies with the rate of production while fixed operating cost is not. (Douglas, 1988 and Turton et al., 2009).

**Table 4.3** Examples of operating cost.

Variable operating cost	Fixed operating cost
Raw materials	Depreciation
Waste treatment	Supplies (office, janitorial, etc.)
Utilities	Plant support
Operating labor	Site services
Etc.	Etc.

#### 4.4.2.1 Raw Material Cost

Raw material cost depends on production rate of the process. Consumption of raw materials can be estimated from material balance of the process. Pricing data of each component can be obtained from purchasing or commercial departments or suppliers. Moreover, some pricing information is collected by many sources such as ICIS Chemical Business (Chemical Market Reporter) and Chemical Market Associates, Inc (Anderson, 2009). For economic evaluations of new, existing, or future plants, it is advisable to establish the true selling or purchase price for all raw materials and products. In most cases, the largest expense is nearly always the cost of raw materials (Green and Perry, 2008 and Turton et al., 2009).

#### 4.4.2.2 Utilities Cost

There are many type of utilities used in the process such as fuel, process steam, cooling water, other heating or cooling fluids, electricity, process water and other service streams. Most utility costs are based on the cost of fuel and

electricity (Towler and Sinnott, 2013). Utilities used in the process can be purchased from a public or private utility providers or self-generated and used by a single process unit. The utilities requirements are obtained from process material and energy balances (Green and Perry, 2008). Therefore, the utilities costs depend on its consumption rate and energy used in each process.

Details of other operating costs that not mentioned in this thesis can be found in many books and references such as Green and Perry (2008), Sinnott (1999), Turton et al. (2009) and Towler and Sinnott (2013).

#### 4.4.3 Production Cost

The production cost of the process can be estimated from the annual production cost divided by the annual production rate of the desired product as expressed in equation (4.3). The annual production cost can be estimated from the various components of the operating costs which are tabulated in Table 4.4 while the annual production rate can be obtained from the process flow sheet diagram (Sinnott, 1999).

$$\text{Production cost (THB/kg)} = \frac{\text{Annual production cost (THB/year)}}{\text{Annual production rate (kg/year)}} \quad (4.3)$$

**Table 4.4** Summary of the production cost (Sinnott, 1999).

<b>Cost Items</b>	<b>Typical Values</b>
<b>Variable Costs</b>	
1. Raw materials	From flow-sheet
2. Miscellaneous materials	10% of maintenance
3. Utilities	From flow-sheet
4. Shipping and packaging	Usually negligible
<b>Sub-total cost A =</b> .....	
<b>Fixed Costs</b>	
5. Maintenance	5-10% of fixed capital
6. Operating labor	From manning estimates
7. Laboratory costs	20-23% of operating labor
8. Supervision	20% of operating labor
9. Plant overheads	50% of operating labor
10. Capital charges	15% of fixed capital
11. Insurance	1% of fixed capital
12. Local taxes	2% of fixed capital
13. Royalties	1% of fixed capital
<b>Sub-total cost B =</b> .....	
<b>Direct production cost A+B =</b> .....	
14. Sales expense	
15. General overheads	20-30% of direct production cost
16. Research and development	
<b>Sub-total cost C =</b> .....	
<b>Annual production cost = A+B+C =</b> .....	

## 4.5 Methodology

Preliminary production costs of ethyl lactate synthesis from esterification of fermentation-derived magnesium lactate were investigated. The production cost of the processes designed in previous chapter, which were Process A and B, was evaluated and compared. The total capital cost was calculated by the percentage of delivered-equipment cost method. Equipment purchased costs, which consisted of column costs, tray costs, and cost of heat exchangers of column, were calculated using Guthire's correlations developed by Douglas (1988) while other expenses of capital cost were

calculated as the percentage of equipment purchased cost. For the operating cost, raw material and utility costs were calculated by price of each item multiply by its consumption rate which obtained from process flow diagram. The utility cost was covered only energy cost, other utilities such as steam and cooling water were not included. Production cost of ethyl lactate was calculated by annual production cost divided by annual production rate of ethyl lactate. All expenses in the process were calculated in Thai Baht (THB). The currency exchange rate used in calculation was obtained from Bank of Thailand's database of August 2014 which was 32.15 THB per USD. Marshall and Swift (M&S) index used in the calculation was 1536.5, which is the value obtained in the 4<sup>th</sup> quarter of 2011.

## **4.6 Results and Discussions**

Ethyl lactate production cost of process A and B as designed in Chapter III were estimated and compared. The production cost of ethyl lactate was estimated using equation (4.3) which the annual production cost can be calculated from the total capital cost and operating cost as in Table 4.4.

### **4.6.1 Capital Cost**

In order to calculate total capital investment using the percentage of delivered-equipment cost method, the purchased cost of major equipment was required to be used in calculation since other expenses of capital cost were considered as percentage of the equipment purchased investment.

#### **4.6.1.1 Equipment Purchased Cost**

Since the difference between Process A and B was the number of fractional distillation columns required in each process. Therefore, major

equipment of each process was considered only reactive distillation column and fractional distillation column as well as heat exchangers of each column. Purchased cost of columns and heat exchangers were evaluated using Guthire's correlations. Currency of costs obtained from Guthire's correlations was US dollar (USD). In order to change all the costs into Thai Baht (THB), the currency exchange rate of 32.15 THB per USD was used, which was obtained from Bank of Thailand's database of August 2014.

#### 4.6.1.1.1 Column Purchased Cost

The purchased costs of reactive distillation column and fractional distillation columns of both processes were considered as the summation of the column cost and tray cost. Guthire's correlation which was developed by Douglas in 1988 for columns purchased cost was shown in equation (4.4). Douglas (1988) did not develop Guthire's correlation to estimate the purchased cost of tray, therefore Guthire's correlation for tray purchased cost calculation was obtained from Albright (2009) which was shown in equation (4.5).

$$\text{Column purchased cost (USD)} = \left( \frac{M \& S}{280} \right) 101.9D^{1.066}HI^{0.802}F_c \quad (4.4)$$

$$\text{Tray purchased cost (USD)} = \left( \frac{M \& S}{273.1} \right) (8.655D - 1.218)(HI \times F_c) \quad (4.5)$$

where  $D$  is column diameter, ft.

$HI$  is column height, ft.

$F_c$  is correction factor,  $F_c = F_m F_p$  where  $F_m$  and  $F_p$  are correction factor for column material and pressure, respectively.

Details of calculation and value of each correction factor were presented in Appendix G. Since the diameter of all columns was equal, the key variable affected the column price was the column height. Costs of each columns in Process A and B were shown in Table 4.5 and 4.6, respectively. It can be seen that the second fractional distillation column in Process B was the costliest column because it have highest total number of stages (18 stages including the reboiler and condenser). The total column cost of Process A was found to be about 0.205 million Baht, which higher than 0.184 million Baht obtained from Process B. As expected, the higher column cost of Process A was due to higher number of fractional distillation columns required.

**Table 4.5** Column costs of Process A.

Column	Purchased cost (THB)		Total cost (THB)
	Column cost	Tray cost	
RD	60368.14	4504.08	64872.22
DIS1	43609.65	3002.72	46612.37
DIS2	43609.65	3002.72	46612.37
DIS3	43609.65	3002.72	46612.37
Total columns cost (THB)			204709.34

**Table 4.6** Column costs of Process B.

Column	Purchased cost (THB)		Total cost (THB)
	Column cost	Tray cost	
RD	39180.78	2627.38	41808.16
DIS1	56299.09	4128.74	60427.83
DIS2	76034.14	6005.44	82039.59
Total columns cost (THB)			184275.58

#### 4.6.1.1.2 Heat Exchanger Costs

Each reactive and fractional distillation column consisted of one reboiler and one condenser, which, in fact, work as a heat exchanger. Type of reboiler used in process designed was Kettle reboiler, while type of heat exchanger for condenser in the process designed was not specified. Since shell and tube heat exchanger is common exchanger which variety used in many applications and u-tube type is small size exchanger with less than 1 ft<sup>2</sup> of heat transfer area required (Seider et al., 1999). Therefore, condenser of each column was assumed to be shell and tube exchanger with u-tube configuration.

Purchased costs of heat exchanger can be calculated from Guthire's correlation modified by Douglas (1988), which was shown in equation (4.6).

$$\text{Heat exchanger purchased cost (USD)} = \left( \frac{M \& S}{280} \right) 101.3A^{0.65}F_c \quad (4.6)$$

where  $A$  is area of heat exchanger, ft<sup>2</sup>.

$F_c$  is correction factor and  $F_c = (F_d + F_p)F_m$ , where  $F_d$ ,  $F_p$  and  $F_m$  are correction factor for design type, pressure and material, respectively.

Heat transfer area for the reboiler and condenser can be estimated from equation (4.7).

$$A = \frac{Q}{U\Delta T} \quad (4.7)$$

where  $A$  is heat transfer area, ft<sup>2</sup>.

$Q$  is heat duty, Btu/hr.

$U$  is overall heat transfer coefficient, Btu/(hr°Fft<sup>2</sup>).

$\Delta T$  is temperature different, °F.

Since this thesis did not specify the configuration of heat exchangers and other operating conditions therefore some parameters are needed to be assumed. The reboiler was assumed to have an overall heat transfer coefficient of 250 Btu/(hr°Fft<sup>2</sup>) and temperature differential of 45°F. The condenser was assumed to have overall heat transfer coefficient of 150 Btu/(hr°Fft<sup>2</sup>) and temperature difference of condenser can be calculated from equation (4.8) (Su et al., 2013).

$$\Delta T_c = \frac{(120 - 90)}{\ln\left(\frac{T_b - 120}{T_b - 90}\right)} \quad (4.8)$$

where  $T_b$  is condenser temperature, °F.

Table 4.7 and 4.8 showed heat exchanger costs of both processes. It can be seen that the total condenser and total reboiler cost of Process A was 0.228 million Baht, which was higher than of 0.129 million Baht of Process B. It was also found that heat exchangers of the last fractional distillation column of both processes were the most expensive ones, which was likely due to highest energy required to purify ethyl lactate in this column. Total purchased cost of major equipment of each process were evaluated and shown in Table 4.9. It was found that the total capital cost of Process A and B were approximated to be 0.433 and 0.313 million Baht, respectively.

**Table 4.7** Heat exchanger cost of process A.

Column	Purchased Cost (THB)		Total cost (THB)
	Condenser cost	Reboiler cost	
RD	15574.74	18229.28	33804.01
DIS1	13834.32	20496.07	34330.38
DIS2	15318.57	26302.43	41621.00
DIS3	47108.09	71250.52	118358.62
Total heat exchanger cost (THB)			228114.01

**Table 4.8** Heat exchanger cost of process B.

Column	Purchased Cost (THB)		Total cost (THB)
	Condenser cost	Reboiler cost	
RD	12161.63	10299.58	22461.21
DIS1	9929.95	16690.83	26620.78
DIS2	32119.78	47326.52	79446.30
Total heat exchanger cost (THB)			128528.29

**Table 4.9** Total equipment purchased cost of Process A and Process B.

Process	Column costs (THB)	Heat exchanger costs (THB)	Total purchased cost (THB)
A	204709.34	228114.01	432823.35
B	184275.58	128528.29	312803.87

#### 4.6.1.2 Total Capital Cost

The total capital investment of Process A and B were evaluated using the percentage of delivered-equipment cost method. The other items of fixed capital cost, such as installed equipment cost, piping cost and land cost, were

evaluated as the percentage of the total purchased equipment cost while working capital cost was evaluated as the percentage based on the total capital investment. The ratio factor of fluid processing plant were used in the calculation because both of Process A and B were designed as distillation separation process which major phase in the process was fluid phase. The results of calculation were shown in Table 4.10. It was found that total capital cost of Process A was about 2.566 million Baht which much higher than that 1.855 million Baht from Process B. As mention before, higher total capital cost of Process A was resulted from higher number of fractional distillation column required in Process A.

**Table 4.10** Total capital cost of Process A and Process B.

Details	Percentage factor	Process	
		Process A	Process B
<b>Direct costs</b>			
Purchased equipment delivered	100	432823.35	312803.87
purchased-equipment installation	47	203426.97	147017.82
Instrumentation and controls (installed)	36	155816.41	112609.39
Piping (installed)	68	294319.88	212706.63
Electrical systems (installed)	11	47610.57	34408.43
Buildings (including services)	18	77908.20	56304.70
Yard improvements	10	43282.34	31280.39
Service facilities (installed)	70	302976.35	218962.71
<b>Total direct cost</b>	<b>360</b>	<b>1558164.06</b>	<b>1126093.93</b>
<b>Indirect costs</b>			
Engineering and supervision	33	142831.71	103225.28
Construction expenses	41	177457.57	128249.59
Legal expenses	4	17312.93	12512.15
Contractor's fee	22	95221.14	68816.85
Contingency	44	190442.27	137633.70
<b>Total indirect cost</b>	<b>144</b>	<b>623265.62</b>	<b>450437.57</b>
<b>Fixed-capital investment</b>	<b>504</b>	<b>2181429.68</b>	<b>1576531.50</b>
<b>Working capital (15% of total capital investment)</b>	<b>89</b>	<b>384958.18</b>	<b>278211.44</b>
<b>Total capital investment</b>	<b>593</b>	<b>2566387.86</b>	<b>1854742.95</b>

## **4.6.2 Operating Cost**

Since Process A and Process B were designed as a pilot plant scale and the aim of this chapter was preliminary estimated the production cost, therefore, the major expense of operating cost were considered to be raw material and utilities costs. Other items of operating cost such as operating labor cost and laboratory cost were not considered.

Since Process A and B were both designed to handle 50 L of fermentation-derived magnesium lactate per day, the raw material cost of both processes were the same while the utility costs were different due to difference in energy requirement and construction of the processes.

### **4.6.2.1 Raw Material Cost**

There are many raw materials used in the process such as fermentation-derived magnesium lactate powder, absolute ethanol, sulfuric acid and water. Price of each component was calculated based on the material balance of the process designed to 50 L fermentation broth per day. Since magnesium lactate powder was produced from fermentation process, its fermentation costs were considered as price of magnesium lactate. Other raw materials costs were calculated from the price obtained from their suppliers. Information of chemical price was shown in Appendix G.

#### **4.6.2.1.1 Magnesium Lactate Fermentation Cost**

Magnesium lactate powder was produced from fermentation of lactic acid using magnesium carbonate ( $\text{MgCO}_3$ ) as a neutralizing agent. Cost of magnesium lactate fermentation was estimated based on the capacity of 50 L fermentation broth per day. Other costs such as cost of precipitation and

separation were discounted. Since the information about composition of culture media was absented, the Man's Rogosa and Sharpe (MRS) broth formula was assumed to be the culture media of this production. Composition of MRS broth was obtained from Sigma Aldrich and Neogen and shown in Table 4.11.

**Table 4.11** Original composition of culture media broth.

Name	Composition	g/L
MRS broth from Sigma Aldrich company	Dipotassium hydrogen phosphate	2
	Glucose	20
	Magnesium sulfate heptahydrate	0.2
	Manganous sulfate tetrahydrate	0.05
	Meat extract	8
	Peptone	10
	Sodium acetate trihydrate	5
	Triammonium citrate	2
	Yeast extract	4
MRS broth from Neogen company	Enzymatic Digest of Animal Tissue	10
	Beef Extract	10
	Yeast Extract	5
	Dextrose	20
	Sodium Acetate	5
	Polysorbate 80	1
	Potassium Phosphate	2
	Ammonium Citrate	2
	Magnesium Sulfate	0.1
	Manganese Sulfate	0.05

From Table 4.11, it can be seen that glucose and dextrose were used as carbon source of MRS broth from Sigma Aldrich and Neogen, respectively. However, in this study, cassava starch was used as the carbon source because this compound is abundantly available in Nakhon Ratchasima region. Carbon source of MRS broth was, therefore, changed to cassava starch in the same proportion and the cost of culture media with different carbon sources were calculated and

compared. Result of the price comparison was shown as in Table 4.12, while details of the price of each chemical were shown in Appendix G. It was found that the price of MRS broth from Sigma Aldrich with cassava starch was the cheapest at 82 THB/L. This price was, therefore, used in calculation of the culture media in this thesis.

**Table 4.12** Price of MRS culture broth with different carbon sources.

Name	Carbon source	Price (THB/L)
MRS broth from Sigma Aldrich	Glucose	93
	Cassava starch	82
MRS broth from Neogen	Dextrose	105
	Cassava starch	108

Magnesium lactate fermentation was operated batchly with 3 days of operation time. Based on 50 L of fermentation broth, volume of culture media and amount of magnesium carbonate required in the fermentation were 10 L and 1.67 kg, respectively. Cost of electricity and water used in the fermentation were considered as operating cost which assumed to be 150 THB/day. Total cost of magnesium lactate fermentation, shown in Table 4.13, was found to be 1457.79 THB.

**Table 4.13** Costs of magnesium lactate fermentation based on 50 L of fermentation broth per day.

Description of cost	Price/Unit	Required quantity	Cost (THB)
Culture media + cassava starch	82.00 THB/L	10 L	820.00
Magnesium carbonate	112.45 THB/kg	1.67 kg	187.79
Electricity and water	150.00 THB/day	3 day	450.00
Total	-	-	1457.79

#### 4.6.1.1.2 Other Raw Material Cost

In addition to fermentation-derived magnesium lactate cost, cost of other raw materials in the production which were sulfuric acid, absolute ethanol, and water were estimated.

Magnesium lactate powder obtained from 50 L of fermentation broth was 5142.86 g. The optimal ratio of magnesium lactate to 1 M sulfuric acid in acidification was 20 g of magnesium lactate per 99 ml of 1 M sulfuric acid (information from Chapter II). Therefore, volume of 1 M sulfuric acid used in acidification was 25.457 L. In order to prepare 1M sulfuric acid, concentrated sulfuric acid was diluted with water and found that 23.069 L of water and 1.388 L of concentrated sulfuric acid were required in this dilution.

Other important raw materials were absolute ethanol and concentrated sulfuric acid, which were used as the reactant and catalyst of the esterification. Quantities of ethanol and concentrated sulfuric acid required were calculated based on the amount of lactic acid in the broth. The maximum concentration of lactic acid produced in the broth was 72 g/L, thus, amount of lactic acid produced was 4.5766 kg or 0.0508 kmol. From Chapter III, Process A and

Process B designed with the same initial molar feed ratio of ethanol-to-lactic acid of 3:1 and catalyst loading of 2 v/v%. Therefore, amount of absolute ethanol required was 0.1524 kmol or 8.953 L and amount of concentrate sulfuric acid required was 0.009 kmol or 0.482 L. Details of calculation was shown in Appendix F.

Costs of all raw materials were shown in Table 4.14. It was found that the total raw materials cost of this process was 2319.18 THB/day or about 846500 THB/year. The details of raw material costs were shown in Appendix G. Since, Process A and B were operated as the same capacity of fermentation-derived magnesium lactate, the raw materials costs of both processes were equal.

**Table 4.14** Raw material costs of ethyl lactate production from fermentation-derived magnesium lactate process.

Component	Volume (L)	Price/unit (THB/L)	Cost (THB)
Fermentation broth	50.000	-	1457.79
Absolute ethanol	8.95	84.62	757.60
Concentrate sulfuric acid	1.87	30.83	57.65
Water	23.07	2.00	46.14
Total	-	-	2319.18

#### 4.6.2.2 Utilities Cost

In this thesis, utilities costs covered only energy costs and other utilities such as steam and cooling water not considered. Daily costs of four different energy sources: electricity, diesel oil, liquefied petroleum gas (LPG) and fuel oil, were evaluated and compared.

Unit of energy required and daily cost of energy can be calculated using equation (4.9) and (4.10), respectively. Net Calorific Value or Lower Heating values of each energy source were obtained from Department of Alternative Energy Development and Efficiency, Thailand and were shown in Table 4.15. Price of petroleum based fuel was reported by the Energy Policy and Planning Office, Ministry of Energy, Thailand, while price of electricity was obtained from the Provincial Electricity Authority, Thailand. Prices of energy were shown in Table 4.16.

$$\text{Unit of energy required per day} = \frac{\text{Heat duty}}{\text{Heating value}} \times 24\text{hr} \quad (4.9)$$

$$\text{Cost of energy} = \text{Energy price} \times \text{Amount of energy required} \quad (4.10)$$

**Table 4.15** Energy content of different fuels.

Energy Type	Heating Value (MJ/Unit)	Unit
Electricity	3.6	kWh
Diesel Oil	36.42	L
LPG	49.30	kg
Fuel oil	39.77	L

**Table 4.16** Price of different energy sources.

Type of energy	Price per unit (THB/unit)	Unit
Electricity	4.58	kWh
Diesel Oil	29.99	L
LPG	30.13	kg
Fuel Oil	23.22	L

Amount of energy required and cost of energy for both processes were evaluated and tabulated in Table 4.17 and 4.18, respectively. As expected, Process A would require more energy than Process B due to higher number of fractional distillation columns used in the process. It can be seen that the amount of energy required and the energy costs in Process A were about two times higher than that required by Process B.

When considered results using different energy sources, it was clearly shown that amount of energy required agreed with the heating value of each energy source. Since the petroleum based fuels have quite high heating value, their required quantities in the both processes were lower than electricity, which has the lowest heating value. Even though the unit price of electricity was lowest here but its requirement was the highest, therefore the cost of electricity was much higher than other energy source. Demands of different petroleum based fuels were in the same order of magnitude, but differences in their prices led to the different total cost of each fuel. Fuel oil had the lowest total cost due to its lower price compared with other petroleum based fuels therefore fuel oil was selected to be an energy source of the process. Total fuel oil costs of Process A and B were found to be 365.35 and 181.88 THB/day or about 133400 and 66400 THB/year respectively.

**Table 4.17** Quantities and cost of energy required in Process A.

Unit operation		Heat Duty (Watt)	Unit of energy required per day				Cost of energy per day (THB)			
Name	Operation type		Electricity (kWh)	Diesel Oil (L)	LPG (kg)	Fuel Oil (L)	Electricity	Diesel Oil	LPG	Fuel oil
HEAT1	Heater	272.984	6.552	0.648	0.478	0.593	30.006	19.422	14.415	13.771
HEAT2	Heater	11.266	0.270	0.027	0.020	0.024	1.238	0.802	0.595	0.568
RD	Condenser	466.131	11.187	1.106	0.817	1.013	51.237	33.163	24.614	23.514
	Reboiler	280.249	6.726	0.665	0.491	0.609	30.805	19.939	14.798	14.137
DIS1	Condenser	333.703	8.009	0.792	0.585	0.725	36.681	23.742	17.621	16.834
	Reboiler	335.625	8.055	0.796	0.588	0.729	36.892	23.878	17.722	16.931
DIS2	Condenser	491.828	11.804	1.167	0.862	1.068	54.062	34.992	25.970	24.810
	Reboiler	492.616	11.823	1.169	0.863	1.070	54.148	35.048	26.012	24.850
DIS3	Condenser	2276.041	54.625	5.400	3.989	4.945	250.182	161.931	120.184	114.815
	Reboiler	2282.140	54.771	5.414	4.000	4.958	250.853	162.365	120.506	115.123
Total		7242.583	173.822	17.182	12.693	15.734	796.105	515.281	382.437	365.354

**Table 4.18** Quantities and cost of energy required in Process B.

Unit operation		Heat Duty (Watt)	Unit of energy required per day				Cost of energy per day (THB)			
Name	Operation type		Electricity (kWh)	Diesel Oil (L)	LPG (kg)	Fuel Oil (L)	Electricity	Diesel Oil	LPG	Fuel oil
HEAT1	Heater	272.984	6.552	0.648	0.478	0.593	30.006	19.422	14.415	13.771
HEAT2	Heater	2.691	0.065	0.006	0.005	0.006	0.296	0.191	0.142	0.136
RD	Condenser	317.623	7.623	0.754	0.557	0.690	34.913	22.598	16.772	16.023
	Reboiler	116.435	2.794	0.276	0.204	0.253	12.799	8.284	6.148	5.874
DIS1	Condenser	221.122	5.307	0.525	0.388	0.480	24.306	15.732	11.676	11.155
	Reboiler	244.700	5.873	0.581	0.429	0.532	26.897	17.409	12.921	12.344
DIS2	Condenser	1213.755	29.130	2.879	2.127	2.637	133.416	86.354	64.091	61.228
	Reboiler	1216.139	29.187	2.885	2.131	2.642	133.678	86.523	64.217	61.348
Total		3605.449	86.531	8.553	6.319	7.833	396.311	256.513	190.382	181.878

### 4.6.3 Production Cost

The production cost of ethyl lactate can be evaluated by dividing the annual production cost by the annual ethyl lactate production rate as expressed in equation (4.3). The annual production cost of Process A and B can be estimated from the operating cost and the fixed capital cost as presented in Table 4.4. The ethyl lactate production rate of both process were obtained from the result of process design in Chapter III and found to be 2043.46 and 1606.04 kilograms of ethyl lactate per year for Process A and B, respectively.

As mention before, Process A and B were designed as a small production process or pilot plant scale therefore cost of operating labor and other expenses involved with operating labor, some expenses of direct production cost and all of indirect production cost were not taken to account with the production cost in this thesis. Since the process to synthesis ethyl lactate from magnesium lactate solution used sulfuric acid as the catalyst, corrosion of equipment in the process might be occurred. Therefore, the maintenance cost of both process were considered to be about 10% of fixed capital cost.

The results of annual production cost estimation were shown in Table 4.19. As expected, the annual production cost of Process A was higher than that optioned from Process B due to higher requirement of number operation unit and energy of Process A. Total annual production cost of Process A and B were found to be about 1.569 and 1.339 million Baht per year, respectively.

**Table 4.19** Annual production cost of Process A and Process B.

Cost Items	Process A	Process B
	THB/year	THB/year
<b>Variable Costs</b>		
1. Raw materials	846500.70	846500.70
2. Miscellaneous materials	21814.30	15765.32
3. Utilities	133352.75	66386.20
4. Shipping and packaging	-	-
Sub-total cost A=	1001667.75	928652.22
<b>Fixed Costs</b>		
5. Maintenance	218142.97	157653.15
6. Operating labor	-	-
7. Laboratory costs	-	-
8. Supervision	-	-
9. Plant overheads	-	-
10. Capital charges	327214.45	236479.73
11. Insurance	21814.30	15765.32
12. Local taxes	-	-
13. Royalties	-	-
Sub-total cost B =	567171.72	409898.19
<b>Direct production cost A+B =</b>	<b>1568839.46</b>	<b>1338550.41</b>
14. Sales expense	-	-
15. General overheads	-	-
16. Research and development	-	-
Sub-total cost C =	-	-
<b>Annual production cost = A+B+C =</b>	<b>1568839.46</b>	<b>1338550.41</b>

The ethyl lactate production cost of Process A and B were shown in Table 4.20. It was found that the production cost of Process A was found to be 767.74 THB/kg, which lower than 833.45 THB/kg obtained from Process B. Higher ethyl lactate production cost of Process B could be due to significantly lower production rate of Process B. In order to reduce the production cost of Process B, the production rate of this process is needed to be increased.

**Table 4.20** Ethyl lactate production cost of Process A and B.

Process	Annual production cost (THB/year)	Annual production rate (kg/year)	Production cost (THB/kg)
Process A	1568839.46	2043.46	767.74
Process B	1338550.41	1606.04	833.45

However, it should be note that ethyl lactate concentration obtained from Process A and B were about 37 w/w% and 76 w/w% which quite lower than other commercial suppliers such as more than 97 w/w% from Acros Organic and higher than 98 w/w% from Sigma Aldrich. Ethyl lactate synthesized from processes proposed in this thesis may more suitable to be used as the solvent or used in other processes where high concentration of ethyl lactate solution is not required.

#### 4.7 Conclusions

Preliminary ethyl lactate production costs of two different production processes were evaluated and compared. Total capital investment of each process was calculated using the percentage delivered-equipment cost method. Other expenses of capital cost were considered as the percentage of major equipment purchased cost. The purchased costs of all reactive and fractional distillation columns and their heat exchangers were evaluated from Guthire's correlation. The total capital cost of Process A was found to be 2.566 million Baht which was higher than 1.855 million Baht of Process B due to higher number of operating unit required. Since the processes were designed as small production process or pilot plant scale. Some expenses of operating cost were not considered. The major expenses considered as the operating cost was cost of raw material and utility. Raw material costs of both

processes were equal because they were designed to handle 50 L of fermentation broth per day, while utilities costs were differed due to different process heat duty required. Fuel oil was selected to be an energy source of the process due to its lowest cost compared with other energy sources. The annual production cost was evaluated from the operating cost and fixed capital cost of each process. The annual production cost of Process A was found to be 1.569 million Baht per year which was higher than 1.339 million Baht per year from Process B. Higher annual production cost of Process A was might be due to higher number of operating unit and heat duty required. Although Process B has lower annual production cost, its ethyl lactate production cost was found to be higher than Process A due to significantly its lower production rate. The ethyl lactate production cost of Process A and B were found to be 767.74 and 833.45 THB/kg, respectively.

#### 4.8 References

- Akerberg, C. and Zacchi, G. (2000). An economic evaluation of the fermentative production of lactic acid from wheat flour. **Bioresource Technology**. 75: 119-126.
- Albright, L.F. (2009). **Albright's Chemical Engineering Handbook**. Tayler and Francis Groiup. Boca Raton, Florida.
- Anderson, J. (2009). Determining Manufacturing Costs. **AIChE, CEP magazine**. 27-31.
- Arpornwichanop, A., Koomsup, K., Kiatkittipong, W., Prasertthdam, P. and Assabumrungrat, S. (2009). Production of n-butyl acetate from dilute acetic

- acid and n-butanol using different reactive distillation systems: Economic analysis. **Journal of the Taiwan Institute of Chemical Engineers**. 40: 21-28.
- Chen, L., Ren, S. and Ye. X.P. (2014). Lactic acid production from glycerol using CaO as solid base catalyst. **Fuel Processing Technology**. 120: 40-47.
- Couper, J.R. (2003). **Process Engineering Economics**. Taylor & Francis Books. Dekker, New York.
- Douglas, J.M. (1988). **Conceptual Design of Chemical Processes**. McGraw-Hill. Singapore.
- Filachione, E.M. and Costello, E.J. (1952). Lactic esters by reaction of ammonium lactate with alcohols. **Industrial and Engineering Chemistry**. 44: 2189-2191.
- Guthrie, K.M. (1969). Capital Cost Estimating. **Chemical Engineering**. 76: 114.
- Kumar, R. and Mahajani, S.M. (2007). Esterification of lactic acid with n-butanol by reactive distillation. **Industrial and Engineering Chemistry Research**. 46: 6873-6882.
- Maki-Arvela, P., Simakova, I.L., Salmi, T. and Murzin, D.Y. (2014). Production of lactic acid/lactates from biomass and their catalytic transformations to commodities. **Chemical Reviews**. 114: 1909-1971.
- Marchetti, J.M., Miguel, V.U. and Errazu, A.F. (2008). Techno-economic study of different alternative for biodiesel production. **Fuel Processing Technology**. 89: 740-748.
- Pereira, C. S., Silva, V. M. and Rodriuges, A. E. (2011). Ethyl Lactate as a Solvent: Properties, Applications and Production Process - a Review. **Green Chemistry**. 13: 2658-2671.

- Green, D.W. and Perry, R.H. (2008). **Perry's Chemical Engineers' Handbook**. 8<sup>th</sup> edition. USA. McGraw-Hill.
- Seider, W.D., Seader, J.D. and Lewin, D.R. (1999). **Process design principles: synthesis, analysis, and evaluation**. USA. John Wiley & Sons.
- Sikder, J., Roy, M., Dey, P. and Pal, P. (2011). Techno-economic analysis of a membrane-integrated bioreactor system for production of lactic acid from sugarcane juice. **Biochemical Engineering Journal**. 63: 81-87.
- Sinnott, R.K. (1999). **Coulson & Richardson's Chemical Engineering**. Volume 6. 3<sup>rd</sup> edition. Miami USA: Butterworth-Heinemann.
- Su, C-Y., Yu, C-C., Chien, I-L. and Ward, J.D. (2013). Plant-wide economic comparison of lactic acid recovery processes by reactive distillation with different alcohols. **Industrial and Engineering Chemistry**. 52:11070-11083.
- Towler, G. and Sinnott, R. (2013). **Chemical engineering design: principles, and economics of plant and process design**. 2<sup>nd</sup> edition. Miami USA: Butterworth-Heinemann.
- Turton, R., Bailie, R.C., Whiting, W.B. and Shaeiwitz. (2009). **Analysis, Synthesis, and Design of Chemical Processes**. 3<sup>rd</sup> edition. Miami USA: Pearson Education International.
- Yusuf, N.N.A.N. and Kamarudin, S.K. (2013). Techno-economic analysis of biodiesel production from *Jatropha curcas* via a supercritical methanol process. **Energy Conversion and Management**. 75: 710-717.

## CHAPTER V

### CONCLUSIONS AND RECOMMENDATIONS

#### 5.1 Conclusions

5.1.1 In preparation of fermentation-derived magnesium lactate solution, optimal molar quantity of sulfuric acid to acidify magnesium lactate powder was found to be the stoichiometric amount, and the optimal sulfuric acid concentration was 1 M.

5.1.2 Kinetics of fermentation-derived magnesium lactate esterification with ethanol was investigated and compared with those of commercial high purity lactic acid esterification. Kinetic parameters of magnesium lactate esterification were found to be lower than those obtained from esterification of high purity lactic acid due to the presence of magnesium sulfate in fermentation-derived magnesium lactate solution.

5.1.3 The kinetic parameters were affected by reaction temperature, initial feed molar ratio of ethanol to lactic acid, catalyst loading as well as concentration of magnesium sulfate in the solution.

5.1.4 Correlations between reaction rate constant with process variables were established. Good agreement between experimental and calculated reaction rate constant were achieved in reaction with high initial molar ratio of ethanol to lactic acid. The deviation between experimental and calculated reaction rate constant may be due to presence of magnesium sulfate and lactic acid oligomers, which could be formed in solution with high lactic acid concentration.

5.1.5 Two different process schematics, Process A and Process B, for synthesis of ethyl lactate from fermentation-derived magnesium lactate by reactive distillation were preliminary designed by Aspen Plus simulator. Optimal operating conditions and configurations of both processes were investigated and proposed. Process A, where ethyl lactate was collected in the top product stream of the reactive distillation column, offered the advantages of higher overall yield and production rate of ethyl lactate. Process B, on the contrary, where ethyl lactate was discharged out of the reactive distillation column via the bottom product stream, produced ethyl lactate aqueous solution of higher concentration than the one produced in Process A. Process B also required less number of fractional distillation columns and lower heat duty required to purify ethyl lactate. To be specific, over 93% of overall ethyl lactate yield with production rate of 0.233 kg/hr were achieved in Process A, which were significantly higher than about 73% and 0.183 kg/hr obtained from Process B. The final product obtained from both processes was in form of aqueous solution with ethyl lactate concentration of 37.18 w/w% in Process A and 76.79 w/w% in Process B.

5.1.6 Total capital cost and annual production cost of Process A were found to be higher than Process B due to its higher number of operating units and heat duty requirement. Nevertheless, the ethyl lactate production cost of Process A was lower than Process B because of the higher ethyl lactate production rate achieved in Process A. The ethyl lactate production cost of Process A was found to be 767.74 THB/kg while the production cost of Process B was 833.25 THB/kg.

## 5.2 Recommendations

Recommendations for future work are summarized as follows:

5.2.1 For development of correlation between the reaction rate constant and operating variables, effect of lactic acid oligomers and concentration of process impurity like magnesium sulfate on value of the rate constant should be taken into account in order to increase accuracy of correlation.

5.2.2 The major impurity in esterification of fermentation-derived magnesium lactate was magnesium sulfate or magnesium (II) ion, which can interrupt the reaction kinetics. This salt should, therefore, be removed from the solution before it is fed into the reactive distillation column. Removal of magnesium sulfate or magnesium (II) ion can be done by separation methods such as adsorption and precipitation.

5.2.3 Water, which is the main component in the acidified fermentation-derived magnesium lactate solution plays significant role in ethyl lactate production in the reactive distillation. For future improvement of process efficiency, it is necessary to remove water from the feed solution before it is fed into the reactive distillation column.

5.2.4 The final ethyl lactate solution obtained from both production processes investigated in this study was still of low concentration. In order to increase ethyl lactate concentration in the product solution, another operating unit such as evaporator or distillation column should be used.

**APPENDIX A**  
**PROPERTIES OF ETHYL LACTATE AND**  
**MAGNESIUM LACTATE**

มหาวิทยาลัยเทคโนโลยีสุรนารี

## A.1 Ethyl Lactate

Ethyl lactate is an important ester also known as lactic acid ester or ethyl(S)-2-hydroxypropanoate. Conventional process to produce ethyl lactate is esterification of lactic acid with ethanol which catalyzed by acid catalyst (Pereira et al., 2011). The structural formula of ethyl lactate is represented in Figure A.1.

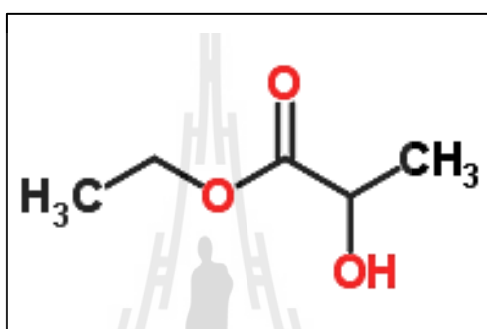


**Figure A.1** Structural formula of ethyl lactate.

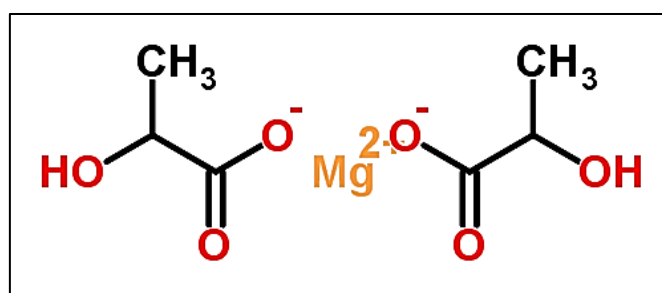
Ethyl lactate is clear to slightly yellow liquid with fruit-like odor. It can be considered as environmentally benign solvent or green solvent due to its nontoxic, biodegradable, renewable as well as excellent solvent properties. There are many industries application of ethyl lactate, i.e. it can be used as a food additive, in perfumery, as flavor chemicals and solvent (Pereira et al., 2011). Some physical and chemical properties of ethyl lactate are shown in Table A.1 (<http://en.wikipedia.org>).

**Table A.1** Physical and chemical properties of ethyl lactate.

Ethyl Lactate Properties	
Molecular formula	$C_5H_{10}O_3$
Molar mass	$118.13 \text{ g mol}^{-1}$
Appearance	Clear to slightly yellow liquid
Density	$1.03 \text{ g/cm}^3$
Melting point	$-26 \text{ }^\circ\text{C}$ ( $-15 \text{ }^\circ\text{F}$ ; $247 \text{ K}$ )
Boiling point	$151 \text{ to } 155 \text{ }^\circ\text{C}$ ( $304 \text{ to } 311 \text{ }^\circ\text{F}$ ; $424 \text{ to } 428 \text{ K}$ )
Solubility in water	Miscible
Solubility in ethanol and most alcohols	Miscible
Odor	Characteristic

## A.2 Magnesium Lactate

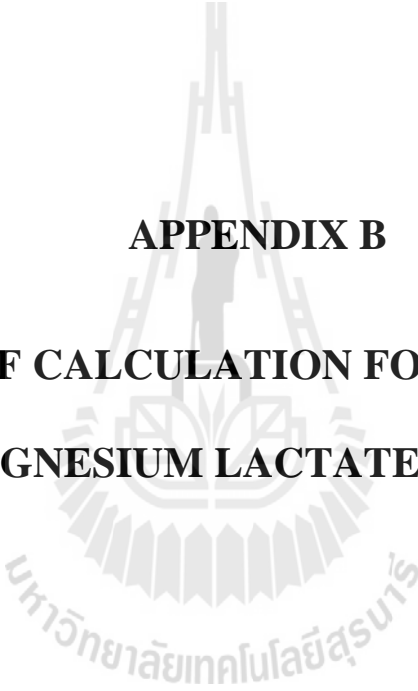
Magnesium lactate is the magnesium salt of lactic acid. Magnesium lactate can be produced in lactic acid fermentation by adding inorganic magnesium compound, i.e. magnesium carbonate, magnesium hydroxide and magnesium oxide, as the lactic acid neutralizing agent (Bode, 1965). The structural formula of magnesium lactate is represented in Figure A.2.

**Figure A.2** Structural formula of magnesium lactate.

There are many advantages of magnesium lactate. It can be used as an antioxidant in food, an anti-microbial agent and an acidity regulator in some food and beverages called E329. For industrial, magnesium lactate is used as a non-hazardous alkali to neutralize acidic waste water, as an antiperspirant armpit deodorant. In the winter, magnesium lactate is used in compound form to clear the snow and ice off highways. Moreover, magnesium lactate is also used in medical supplements. Some properties of magnesium lactate are presented in Table A.2 ([www.chm.bris.ac.uk](http://www.chm.bris.ac.uk), [www.inrfood.com](http://www.inrfood.com), and [www.chemspider.com](http://www.chemspider.com)).

**Table A.2** Physical and chemical properties of magnesium lactate.

Magnesium lactate properties	
Name and synonyms	Magnesium lactate L-lactic acid magnesium salt Magnesium bis(2-hydroxypropanoate) Magnesium lactate, anhydrous
Formula	$C_6H_{10}MgO_6$
Mol. mass	202.45 g/mol
Boiling Point	227.6 °C at 760 mmHg
Vapor Pressure	0.015 mmHg at 25°C
Enthalpy of Vaporization	53.96 kJ/mol
Flash Point	109.9 °C



**APPENDIX B**

**EXAMPLE OF CALCULATION FOR PREPARATION  
OF MAGNESIUM LACTATE SOLUTION**

In magnesium lactate solution preparation study, fermentation-derived magnesium lactate powder was acidified with sulfuric acid. The acidification reaction of magnesium lactate with sulfuric acid was shown in equation (B.1).



From equation B.1, stoichiometric coefficient of magnesium lactate to sulfuric acid was 1:1. Molar quantity and concentration of sulfuric acid used in acidification were varied. The optimal concentration and amount of sulfuric acid to obtain maximum molar quantity of lactic acid were investigated.

The molar ratio of magnesium lactate to sulfuric acid at 1:1 and concentration of sulfuric acid at 1M were used as an example of calculation. From Table 2.2, 20.0896 g of magnesium lactate was used.

$$\text{Molar quantity of magnesium lactate} = 20.0896 \text{ g} \times \frac{1 \text{ gmole}}{202.45 \text{ g}} = 0.099 \text{ gmole}$$

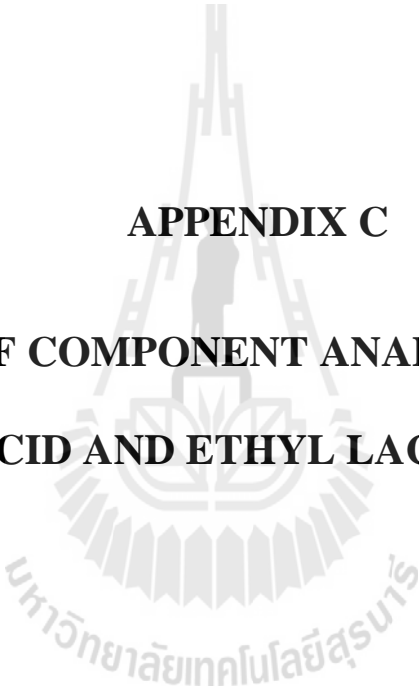
Since the molar ratio required was 1:1, molar quantity of 1 M sulfuric acid required = 0.099 gmole

Thus, volume of 1 M sulfuric acid required to use in the acidification of magnesium lactate =  $0.099 \text{ gmole} \times \frac{1 \text{ L}}{1 \text{ gmole}} \times \frac{1000 \text{ ml}}{1 \text{ L}} = 99 \text{ ml}$

Amount of lactic acid obtained from this acidification was analyzed by HPLC and found to be 0.180 gmole.

Therefore, percentage of lactic acid dissolved =

$$\left( \frac{0.180 \text{ gmole LA}}{\frac{2 \text{ gmole LA}}{1 \text{ gmole MgLA}_2} \times 0.099 \text{ gmole MgLA}_2} \right) \times 100\% = 90.8\%$$



**APPENDIX C**

**EXAMPLE OF COMPONENT ANALYSIS OF LACTIC  
ACID AND ETHYL LACTATE**

### C.1 Calibration Standard Curve of Lactic Acid by HPLC

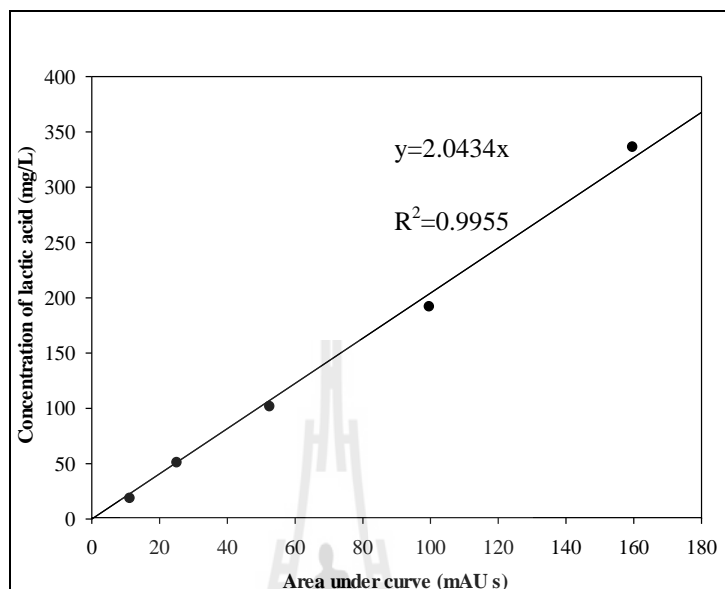


Figure C.1 Calibration standard curve of lactic acid.

### C.2 Calibration Standard Curve of Ethyl Lactate by GC

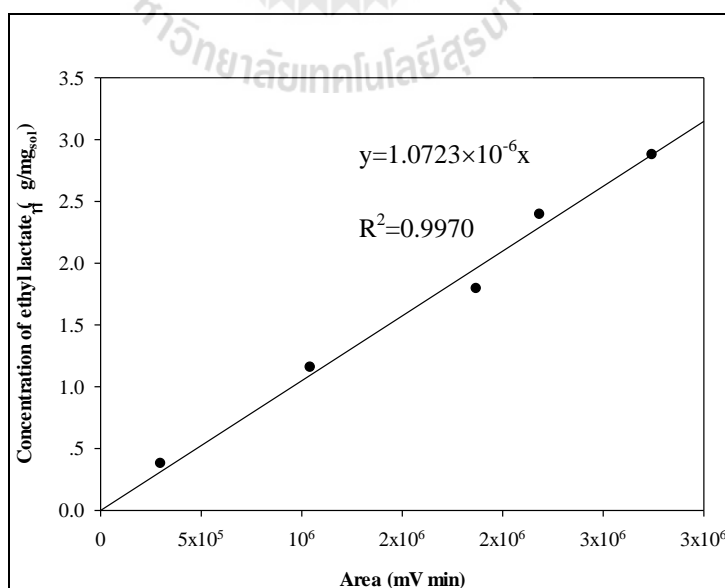


Figure C.2 Calibration standard curve of ethyl lactate.

### C.3 Lactic Acid Analysis

Lactic acid was obtained from acidification of fermentation-derived magnesium lactate with sulfuric acid. Example of calculation of lactic acid which analyzed by HPLC was shown as followed.

Sample of the magnesium lactate solution was diluted with DI water.

Weight of DI water = 9.9318 g (per 10ml of water)

Weight of sample = 0.0113 g (per 0.01ml of sample)

Total weight = (9.9318 + 0.0113) g = 9.9431 g

Chromatogram of lactic acid peak by HPLC was shown in Figure C.3. The calculation of acid concentration from calibration curve was 160.49657 mg/L.

Therefore amount of lactic acid in the solution:

$$= \frac{160.49657 \text{ mg}_{\text{LA}}}{1000 \text{ ml}_{\text{sol}}} \times \frac{10.01 \text{ ml}_{\text{sol}}}{0.01 \text{ ml}_{\text{sample}}} \times \frac{1 \text{ g}_{\text{LA}}}{1000 \text{ mg}_{\text{LA}}} \times \frac{1 \text{ mol}_{\text{LA}}}{90.08 \text{ g}_{\text{LA}}} \times 101.7 \text{ ml}_{\text{sample}}$$

$$= 0.180 \text{ mol}_{\text{LA}}$$

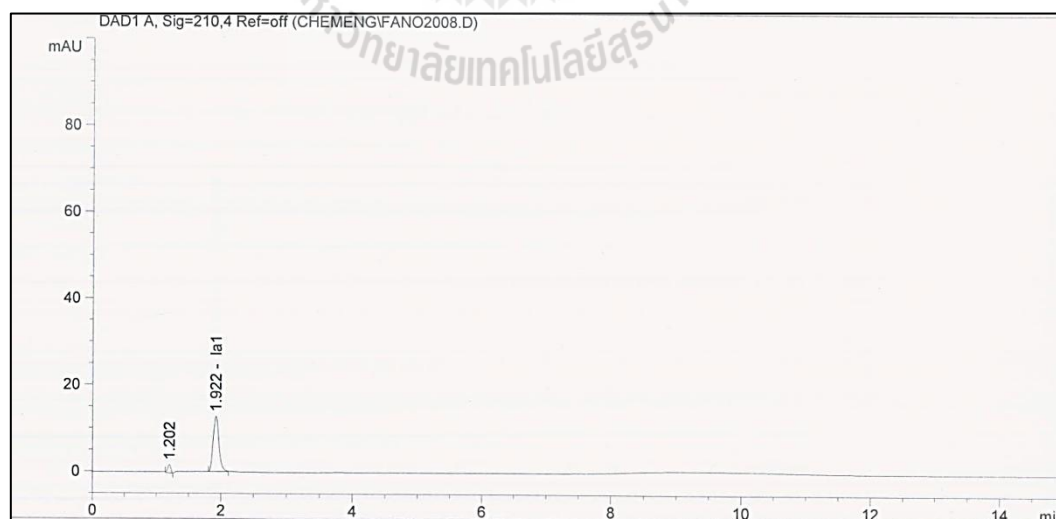


**Figure C.3** Chromatogram of lactic acid from HPLC.

## C.4 Ethyl Lactate Analysis

Example of calculation of ethyl lactate in the solution from esterification of magnesium lactate solution with ethanol was shown as followed.

Sample of the solution was diluted with DI water.

Weight of DI water = 0.8191 g

Weight of sample = 0.0465 g (density of sample is 1.013 g/ml)

Total weight = (0.8191 + 0.0465) g = 0.8656 g

Chromatogram of ethyl lactate by GC was shown in Figure C.4. The area under curve was 5,141,423 mAU. Concentration of ethyl lactate was calculated from calibration curve and found to be = 5.501  $\mu\text{g}/\text{mg}$

Thus, ethyl lactate concentration in the solution:

$$= \frac{5.501 \times 10^{-6} \text{ g}_{\text{EL}}}{1 \text{ mg}_{\text{sol}}} \times \frac{865.6 \text{ mg}_{\text{sol}}}{0.0465 \text{ g}_{\text{sample}}} \times \frac{1.013 \text{ g}_{\text{sample}}}{1 \text{ ml}_{\text{sample}}} \times \frac{1 \text{ mol}_{\text{EL}}}{118.13 \text{ g}_{\text{EL}}} \times \frac{1000 \text{ ml}_{\text{sample}}}{1 \text{ L}_{\text{sample}}}$$

$$= 0.878 \text{ M}$$

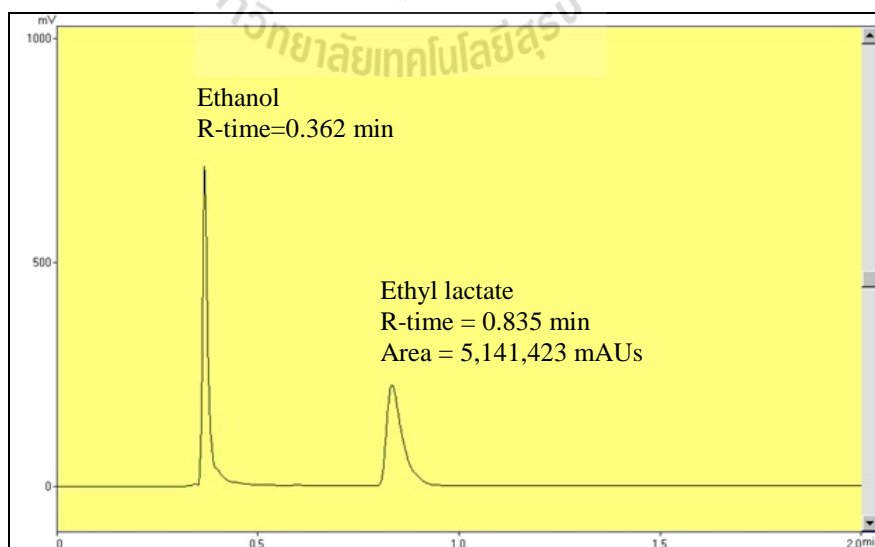
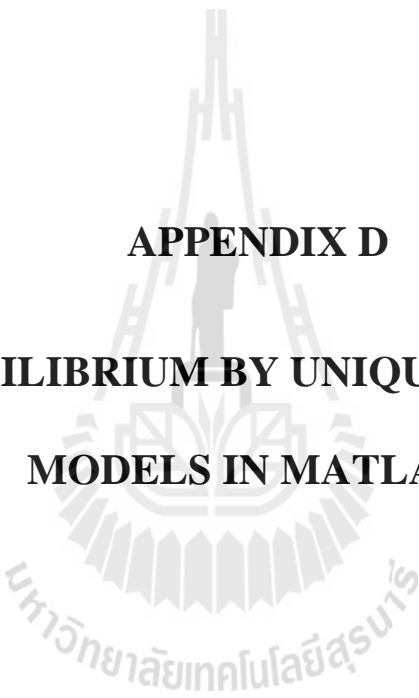


**Figure C.4** Chromatogram of ethyl lactate from GC.



**APPENDIX D**

**LIQUID EQUILIBRIUM BY UNIQUAC AND UNIFAC**

**MODELS IN MATLAB®**

UNIQUAC and UNIFAC model were used to determine liquid phase activity coefficient in the equilibrium of lactic acid + ethanol + ethyl lactate + water. For the UNIQUAC model, binary interaction parameters of each pair composition were obtained from Delgado et al. (2007) while the binary interaction parameters of the UNIFAC model were calculated using functional-group of each component in the solution from Chan and co-workers (2001).

MATLAB built-in function, *ode45* solver, was used to solve the ordinary differential equations. The *ode45* solver was based on explicit 4<sup>th</sup>-order Runge-Kutta method. The liquid phase activity coefficient and calculated conversion were calculated at initial guess of reaction rate constant. Then, the calculation conversions at any time were sent to nonlinear least-square regression solver, *lsqnonlin*, to minimize the sum of squared errors between the experimental and the calculated conversion. Both solvers were simultaneously operated. The optimal reaction rate constant was obtained from nonlinear least-square regression. The flowchart of program algorithm was shown in Figure D.1.

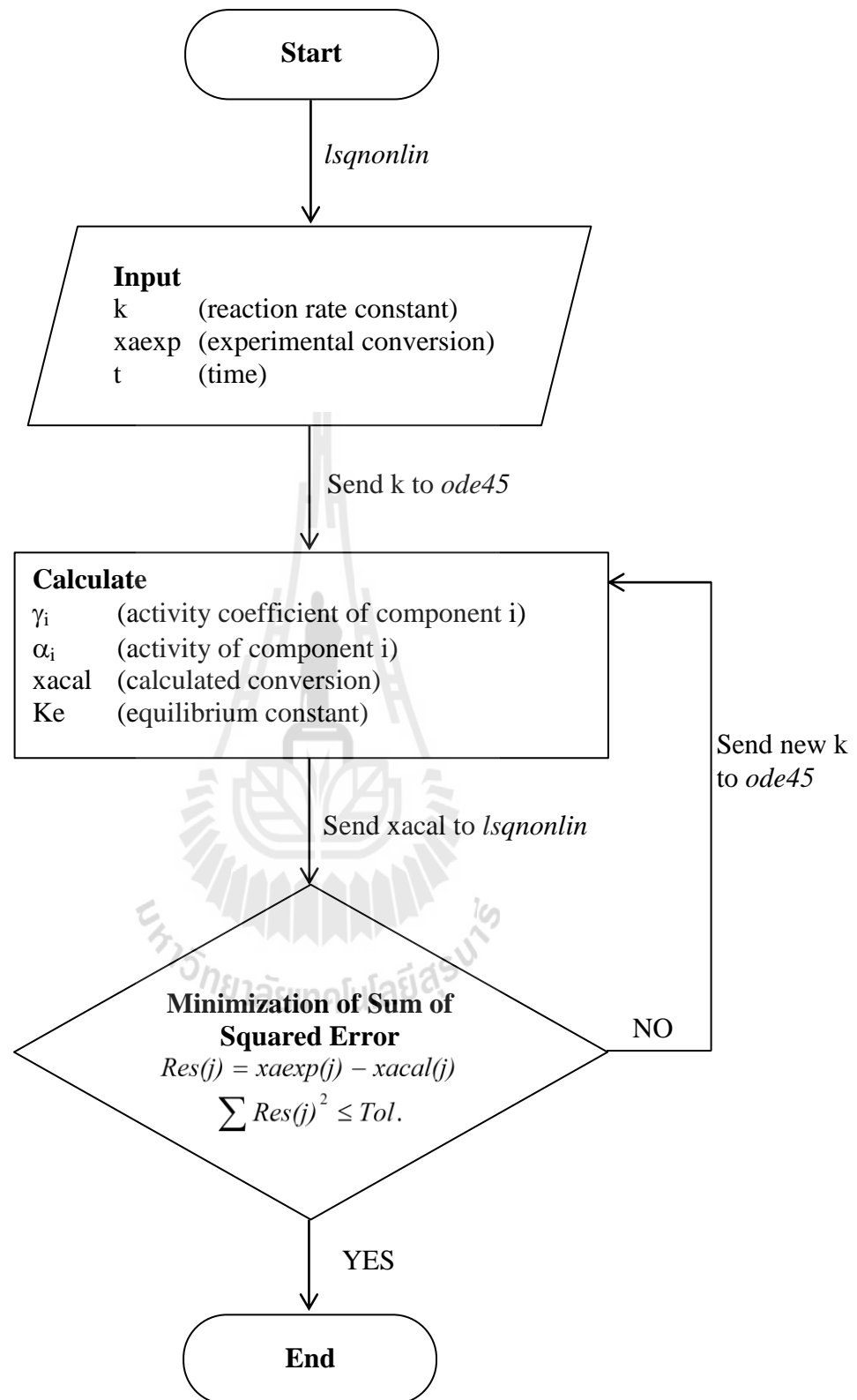


**Figure D.1** Flowchart of non-linear least square combined with *ode45*.

### D.1 The *lsqnonlin* program

Example of non-linear least square program in m-file was shown as followed:

Determining of reaction rate constant of esterification of lactic acid without presence of magnesium sulfate:

```
function res=kqcmg(m)

global k

k=m;

%a=LA

%-----input-----

%0g MgSO4

[t,xa]=ode45(@qcmg0,[0 4 20 40 60 90 120 180 240 300 360],0);

xaexp=[0.0000 0.0339 0.3264 0.3811 0.4159 0.4263 0.4351 0.4334 0.4361 0.4378

0.4555];

%-----

xacal=xa;

%-----Equation for non-lin-----

for j=1:11

    res(j)=xaexp(j)-xacal(j);

end
```

## D.2 The *ode45* Program with UNIQUAC Model

Example of *ode45* program with the UNIQUAC model in m-file was shown as followed:

```
function dxa=qcmg0(time,xa)

%Reaction temperature (K)

T=348.15;

dxa=zeros(1,1);

%Conversion at equilibrium

xae=0.4555;

%Constant for the reaction

m=3.095; n=12.182;

global k

%=====

%Assumed UNIQUAC model in liquid phase

%This system is esterification of lactic acid with ethanol

%EtOH(1)+LA(2)<--->EtLA(3)+W(4)

%=====

%+++++CONSTANT+++++

%Volume parameters related to pure component i (Van der Waals properties)

r=[2.1055 3.1648 4.4555 0.9200];

%Area parameters related to pure component i (Van der Waals properties)

q=[1.9720 2.8800 3.9280 1.4000];

z=10; %Coordination number
```

```

for i=1:4

    L(i)=(z/2)*(r(i)-q(i))-(r(i)-1);

end

%Interaction parameter for bicomponent

%Find a(i,j) and b(i,j)

a=[0 191.28 -148.67 728.97; -43.32 0 125.29 155.18; 341.77 52.64 0 99.8; -
756.95 -39.61 64.53 0];

b=[0 0 0 -2.0046; 0 0 0 0; 0 0 0 0; 2.4936 0 0 0];

%Find Tij

for i=1:4

    for j=1:4

        f(i,j)=exp(-(a(i,j)+b(i,j).*T)/T);

    end

end

end

%+++++Find Ke+++++

%Find mole fraction x(i) at equilibrium

x1e=(m-xae)/(1+m+n);

x2e=(1-xae)/(1+m+n);

x3e=xae/(1+m+n);

x4e=(n+xae)/(1+m+n);

xe=[x1e x2e x3e x4e];

%-----

%For combinatorial part at equilibrium

%-----

```

```

%Find volume fraction (Phi,p) and area fraction (Theta, t) for component i

for i=1:4

    pe(i)=xe(i).*r(i)./(xe(1).*r(1)+xe(2).*r(2)+xe(3).*r(3)+xe(4).*r(4));

    te(i)=xe(i).*q(i)./(xe(1).*q(1)+xe(2).*q(2)+xe(3).*q(3)+xe(4).*q(4));

end

%Activity coefficient for combinatorial part (ln gammaC)

sumxLe=xe(1).*L(1)+xe(2).*L(2)+xe(3).*L(3)+xe(4).*L(4);

for i=1:4

    gammaCe(i)=(log(pe(i)./xe(i))+(z/2).*q(i).*log(te(i)./pe(i))+L(i)-
(pe(i)./xe(i)).*sumxLe);

end

%-----

%For residual part at equilibrium

%-----

for i=1:4

    Be(i)=te(1).*f(1,i)+te(2).*f(2,i)+te(3).*f(3,i)+te(4).*f(4,i);

end

for i=1:4

    gammaRe(i)=-
q(i).*log(te(1).*f(1,i)+te(2).*f(2,i)+te(3).*f(3,i)+te(4).*f(4,i))+q(i)-
q(i).*((te(1).*f(i,1)./Be(1))+te(2).*f(i,2)./Be(2))+te(3).*f(i,3)./Be(3))+te(4).*
f(i,4)./Be(4));

end

```

```

%-----
%Find activity coefficient and activity at equilibrium
%-----
for i=1:4
    gammae(i)=exp(gammaCe(i)+gammaRe(i)); % activity coefficient
    acte(i)=xe(i).*gammae(i); % activity
end
%-----
%Find equilibrium constant, Ke
%-----
Ke=acte(3).*acte(4)./(acte(1).*acte(2))
%+++++For
ODE+++++
%Find mole fraction x(i) as a function of conversion (xa)
x1=(m-xa(1))/(1+m+n);
x2=(1-xa(1))/(1+m+n);
x3=xa(1)/(1+m+n);
x4=(n+xa(1))/(1+m+n);
x=[x1 x2 x3 x4];
%-----
%For combinatorial part
%-----
%Find volume fraction (Phi,p) and area fraction (Theta, t) for component i
for i=1:4

```

```

p(i)=x(i).*r(i)./(x(1).*r(1)+x(2).*r(2)+x(3).*r(3)+x(4).*r(4));
t(i)=x(i).*q(i)./(x(1).*q(1)+x(2).*q(2)+x(3).*q(3)+x(4).*q(4));
end
%Activity coefficient for combinatorial part (ln gammaC)
sumxL=x(1).*L(1)+x(2).*L(2)+x(3).*L(3)+x(4).*L(4);
for i=1:4
    if x(i)==0
        gammaC(i)=0;
    else
        gammaC(i)=(log(p(i)./x(i))+(z/2).*q(i).*log(t(i)./p(i))+L(i)-
(p(i)./x(i)).*sumxL);
    end
end
%-----
%For residual part
%-----
for i=1:4
    B(i)=t(1).*f(1,i)+t(2).*f(2,i)+t(3).*f(3,i)+t(4).*f(4,i);
end
for i=1:4
    gammaR(i)=-q(i).*log(t(1).*f(1,i)+t(2).*f(2,i)+t(3).*f(3,i)+t(4).*f(4,i))+q(i)-
q(i).*((t(1).*f(i,1)/B(1))+t(2).*f(i,2)/B(2))+t(3).*f(i,3)/B(3))+t(4).*f(i,4)/B(4));
end

```

```

%-----
%Find activity coefficient and activity
%-----
for i=1:4
    gamma(i)=exp(gammaC(i)+gammaR(i)); % activity coefficient
    act(i)=x(i).*gamma(i); % activity
end
%-----
%Differential Equation
%-----
dxa=k.*(act(1).*act(2)-(act(3).*act(4)./Ke));

```

### D.3 The *ode45* Program with UNIFAC Model

Example of *ode45* program with the UNIFAC model in m-file was shown as followed:

```

function dxa=qfmg0(time,xa)
%Reaction temperature (K)
T=348.15;
dxa=zeros(1,1);
%Conversion at equilibrium
xae=0.4555;
%Constant for the reaction
m=3.095; n=12.182;

```

```

global k

%=====

%Assumed UNIFAC in liquid phase

%=====

%This system is esterification of lactic acid with ethanol

%EtOH(1)+LA(2)<--->EtLA(3)+W(4)

%Functional group of any component (i)

%   EtOH = 1CH3+1CH2+1OH
%   LA   = 1CH3+1CH+1OH+1COOH
%   EtLA = 2CH3+1CH2+1CH+1OH+1COO
%   W    = 1H2O

%   let k--> CH3=1, CH2=2, CH=3, OH=4, H2O=5, COOH=6, COO=7

%+++++CONSTANT+++++

%From UNIFAC Structural Groups and Parameters

%Ref :: www.aim.env.uea.ac.uk/aim/info/UNIFACgroups.html

%Volume parameters of functional group k

    R=[0.9011 0.6744 0.4469 1.0000 0.9200 1.3013 1.3800];

%Area parameters of functional group k

    Q=[0.848 0.540 0.228 1.200 1.400 1.224 1.200];

%Find volume parameters and area parameters of chemical i (r(i) and q(i))

    z=10; %Coordination number

    for i=1:4

        if i==1

            r(i)=R(1)+R(2)+R(4);

```

```

q(i)=Q(1)+Q(2)+Q(4);

L(i)=(z/2)*(r(i)-q(i))-(r(i)-1);

elseif i==2

r(i)=R(1)+R(3)+R(4)+R(6);

q(i)=Q(1)+Q(3)+Q(4)+Q(6);

L(i)=(z/2)*(r(i)-q(i))-(r(i)-1);

elseif i==3

r(i)=2*R(1)+R(2)+R(3)+R(4)+R(7);

q(i)=2*Q(1)+Q(2)+Q(3)+Q(4)+Q(7);

L(i)=(z/2)*(r(i)-q(i))-(r(i)-1);

else

r(i)=R(5);

q(i)=Q(5);

L(i)=(z/2)*(r(i)-q(i))-(r(i)-1);

end

end

%Energy interaction parameter a(i,j)

%Ref ::www.aim.env.uea.ac.uk/aim/info/UNIFACgroups.html

a=[0 0 0 986.5 1318 663.5 387.1; 0 0 0 986.5 1318 663.5 387.1; 0 0 0 986.5 1318
663.5 387.1; 156.4 156.4 156.4 0 353.5 199 190.3; 300 300 300 -229.1 0 -14.09 -
197.5; 315.3 315.3 315.3 -151 -66.17 0 -337; 529 529 529 88.63 284.4 1179 0];

%Group interaction parameters f(i,j)

for i=1:7

for j=1:7

```

```

f(i,j)=exp(-a(i,j)./T);

end

end

%Mole fraction of group m(k=1-7) in any component i, X,mi

%Area fraction of group m(k=1-7) in any component i, Th,mi

%let m--> CH3=1, CH2=2, CH=3, OH=4, H2O=5, COOH=6, COO=7

%for component 1: EtOH = 1CH3+1CH2+1OH

Th11=Q(1)./(Q(1)+Q(2)+Q(4));
Th21=Q(2)./(Q(1)+Q(2)+Q(4));
Th41=Q(4)./(Q(1)+Q(2)+Q(4));

%for component 2: LA = 1CH3+1CH+1OH+1COOH

Th12=Q(1)./(Q(1)+Q(3)+Q(4)+Q(6));
Th32=Q(3)./(Q(1)+Q(3)+Q(4)+Q(6));
Th42=Q(4)./(Q(1)+Q(3)+Q(4)+Q(6));
Th62=Q(6)./(Q(1)+Q(3)+Q(4)+Q(6));

%for component 3: EtLA = 2CH3+1CH2+1CH+1OH+1COO

X13=2/6;
X23=1/6;
X33=1/6;
X43=1/6;
X73=1/6;

Th13=Q(1).*X13./(Q(1).*X13+Q(2).*X23+Q(3).*X33+Q(4).*X43+Q(7).*X73);
Th23=Q(2).*X23./(Q(1).*X13+Q(2).*X23+Q(3).*X33+Q(4).*X43+Q(7).*X73);
Th33=Q(3).*X33./(Q(1).*X13+Q(2).*X23+Q(3).*X33+Q(4).*X43+Q(7).*X73);

```

```

Th43=Q(4).*X43./(Q(1).*X13+Q(2).*X23+Q(3).*X33+Q(4).*X43+Q(7).*X73);
Th73=Q(7).*X73./(Q(1).*X13+Q(2).*X23+Q(3).*X33+Q(4).*X43+Q(7).*X73);

%for component 4: W = 1H2O

Th54=1;

%find lnGmi

%let k--> CH3=1, CH2=2, CH=3, OH=4, H2O=5, COOH=6, COO=7

%for component 1: EtOH = 1CH3+1CH2+1OH

B11=Th11.*f(1,1)+Th21.*f(2,1)+Th41.*f(4,1);
B21=Th11.*f(1,2)+Th21.*f(2,2)+Th41.*f(4,2);
B41=Th11.*f(1,4)+Th21.*f(2,4)+Th41.*f(4,4);

G11=Q(1).*(1-log(Th11.*f(1,1)+Th21.*f(2,1)+Th41.*f(4,1))-
(Th11.*f(1,1)/B11)-(Th21.*f(2,1)/B21)-(Th41.*f(4,1)/B41));

G21=Q(2).*(1-log(Th11.*f(1,2)+Th21.*f(2,2)+Th41.*f(4,2))-
(Th11.*f(1,2)/B11)-(Th21.*f(2,2)/B21)-(Th41.*f(4,2)/B41));

G41=Q(4).*(1-log(Th11.*f(1,4)+Th21.*f(2,4)+Th41.*f(4,4))-
(Th11.*f(1,4)/B11)-(Th21.*f(2,4)/B21)-(Th41.*f(4,4)/B41));

%for component 2: LA = 1CH3+1CH+1OH+1COOH

B12=Th12.*f(1,1)+Th32.*f(3,1)+Th42.*f(4,1)+Th62.*f(6,1);
B32=Th12.*f(1,3)+Th32.*f(3,3)+Th42.*f(4,3)+Th62.*f(6,3);
B42=Th12.*f(1,4)+Th32.*f(3,4)+Th42.*f(4,4)+Th62.*f(6,4);
B62=Th12.*f(1,6)+Th32.*f(3,6)+Th42.*f(4,6)+Th62.*f(6,6);

G12=Q(1).*(1-log(Th12.*f(1,1)+Th32.*f(3,1)+Th42.*f(4,1)+Th62.*f(6,1))-
(Th12.*f(1,1)/B12)-(Th32.*f(3,1)/B32)-(Th42.*f(4,1)/B42)-(Th62.*f(6,1)/B62));

```

$$G32=Q(3).\*(1-\log(\text{Th12.}\*f(1,3)+\text{Th32.}\*f(3,3)+\text{Th42.}\*f(4,3)+\text{Th62.}\*f(6,3))-$$

$$(\text{Th12.}\*f(3,1)/\text{B12})-(\text{Th32.}\*f(3,3)/\text{B32})-(\text{Th42.}\*f(3,4)/\text{B42})-(\text{Th62.}\*f(3,6)/\text{B62});$$

$$G42=Q(4).\*(1-\log(\text{Th12.}\*f(1,4)+\text{Th32.}\*f(3,4)+\text{Th42.}\*f(4,4)+\text{Th62.}\*f(6,4))-$$

$$(\text{Th12.}\*f(4,1)/\text{B12})-(\text{Th32.}\*f(4,3)/\text{B32})-(\text{Th42.}\*f(4,4)/\text{B42})-(\text{Th62.}\*f(4,6)/\text{B62});$$

$$G62=Q(6).\*(1-\log(\text{Th12.}\*f(1,6)+\text{Th32.}\*f(3,6)+\text{Th42.}\*f(4,6)+\text{Th62.}\*f(6,6))-$$

$$(\text{Th12.}\*f(6,1)/\text{B12})-(\text{Th32.}\*f(6,3)/\text{B32})-(\text{Th42.}\*f(6,4)/\text{B42})-(\text{Th62.}\*f(6,6)/\text{B62});$$

%for component 3: EtLA= 2CH<sub>3</sub>+1CH<sub>2</sub>+1CH+1OH+1COO

$$B13=\text{Th13.}\*f(1,1)+\text{Th23.}\*f(2,1)+\text{Th33.}\*f(3,1)+\text{Th43.}\*f(4,1)+\text{Th73.}\*f(7,1);$$

$$B23=\text{Th13.}\*f(1,2)+\text{Th23.}\*f(2,2)+\text{Th33.}\*f(3,2)+\text{Th43.}\*f(4,2)+\text{Th73.}\*f(7,2);$$

$$B33=\text{Th13.}\*f(1,3)+\text{Th23.}\*f(2,3)+\text{Th33.}\*f(3,3)+\text{Th43.}\*f(4,3)+\text{Th73.}\*f(7,3);$$

$$B43=\text{Th13.}\*f(1,4)+\text{Th23.}\*f(2,4)+\text{Th33.}\*f(3,4)+\text{Th43.}\*f(4,4)+\text{Th73.}\*f(7,4);$$

$$B73=\text{Th13.}\*f(1,7)+\text{Th23.}\*f(2,7)+\text{Th33.}\*f(3,7)+\text{Th43.}\*f(4,7)+\text{Th73.}\*f(7,7);$$

$$G13=Q(1).\*(1-$$

$$\log(\text{Th13.}\*f(1,1)+\text{Th23.}\*f(2,1)+\text{Th33.}\*f(3,1)+\text{Th43.}\*f(4,1)+\text{Th73.}\*f(7,1))-$$

$$(\text{Th13.}\*f(1,1)/\text{B13})-(\text{Th23.}\*f(1,2)/\text{B23})-(\text{Th33.}\*f(1,3)/\text{B33})-(\text{Th43.}\*f(1,4)/\text{B43})-$$

$$(\text{Th73.}\*f(1,7)/\text{B73}));$$

$$G23=Q(2).\*(1-$$

$$\log(\text{Th13.}\*f(1,2)+\text{Th23.}\*f(2,2)+\text{Th33.}\*f(3,2)+\text{Th43.}\*f(4,2)+\text{Th73.}\*f(7,2))-$$

$$(\text{Th13.}\*f(2,1)/\text{B13})-(\text{Th23.}\*f(2,2)/\text{B23})-(\text{Th33.}\*f(2,3)/\text{B33})-(\text{Th43.}\*f(2,4)/\text{B43})-$$

$$(\text{Th73.}\*f(2,7)/\text{B73}));$$

$$G33=Q(3).\*(1-$$

$$\log(\text{Th13.}\*f(1,3)+\text{Th23.}\*f(2,3)+\text{Th33.}\*f(3,3)+\text{Th43.}\*f(4,3)+\text{Th73.}\*f(7,3))-$$

$$(\text{Th13.}\*f(3,1)/\text{B13})-(\text{Th23.}\*f(3,2)/\text{B23})-(\text{Th33.}\*f(3,3)/\text{B33})-(\text{Th43.}\*f(3,4)/\text{B43})-$$

$$(\text{Th73.}\*f(3,7)/\text{B73}));$$

```

G43=Q(4).*(1-
log(Th13.*f(1,4)+Th23.*f(2,4)+Th33.*f(3,4)+Th43.*f(4,4)+Th73.*f(7,4))-
(Th13.*f(4,1)/B13)-(Th23.*f(4,2)/B23)-(Th33.*f(4,3)/B33)-(Th43.*f(4,4)/B43)-
(Th73.*f(4,7)/B73));

G73=Q(7).*(1-
log(Th13.*f(1,7)+Th23.*f(2,7)+Th33.*f(3,7)+Th43.*f(4,7)+Th73.*f(7,7))-
(Th13.*f(7,1)/B13)-(Th23.*f(7,2)/B23)-(Th33.*f(7,3)/B33)-(Th43.*f(7,4)/B43)-
(Th73.*f(7,7)/B73));

%for component 4: W= 1H2O

G54=Q(5).*(1-log(Th54.*f(5,5))-(Th54.*f(5,5)/Th54.*f(5,5)));

%+++++Find Ke+++++

%Find mole fraction x(i) at equilibrium
x1e=(m-xae)/(1+m+n);
x2e=(1-xae)/(1+m+n);
x3e=xae/(1+m+n);
x4e=(n+xae)/(1+m+n);
xe=[x1e x2e x3e x4e];

%-----

%For combinatorial part at equilibrium

%-----

%Find volume fraction (Phi,p) and area fraction (Theta, t) for component i
for i=1:4
    pe(i)=xe(i).*r(i)/(xe(1).*r(1)+xe(2).*r(2)+xe(3).*r(3)+xe(4).*r(4));
    te(i)=xe(i).*q(i)/(xe(1).*q(1)+xe(2).*q(2)+xe(3).*q(3)+xe(4).*q(4));

```

```

end

%Activity coefficient for combinatorial part (ln gammaC,e)

sumxLe=xe(1).*L(1)+xe(2).*L(2)+xe(3).*L(3)+xe(4).*L(4);

for i=1:4

    gammaCe(i)=log(pe(i)./xe(i))+(z/2).*q(i).*log(te(i)./pe(i))+L(i)-
((pe(i)./xe(i)).*sumxLe);

end;

%-----

%For residual part at equilibrium

%-----

%Mole fraction of group m (k=1-7)

xte=3.*xe(1)+4.*xe(2)+6.*xe(3)+xe(4);

for i=1:7 %i=k

    if i==1

        Xe(i)=(xe(1)+xe(2)+2*xe(3))./xte;

    elseif i==2

        Xe(i)=(xe(1)+xe(3))./xte;

    elseif i==3

        Xe(i)=(xe(2)+xe(3))./xte;

    elseif i==4

        Xe(i)=(xe(1)+xe(2)+xe(3))./xte;

    elseif i==5

        Xe(i)=xe(4)./xte;

    elseif i==6

```

```

Xe(i)=xe(2)./xte;

else

Xe(i)=xe(3)./xte;

end

end

%Area fraction of group m (k=1:7)
Thte=Q(1).*Xe(1)+Q(2).*Xe(2)+Q(3).*Xe(3)+Q(4).*Xe(4)+Q(5).*Xe(5)+Q(6).*
Xe(6)+Q(7).*Xe(7);

for i=1:7 %i=k

The(i)=Q(i).*Xe(i)./Thte;

end

for i=1:7

Be(i)=The(1).*f(1,i)+The(2).*f(2,i)+The(3).*f(3,i)+The(4).*f(4,i)+The(5).*
f(5,i)+The(6).*f(6,i)+The(7).*f(7,i);

end

for i=1:7

Ge(i)=Q(i).*(1-
log(The(1).*f(1,i)+The(2).*f(2,i)+The(3).*f(3,i)+The(4).*f(4,i)+The(5).*f(5,i)+
The(6).*f(6,i)+The(7).*f(7,i))-(The(1).*f(i,1)./Be(1))-(The(2).*f(i,2)./Be(2))-
(The(3).*f(i,3)./Be(3))-(The(4).*f(i,4)./Be(4))-(The(5).*f(i,5)./Be(5))-
(The(6).*f(i,6)./Be(6))-(The(7).*f(i,7)./Be(7)));

end

%find gammaR

gammaRe(1)=(Ge(1)-G11)+(Ge(2)-G21)+(Ge(4)-G41);

```

```

gammaRe(2)=(Ge(1)-G12)+(Ge(3)-G32)+(Ge(4)-G42)+(Ge(6)-G62);

gammaRe(3)=2.*(Ge(1)-G13)+(Ge(2)-G23)+(Ge(3)-G33)+(Ge(4)-
G43)+(Ge(7)-G73);

gammaRe(4)=(Ge(5)-G54);

%-----

%Find activity coefficient and activity at equilibrium

%-----

for i=1:4

    gammae(i)=exp(gammaCe(i)+gammaRe(i)); % activity coefficient

    acte(i)=xe(i).*gammae(i); % activity

end

%-----

%Find Equilibrium constant, Ke

%-----

Ke=acte(3).*acte(4)./(acte(1).*acte(2))

%+++++++For ODE+++++++

%Find mole fraction x(i) as a function of conversion (xa)

x1=(m-xa(1))/(1+m+n);

x2=(1-xa(1))/(1+m+n);

x3=xa(1)/(1+m+n);

x4=(n+xa(1))/(1+m+n);

x=[x1 x2 x3 x4];

%-----

```

```

%For combinatorial part

%-----

%Find volume fraction (Phi,p) and area fraction (Theta, t) for component i

for i=1:4

    p(i)=x(i).*r(i)./(x(1).*r(1)+x(2).*r(2)+x(3).*r(3)+x(4).*r(4));

    t(i)=x(i).*q(i)./(x(1).*q(1)+x(2).*q(2)+x(3).*q(3)+x(4).*q(4));

end

%activity coefficient for combinatorial part (ln gammaC)

sumxL=x(1).*L(1)+x(2).*L(2)+x(3).*L(3)+x(4).*L(4);

for i=1:4

    if x(i)==0

        gammaC(i)=0;

    else

        gammaC(i)=log(p(i)./x(i))+z/2.*q(i).*log(t(i)./p(i))+L(i)-((p(i)./x(i)).*sumxL);

    end

end

end

%-----

%For residual part

%-----

%mole fraction of group m (k=1-7)

xt=3.*x(1)+4.*x(2)+6.*x(3)+x(4);

for i=1:7 %i=k

    if i==1

        X(i)=(x(1)+x(2)+2.*x(3))./xt;
    end
end

```

```

elseif i==2
    X(i)=(x(1)+x(3))./xt;
elseif i==3
    X(i)=(x(2)+x(3))./xt;
elseif i==4
    X(i)=(x(1)+x(2)+x(3))./xt;
elseif i==5
    X(i)=x(4)./xt;
elseif i==6
    X(i)=x(2)./xt;
else
    X(i)=x(3)./xt;
end
end
end
%area fraction of group m (k=1:7)
ThT=Q(1).*X(1)+Q(2).*X(2)+Q(3).*X(3)+Q(4).*X(4)+Q(5).*X(5)+Q(6).*X(6)+
Q(7).*X(7);
for i=1:7 %i=k
    Th(i)=Q(i).*X(i)./ThT;
end
for i=1:7
    B(i)=Th(1).*f(1,i)+Th(2).*f(2,i)+Th(3).*f(3,i)+Th(4).*f(4,i)+Th(5).*f(5,i)+
Th(6).*f(6,i)+Th(7).*f(7,i);
end

```

```

for i=1:7

    G(i)=Q(i).*(1-
log(Th(1).*f(1,i)+Th(2).*f(2,i)+Th(3).*f(3,i)+Th(4).*f(4,i)+Th(5).*f(5,i)+Th(6).*
f(6,i)+Th(7).*f(7,i))-Th(1).*f(i,1)./B(1)-Th(2).*f(i,2)./B(2)-Th(3).*f(i,3)./B(3)-
Th(4).*f(i,4)./B(4)-Th(5).*f(i,5)./B(5)-Th(6).*f(i,6)./B(6)-Th(7).*f(i,7)./B(7));

    end

    %find gammaR

    gammaR(1)=(G(1)-G11)+(G(2)-G21)+(G(4)-G41);

    gammaR(2)=(G(1)-G12)+(G(3)-G32)+(G(4)-G42)+(G(6)-G62);

    gammaR(3)=2.*(G(1)-G13)+(G(2)-G23)+(G(3)-G33)+(G(4)-G43)+(G(7)-
G73);

    gammaR(4)=(G(5)-G54);

%-----

%Find activity coefficient and activity

%-----

    for i=1:4

        gamma(i)=exp(gammaC(i)+gammaR(i)); % activity coefficient

        act(i)=x(i).*gamma(i); % activity

    end

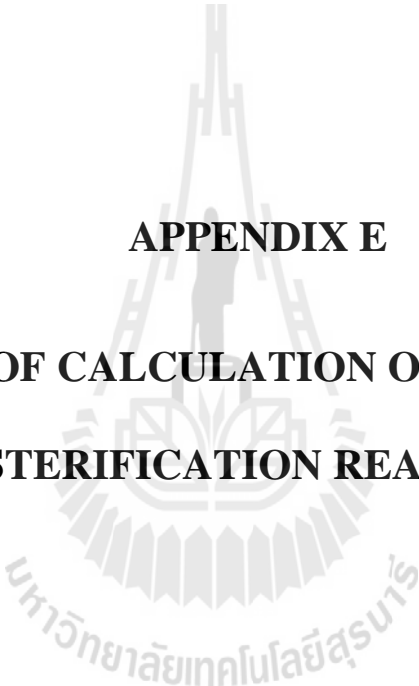
%-----

%Different Equation

%-----

dxa=k.*(act(1).*act(2)-(act(3).*act(4)./Ke));

```



**APPENDIX E**

**EXAMPLE OF CALCULATION OF CONSTANT IN  
ESTERIFICATION REACTION**

### E.1 Mole Fraction of Composition in the Solution

The esterification of lactic acid (LA) with ethanol (EtOH) to produce ethyl lactate (EtLA) and water (W) can be written as:



Let  $x_A$  is conversion of lactic acid at any time. Mole fractions of each component,  $x_i$ , in term of conversion of lactic acid are shown as followed:

$$\text{Mole fraction of lactic acid: } x_{LA} = \frac{C_{LA}}{C_{total}} = \frac{C_{LA0}(1-x_A)}{C_{EtOH} + C_{LA} + C_{ETLA} + C_W} \quad (E.2)$$

$$\text{From } C_{total} = C_{EtOH} + C_{LA} + C_{ETLA} + C_W$$

$$C_{total} = (C_{LA0}(m-x_A)) + (C_{LA0}(1-x_A)) + (C_{LA0}(x_A)) + (C_{LA0}(n+x_A)) \quad (E.3)$$

$$\text{where } m = \frac{C_{EtOH0}}{C_{LA0}} \text{ and } n = \frac{C_{W0}}{C_{LA0}}$$

Substitute (E.3) into (E.2) will obtain:

$$x_{LA} = \frac{C_{LA0}(1-x_A)}{(C_{LA0}(m-x_A)) + (C_{LA0}(1-x_A)) + (C_{LA0}(x_A)) + (C_{LA0}(n+x_A))}$$

$$x_{LA} = \frac{(1-x_A)}{(m-x_A) + (1-x_A) + (x_A) + (n+x_A)} = \frac{(1-x_A)}{1+m+n}$$

$$\text{Thus, } x_{LA} = \frac{(1-x_A)}{1+m+n} \quad (E.4)$$

Similarly with mole fraction of lactic acid, mole fraction of ethanol, ethyl lactate and water are shown in equation (E.5) to (E.7).

$$x_{EtOH} = \frac{(m-x_A)}{1+m+n} \quad (E.5)$$

$$x_{EtLA} = \frac{x_A}{1+m+n} \quad (E.6)$$

$$x_W = \frac{n + x_A}{1 + m + n} \quad (\text{E.7})$$

## E.2 Initial concentration ratio of ethanol to lactic acid constant, $m$

Volume of initial ethanol = 94.2 ml

Volume of initial lactic acid = 150.7 ml

Volume of sulfuric acid (96wt%) = 5.1 ml

Total volume of solution = 250 ml

Initial concentration of lactic acid = 3.4465 M

Initial mole of lactic acid =  $150.7 \text{ ml} \times \frac{3.4465 \text{ mol}}{1 \text{ L}} \times \frac{1 \text{ L}}{1000 \text{ ml}} = 0.5194 \text{ mole}$

Initial concentration of lactic acid in solution =  $\frac{0.5194 \text{ mol}}{250 \text{ ml}} \times \frac{1000 \text{ ml}}{1 \text{ L}} = 2.078 \text{ M}$

Initial concentration of ethanol

$$= 94.2 \text{ ml} \times \frac{0.78 \text{ g}}{1 \text{ ml}} \times \frac{1 \text{ mole}}{46 \text{ g}} \times \frac{1}{250 \text{ ml}} \times \frac{1000 \text{ ml}}{1 \text{ L}} = 6.389 \text{ M}$$

From  $m = \frac{C_{\text{ETOH, initial}}}{C_{\text{LA, initial}}}$

Thus,  $m = \frac{6.389 \text{ M}}{2.078 \text{ M}} = 3.075$

## E.3 Initial concentration ratio of water to lactic acid constant, $n$

Volume of initial ethanol = 94.2 ml

Volume of initial lactic acid = 150.7 ml

Volume of sulfuric acid (96wt%) = 5.1 ml

Total volume of solution = 250 ml

Initial concentration of lactic acid = 3.4465 M

Initial amount of water is obtained from sulfuric acid and lactic acid solution.

Water obtained from sulfuric acid 96wt%:

$$= 5.1 \text{ ml sol} \times \frac{1.834 \text{ g sol}}{1 \text{ ml sol}} \times \frac{4 \text{ g water}}{100 \text{ g sol}} \times \frac{1 \text{ ml water}}{1 \text{ g water}} = 0.374 \text{ ml water}$$

Water obtained from lactic acid solution

Lactic acid 88wt% volume:

$$= 150.7 \text{ ml} \times \frac{3.4465 \text{ mol}}{1000 \text{ ml}} \times \frac{90.08 \text{ g}}{1 \text{ mol}} \times \frac{1 \text{ ml LA}_{88\text{wt}\%}}{1.22 \text{ g LA}_{88\text{wt}\%}} \times \frac{100 \text{ g LA}_{88\text{wt}\%}}{88 \text{ g}} = 43.5645 \text{ ml}$$

$$\therefore \text{Water in the solution} = 150.7 \text{ ml sol} - 43.5645 \text{ ml LA}_{88\text{wt}\%} = 107.1355 \text{ ml water}$$

Water in lactic acid 88wt%:

$$= 43.5645 \text{ ml LA}_{88\text{wt}\%} \times \frac{1.22 \text{ g LA}_{88\text{wt}\%}}{1 \text{ ml LA}_{88\text{wt}\%}} \times \frac{12 \text{ g water}}{100 \text{ g LA}_{88\text{wt}\%}} \times \frac{1 \text{ ml water}}{1 \text{ g water}} = 6.3778 \text{ ml water}$$

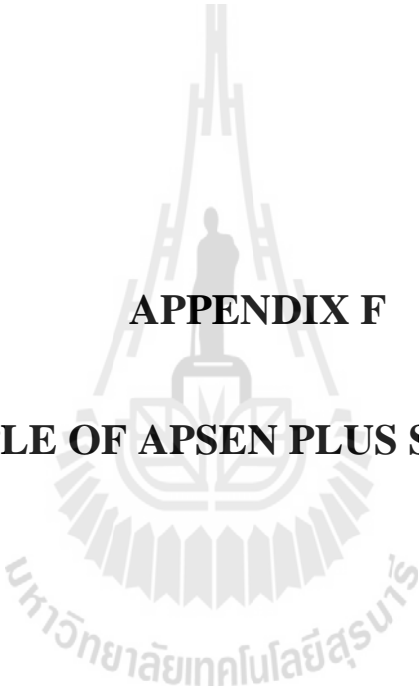
$$\text{Total volume of water} = 107.1355 + 6.3778 = 113.8875 \text{ ml}$$

Initial concentration of water =

$$\frac{113.8875 \text{ ml water}}{250 \text{ ml sol}} \times \frac{1 \text{ g water}}{1 \text{ ml water}} \times \frac{1 \text{ mol}}{18 \text{ g water}} \times \frac{1000 \text{ ml}}{1 \text{ L}} = 25.3083 \text{ M}$$

$$\text{From} \quad n = \frac{C_{\text{water,initial}}}{C_{\text{LA,initial}}}$$

$$\text{Thus,} \quad n = \frac{25.3083 \text{ M}}{2.078 \text{ M}} = 12.182$$



**APPENDIX F**

**EXAMPLE OF APSEN PLUS SIMULATOR**

Aspen Plus simulator is a product of Aspen Technology, Inc. It is a part of the Aspen Engineering Suite™ (AESTM). Aspen Plus program is a powerful and flexible tool for a wide variety of engineering tasks. It can handle very complex processes, including multiple-column separation systems, chemical reactors, distillation of chemically reactive compounds, and even electrolyte solutions like mineral acids and sodium hydroxide solutions. Another advantage of Aspen Plus simulator is Aspen Plus library which contains information on property of chemicals, unit operations, reactions, and much more (<http://www.chems.msu.edu/resources/tutorials/ASPEN>).

For process simulation using Aspen Plus simulator (V.7.3.2), details of the simulation in Aspen Plus are shown as followed. Process to produce ethyl lactate via top product stream or Process A is selected to be an example. The production is handled with 50 L of fermentation broth and UNIQUAC activity coefficient model is used to present non-ideality of all solution in the process.

### F.1 Composition of Feed Streams

Process simulation is based on the target of 50 L of fermentation broth.

Concentration of lactic acid in broth	72 g/L
Purity of lactic acid in magnesium lactate	70 w/w%
Amount of magnesium lactate obtained from broth	5142.86 g
Preparation of magnesium lactate solution by acidification with sulfuric acid	
Total volume of 1 M sulfuric acid required	25457.14 mL
Evaporation of water from solution 60%, remained water	10182.86 mL
Mass of water remained after evaporation	10162.49 g
Amount of magnesium sulfate in solution	3953.21 g

Thus the composition in fermentation-derived magnesium lactate solution and molar flow rate of each component which based on 50 L/day of fermentation broth are shown in Table F.1.

**Table F.1** Composition and molar flow rate of each component in fermentation-derived magnesium lactate solution.

Component	Weight (g)	Mole	Molar flow rate (kmol/day)
LA	4576.62	50.81	0.0508
Water	10162.49	564.58	0.5646
MgSO <sub>4</sub>	3953.21	32.84	0.0328

Feed stream F1 is the fermentation-derived magnesium lactate solution mixed with sulfuric acid. Flow rate of concentrated sulfuric acid used as catalyst based on 2v/v% is 0.0090 kmol/day. Therefore the composition and molar flow rate of each component in feed stream F1 are presented in Table F.2.

**Table F.2** Molar flow rate and mole fraction of feed stream F1.

Composition	Molar flow rate (kmol/day)	Mole fraction
LA	0.0508	0.0773
W	0.5646	0.8590
MgSO <sub>4</sub>	0.0328	0.0500
H <sub>2</sub> SO <sub>4</sub>	0.0090	0.0137
Total	0.6573	1.0000

Initial feed molar ratio of ethanol to lactic acid in this process is 3:1. Feed stream F2 is pure absolute ethanol. Therefore, molar flow rate of feed stream F2 is 0.1524 kmol/day.

## F.2 Reaction Rate Constants

From the results of effect of temperature on fermentation-derived magnesium lactate in Chapter II, reaction rate constants can be presented in term of Arrhenius's equation followed equation (F.1).

$$k = A_0 \exp\left(-\frac{E_A}{RT}\right) \quad (\text{F.1})$$

where  $k$  is reaction rate constant,  $\text{s}^{-1}$

$A_0$  is frequency factor,  $\text{s}^{-1}$

$E_A$  is activation energy,  $\text{Jmol}^{-1}$

$R$  is universal gas constant,  $\text{Jmol}^{-1}\text{K}^{-1}$

$T$  is absolute temperature,  $\text{K}$

The activation energy and frequency factor of both forward and backward reactions from UNIQUAC model are shown in Table F.3.

**Table F.3** Arrhenius's parameter of reaction obtained from UNIQUAC model.

Parameter	Forward reaction	Backward reaction
$E_A$ (J/mol)	30400	7022.67
$A_0$ ( $\text{s}^{-1}$ )	13300	0.799

## F.3 Aspen Plus Program

### F.3.1 Starting a New Aspen Plus Simulation

After open the Aspen Plus program, an Aspen Plus Startup window will appear, as below in Figure F.1. Select 'Blank Simulation' and click **Create** button to create new file.

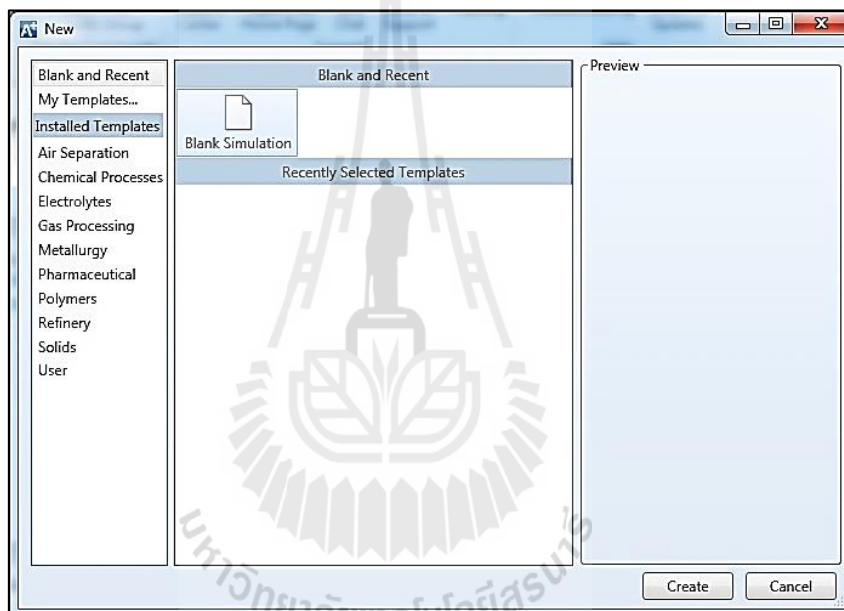


**Figure F.1** Aspen Plus startup window.

### F.3.2 Properties Input

In Aspen Plus simulator V.7.3.2, Properties window will appear after create new file as Figure F.2. In this window, components and method of calculation in the process are needed to be specified before create process flowsheet of simulation.

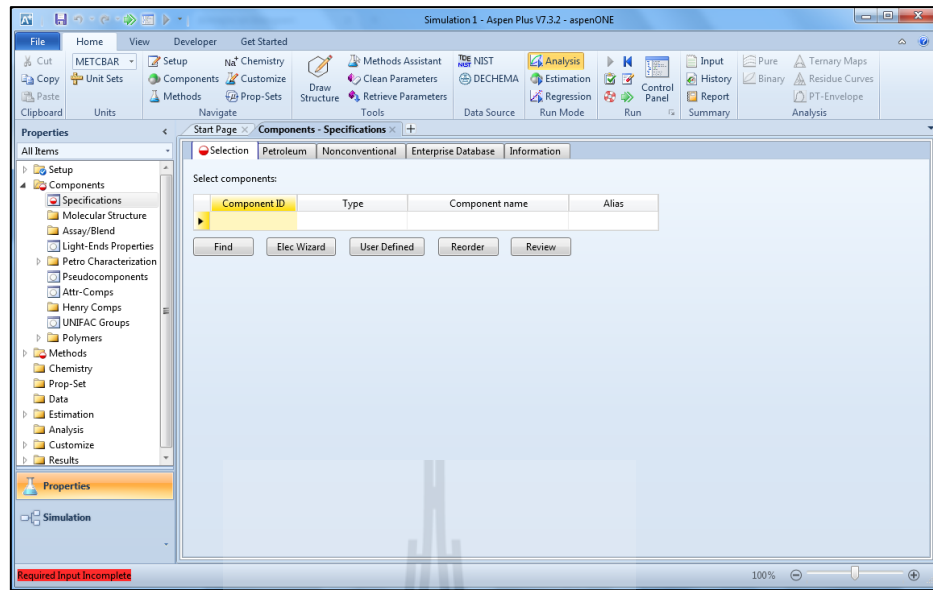


Figure F.2 Properties window.

### F.3.2.1 Components Input

Click **'Components'** folder to open subfolder for input components. Then click the **'Selection'** tab in **'Specifications'** subfolder to entering each component name in the box labeled **'Component ID'**. Use **'Find'** button located near the bottom and entered name of component as Figure F.3. Click **'Find Now'** and double click on desired component. After all components are specified, Figure F.4 is obtained.

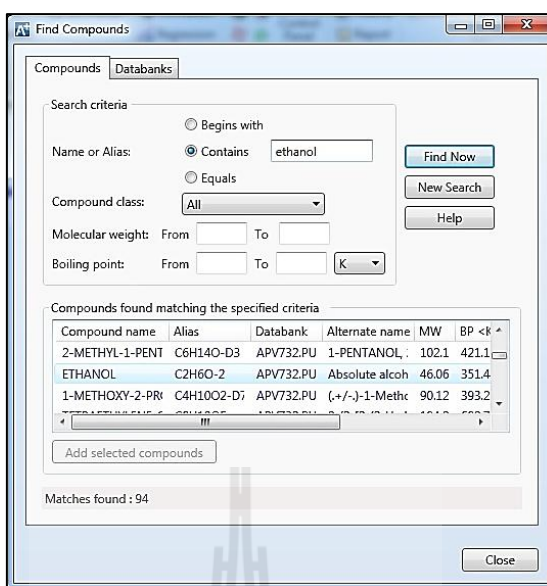


Figure F.3 Find components.

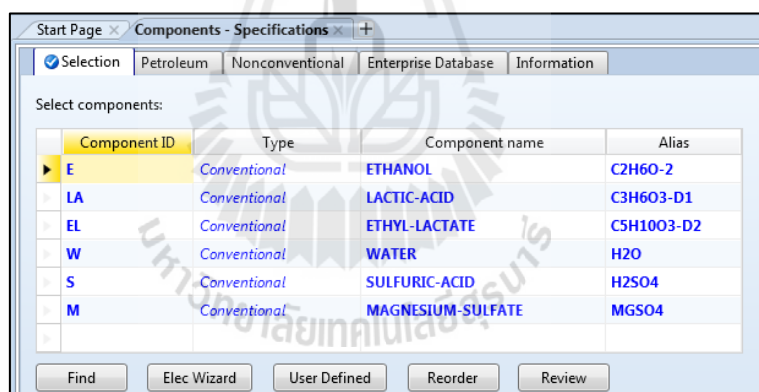
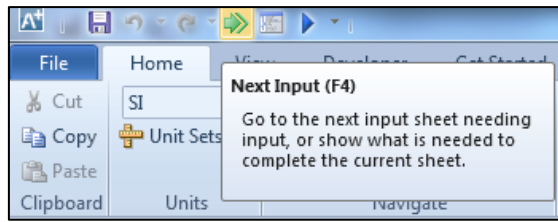


Figure F.4 All component specification.

### F.3.2.2 Method Input

Click 'Next' button, in Figure F.5, to go to next step automatically or choose 'Method' folder to specified thermodynamic method used in the simulation and choose 'UNIQUAC' as in Figure F.5.



**Figure F.5** Next Input button in the toolbar.

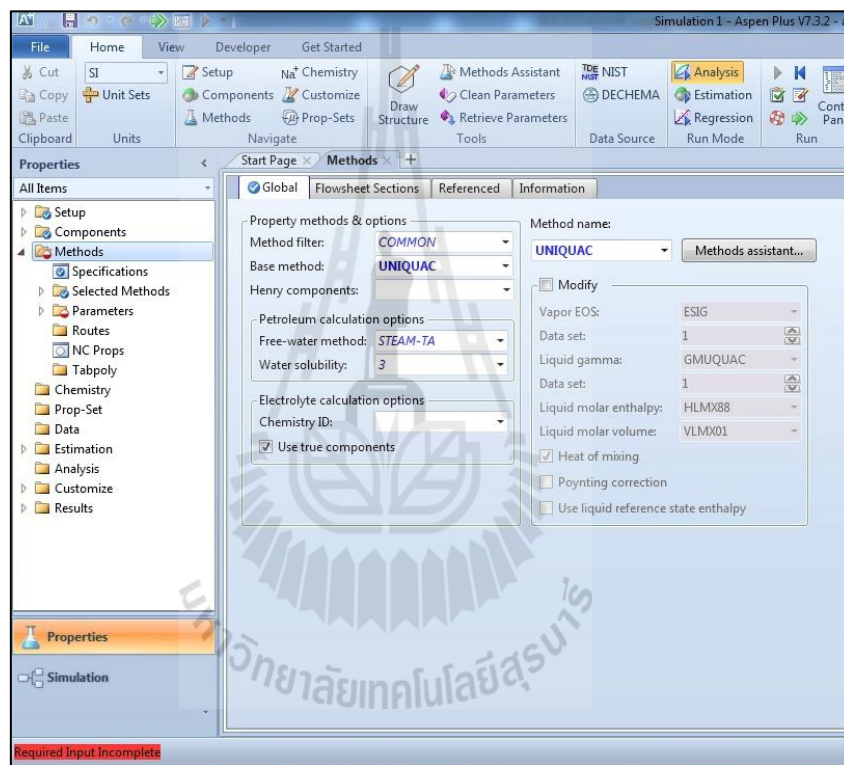


**Figure F.6** Thermodynamic method specification.

Click ‘Next’ button to go next step. At ‘Binary Interaction’ subfolder, input all binary interaction parameter obtained from Delgado et al. (2007) as showed in Figure F.7. It should be note that form of binary interaction of Aspen Plus simulator is  $\tau_{ij} = \exp(a_{ij} + bi_j/T + c_{ij} \ln T + d_{ij}T + e_{ij}/T^2)$  while the form of the

parameters from Delgado et al. is  $\tau_{ij} = \exp\left(-\frac{(a_{ij} + b_{ij}T)}{T}\right)$ , therefore the published parameters are related to the aspen parameters as :

$$a_{ij}(\text{aspen}) = -b_{ij}(\text{published})$$

$$b_{ij}(\text{aspen}) = -a_{ij}(\text{published})$$

The screenshot shows the Aspen Plus software interface for inputting binary interaction parameters for the UNIQUAC model. The main window displays a table of temperature-dependent binary parameters for various component pairs. The status bar at the bottom indicates that the required properties input is complete.

Component i	E	E	E	W	W	EL
Component j	W	L	EL	L	EL	L
Temperature units	K	K	K	K	K	K
Source	APV732 VLE-IG	USER	USER	USER	USER	USER
Property units						
AU	2.0046	0	0	0	0	0
AL	-2.4936	0	0	0	0	0
BU	-728.971	-191.28	148.67	39.61	-64.53	-52.64
BL	756.948	43.32	-341.77	-155.18	-99.8	-125.29
CU	0	0	0	0	0	0
CL	0	0	0	0	0	0
DU	0	0	0	0	0	0
DL	0	0	0	0	0	0
TLOWER	298.14	0	0	0	0	0
TUPPER	373.15	1000	1000	1000	1000	1000
ETU	0	0	0	0	0	0

**Figure F.7** Binary interaction parameter of UNIQUAC model input.

After input all binary interaction parameters, status in the status bar is changed to be ‘Required Properties Input Complete’ and all red signs are changed to be blue signs then click on ‘Simulation’ above status bar to input the process simulation.

### F.3.3 Simulation Input

#### F.3.3.1 Process Flowsheet window

Process flowsheet window and its features are shown in Figure F.8. Details of process flowsheet are as followed:

1. Toolbar: provides shortcuts through the Aspen Plus features.
2. Status bar: notifies user of equipment functions and of simulation status (i.e. if all required information has been inputted).
3. Model palette:
  - 3.1 Stream library: contains options for the addition of various streams to flow sheet.
  - 3.2 Process equipment library: contains process equipment that can be added to flow sheet.

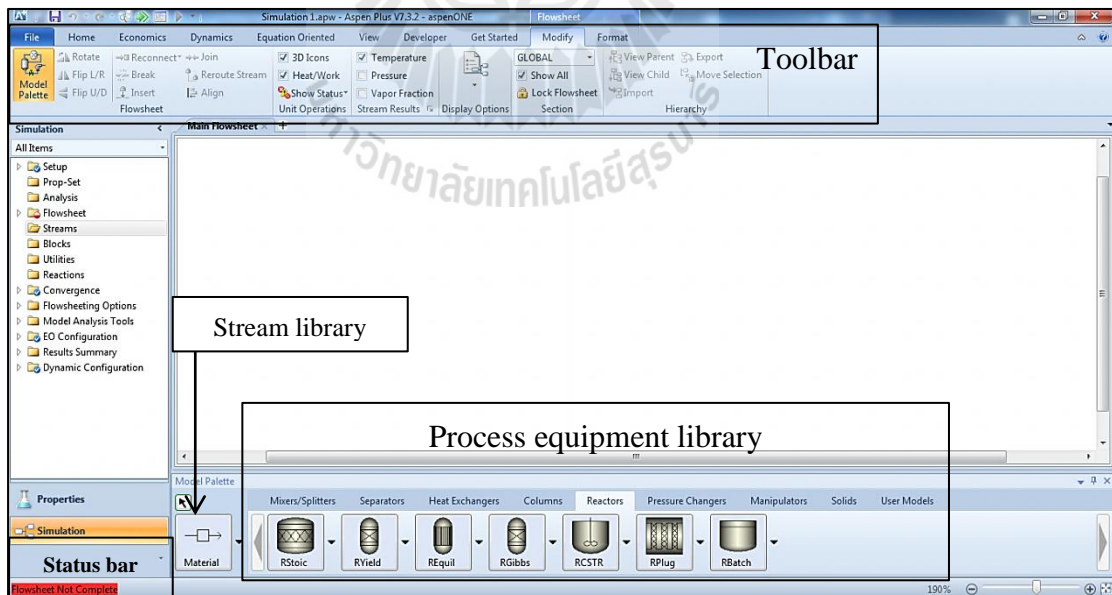


**Figure F.8** Details of process flow sheet window.

### F.3.3.2 Adding Equipment and Stream to Process Flowsheet

To adding a unit operation in the process flowsheet window, select desired unit from **'Process equipment library'** as followed procedures:

- a. Choose **'Column'** Tab, click on right button of **'RadFrac'** column to select desired block which is **FRACT1** and then click on workspace or drag it on workspace of main flowsheet to add the block. An example is shown in Figure F.9.

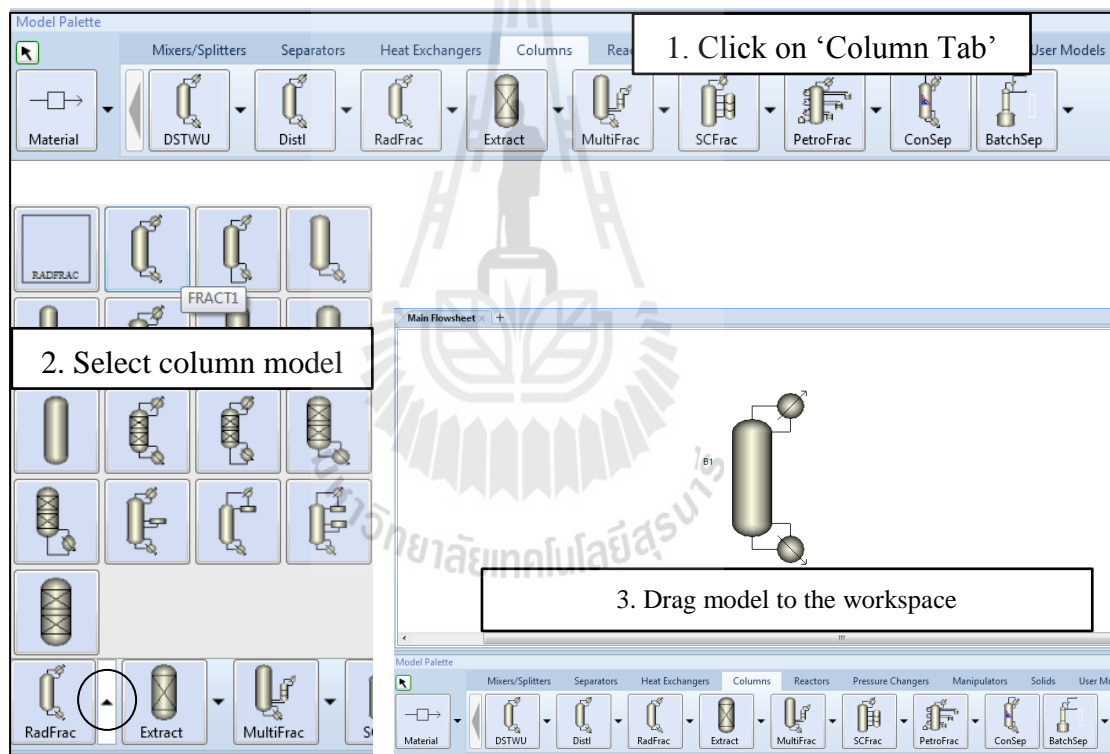


**Figure F.9** Selection of unit operation.

- b. Choose **'Material'** in stream library to create stream input and output from the column. Notice that when the mouse is pointing at a piece of equipment, arrows appear. Red arrows indicate streams that are required for the unit,

and blue arrows indicate optional stream. Connect all streams to the column and rename all streams as shown in Figure F.10.

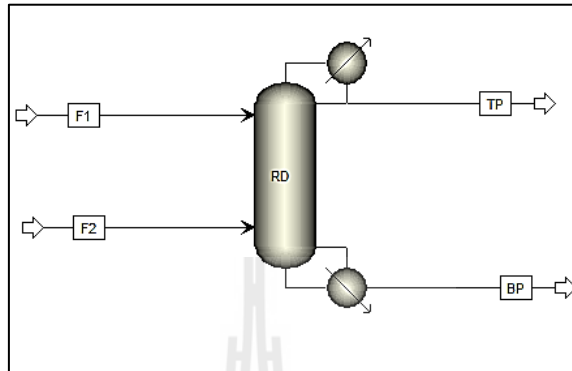


**Figure F.10** Adding streams to the column.

### F.3.3.3 Data Input

Notice a blue check mark  to indicate completed information and a half-filled red circle  to indicate information that needs to be completed. However, to ensure that all required input has been entered into the simulation, it is best to go through each section systematically. By selecting the ‘**Next icon**’ on the toolbar, Aspen will guide through all required steps of data entry.

**Stream Input:** Click on ‘**Stream**’ folder to modify streams details. Temperature, pressure, molar flow rate, composition, etc. of each stream are need to specified.

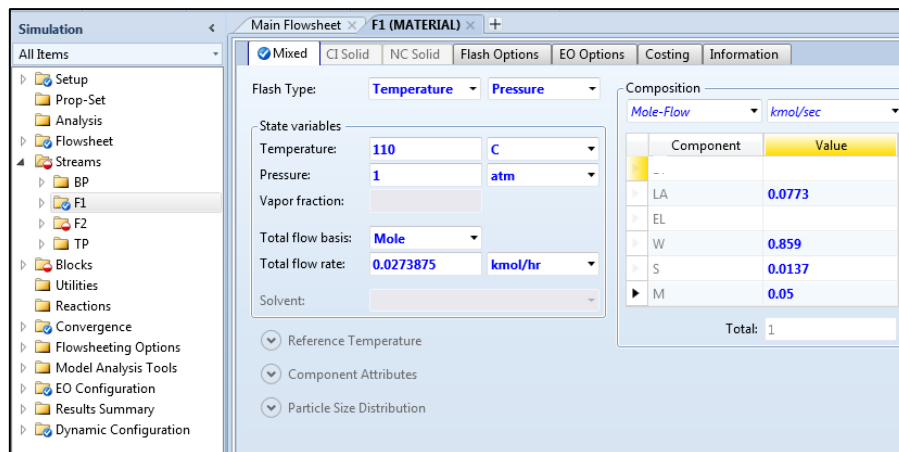


**Figure F.11** Feed stream details input.

**Block Input:** Click on **'Blocks'** folder, select desired unit operation name to specify unit details.

**a. Set Up Subfolder**

In the **'Configurations'** tab, the details of column such as number of total stages, condenser and reboiler types, convergence method and two operating specifications are set.

In **'Streams'** tab, location of feed streams and product streams are specified.

In **'Pressure'** tab, pressure of the column is input.

Since, the reactive distillation column is used to be an example. Rate-Based calculation type is selected due to reaction occurred in the column. Strongly non-ideal liquid convergence method is chose due to non-ideal property of liquid phase. Locations of feed stream are 2<sup>nd</sup> and 13<sup>th</sup> stage because 1<sup>st</sup> and 14<sup>th</sup> stages are reboiler and condenser of the column. Pressure of the column is

atmospheric with assuming of no pressure drop of the column. All inputs are shown in Figure F.12.

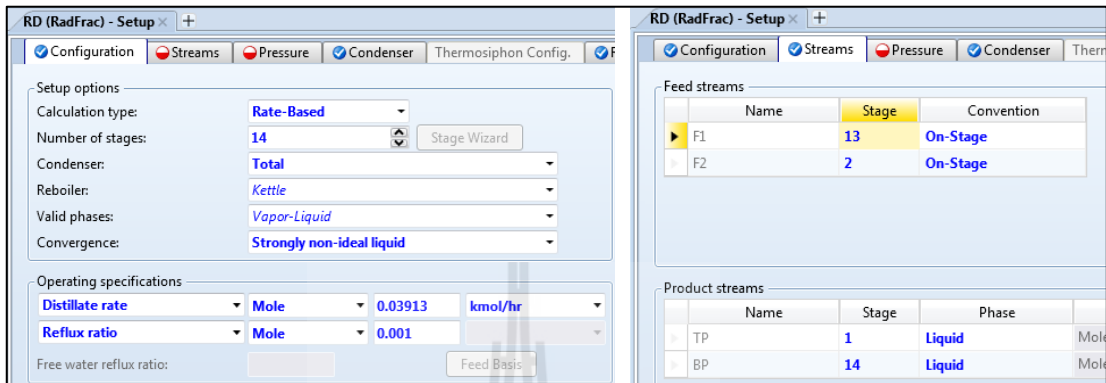


**Figure F.12** Reactive distillation column setup.

### b. Reaction Subfolder

Specify section of the column that reaction occurred. Since, the 1<sup>st</sup> and 14<sup>th</sup> stages are condenser and reboiler. The reaction is assumed to be occurred at 2<sup>nd</sup> to 13<sup>th</sup> stage.

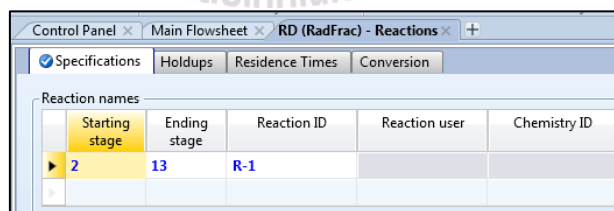


**Figure F.13** Section of reaction in reactive distillation column.

### c. Tray Rating Subfolder

Tray specifications are defined in this subfolder.

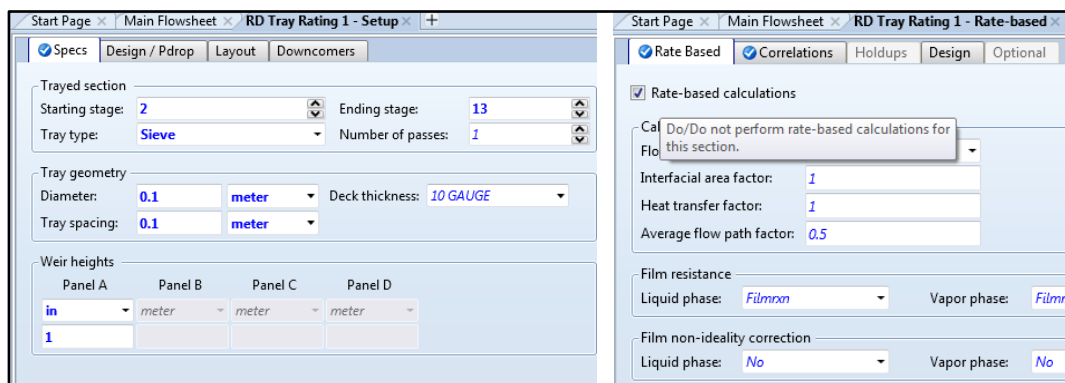


Figure F.14 Tray specification.

**Reaction Input:** Click on ‘Reaction’ folder, create new reaction file as step (1) of Figure F.15. The ‘Kinetic’ reaction type is selected. For reversible reaction, both of forward reaction and backward reaction are needed to specify as in step (2). Kinetic parameter is set as step (3) of Figure F.15.

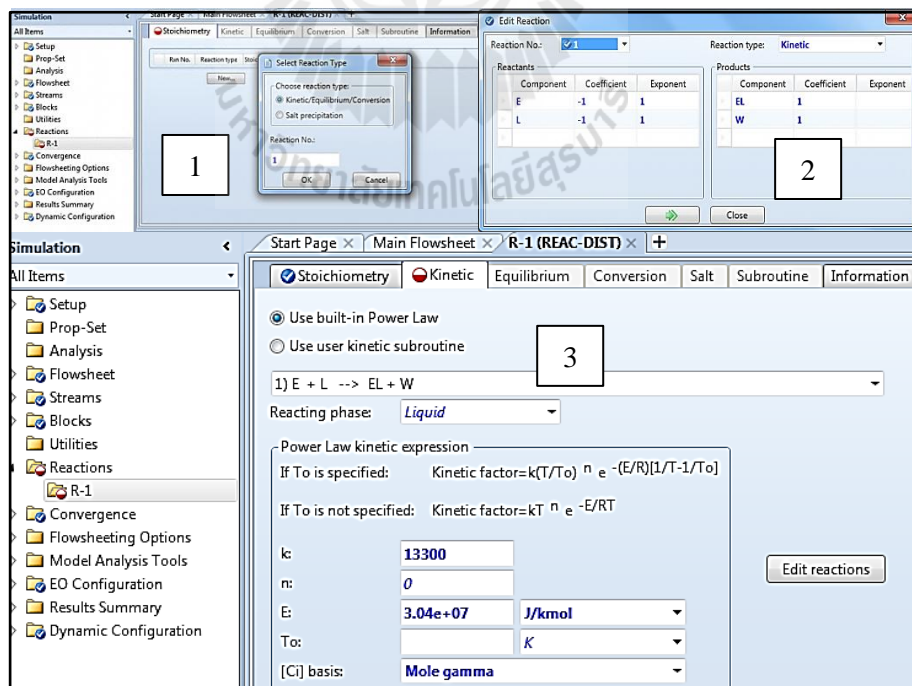


Figure F.15 Reaction specification.

After input all data, the status in status bar is changed to be **‘Required Input Complete’**. Then click on **‘Run’** symbol  on the toolbar to run simulation and click on **‘Results Summary’** to show simulation results.

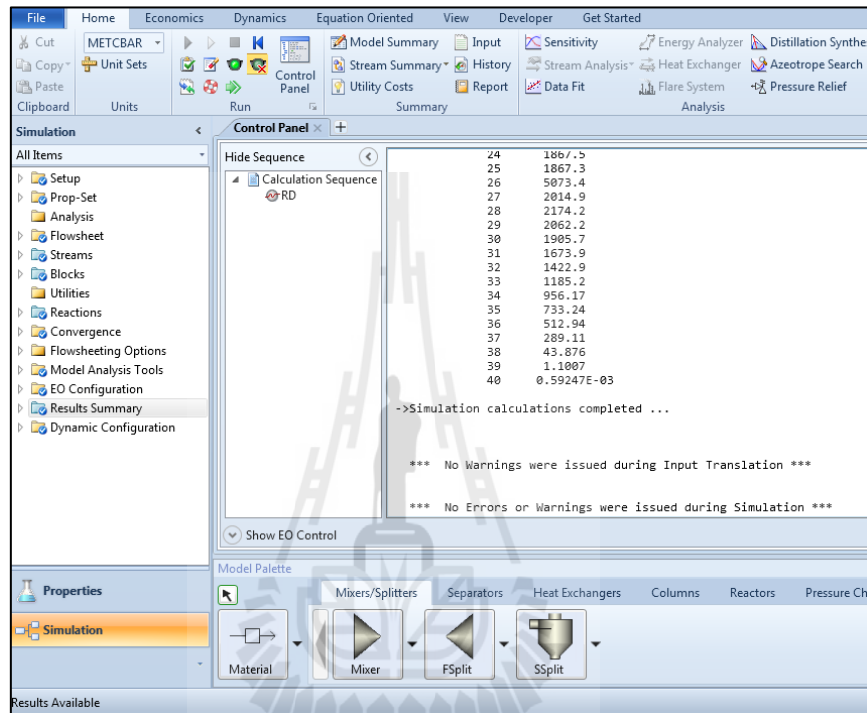


Figure F.16 Control Panel.

From	To	Units	BP	F1	F2	TP
			RD			RD
Substream: MIXED						
Phase:			Liquid	Mixed	Liquid	Liquid
Component Mole Flow						
E		KMOL/HR	1.10334e-05	0	0.00635	0.00428088
L		KMOL/HR	1.37083e-07	0.00211705	0	5.88299e-05
EL		KMOL/HR	7.68695e-05	0	0	0.00198122
W		KMOL/HR	6.09257e-08	0.0235258	0	0.0255838
S		KMOL/HR	0.000280027	0.000375209	0	9.51816e-05
M		KMOL/HR	0.00136938	0.00136938	0	1.4771e-28
Component Mole Fraction						
E			0.00635017	0	1	0.133778
L			7.88967e-05	0.0773	0	0.00183843
EL			0.0442396	0	0	0.0619131

Figure F.17 Streams result of simulation.

### F.3.4 Model Analysis Tools

In order to do sensitivity analysis or optimization, click on ‘**Model Analysis Tools**’ Folder

#### F.3.4.1 Sensitivity Analysis

Create new sensitivity file in ‘**Sensitivity**’ folder. Choose manipulated variable and range of manipulated variable in ‘**Vary**’ tab.

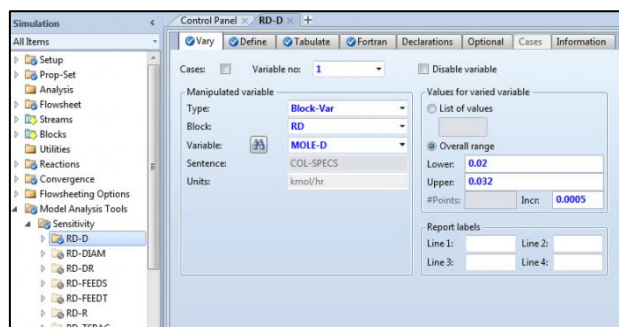
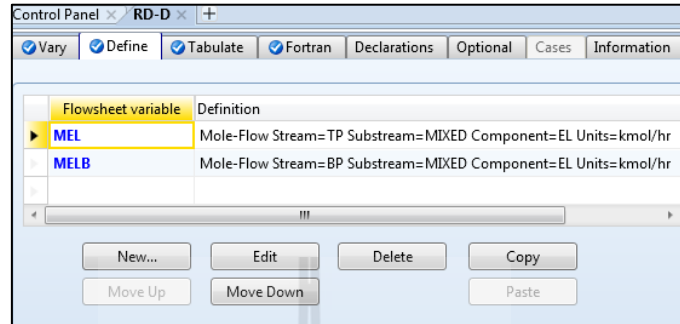


Figure F.18 Selecting manipulated variable in sensitivity analysis.

Use **‘Define’** tab to identify the flowsheet variables that are to be calculated or used to compute the tabulated results.



**Figure F.19** Define variable to be studied in the sensitivity analysis.

In **‘Tabulate’** tab, define the parameter want Aspen Plus to tabulate. Click on **Fill variables** button to automatic put variables from **‘Define Tab’** or input the variables by manual.

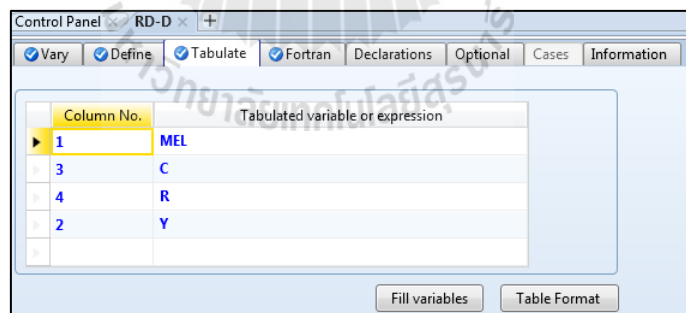


**Figure F.20** Input variable to table result.

The FORTRAN statements used in calculation the tabulated results can be enter in **‘Fortran’** tab.

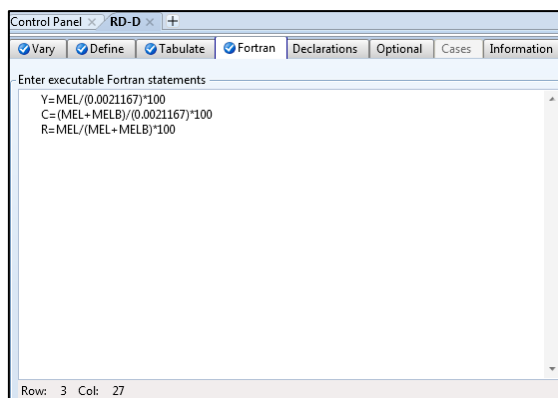


Figure F.21 FORTRAN statements input.

Results of sensitivity study are shown in **'Results'** subfolder. The variables which filled in **'Tabulate'** tab are shown. Results curve can be generated by **'Plot'** function in tool bars.

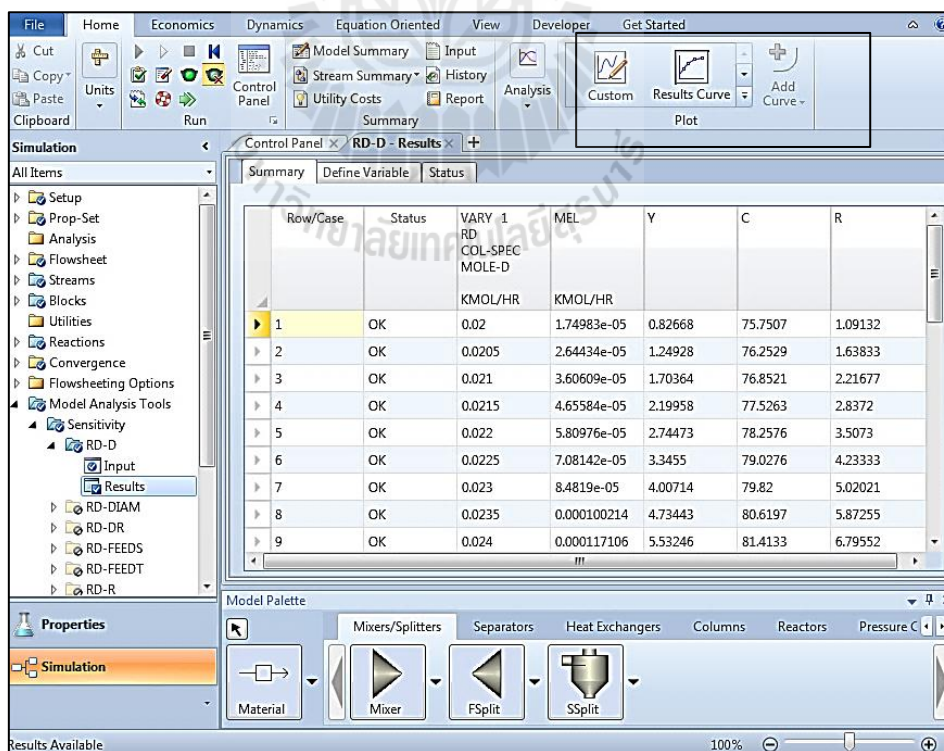
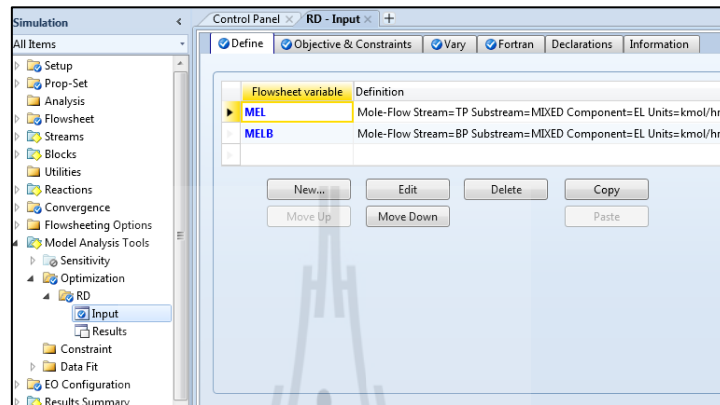


Figure F.22 Sensitivity result.

### F.3.4.2 Optimization

To perform optimization of simulation, create new optimization file in **‘Optimization’** folder and create flowsheet variables in **‘Define’** tab.



**Figure F.23** Identify flowsheet variables in optimization.

Identify objective function in **‘Objective & Constraints’** tab. If constraint of simulation is set, details of constraint must be specified in **‘Constraint’** subfolder.

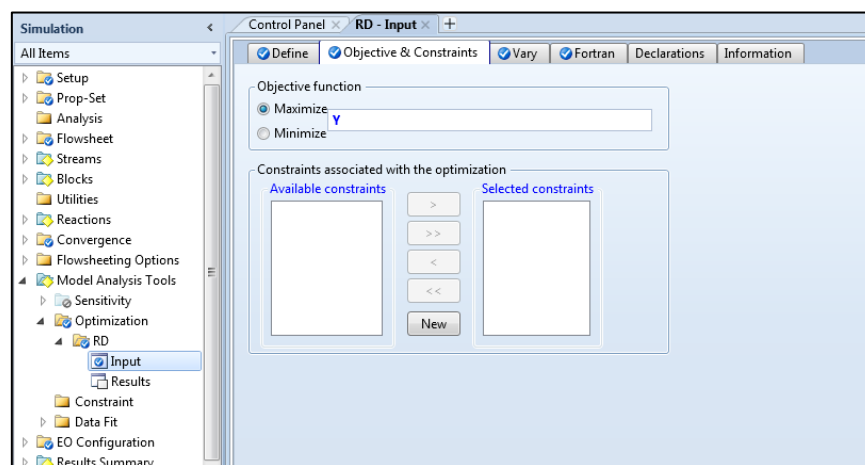


**Figure F.24** Identify objective function in optimization.

In **'Vary'** tab, choose manipulated variables and set range of manipulated variables. As the same as in sensitivity analysis, FORTRAN statements used to calculated objective function are entered in **'Fortran'** tab.

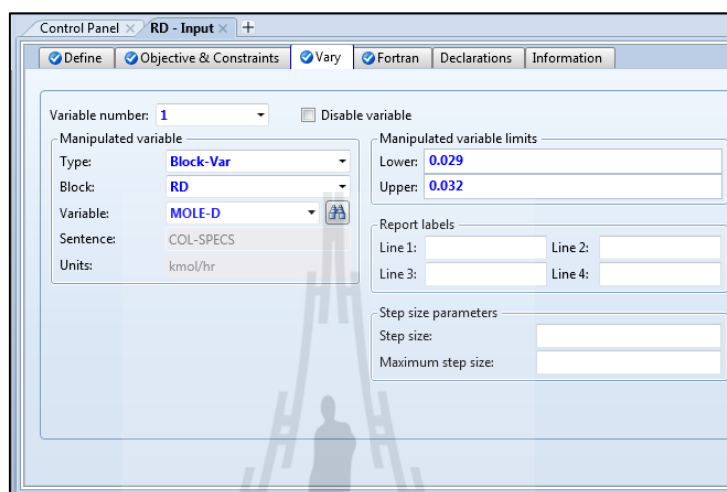


**Figure F.25** Selecting manipulated variable in optimization.

Results of optimization are shown in **'Results'** subfolder. Value of flowsheet variables are shown in **'Results Tab'** as in Figure F.26. Value of objective function and optimal manipulated variables are shown in **'Convergence'** folder. In **'Summary'** tab, result of objective function is shown as in Figure F.27 while optimal manipulated variables are shown in **'Manipulated Variables'** tab as shown in Figure F.28.

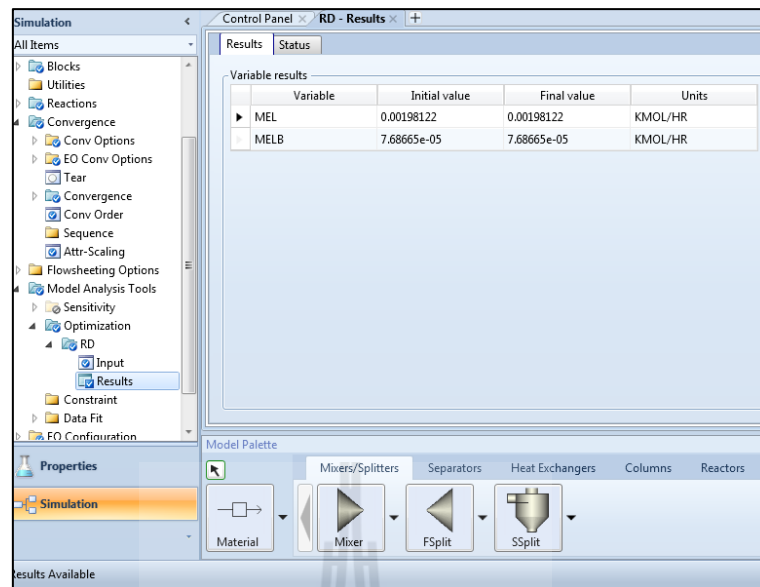


Figure F.26 Results of flowsheet variables in optimization.

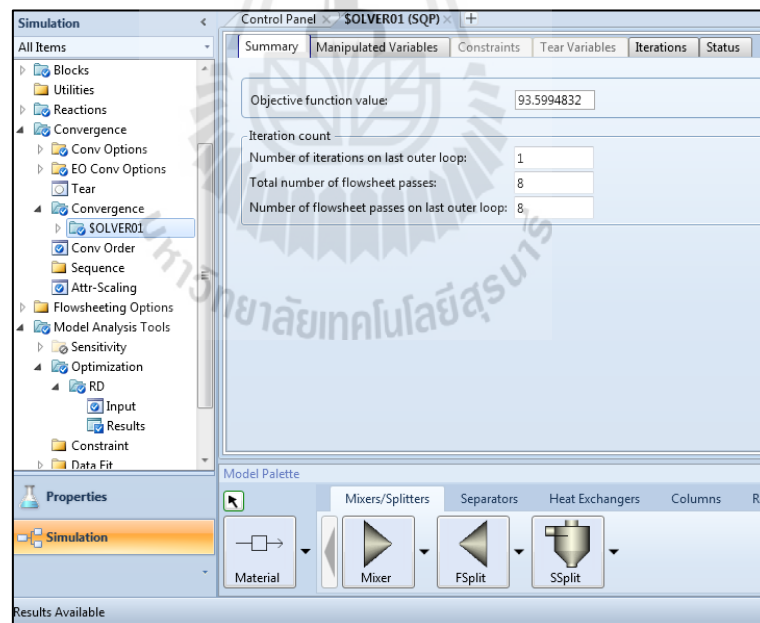
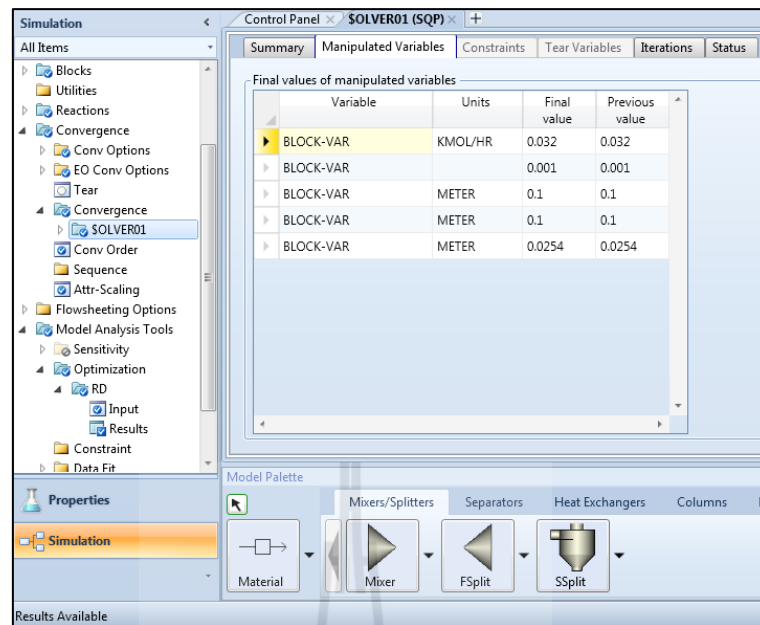
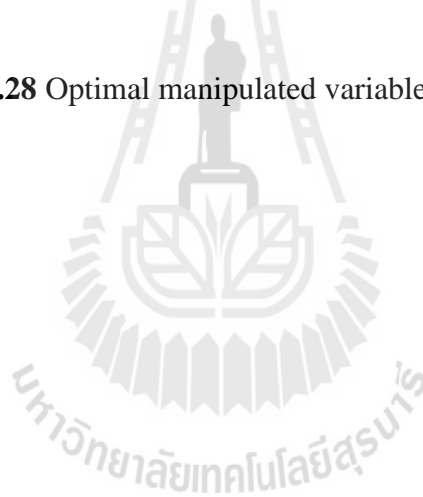
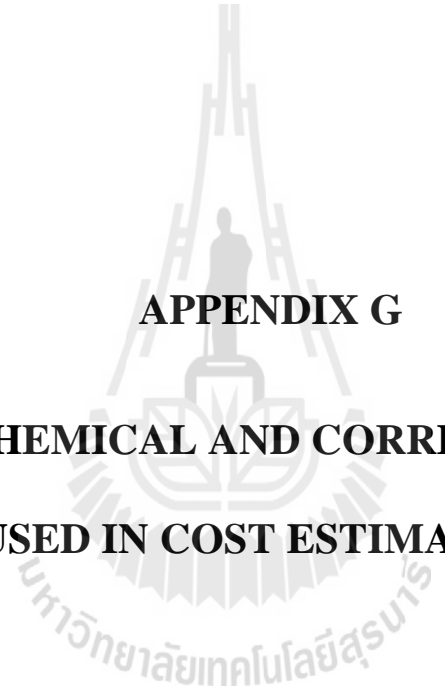


Figure F.27 Objective function value in optimization.



**Figure F.28** Optimal manipulated variables in optimization.





**APPENDIX G**

**PRICE OF CHEMICAL AND CORRECTION FACTOR**

**USED IN COST ESTIMATION**

## G.1 Raw Materials Costs

Price of chemicals used to be the composition in MRS culture media of fermentation is tabulated in Table G.1.

**Table G.1** Prices of chemical in culture media.

Composition	Price (THB/g)	Supplier
Universal peptone M66	13.01	Merck
Soya peptone obtained by papain digestion	2.34	Sigma Aldrich
Casein peptone obtained by pancreatic digestion	4.54	Acumedia
Yeast extract	3.22	Biomatik
Meat extract	2.97	Thomas Scientific
MgSO <sub>4</sub> ·7H <sub>2</sub> O	1.06	Amresco
NaCl	0.20	Vittayapun Thailand
(NH <sub>4</sub> ) <sub>2</sub> SO <sub>4</sub>	0.45	Vittayapun Thailand
K <sub>2</sub> HPO <sub>4</sub>	1.77	Biomatik
Prolabo soluble starch	2.17	Fisher Scientific
Tween 80	1.13	Biomatik
Cassava starch	0.01	Thai Tapioca Starch Association
Peptone	2.23	US Biological
D-glucose	0.55	Biomatik
Sodium acetate	1.00	US Biological
Tri-ammonium citrate	7.02	The Lab Depot Inc.
MnSO <sub>4</sub> ·4H <sub>2</sub> O	4.21	Merck
Corn steep liquor	1.36	Santa Cruz Bio.
Sugar cane molasses	0.01	Mitr Phol group
Peptone A	3.29	US Biological
Beef extract	3.43	US Biological
Dextrose	0.26	Affymetrix
Sodium acetate trihydrate	0.98	Santa Cruz Bio.

Cost of MRS culture media with original formula from Sigma Aldrich and Neogen are shown in Table G.2 and G.3 while cost of culture media which used cassava starch as carbon source based on formula from Sigma Aldrich and Neogen

are shown in Table G.4 to G.5, respectively. In addition, price of other raw materials such as absolute ethanol and sulfuric acid are shown in Table G.6.

**Table G.2** Price of culture media with original Sigma Aldrich formula.

Composition	Amount (g/10L)	Price (THB)
Dipotassium hydrogen phosphate	20	35
Glucose	200	109
Magnesium sulfate heptahydrate	2	2
Manganous sulfate tetrahydrate	0.5	2
Meat extract	80	238
Peptone	100	223
Sodium acetate trihydrate	50	49
Triammonium citrate	20	140
Yeast extract	40	129
Total (THB/10L)		928

**Table G.3** Price of culture media with original Neogen formula.

Composition	Amount (g/10L)	Price (THB)
Enzymatic Digest of Animal Tissue	100	329
Beef Extract	100	343
Yeast Extract	50	161
Dextrose	200	51
Sodium Acetate	50	5
Polysorbate 80	10	11
Potassium Phosphate	20	4
Ammonium Citrate	20	140
Magnesium Sulfate	1	1
Manganese Sulfate	0.5	2
Total (THB/10L)		1047

**Table G.4** Price of culture media with Sigma Aldrich formula which was applied with cassava starch.

Composition	Amount (g/10L)	Price (THB)
Dipotassium hydrogen phosphate	20	35
Cassava starch	200	3
Magnesium sulfate heptahydrate	2	2
Manganous sulfate tetrahydrate	0.5	2
Meat extract	80	238
Peptone	100	223
Sodium acetate trihydrate	50	49
Triammonium citrate	20	140
Yeast extract	40	129
Total (THB/10L)		821

**Table G.5** Price of culture media with Neogen formula which was applied with cassava starch.

Composition	Amount (g/10L)	Price (THB)
Enzymatic Digest of Animal Tissue	100	329
Beef Extract	100	343
Yeast Extract	50	161
Cassava starch	200	3
Sodium Acetate	50	50
Polysorbate 80	10	11
Potassium Phosphate	20	35
Ammonium Citrate	20	140
Magnesium Sulfate	1	1
Manganese Sulfate	0.5	2
Total (THB/10L)		1076

**Table G.6** Price of other raw material.

Composition	Price (THB/L)	Supplier
Ethanol (Absolute)	84.62	P.WAI Co., Ltd.
H <sub>2</sub> SO <sub>4</sub> (98w/w%)	30.83	Moral Compound Co.,Ltd.
water RO	2.00	Goonchon Technology

## G.2 Correction Factor

Purchased costs and installed costs of equipment from Guthire's correlation were based on equipment with carbon steel material. A series of correction factors can be used to account for other material of construction and design type as well as operating pressure. All correction factors for column, tray and heat exchanger were presented in Table G.7 to G.12.

**Table G.7** Pressure correction factors of column.

Design Pressure Psi	up to 50	100	200	300	400	500	600	700	800	900	1000
F <sub>p</sub>	1	1.05	1.1	1.2	1.35	1.45	1.6	1.8	1.9	2.3	2.5

**Table G.8** Material correction factors of column.

Shell material	Carbon steel	Stainless steel	Monel	Titanium
F <sub>m</sub> clad	1	2.25	3.89	4.25
F <sub>m</sub> solid	1	3.67	6.34	7.89

**Table G.9** Correction factors for column trays.

Tray spacing (inch)	24	18	12			
$F_s$	1	1.4	2.2			
Tray type	Grid	Plate	Sieve	Trough or valve	Bubble cap	Koch Cascade
$F_t$	0	0	0	0.4	1.8	3.9
Tray materials	Carbon steel	Stainless steel	Monel			
$F_m$	0	1.7	8.9			

**Table G.10** Material factors of heat exchanger.

Shell and tube material	$F_m$
Carbon steel/Carbon steel	1.00
Carbon steel/Brass	1.30
Carbon steel/Monel	2.15
Carbon steel/Stainless steel	2.81
Stainless steel/Stainless steel	3.75
Carbon steel/Monel	3.10
Monel/Monel	4.25
Carbon steel/Titanium	8.95
Titanium/Titanium	13.05

**Table G.11** Correction factors for pressure of heat exchanger.

Design pressure (Psi)	up to 150	300	400	800	1000
$F_p$	0.00	0.10	0.25	0.52	0.55

**Table G.12** Correction factors for type of heat exchanger.

Design Type	Kettle reboiler	Floating head	U-tube	Fixed tube sheet
$F_d$	1.35	1.00	0.85	0.80

### G.2.1 Correction Factor of Column

All columns of each process were operated at atmospheric pressure and stainless steel was selected to be material of construction.

$$\text{From } F_c = F_m F_p$$

$$\therefore F_c = 1 \times 3.67 = 3.67$$

### G.2.2 Correction Factor of Tray

Tray of column was designed to be sieve tray with stainless steel and the pressure in operation was 1 atm. For tray spacing correction factor, minimum spacing (12 inch) was selected.

$$\text{From } F_c = F_m + F_s + F_t$$

$$\therefore F_c = 1.7 + 2.2 + 0 = 3.9$$

### G.2.3 Correction Factor of Condenser

Stainless steel was selected to be material of both shell and tube sides of u-tube exchanger. Pressure in operation was atmospheric.

$$\text{From } F_c = (F_d + F_p) F_m$$

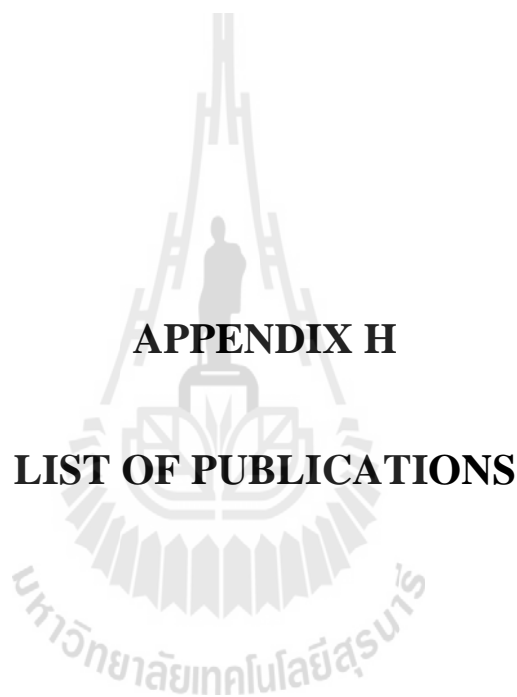
$$\therefore F_c = (0.85 + 0) \times 3.75 = 3.1875$$

### G.2.4 Correction Factor of Reboiler

Stainless steel was selected to be material of both shell and tube sides of Kettle reboiler. Pressure in operation was atmospheric.

$$\text{From } F_c = (F_d + F_p) F_m$$

$$\therefore F_c = (1.35 + 0) \times 3.75 = 5.0625$$



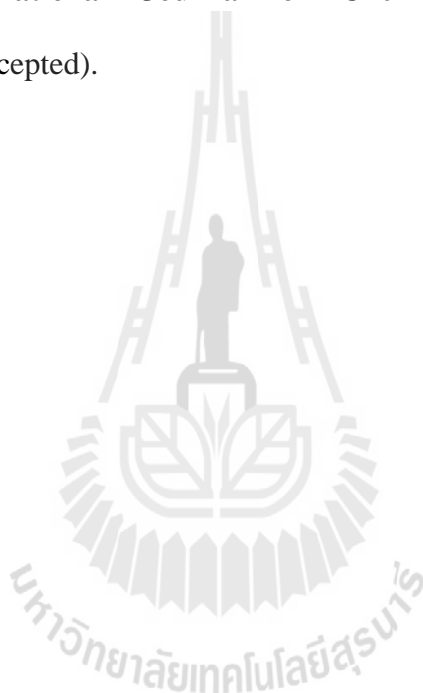
**APPENDIX H**

**LIST OF PUBLICATIONS**

**List of Publications**

Daengpradab, B. and Rattanaphanee, P. (2012). Kinetic study of ethyl lactate synthesis from magnesium lactate. **Engineering Transactions**. 15(2): 84-90.

Daengpradab, B. and Rattanaphanee, P. (2014). Process intensification for production of ethyl lactate from fermentation-derived magnesium lactate: a preliminary design. **International Journal of Chemical Reactor Engineering**. (Manuscript accepted).



# Kinetic Study of Ethyl Lactate Synthesis from Magnesium Lactate

Boonpradab Daengpradab and Panarat Rattanaphanee\*

School of Chemical Engineering, Institute of Engineering,  
Suranaree University of Technology, Nakhon Ratchasima, 30000, Thailand

\*E-mail: panarat@sut.ac.th

Manuscript received October 12, 2012

Revised November 9, 2012

## ABSTRACT

*Ethyl lactate is widely used as solvent for several industries and usually produced from lactic acid esterification with ethanol. In order to lower the production cost, attempt to synthesis ethyl lactate directly from fermentation-derived magnesium lactate was made. In this research, kinetics of magnesium lactate esterification with ethanol catalyzed by sulfuric acid was studied. Effect of reaction temperature, initial feed molar ratio, and catalyst loading on the production yield were investigated. Specific rate and equilibrium constant were determined and found that both parameters were influenced by reaction temperature, initial feed molar ratio, and catalyst loading. Relationship between the rate constant and process variables was elucidated. The result was compared with commercial lactic acid esterification under the same process condition. It was found that the values of kinetic parameters obtained from magnesium lactate esterification were lower, which could be due to the presence of impurities in fermentation-derived magnesium lactate.*

**Keyword:** Ethyl lactate, lactic acid, magnesium lactate, esterification, kinetic study.

## 1 INTRODUCTION

Ethyl lactate ( $\text{CH}_3\text{CHOHCOOCH}_2\text{CH}_3$ ) is an acid ester that can be considered as a green chemical due to its nontoxic, biodegradable and excellent solvent properties [1]. It was used in many industries with general application as solvent for production of nitrocellulose, food additive, perfumery, flavor chemicals as well as drug industries [2].

Normally, ethyl lactate is produced from esterification of lactic acid with ethanol. Sulfuric acid

and cation exchange resins can be used as homogeneous and heterogeneous catalyst, respectively. However, this process is expensive due to the high cost of lactic acid separation and purification [3]. Using lactate salt such as magnesium lactate or calcium lactate, which can be obtained directly from fermentation to produce lactic acid, might be an approach that help decreasing the production cost of this chemical.

Several studies concerned kinetics of esterification reaction between commercial lactic acid and ethanol had been conducted and reported [4] – [5]. The important variables which are affecting to the kinetics of reaction is temperature, initial feed molar ratio of the reactant, as well as percent catalyst loading.

The purpose of this research is therefore to study the kinetics of magnesium lactate esterification with ethanol by study effect of reaction temperature, initial feed molar ratio, and catalyst loading on the reaction. The yield of ethyl lactate production is also evaluated. The relationship between reaction rate constant and involved parameters was determined.

## 2 RESEARCH METHODOLOGY

### 2.1 Materials and Equipments

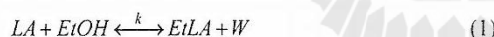
Lactic acid (88 %w/w), absolute ethanol (99+ %w/w), and sulfuric acid (96 %w/w) were obtained from CARLO ERBA. Magnesium lactate is produced from lactic acid fermentation using magnesium oxide as neutralizing agent. Deionized water was produced from an Aquinity P LifeScience TI water purifier. Compositions of the reaction solution were analyzed by gas chromatography analyzer (GC) and high performance liquid chromatography (HPLC) from Shimadzu and Agilent Technologies, respectively. Rotary vacuum evaporator used for evaporation from BUCHI Thailand.

## 2.2 Experimental Procedure

Magnesium lactate was dissolved in 1 M sulfuric acid solution. The solution was stirred for 10 min, before it was left for precipitation for 90 min. Solid residue was separated by vacuum filtration. About 60% of water was removed from the solution by rotary vacuum evaporator in order to reduce its interference in esterification reaction. Lactic acid concentration in the magnesium lactate solution was analyzed by HPLC. Esterification reaction of magnesium lactate solution and commercial lactic acid with ethanol were performed in a 500-ml glass vessel using sulfuric acid as homogeneous catalyst. Total volume of the reaction solution was constant at 250 ml. The solution was stirred by magnetic stirrer and the reaction temperature was maintained by thermally-controlled oil bath. Kinetics of the reaction was studied by analyzing the reaction solution contents by GC. The effect of temperature, initial feed molar ratio, and catalyst loading were studied. The catalyst loading was expressed as volume percent of concentrated sulfuric acid in the reaction solution.

## 3 RESULTS AND DISCUSSION

In this study, kinetics experiment were performed in reaction temperature, initial feed molar ratio, and catalyst loading ranges of 65°C to 85°C, 3:1 to 30:1 and 1 to 3 %v/v, respectively. The esterification of lactic acid (LA), also lactic acid in magnesium lactate solution, with ethanol (EtOH) to produce ethyl lactate (EtLA) and water (W) can be written as



The rate expression of esterification reaction of lactic acid and the equilibrium constant of the reaction can be described in equation (2) and (3)

$$-r_{LA} = -\frac{dC_{LA}}{dt} = k \left( C_{LA} C_{EtOH} - \frac{C_{EtLA} C_W}{K_e} \right) \quad (2)$$

$$K_e = \frac{C_{EtLA,e} C_{W,e}}{C_{LA,e} C_{EtOH,e}} \quad (3)$$

where  $-r_{LA}$  is rate of esterification ( $\text{mol L}^{-1} \text{min}^{-1}$ ),  $C_i$  and  $C_{i,e}$  are concentration of reaction species  $i$  at time  $t$  and at equilibrium ( $\text{mol L}^{-1}$ ), respectively,  $t$  is reaction time (min),  $k$  is the reaction rate constant ( $\text{L mol}^{-1} \text{min}^{-1}$ ), and  $K_e$  is equilibrium constant.

Reaction rate constant ( $k$ ) and equilibrium constant ( $K_e$ ) of the reaction were determined by minimization the sum of squared of the errors (SSE) [6] between the

experimental conversion ( $x_{exp}$ ) and the calculated conversion ( $x_{cal}$ ) as shown in equation (4). The calculated conversion was evaluated by 4<sup>th</sup>-order Runge-Kutta method.

$$SSE = \sum_1^n (x_{exp} - x_{cal})^2 \quad (4)$$

The reaction rate constant can be expressed using Arrhenius equation:

$$k = A \exp\left(-\frac{E_A}{RT}\right) \quad (5)$$

where  $A$  is pre-exponential factor,  $E_A$  is activation energy of the reaction ( $\text{J mol}^{-1}$ ),  $R$  is universal gas constant ( $\text{J mol}^{-1} \text{K}^{-1}$ ), and  $T$  is absolute temperature (K), respectively.

### 3.1 Effect of Reaction Temperature

In order to study effect of reaction temperature, both esterification of magnesium lactate solution and commercial lactic acid were carried out in the reaction temperature range of 65-85 °C with constant initial feed molar ratio of ethanol to lactic acid and catalyst loading at 3:1 and 2 %v/v, respectively. The results are shown in Fig. 1. As expected, conversion of lactic acid in both processes was increased with reaction temperature. However, the conversion of magnesium lactate esterification was lower than that obtained from esterification of commercial lactic acid. This could be due to the presence of impurities in magnesium lactate solution, one of which is magnesium sulfate formed during the acidification of magnesium lactate with sulfuric acid. The reaction rate and equilibrium constants were determined and found that both parameters were increased with reaction temperature. The Arrhenius plots are shown in Fig. 2. The activation energy of magnesium lactate and commercial lactic acid esterification were approximately 26.7 and 53.5 kJ/mol, respectively. Activation energy for esterification of 88%w/w lactic acid evaluated in this study is in the region of the values reported by Troupe and Dimilla, whose obtained the activation energies of 62.4 and 50.6 kJ/mol for esterification of  $\text{H}_2\text{SO}_4$ -catalyzed esterification of 85%w/w and 44%w/w commercial lactic acid, respectively[7].

### 3.2 Effect of Initial Feed Molar Ratio

In this part, effect of initial feed molar ratio was investigated by varying the initial feed molar ratio of

ethanol to lactic acid from 3:1 to 30:1 which constant reaction temperature at 75°C and catalyst loading at 2 %v/v. The results are shown in Fig.3. It was found that the conversion of lactic acid in both processes was increased with initial feed molar ratio. According to Le Chatelier's principle, increasing of initial feed molar ratio will increase the forward reaction rate. In this situation, ethyl lactate is produced more, and the conversion of lactic acid is increased.

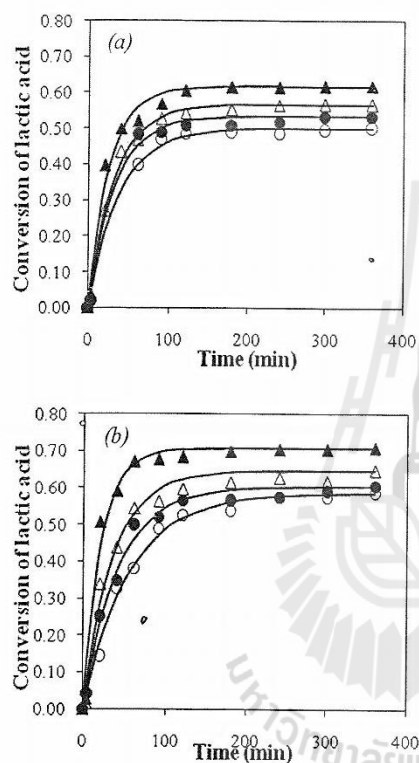


Fig. 1 Effect of Reaction Temperature on Conversion of Lactic Acid in Esterification of (a) Magnesium Lactate and (b) Commercial Lactic Acid. Reaction Temperature (▲) 85°C; (△) 80°C; (●) 75°C; (○) 65°C; Lines Indicated the Value from Calculation.

### 3.3 Effect of Catalyst Loading

The effect of catalyst loading was investigated by varying the concentration of sulfuric acid in the reaction solution from 1 to 3 %v/v with constant reaction temperature and initial feed molar ratio of ethanol to lactic acid at 75°C and 30:1, respectively. The results are shown in Fig. 4. Esterification favors the acidic environment, therefore, the conversion of lactic acid in

both processes was increased with concentration of sulfuric acid in the process.

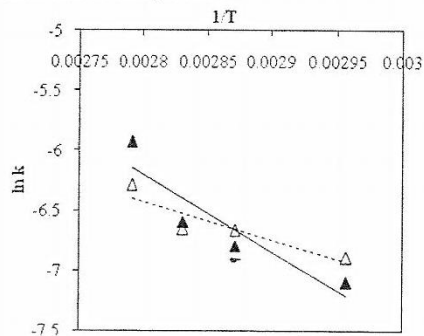


Fig. 2 The Arrhenius Plots between  $\ln k$  and  $1/T$  ( $K^{-1}$ ) for Esterification Reaction; (△) Magnesium Lactate; (▲) Commercial Lactic Acid.

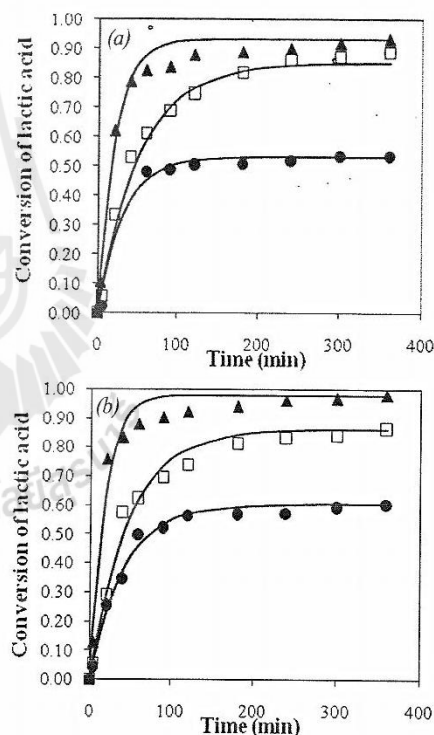
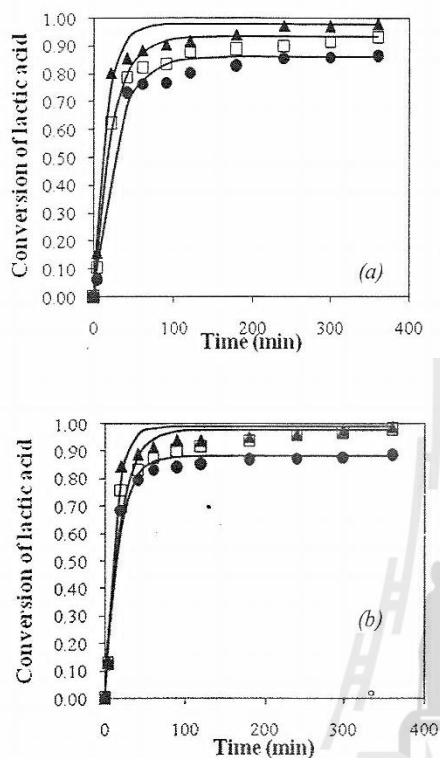


Fig. 3 Effect of Initial Feed Molar Ratio on Conversion of Lactic Acid in Esterification of (a) Magnesium Lactate and (b) Commercial Lactic Acid. Initial Feed Molar Ratio of Ethanol to Lactic Acid (▲) 30:1; (□) 10:1; (●) 3:1; Lines Indicated the Value from Calculation.



**Fig. 4** Effect of Catalyst Loading on Conversion of Lactic Acid in Esterification of (a) Magnesium Lactate and (b) Commercial Lactic Acid. Reaction Conditions: Constant Reaction Temperature at 75°C and Initial Feed Molar Ratio at 30:1, Catalyst Loading (▲) 3 %v/v; (◻) 2 %v/v; (●) 1 %v/v; Lines Indicated the Value from Calculation.

### 3.4 Kinetic Parameters

The reaction rate and equilibrium constant were calculated and shown in Table 1. Both kinetic parameters were found to increase with reaction temperature, initial feed molar ratio as well as catalyst loading. The parameters obtained from magnesium lactate esterification were less than that obtained from esterification of commercial lactic acid. Increasing of equilibrium constant is due to high equilibrium concentration of products in the reaction solution. The range of reaction rate constant of magnesium lactate and commercial lactic acid esterification are 0.0010-0.0098 and 0.0008-0.0123  $\text{Lmol}^{-1}\text{min}^{-1}$ , respectively, as well as the range of equilibrium constant of magnesium lactate and commercial lactic acid esterification are 2.1778-17.4077 and 2.4653-31.9546, respectively. The

coefficient of determination ( $R^2$ ) in every experiment is close to unity, which indicates good agreement between the experimental and the calculated conversion. Variation of the rate constant with the initial feed molar ratio clearly indicates the non-ideal nature of the solution mixture.

### 3.5 Correlation for Reaction Rate Constant

Relationships between reaction rate constant and reaction temperature, initial feed molar ratio, and catalyst loading have been reported for esterification of commercial lactic acid with concentration of 85%w/w and 44%w/w by Troupe and Dimilla [7]. In this research, these relationships were determined by plotting the rate constant against each corresponding variable. The plot of rate constant against catalyst loading is shown in Fig. 5. Correlations that obtained from Fig. 5 are as following equation (6)-(9).

For esterification of magnesium lactate:

For catalyst loading in %v/v:

$$k = 0.0027C_1 + 0.0016 \quad (6)$$

For catalyst loading in %w/w

$$k = 0.1286C_2 + 0.0015 \quad (7)$$

For esterification of commercial 88%w/w lactic acid:

For catalyst loading in %v/v:

$$k = 0.0024C_1 + 0.0044 \quad (8)$$

For catalyst loading in %w/w:

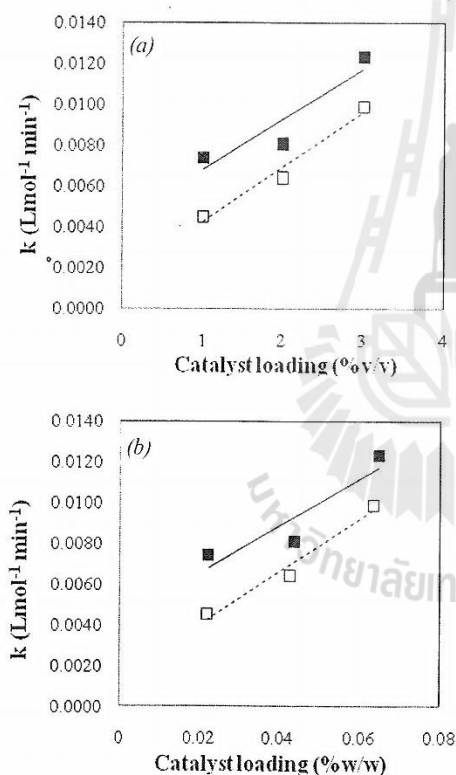
$$k = 0.1145C_2 + 0.0043 \quad (9)$$

$C_1$  and  $C_2$  are catalyst loading in %v/v and %w/w, respectively. Intercepts of equation (6) to (9) are not at origin, which signifies the autocatalytic nature of the reaction. Equation (9) agrees quite well with the one reported by Troupe and Dimilla who studied  $\text{H}_2\text{SO}_4$ -catalyzed esterification of 85%w/w lactic acid and obtained  $k=0.117C+0.001895$  for the correlation between the reaction rate constant and %w/w of  $\text{H}_2\text{SO}_4$  in the reaction solution. The difference in coefficients of the correlation for esterification of magnesium lactate and commercial lactic acid shown in this study is likely due to the process impurities as previously explained.

Effect of initial feed molar ratio of ethanol to lactic acid (E/L) on the reaction rate constant of magnesium lactate esterification was established by plotting the parameter  $(k-a)/C$  against the initial feed molar ratio

**Table 1** Kinetic Parameters for Esterification of Magnesium Lactate and Commercial Lactic Acid with Ethanol

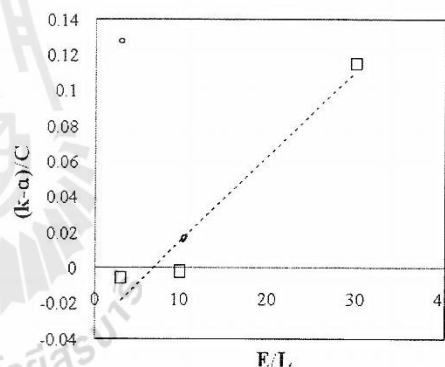
Process condition			Magnesium lactate				Commercial lactic acid			
Temperature (°C)	Initial feed molar ratio	Catalyst loading (%v/v)	Ke	k	SSE	R <sup>2</sup>	Ke	k	SSE	R <sup>2</sup>
85	3	2	7.8574	0.00185	0.0092	0.9823	12.9684	0.00266	0.0161	0.9753
80	3	2	5.7343	0.00128	0.0024	0.9948	9.0088	0.00136	0.0098	0.9854
65	3	2	4.7720	0.00102	0.0017	0.9947	7.3199	0.00082	0.0030	0.9937
75	3	2	5.4337	0.00127	0.0039	0.9899	7.8570	0.00112	0.0047	0.9918
75	10	2	9.5951	0.00141	0.0107	0.9905	10.1015	0.00158	0.0128	0.9891
75	30	2	6.0220	0.00641	0.0183	0.9906	18.7719	0.00809	0.0311	0.9797
75	30	1	2.1778	0.00451	0.0121	0.9899	2.4652	0.00741	0.0130	0.9884
75	30	3	17.4077	0.00987	0.0263	0.9856	31.9546	0.01230	0.0178	0.9896

**Fig. 5** Relationship between Reaction Rate Constant and Catalyst Loading; (a) Catalyst Loading in %v/v; (b) Catalyst Loading in %w/w; (□--) Magnesium Lactate Solution; (■—) Commercial Lactic Acid.

as shown in Fig. 6. Here, C is the catalyst loading in %w/w, and  $a$  is the rate constant of the autocatalytic

esterification when no  $H_2SO_4$  was added. This parameter can be evaluated from the intercept of equation (7). The correlation involved effect of initial feed molar ratio and catalyst loading is written as:

$$k = 0.0048(E/L)C - 0.0325C + 0.0015 \quad (10)$$

**Fig. 6** Relationship between  $(k-a)/C$  and  $E/L$  from Magnesium Lactate Esterification

Effect of reaction temperature to reaction rate constant was acquired by plotting  $\log k$  against the reciprocal of the absolute temperature (K) at constant initial feed molar ratio and catalyst loading as shown in Fig. 7.

The relationship obtained from the plot was:

$$\log k = 1.1151 - 1394.6/T \quad (11)$$

Equation (11) may also be able to express in form:

$$k = 10^{(1.1151-1394.6/T)} \quad (12)$$

where  $k$  is the reaction rate constant in  $\text{Lmol}^{-1}\text{min}^{-1}$  and  $T$  is the absolute temperature in K. In this research, effect of catalyst loading and initial feed molar ratio was studied at the reaction temperature of  $75^\circ\text{C}$  or  $348.15\text{ K}$ . The reaction rate constant at this temperature is

$$k_{348.15\text{K}} = 0.001286 \quad (13)$$

The ratio of reaction rate constant at any temperature to that at  $348.15\text{ K}$  can be written as:

$$\frac{k_T}{k_{348.15\text{K}}} = \left( \frac{10^{(1.1151-1394.6/T)}}{0.001286} \right) \quad (14)$$

Equation (10) and (14) were then combined to obtain the relationship between reaction rate constant and all the process variables, equation (15).

$$k = (0.0048(E/L)C - 0.0325C + 0.0015) \left( \frac{10^{(1.1151-1394.6/T)}}{0.001286} \right) \quad (15)$$

Equation (15) was used to re-calculate the reaction rate constant of each experiment. The experimental and calculated reaction rate constants were compared and shown in Table 2. Good agreement between the calculated and experimental reaction rate constant was achieved only in the experiments with high initial feed molar ratio. The large deviation between the two values in experiments with low initial feed molar ratio is likely caused by high concentration of magnesium sulfate in the reaction solution, which was resulted from large amount of magnesium lactate used in order to increase the number of moles of lactic acid, in other words, to lower the molar ratio between ethanol and lactic acid in the experiment. To have a clear point of view on this observation, effect of magnesium sulfate on kinetics of lactic acid esterification should be extensively investigated in the future study.

Table 2 Comparison between Experimental and Calculated Rate Constant of Magnesium Lactate Esterification

Temperature ( $^\circ\text{C}$ )	Molar ratio E/L	Catalyst loading (%v/v)	Catalyst loading (%w/w)	k ( $\text{Lmol}^{-1}\text{min}^{-1}$ )	
				Calculation	Experiment
85	3	2	0.0426	0.00094	0.00185
80	3	2	0.0426	0.00083	0.00128
65	3	2	0.0426	0.00056	0.00102
75	3	2	0.0426	0.00073	0.00127
75	10	2	0.0426	0.00216	0.00141
75	30	2	0.0426	0.00625	0.00641
75	30	1	0.0217	0.00392	0.00451
75	30	3	0.0633	0.00856	0.00987

#### 4 CONCLUSION

Kinetics of magnesium lactate esterification was studied. The activation energy of magnesium lactate esterification was found to be  $26.7\text{ kJ/mol}$ . The reaction rate and equilibrium constants, were influenced by reaction temperature, initial feed molar ratio as well as catalyst loading. Both of parameters were increased with temperature, initial feed molar ratio and catalyst loading. The relationship between the reaction rate constant of magnesium lactate esterification and the process variables was established. Good agreement between the calculated and the experimental rate constant was achieved in experiments with high initial feed molar ratio. The deviation observed may be a result of high

amount of magnesium sulfate in the reaction mixture when small initial feed molar ratio was used. Effect of magnesium sulfate quantity on the reaction kinetics should be further studied in order to gain accurate relationship between the reaction rate constant and the process variables.

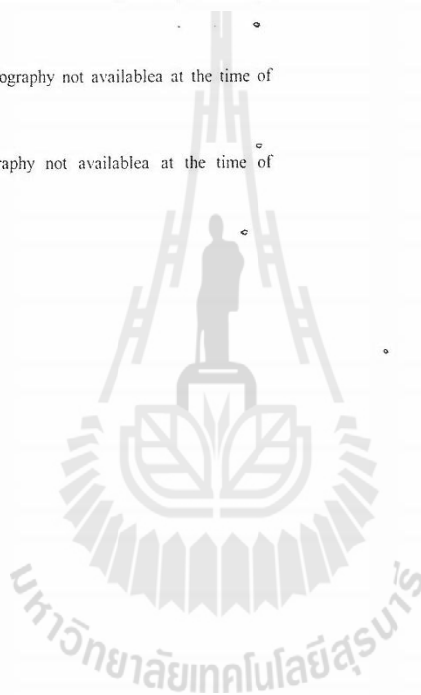
#### REFERENCES

- [1] P.T. Anastas, "Green Chemistry as Applied to Solvents", *ACS Symposium Series*, vol. 819, pp.1-9, 2002.
- [2] R.J. Lewis, *Hawley's Condensed Chemical Dictionary*, John Wiley and Sons, Inc., New York, 2007.
- [3] K. Palraj, K. Hyejin, L. Uhwang, W.H. Dong, K.H. Young, and C. Jong-San, "Synthesis of ethyl lactate from ammonium lactate solution by coupling solvent extraction with esterification",

- Separation and Purification Technology*, vol. 76, no. 1, pp.1-7, 2010.
- [4] P. Delgado, M. T. Sanz, and S. Beltran, "Kinetic Study for Esterification of Lactic acid with Ethanol and Hydrolysis of Ethyl Lactate Using an Ion-Exchange Resin Catalyst", *Chemical Engineering Journal*, vol. 126, pp. 111-118, 2007.
- [5] N. S. Asthana, A. K. Kolah, T. Vu, C. T. Lira, and D. J. Miller, "A Kinetic Model for the Esterification of Lactic Acid and Its Oligomers", *Industrial and Engineering Chemistry Research*, vol.45, pp. 5251-5257, 2006.
- [6] Y. Qu, S. Peng, S. Wang, Z. Zhang, and J. Wang, "Kinetic Study of Esterification of Lactic Acid with Isobutanol and n-Butanol Catalyzed by Ion-exchange Resins", *Chinese Journal of Chemical Engineering*, vol. 17, no.8, pp. 773-780, 2009.
- [7] R.A. Troupe and E. Dimilla, "Kinetics of the ethyl alcohol-lactic acid reaction", *Journal of Industrial and Engineering Chemistry*, vol.49, pp.847-855, 1957.

**Boompradab Daengpradab**, Biography not available at the time of publication.

**Panarat Rattanaphanee**, Biography not available at the time of publication.



## **BIOGRAPHY**

Miss Boonpradab Daengpradab was born on December 18, 1987 in Prachuap Khiri Khan Province, western part of Thailand. In 2006, she started her Bachelor's degree study at School of Chemical Engineering, Institute of Engineering, Suranaree University of Technology, Nakhon Ratchasima Province and earned her degree in 2009. Her senior project topic was about the comparative study of lactic acid esterification with ethanol and n-butanol. After graduation, she then continued her Master's degree at the School of Chemical Engineering, Institute of Engineering, Suranaree University of Technology under the supervision of Asst. Prof. Dr. Panarat Rattanaphanee. During her Master's degree study, she presented two oral presentations in entitled of "Kinetic study of ethyl lactate synthesis from magnesium lactate" in the 22<sup>nd</sup> Thai Institute of Chemical Engineering and Applied Chemistry Conference (TICHe 2012), Nakhon Ratchasima and "Effect of magnesium sulfate salt on kinetics of lactic acid esterification with ethanol" in the Pure and Applied Chemistry International Conference 2013 (PACCON 2013), Chonburi, Thailand. In addition, her article in topic of "Kinetic study of ethyl lactate synthesis from magnesium lactate" was published in Engineering Transaction (volume 2 in 2012) and manuscript of "Process intensification for production of ethyl lactate from fermentation-derived magnesium lactate: a preliminary design" was accepted to be published in the International Journal of Chemical Reactor Engineering.